Bone Formation on Calcium Phosphate Bone Substitute Materials

Sorousheh Samizadeh

Submitted for the degree of Doctor of Philosophy
Department of Biomedical Engineering
University College London

April 2010

The Centre for Biomedical Engineering
Institute of Orthopaedics and Musculoskeletal Science
University College London
Royal National Orthopaedics Hospital
Stanmore, HA7 4LP
United Kingdom

I, Sorousheh Samizadeh confirm that the work presented in this thesis is my own. Where information has been derived from other sources, I confirm that this has been indicated in the thesis.

Abstract

A large number of bone substitute materials are available; for which some authors claim osteoconductivity and some osteoinductivity. In order to rank these materials an *in vivo* analysis was carried out. These materials were chosen based on their availability and claimed mode of action. Silicon substituted Hydroxyapatite (SiHA), Hydroxyapatite (HA), Resorbable Calcium Phosphate Silicon, Skelite [silicon-stabilized tricalcium phosphate-based bone substitute], Pro Osteon 500R [coralline HA], BiIonic [Yttrium stabilized SiHA] and two non-calcium phosphate, Dimeneralised Bone Matrix (DBM) based biomaterials: Accell Connexus DBM putty and Grafton crunch DBM were implanted in sheep femoral condyle defects for 6 weeks. Implanted calcium phosphate (CaP) based biomaterials demonstrated superior bone formation in comparison with the DBM samples. Silicon within CaPs increased the rate of bone formation *in vivo*. Silicon substituted HA showed increased proliferation rate ($P<0.05$) of human marrow stromal cells compared to pure HA *in vitro*. Expression of osteoblastic marker genes RUNX2, Osterix and Osteopontin within the hMSCs indicated the differentiation of preosteoblasts into osteoblasts, and osteogenic development on both HA and SiHA. Expression of osteocalcin and bone sialoprotein genes on HA and SiHA samples indicated the activation of mineralisation process. Differentiation of hMSCs into osteoblasts *in vitro* suggested a role in promotion of osteoinduction by both HA and SiHA. Implantation of porous SiHA and HA in paraspinous muscle of sheep, exhibited new bone formation through osteoinduction. SiHA indicated significantly higher new bone formation ($P<0.01$) compared to HA. SiHA and HA biomaterials with higher strut porosity (30%) indicated greater bone formation ($P<0.05$).

In conclusion, CaP based biomaterials demonstrate superior bone formation in comparison with DBM biomaterials. Silicon substitution within HA enhances the cellular activity of hMSCs. Osteoinduction was greatest on SiHA with higher strut porosity. This result is believed to be due to a combination of the effect of interconnected porosity and chemical composition of the bone substitute.

Acknowledgement

This thesis would not have been possible without the inexhaustible supervision of Professor Gordon Blunn. I cannot thank him enough for all the guidance, support and encouragement that he provided me throughout my PhD. His vast knowledge, patience and inspirational character throughout the past four years helped my PhD progress in the right direction. I see myself exceptionally privileged for having him as my supervisor and I will always take pride in introducing myself as one of his students.

I would like to thank Dr Melanie Coathup for all her kind support and help throughout my PhD and thesis. Without her support I would not have gained my confidence in performing surgical experiments. Her calm and peaceful yet professional character has always been admirable for me.

I would also like to thank Annie Bartram for her time for proofreading this thesis and all her support throughout these years, had it been conference booking or emotional support. I am also thankfully to Josie Marshal for her kind words and valuable advice within the past year, it was a hard year and her support helped me overcome it easier. I would also like to thank Mark Harrison and Rebecca Porter for their technical and lab support.

My BME buddies, Jonathan Caruana's wisdom and intelligence, Elena Garcia's bubbly character, Carolina Alevaro Rodrigez's assertiveness, Kevin Ho's hard work and Kunalan Maruthainar's caring character, shape the best memories of my time at BME and I have learnt so much from each and every one of them.

Finally, thanks to my mum who cared for me and nurtured me throughout these years despite all my grumpiness, moodiness and bad manners! She was there for me, whenever even I could not put up with myself. She provided a peaceful, comfortable and loving home for me to be able to work on my PhD. I could not have finished the PhD without her love and support. And, my dad who put me on the path he

knew I would succeed in; it's only for him that I am able to achieve the goals of my life. His understanding of me and my needs is exceptional; I am who I am because of him. Also, Ali, Iman and Souphiyeh thank you for being supportive and patient with me while I was busy with the PhD, without you my life would be empty.

And to my better half who stood by my side throughout these years, helped me process my samples when I had wounded my hand and kept me company on Sundays and late evenings when I had to be in the cutting room or the lab on my own; thank you for all your love, support and encouragement, I know with you by my side, I can achieve anything I aim for.

Table of Contents

1 Chapter I. Introduction 13

1.1 Bone 13
1.2 Bone Grafts 19
1.2.1 Autograft 22
1.2.2 Allografts 23
1.2.3 Bone Substitutes 23
1.2.4 The effect of silicate ion substitution on bone formation 42
1.3 Aim and Hypothesis 47

2 Chapter II. In vivo Osteoconduction by Calcium Phosphate Bone Substitutes: A Comparative Study 48

2.1 Introduction 48
2.2 Calcium phosphate based bone substitute materials 48
2.2.1 ApaPore: Hydroxyapatite (HA) 48
2.2.2 Actifuse: Silicon Substituted Hydroxyapatite (SiHA) 49
2.2.3 BiIonic: Yttrium stabilized SiHA 49
2.2.4 CPS: Calcium Phosphosilicate 50
2.2.5 Pro Osteon 500R 51
2.2.6 Skelite 51
2.3 DBM based biomaterials 52
2.3.1 Grafton DBM crunch 52
2.3.2 Accell Connexus DBM Putty 53
2.4 Aims and Hypothesis 54
2.5 Materials and Methods 55
2.5.1 Study design 55
2.5.2 Surgery 56
2.5.3 Undecalcified Hard Resin Histology 57
2.5.4 Histomorphometry 58
2.5.5 Back scattered electron microscopy 59
2.5.6 Statistics 59
2.6 Results 60
2.6.1 Histomorphometry 60
2.6.2 Biomaterial Area 63
2.6.3 Dense vs. Porous biomaterials 65
2.6.4 Histological Analysis 66
2.7 Discussion 87
2.8 Conclusions 94

3 Chapter III. Cellular and Molecular Mechanism of Osteoinductivity by Silicon Substituted Hydroxyapatite 95

3.1 Introduction 95
3.2 Osteoblast Proliferation and Differentiation 95

3.2.1 Transcription factors....96
3.2.2 Osteoblastic marker proteins....97
3.3 Aims and Hypothesis....101
3.4 Materials and Methods....102
3.4.1 Disc production....102
3.4.2 Human Marrow Stromal Cells (hMSCs) culture....103
3.4.3 Cell seeding on discs....106
3.4.4 Osteogenic Differentiation- Morphology....107
3.4.5 Cellular Proliferation....107
3.4.6 Osteogenic Protein Expression....108
3.4.7 Osteogenic Gene Expression....110
3.4.8 Statistical analysis....111
3.5 Results....112
3.5.1 Characterisation of MSCs....112
3.5.2 Osteoblastic Differentiation- Morphology....114
3.5.3 Cellular Proliferation....118
3.5.4 Osteoblastic Protein Expression....121
3.5.5 Osteoblastic gene expression....125
3.6 Discussion....129
3.7 Conclusions....135

4 Chapter IV. Osteoinduction by Silicon substituted HA....136

4.1 Introduction....136
4.2 Aims and Hypothesis....138
4.3 Materials and methods....139
4.3.1 Study design....139
4.3.2 XRD and XRF Chemical Analysis....140
4.3.3 Surgery....141
4.3.4 Undecalcified Hard Resin Histology....142
4.3.5 Histomorphometry Analysis....143
4.3.6 BSEM and EDAX Analysis....143
4.3.7 Statistical analysis....143
4.4 Results....144
4.4.1 Histomorphometry....144
4.4.2 Histology (Light microscopy and SEM analysis)....150
4.5 Discussion....160
4.5.1 The effect of Silicate ion substitution on osteoinduction....160
4.5.2 The effect of strut porosity and physical structure....164
4.6 Conclusions....167

5 Chapter V. Discussion and Conclusions....168

5.1 Discussion....168
5.2 Conclusions....173

6 Bibliography....175

7 Conference presentations....205

Table of Figures

Figure 1. Osteoblast differentiation (from: Current Opinion in Genetic and Development) 16
Figure 2. Events at the interface between bioactive ceramics and the surrounding biological environment (Ducheyne and Qui, 1999) 26
Figure 3 . Bone-bone substitute material communication pathways (Hing et al., 2005) 27
Figure 4. Crystal Structure of HA (Vallet Regi and Acros, 2005) 38
Figure 5. Defects within femoral condyle head filled with test biomaterial 57
Figure 6. A photo micrograph showing the grid placed over the image and the type of tissue (I: Biomaterial, Red stain/NB: Bone or ST: Soft Tissue) present was measured at each intersection 58
Figure 7. New bone area percentage within Actifuse (AF), ApaPore (AP), BiIonic (BI), CPS, DBM Crunch (CR), DBM putty (CO), Pro Osteon 500R (PO) and Skelite (SK) samples at weeks 1, 3 and 6. (Numbers 1, 3 and 6 next to the letters indicate time point. e.g. AF1: Actifuse at week 1) 60
Figure 8. % bone contact for samples at weeks 1, 3 and 6. AF: Actifuse, AP: ApaPore, CO: Connexus, BI: BiIonic, CPS, PO: Pro Osteon 500R, SK: Skelite 62
Figure 9. Percentage of biomaterial area within calcium phosphate based and DBM based biomaterials 63
Figure 10. % bone area within porous and dense ApaPore and Actifuse calcium phosphates within 6 weeks 65
Figure 11. New bone formed within Actifuse at 6 weeks. A) Histology image: "*"/ Red stain indicating new bone. I: Biomaterial, ST: Soft tissue; Bar=100 μm B) BSEM image, Arrows: new bone, I: Actifuse, Bar = 100 μm 66
Figure 12. Actifuse sample at week 1. 67
Figure 13. Actifuse at week 3. Red, Bone, Arrows: Osteoblast. 67
Figure 14. Image of new bone formed within Actifuse at week 6. Arrows: osteoblasts, I: Biomaterial, NB: New bone, ST: Soft tissue. Circle: mesenchymal condensation. Yellow arrow: osteoclasts. 68
Figure 15. Lamellar bone within Actifuse sample at week 6. 68
Figure 16. Actifuse at week 3. Arrow: Multinucleated giant cell. 69
Figure 17. New bone formation within ApaPore at week 3. Red stain/arrows: New bone, I: Implant; ST: Soft tissue. HB: Host bone 70
Figure 18. BSEM image indicating new bone within and between ApaPore pores. Arrows: new bone 70
Figure 19. Lamellar bone within ApaPore at 6 weeks. Red stain: Bone; Green Arrow: Mesenchymal condensation. 70
Figure 20. New bone within ApaPore at week 6. Black Arrows: osteoblast. Yellow arrow: Blood vessel, Red stain: NB: New bone, ST: Soft tissue 71
Figure 21. New bone within ApaPore at 6 weeks. Black arrows: osteoblasts, white arrows: osteocytes, Green arrow: osteoclasts and implant resorption zone. 71
Figure 22. New bone within BiIonic sample at 6 weeks. Red stain/ *: New bone, ST: Soft Tissue 72
Figure 23. BSEM image indicating new bone within BiIonic. Arrows: New Bone 72

Figure 24. Osteoblast cells surrounding BiIonic particles at 3 weeks. Arrows: Osteoblasts, ST: Soft Tissue. 73
Figure 25. New bone formation within a BiIonic sample at 6 weeks. Arrows: Osteoblasts, NB: New Bone. 73
Figure 26. New bone formation within a CPS samples at week 6. Red stain indicating new bone. 74
Figure 27. BSEM image indicating new bone within CPS. NB: New bone. Magnified image indicates new bone attachment to CPS. Green arrow indicates material dissolution 74
Figure 28. Presence of osteoblasts adjacent to CPS at 6 weeks. NB: New bone. 75
Figure 29. CPS sample at 3 weeks. Yellow arrows: Osteoclasts, Green arrows: blood vessel. 75
Figure 30. Pro Osteon 500R. Red stain indicating bone. NB: New Bone, ST: Soft Tissue, PO: Pro Osteon 500R 76
Figure 31. New bone within Pro Osteon 500R. White arrows: HA layer surrounding the PO particle, Star: blood vessels, Black arrows: Osteoblasts, Yellow arrows: Osteocytes and NB: New Bone. 77
Figure 32. BSEM image indicating bone formation in between Pro Osteon 500R particles. Arrows: HA layer 77
Figure 33. BSEM image indicating bone formation on Pro Osteon 500R and zones of biomaterial resorption. Yellow arrows: HA, Red arrows: resorption zone, NB: New Bone 78
Figure 34. High magnification BSEM image. Zones of Pro Osteon 500R (PO) resorption and presence of CaP nodules. Yellow Arrows: HA, stars *: zones of resorption 78
Figure 35. EDAX spectrums of elemental composition of PO samples and the surrounding HA composition 79
Figure 36. New bone formation on a Skelite at 6 weeks. Red stain/Arrow indicates new bone. ST: Soft tissue 80
Figure 37. BSEM image indicating new bone within Skelite at 6 weeks 80
Figure 38. Skelite sample at 3 weeks. SK: Skelite; ST: Soft Tissue. 81
Figure 39. Skelite at 6 weeks. Arrows indicating osteoclasts and nucleated giant cells 81
Figure 40. BSEM image. Arrows indicate implant resorption sites within Skelite 82
Figure 41. Skelite at 6 weeks. Arrow indicating multinucleated giant cells 82
Figure 42. New bone within Grafton crunch at 6 weeks. Arrow indicating remineralised DBM 83
Figure 43. BSEM Image indicating Grafton Crunch DBM. 83
Figure 44. B). Remineralised Grafton Crunch DBM particle. Arrow: bone. NB: New bone 84
Figure 45. Grafton crunch sample. Blue arrow: multi nucleated giant cell. Yellow arrows: osteoid and osteoblasts. 84
Figure 46. Accell Connexus DBM putty sample at week 6. CO: DBM putty, ST: Soft tissue 85
Figure 47. BSEM image of Accell Connexus DBM particles (CO) 85
Figure 48. DBM putty particles. CO: Connexus DBM. Red arrows: osteoblasts. Green arrow: Osteocytes, Yellow arrows: osteoclast cells. 86

Figure 49. a) Discs of SiHA/HA. b) SEM image of SiHA surface 102
Figure 50. Confluent Passage 3 hMSCs after 14 days. Arrows: Spindle like cells Thermanox cover slips 112
Figure 51. Von Kossa stain indicating mineralisation and calcium deposits within osteogenic differentiated hMSCs on Thermanox discs. Black Arrows: Calcium; Red Arrows: Cells. 2.5 X magnification 113
Figure 52. Oil red O stained hMSCs. Arrows: Lipids within the cultured cells on Thermanox discs. 2.5X magnification 113
Figure 53. Day 1 hMSC on Control and HA discs. White arrows: adherent hMSCS cells. Yellow arrow: Presence of cell filopodia in contact with SiHA. 114
Figure 54 . Day 7 hMSCs on SiHA and HA discs. Arrow: spindle like cell. Stars: Cuboidal cells. 115
Figure 55. Control, HA and SiHA d14. Stars: cuboidal osteoblasts. 116
Figure 56. Day 24 hMSCs on Control, HA and SiHA discs. White arrow: Spindle like cells, Star: Osteoblast cells, Yellow arrow: Globular nodules 117
Figure 57. Total DNA content within hMSCs seeded on SiHA, HA and Control discs grown in Normal (-) and Osteogenic (+) medium. 118
Figure 58. Alamar Blue absorbency of hMSCs seeded on SiHA, HA and Control Therminox disc in Normal (-) and Osteogenic (+) medium within 24 days 120
Figure 59. Total protein production within hMSCs seeded on SiHA, HA and Control discs in Osteogenic (+) or Normal medium (-) 122
Figure 60. Total protein production normalized to DNA levels 122
Figure 61. Normalised data for Osteocalcin/DNA production by hMSC seeded on SiHA (SiHA+/-), HA (HA+/-) and control discs (Cntrl+/-) grown in Normal (-) or Osteogenic medium (+) 123
Figure 62. Normalized Osteopontin/DNA production by hMSC seeded on SiHA, HA and Control discs grown in Normal (-) and Osteogenic (+) medium. 124
Figure 63. The relative expression of transcription factors RUNX2 and Osterix ... 125
Figure 64. Relative expression levels of osteopontin gene. 126
Figure 65. Relative expression of Osteonectin, Bone sialoprotein and Osteocalcin genes 127
Figure 66. Relative expression of VEGF gene 128
Figure 67. XRD patterns for HA and SiHA samples. 140
Figure 68. a) Image illustrating the location of the implants. b) Radiograph of granular and block implants. 142
Figure 69. Bone area within SiHA implants compared to HA implants. 144
Figure 70. Graph showing % bone contact within SiHA and HA samples. 145
Figure 71. Bone area within SiHA and HA samples with different levels of strut porosity. 146
Figure 72. Bone contact measurements for SiHA and HA implants with different strut porosity. 147
Figure 73. Bone area within granular and blocks of SiHA and HA implants. 148
Figure 74. Bone contact in granular and blocks of SiHA and HA samples. 149
Figure 75. Images illustrating bone formation on HA 20 and 30% and SiHA 10, 20 and 30% samples. FT: Fibrous Tissue. NB: New Bone. No bone formation was observed in SiHA10 samples. 150
Figure 76. Blood cells at the implant interface within a pore. 151

Figure 77. Soft tissue infiltration within implant pores. FT: Fibrous tissue, BC: Blood cells. 151
Figure 78. New bone formation within SiHA and HA. Black arrows indicate osteoblasts, white arrow indicates osteocyte. Star indicates bone matrix. FT: Fibrous Tissue. 152
Figure 79. High magnification image of osteoid formation within SiHA and HA implants. 153
Figure 80. Histology images illustrating new bone within HA20 and SiHA20 implants. NB: New bone, FT: Fibrous tissue. 154
Figure 81. Light microscopy images of newly formed bone within HA30 and SiHA30 samples. NB: New Bone; FT: Fibrous tissue. 155
Figure 82. BSEM images illustrating new bone within SiHA30 and HA30% samples. White star indicates woven bone. Black star indicates biomaterial. 156
Figure 83. Histology and BSEM images indicating bone formation within..... 157
Figure 84. Histology images of block (SiHA30-B) and granular (SiHA30-G) implants illustrating new bone formed within the implant NB: new bone, FT: fibrous tissue. 158
Figure 85. EDAX map of SiHA. Yellow star: Soft tissue, Red star: Implant. 159

List of Tables

Table 1. Bone grafts (Bauer et al., 2007).....24
Table 2. The mechanical properties of bone and metallic and calcium phosphate implant materials (Kokubo et al., 2003;, Mahmoud et l., 2005, Levy et al., 2007)) 29
Table 3. Bone hydroxyapatite and different calcium phosphates and their composition (Wopenka and Pasteries, 2005).....34
Table 4. Bone substitute materials. P-G: Porous granules, D-G: Dense granules, P-C: Porous cylinder.....55
Table 5. Mean values (±standard error values) of the cellular activity (RFU/1000s) of hMSCs grown on SiHA, HA and Control discs in osteogenic (+) and normal (-) medium on days1, 3, 6, 12 and 24. 119
Table 6. Mean total protein/DNA (ng/ml)/(μg/ml) content of hMSCs seeded on SiHA, HA and Control discs in normal (+) and osteogenic (-) medium on days 3, 12 and 24..... 121
Table 7. Mean osteocalcin protein expression values (±standard error values) 123
Table 8. Mean osteopontin protein expression values (± standard error values) 124
Table 9. SiHA and HA implants porosity levels..... 139

1 Chapter I. Introduction

Natural bone composition, structure and the interconnected trabecular structure of bone tissue have provided the structural model for design and construction of bone substitute materials. The aim of this thesis was to investigate the mechanisms involved in the promotion of bone formation by calcium phosphate bone substitute materials including the effects of elemental substitution, specifically silicate ion substitution and material porosity.

1.1 Bone

Bone is a complex form of dense connective tissue that consists of collagen fibres, contributing to bone toughness, surrounded by a hard matrix of calcium salt deposits which provides the tissue with stiffness (Vander et al., 1994). Bones are rigid, porous and calcified structural organs of the body, responsible for the body's shape and movement. Seventy percent of the composition of the bone is made of calcium phosphates chemically arranged in a structure known as hydroxyapatite ($[Ca_3(P)_4)_2]_3.Ca(OH)_2$). Calcium phosphate, calcium carbonate, calcium fluoride, calcium hydroxide and citrate make up the crystalline structure of hydroxyapatite (Hedges and van Klinken, 1992).

The bones of the skeleton are all made of an outer layer of dense, compact bone, known as the cortical bone, surrounding the cancellous bone; the spongy inner bone is composed of thin trabeculae (Cornuelle and Gronefeld, 1997). The skeleton is composed of different types of bone including flat bones, short bones, and long bones, irregular, sesamoid and wormian bones. The mechanical properties of bone provide the skeleton with the required support, shape, protection and locomotion. Cortical bone is stiffer and resists higher stress, but is less strain resistant than cancellous bone. The porous structure of cancellous bone has a large capacity for energy storage and consequently is less stiff and withstands more strain (Table 2) (Nordin and Frankel, 2001). Bones provide protection to the internal organs, support for soft tissues and attachment sites for muscles and tendons. Bone also has a

function in calcium homeostasis, metabolism of minerals, and is a site for haematopoiesis.

Skeletal development involves close co-ordination of genetic processes controlling the specification, proliferation and differentiation of cells with apoptosis (programmed cell death) and remodelling of the extracellular matrix alongside vasculogenesis (Miclau et al., 2005). Skeletal development starts within 6 weeks of conception through the process of ossification. In the embryo the precursor cartilaginous tissue exhibits the characteristic shape of the forming bone tissues (Bell, 1952). During fetus development, bones are formed through endochondral ossification for the formation of long bones or intramembranous ossification for the formation and development of flat bones (Cornuelle and Gronefeld, 1997). The process of bone formation or osteogenesis continues throughout adult life as a bone remodelling process and is re-instigated during the course of fracture repair (Ferguson et al., 1999).

Bone formation is a tightly controlled mechanism which involves the morphogen mediated patterning signals for identification of areas of initial mesenchyme condensation, followed by stimulation of cell specific differentiation processes involving specific genes and protein expression for the production of chondrocytes and osteoblast cells (Franceschi, 1999). Intramembranous ossification starts with the condensation and differentiation of unspecialised MSCs into osteoprogenitor cells and ultimately differentiation of osteoblasts, which then create the extracellular osteoid matrix (Komori and Koshimoto, 1998). Osteoblasts, which originate from multipotential undifferentiated progenitor cells known as marrow stromal cells (MSCs) (Beresfrod, 1989), do not divide and contain a large eccentric nucleus with one or two nucleioli and prominent rough endoplasmic reticulum (RER) (Franz-Odendal et al., 2005). Marrow stromal cells are known as a heterogeneous population of stem/progenitor cells with a pluripotent capacity to self-renew and differentiate into many cell types, including the osteoblasts, osteocytes, adipocytes, chondrocytes, myocytes, cardiomyocytes, fibroblasts, myo-fibroblasts, epithelial cells, and neurons. Bone marrow is the primary source of MSCs, however adipose tissue, peripheral blood, cord blood, liver, and fetal tissues are also known to be sources of these cells (Peleld et al., 2002; Bobis et al., 2006; Liu et al., 2009). Osteoblastic cells exhibit a

variety of structural morphologies and activities, ranging from polygonal preosteoblasts to cuboidal osteoblasts, matrix-synthesizing osteoblasts, matrix and mineral-embedded osteocytes and very flattened or thin bone lining cells (Malaval et al., 1999). Extracellular signals, including hormones, growth factors, or cytokines, regulate the osteoblasts' function (Masato, 2001). The differentiated osteoblasts or the bone forming cells secrete the bone matrix proteins and synthesise the extracellular matrix or osteoid (Lecanda et al., 1997; Bronner and Farach-Carson, 2003; Yoshiko, 2007). The secreted extracellular matrix undergoes modification by osteoblasts to meet the mechanical requirements of the bone (Franceschi, 1999). Bone matrix deposited by osteoblasts is composed of collagenous and non-collagenous proteins with Type I collagen being the major component (90%) of the matrix, in addition to a small number of other collagen types (Fujisawa and Kuboki, 1998). The collagen in the bone provides a scaffold for the formation of crystals of dahllite or carbonated apatite (Ca_5 (PO_4, CO_3) (OH)) (Robinson, 1952). Collagen is a fibrous protein and the orientation of the collagen fibres within the bone matrix determines the cortical or trabecular/cancellous types of the bone in the body (Robinson, 1952). Osteopontin, osteocalcin, osteonectin, Bone Gla protein (BGP) and bone sialoprotein (BSP), in addition to a few other proteins, are the non-collagenous proteins of the bone matrix (Roach et al., 1994; Aerssens *et al.*, 1994; Fujisawa and Kuboki, 1998) expressed at different stages of osteoblastic differentiation (Figure 1). Bone matrix proteins are important for processes such as cell differentiation, cell attachment, cell maturation, hydroxyapatite and calcium ion bonding, in addition to mineralization of the bone tissue (Castano-Izquierdo et al., 2006; Young, 1991; Young 2003). As osteoid production by osteoblasts progresses some of the osteoblasts become embedded within the extracellular matrix, which subsequently becomes calcified. These cells develop into osteocytes (Figure 1) which exhibit reduced endoplasmic reticulum and golgi apparatus and consequently reduced protein synthesis and secretion (Franz-Odendaal et al., 2005). Osteocytes are mature, non-dividing, the longest living and the most abundant cell type of the bone whose precise functions are still obscure and are suspected to be involved in the regulation of calcium homeostasis, in addition to modulation of the function of other bone cells (Palumbo et al., 1990; Gu and Vanaanen, 2008). They contain numerous long cell

processes through which they connect with each other and the osteoblasts on the bone surface (Ikeda, 2008).

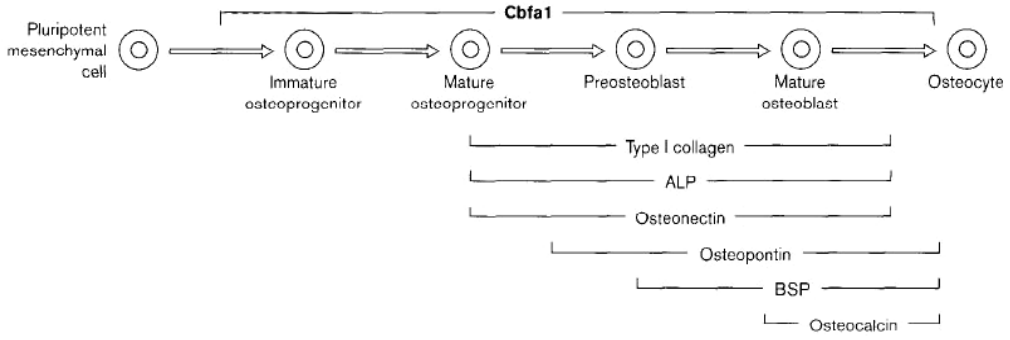

Figure 1. Osteoblast differentiation (from: Current Opinion in Genetic and Development)

Following deposition of the bone matrix, randomly orientated deposited bone matrices form weak, woven or coarse fibred bone, which is then replaced with mechanically stronger new linear or lamellar structured bone (Shapiro, 2008). The deposited osteoid matrix undergoes mineralisation. Osteoblasts secrete matrix vesicles in the osteoid which form the nucleation sites for the deposition of the first mineral crystals (Ray et al., 1997). Bone stiffness and rigidity is the result of the integration of minerals into the bone matrix. During the process of bone mineralisation, osteoblasts mineralize the deposited matrix by inducting the diffusion of Calcium (Ca^{2+}) and Phosphorous (PO_4^{3-}) ions through the interstitial space and pores of collagen present in the unmineralised matrix (Yokobori, 1998; Toshimitsu et al., 2002) and seeding of calcium phosphate crystals of carbonated hydroxyapatite $(Ca, X)_{10}(PO_4, HPO_4, CO_3)_6)(OH, Y)_2$ (LeGeros, 2002) in the sheltered interior of membrane-limited matrix vesicles. This is followed by spreading the hydroxyapatite mineral as needles orientated in the direction of collagen fibres onto the collagenous extracellular matrix (Posner, 1985; Hessle et al., 2002; Webster et al., 2003). The HA crystals in mineralized bone are in the form of irregular shaped thin plates which contribute to the exposure of a large surface area for rapid exchange of ions with the extracellular fluids (Barrere et al., 2006). The mineralised bone contains narrow tunnels, known as the osteocytic canaliculi, filled with extracellular fluid through

which osteocytic cell processes travel and mediate the transport and exchange of ions and other bioactive substances (Bonewald et al., 2006; Lane et al., 2008).

Following mineralization of the bone matrix, resorption and remodelling of the newly formed bone tissue usually follows (Gerstenfeld et al., 2003). Bone is replaced through osteoclast-mediated bone resorption and bone replacement by osteoblast-mediated bone formation as tightly coupled processes (Pederson et al., 2008). Osteoclast activation involves the receptor activator of nuclear factor- kB ligand, RANKL/RANK (a member of the tumour necrosis family) signalling and the production of pro-inflammatory cytokines and chemokines for regulation of an inflammatory response (Xing et al., 2005). RANKL resides on the osteoblast surface and RANK on the preosteoclast surface therefore in order for osteoclast differentiation these two different cell types must be in contact. Osteoclasts are specialized multinucleated macrophages of hematopoietic origin (Susa et al., 2004) which attach to the bone surface and develop a specialized cytoskeleton and other structures, such as the "ruffled border" associated with the degradation of the bone matrix. Bone resorption by these cells is carried out by secretion of hydrochloric acid and protease enzymes through extensive vesicle transport to the ruffled border and formation of an isolated acidic microenvironment on the bone-osteoclast interface called the resorption lacuna or Howships lacuna, within which hydroxyapatite crystals dissolve and the organic matrix of the bone degrades (Blair et al., 1986; Teitelbaum, 2000; Vaananen et al., 2000; Boyle et al., 2003; Takahashi et al., 2007).

Osteocytes mediate the mechanotransduction of the bone and translation of the mechanical strains into biochemical signals between osteocytes and to cells on the bone surface for the process of bone remodelling (Bonewald et al., 2006; Feng et al., 2006). Bone resorption and formation processes are in balance and maintain a constant, homeostatically controlled amount of bone within the body (Rodan, 1998).

During the process of endochondral ossification, unspecialised mesenchymal stem cells condensate at a location where a future bone is formed. The cells within the centre of this structure then differentiation into chondrocytes and the cells on the outside edges differentiate into fibroblast-like perichondrial cells. The formed chondrocytes proliferate and form cartilage templates. This is followed by the formation of vascular networks around these templates and the expression of

angiogenic growth factor, VEGF, for differentiation and enlargement of chondrocytes to hypertrophic chondrocytes. Vascular invasion is an essential factor for bone formation for repair/replacement of bone tissue. Vascular endothelial growth factor (VEGF) is the most effective angiogenic factor involved in osteogenesis (Ferrera and Davis-Smyth, 1997). Neo-angiogenesis by VEGF signaling is known to be crucial for endochondral ossification as inhibition of bone formation and resorption in juvenile mice has been observed in the absence of VEGF activity (Gerber et al., 1999). Following the formation of hypertrophic chondrocytes, secretion of collagen and other proteoglycans ceases and secretion of alkaline phosphatase which is essential for mineral deposition initiates. The hypertrophic chondrocytes further differentiate and mature and eventually, subsequent to calcification of the matrix, the chondrocytes die resulting in the formation of cavities which are then filled with blood vessels, nerves and lymph vessels. Concomitant with this process, the perichondrial cells on the periphery differentiate into osteoblasts and form the bone collar. The vascularisation ultimately recruits chondroclasts, the bone forming osteoblasts, and the bone resorbing osteoclasts for degradation of the mineralized cartilaginous matrix, osteoid secretion and remodelling of the extracellular matrix (ECM) respectively. The process of ECM remodelling eventually results in the synthesis of trabecular bone by osteoblasts' precursor cells and the consequent formation of the bone marrow cavity (Chung et al., 2004; Ortega et al., 2004).

Following completion of the skeletal growth, bone remodelling controls the bone turnover through which old bone tissue is replaced with new bone and consequently mineral homeostasis is regulated (Hill et al., 1998). Bone remodelling is a coordinated cycle of tissue resorption by osteoclast cells and bone formation by osteoblasts throughout life (Vaananen, 1993). Bone remodelling happens in small packets of cells known as basic multicellular units and new bone formation happens at approximately the same place as the resorbed bone and without any change in the density or shape of the bone. Healing of non critical sized defects and fractures of the bone is achieved through this remodelling process; however, promotion of bone formation for repair of critical sized defects requires human intervention (Hill et al., 1998). Since the functionality of the bone is dependent on the balanced mechanism of bone

resorption and formation (Frost, 1964), alteration of this balance for the purpose of increasing bone formation has been the focus of many studies. The complex structure of bone tissue contributes to its function in resisting mechanical forces and fractures. The mass and the quality of bone tissue characterised by the geometry, bone shape, the microstructure of the trabecular bone, bone turnover, the mineral content, and the collagen levels are important factors contributing to bone strength (Viguet-Carrin *et al.*, 2006).

1.2 Bone Grafts

Bone is known for its ability to self repair and remodel without the creation of scar tissue. However, large bony defects or poor bone healing, in addition to bone pathologies, require augmention to facilitate bone formation. The augmentation of bone tissue regeneration for repair of fracture defects, lesions, non unions or spinal fusions have been investigated for many years. Bone repair is described as restoration of the connection of the injured tissues, whereas bone regeneration involves the differentiation and proliferation of new cells and ultimately formation of new bone tissue with an increased volume (Al Aql et al., 2008). Regeneration of bone tissue was first achieved by a Dutch surgeon, Job van Meekeren, in 1668 through the repair of a soldier's cranium using bone tissue from a dog (de Boer., 1988). Since the 1920s, various types of substances such as Osmic acid, fibrin, blood, gelatine, calcium chloride, zinc chloride, thyroidin, glacial acetic acid, iodine tincture, adrenalin, hypophysis extract, bone marrow, copper sulphate, oil of turpentine, ammonia, lactic acid, silver nitrate solution, alcohol, carbolic acid, oak bark extract(tannic), vaccines, and sera have been used to promote bone regeneration; however, none of these are effective in promoting osteogenesis (Albee and Morrison, 1920).

Replacement of lost mineralised tissue and regeneration of bone has inspired the study of the inorganic chemistry associated with bone and its role in bone formation. The enhancement of bone formation using bone substitute materials is one of the mostly focused areas of orthopaedics and maxillofacial research. Bone grafts for the replacement or repair of bone defects have been used since the 17th century (Yaszemski et al., 1968). Natural or synthetic scaffolds/implants, undifferentiated or

osteoblastic cells and many growth factors and proteins are known to promote bone growth within osseous or non-osseous tissue for the purposes of tissue repair/replacement (Meijer et al., 2007). Autografts, allografts, xenografts (Brown and Cruess, 1982) and synthetic bone graft/substitute biomaterials have been used in orthopaedics and maxillofacial surgery over recent years. Spinal fusion in orthopaedics is one of the common techniques that employs the use of bone substitute materials. This technique involves the stabilisation of the spine by fusing two or more vertebrae together by placing bone graft material between the vertebrae. Bioactive bone grafts are available as dense or porous granules or blocks, wedges or cylinders, cements or as coatings on orthopaedic or dental implants (LeGeros et al., 2008). The success of bone formation by bone graft depends on the intrinsic bone forming properties of the graft including surface composition, surface roughness, surface topography, porosity and crystallinity (Keiswetter et al, 1996), the bone forming potential of the host, the graft's mechanical stability, and the surface area of the host-graft contact (Taylor et al., 2007). Direct interactions between matrix proteins and their cell surface receptors contribute to the host response to the bone graft. *In vivo* and *in vitro* different bone graft materials induce specific biological and local responses (Figure 2) leading to initiation of specific mechanism of ossification (Boyan et al., 1996).

Different types of bone grafts stimulate different osteogenic, osteoinductive and conductive mechanisms (Bauer et al., 2000). Osteogenesis involves new bone formation through the effect of the host tissue or a bone graft material and the activity of osteoprogenitor cells and osteogenic precursor cells (Lieberman and Friedlaender, 2005). Osteoblasts and preosteoblasts transplanted from one part of the body to the repair site induce the mechanism of osteogenesis through which osteoid deposition by osteoblasts, release of growth factors, initiation of capillary formation and vascularisation ultimately leads to new bone formation (Kontio et al., 2004). Osteoinduction is the induction of osteogenesis through the activation of cytokines, growth factors and also extracellular matrix proteins for proliferation and differentiation of pluripotent marrow stromal cells into osteoblasts (Helm, 1951; Albrektsson and Johansson, 2001). This mechanism involves the attraction of mesenchymal stem cells for induction of the repair or replacement of bone tissue

within osseous or non-osseous tissue (Luo et al., 2005). Bone grafts which transform connective tissue to bone in exoskeletal sites are osteoinductive. Urist et al. (1960s) demonstrated bone formation through osteoinduction by the intramuscular implantation of demineralised bone, which is bone tissue without the mineral constituents. Further identification of osteoinductive agents demonstrated the involvement of a soluble glycoprotein known as the bone morphogenic protein (BMP) in the mechanism of osteoinduction. BMPs are inductive agents naturally released in response to trauma for formation of bone or cartilage or during the process of bone remodelling. The mechanism of induction of bone formation by bone graft materials is suggested to be species dependant and dependant on the species' specific concentrations of the BMPs (Ripamonti et al., 1996). An illustration of the species specific nature of the bone response was demonstrated by Ripamonti et al. (1996) using bone substitute materials. They reported that intramuscular implantation of porous coralline hydroxyapatite within rat and rabbit animal models does not promote any bone formation; however, substantial bone formation was observed in porous HA samples implanted in canine or primate animal models. Apart from the chemical inductive agents, including BMPs, physical stimuli such as stress, the bone graft's physical structure and also electrical signals (Dealler, 1981) have also been shown to influence the mechanism of osteoinduction (Alberktsson and Johansson, 2001).

A bone graft is osteoconductive if it promotes bone formation within osseous tissue due to the effect of its composition, shape and surface texture (Bauer, 2007). Osteoconduction is the mechanism of stimulation of the attachment, migration and distribution of differentiated osteogenic and vascular cells for conduction of bone formation through the surrounding tissue into the repair/replacement site (Helm, 1951). The sources of the differentiated osteoblasts that promote osteoconduction can be the primitive mesenchymal cells or the preosteoblasts activated by trauma. Therefore it can be suggested that osteoconduction is the continuation of an earlier mechanism of osteoinduction (Alberktsson and Johansson, 2001). Bone tissue, specifically cancellous bone, is osteoconductive. The porous and highly interconnected trabecular structure of the bone promotes the migration of cells and vessels from the surrounding tissue for new bone formation. Adequate

vascularisation and development of a network of blood vessels for the provision of growth factors, proteins, hormones and nutrition is essential for bone formation (Trueta, 1963). In 1763, Albrecht von Haller stated that "the origin of the bone is the artery carrying the blood and in it the mineral elements". It is known that endochondral and intramembranous ossification are both associated with blood vessels' growth (Yeh and Lee, 1999). Differentiation of chondrocytes in endochondral ossification and their appropriate alignment in the growth plate are dependant on the formation of an appropriate vascular network. Osteogenesis is suggested to be coupled with angiogenesis as endothelial cells in blood vessels are known to be adjacent to osteoprogenitor and osteoblast cells present at the site of new bone formation (Trueta, 1963; Yeh and Lee, 1999). Osteoblasts are sensitive to oxygen levels and oxygen tension and hypoxia trigger the processes of angiogenesis and osteogenesis by elevating the expression of the angiogenic gene, vascular endothelial growth factor (VEGF) in osteoblasts (Wang et al., 2007).

A wide range of mitogenic and angiogenic growth factors have been identified to be involved in the mechanism of osteoconduction (Alberktsson and Johansson, 2001). Osteoconduction by bone grafts is achieved through the use of natural or synthetic scaffolds exhibiting porosity and chemical composition similar to that of natural bone, for the ingrowth of differentiated bone cells and blood vessels from the surrounding bone tissue concomitant with promotion of bone formation through osteoinduction (Cornell and Lane, 1963; Glowaschi and Mulliken, 1985).

1.2.1 Autograft

Autograft is transplanted fresh cancellous or cortical bone tissue or a combination of both, from one site (i.e. fibula, iliac crest, ribs or the removed bony process associated with the spine during spinal surgery) in the body to another within the same patient. Autologous bone graft is the "gold standard" and the most effective method of bone regeneration as this source of bone tissue provides scaffolding for osteoconduction, growth factors for osteoinduction, and progenitor cells for osteogenesis and also osteoindution (Vaccaro, 2002; Weinand et al., 2005) without any associated immune response. The most common use of autograft is in spinal

fusions, which involve the stabilisation of the spine by fusing two or more vertebrae together by placing small pieces of bone graft material between the vertebrae to be fused for the elimination of problems of the vertebrae and back pain. Disadvantages such as limited supply, the harvest procedure and high donor site morbidity limit the use of this type of bone graft (Goulet et al., 1997).

1.2.2 Allografts

Allografts are transplanted cancellous, cortical or dimeneralised bone matrixes from a living/cadaver donor to a patient (Delloy et al., 2007). Allografts are an osteoconductive source of bone graft usually harvested from femoral heads taken from patients during total hip replacement surgery or sections of the pelvis from cadaveric donors. They also possess limited osteoinductive properties if used as fresh frozen or in a demineralised form (Moore et al., 2001; Nguyen et al., 2007). Complications such as risk of disease transmission, inconsistency in graft preparation techniques, immune rejection, bacterial infection, fracture and also non-union due to differential donor related bone quality have been related to the limitations of the use of this type of bone grafts (Ferrara et al., 2005). The risk of disease transmission is reducing the use of fresh frozen allograft. Preparation for sterilisation and the sterilisation procedure itself reduce the bone forming potency of allograft.

1.2.3 Bone Substitutes

Due to the limitations of autograft and allograft, a variety of natural and synthetic bone substitutes have been identified and developed for the repair, reconstruction or replacement of bone tissue in procedures such as revision impaction grafting and spinal fusions. Calcium phosphate composition of natural bone and the interconnected trabecular structure of bone tissue have provided the structural model for development of bone substitute materials. Plaster of Paris, a calcium sulphate based biomaterial was one of the very first synthetic bone substitutes developed in the 1890s. Non-metallic bone substitutes include calcium phosphate ceramics, bioactive glasses, glass ceramics, aluminium oxide/alumina, tricalcium phosphates

(TCP), synthetic hydroxyapatite, dimeneralised bone matrix (DBM) and also coralline hydroxyapatite (Table 1) (Moore et al., 2001; Bjerre et al., 2008). Metallic bone substitutes include tantalum and titanium based alloys which are prominently used for load bearing purposes. Bioactive glasses are composed of SiO_2, CaO, Na_2O, and P_2O_5 with low mechanical strength and a greater osteoblastic activity compared to hydroxyapatite. The very first developed bioglass (45S5) is silica based (<60%) melt-derived glass with a high CaO/PO ratio. The surface reactivity of the silica, calcium and phosphates within this biomaterial promote bone bonding and bone formation in osseous tissue (Thomas et al., 2005).

Table 1. Bone grafts (Bauer et al., 2007)

Type	Characteristics
I.	Autograft
	A. Iliac crest
	B. Locally harvested
	C. Vascularized or non-vascularized cortical
	D. Aspirated and/or enriched bone marrow stromal cells
II.	Allograft
	A. Mineralized
	B. Demineralized [demineralized bone matrix (DBM)]
III.	Hydroxyapatite (HA) blocks and granules
	A. Formed by sintering or precipitation
	B. Formed by conversion of calcium carbonate
IV.	Soluble calcium-based granules
	A. Tri-calcium phosphate (TCP)
	B. Calcium sulfate
V.	Silicon-containing calcium phosphates
VI.	Bone morphogenetic proteins (BMPs)
	A. BMP-2
	B. BMP-7
	C. Growth differentiation factor-5 (GDF-5)
VII.	Injectable cements
	A. Polymethyl methacrylate
	B. Calcium phosphate cements
	C. Silica-containing cements

Calcium phosphates are the most popular non-metallic bone substitute materials due to their similar chemical composition to the inorganic phase of bone, plentiful amounts and low cost (Bohner, 2000; Brandoff et al., 2008). Tricalcium phosphates (TCP), synthetic hydroxyapatite (HA) and combinations of TCP and HA were the

very first and most popular bone substitute materials due to their biocompatibility and osteoconductive potential (Knaack et al., 1998; Bjerre et al., 2008).

Metallic implants, such as titanium and its alloys are commonly used for the repair of skeletal tissue where mechanical strength is required (Table 2). However these biomaterials are perpetual non-biodegradable grafts and do not elicit a biologically functional bone/biomaterials interface for promotion of osteointegration and direct contact of bone tissue with the implant surface. Synthesis of bone substitute materials as coatings for metallic implants is required for enhanced osteointegration and consequent implant fixation (Thian et al., 2005; Bjerre et al., 2008).

Bone substitute materials are required to be biocompatible, osteoconductive and/or osteoinductive, in addition to ultimately being totally replaced by natural bone. Bone substitute materials represent differential resorbablity; some indicate complete replacement by new bone whereas only partial resorption has been identified in others. Bioglasses, silica-calcium phosphate nanocomposites, biphasic calcium phosphates such as ß-TCP/HA or a-TCP/HA and calcium deficit or amorphous calcium phosphates are amongst clinically used bone substitutes (Soballe et al., 1999; Hing et al., 2007). Porous bone substitute scaffolds have been shown to promote enhanced cellular and vascular ingrowth which is required for mechanical fixation to the surrounding tissue (Klawitter et al., 1976; Hing et al., 2004; Karageorgiou and Kaplan, 2005). The presence of the porous structure contributes to in-growth of vascular networks within the implant and enhanced angiogenesis, in addition to increased levels of fluids, nutrients and growth factors permeability into the implant area (Bonfield, 2006). Pore sizes of ~300-400μm have been identified as the optimal pore size for attachment, differentiation, growth of osteoblasts and also vascularisation (Tsurugo et al., 1997). Further, interconnected macro (>50μm) and micro (<20μm) structures provide greater surface area for exchange of ions (Daculsi et al., 1990), which is believed to be important.

The specific surface interactions of bone substitutes with the host cells and the extracellular fluids, in addition to their influence on ionic exchange and molecular and/or cellular activities within the tissue, contribute to their function in promotion of bone formation (Barrère et al., 2006). At the interface between bone substitutes and the surrounding environment (Figure 2), dissolution of ions from the material (1)

and precipitation from the solution onto the biomaterial (2) contribute to the process of ionic exchange and structural rearrangement (3) at the biomaterial-tissue interface. This is followed by interdiffusion of elements from the surface boundary layer into the biomaterial (4). Further, elements present in the solution influence the activity of cells (5), which attach following deposition of mineral (6a) or organic phases (6b). These phases may be integrated (7) into the biomaterial surface promoting chemotaxis on the biomaterial surface (8), stimulation of cell attachment and proliferation (9), followed by differentiation (10) and extracellular matrix production(11).

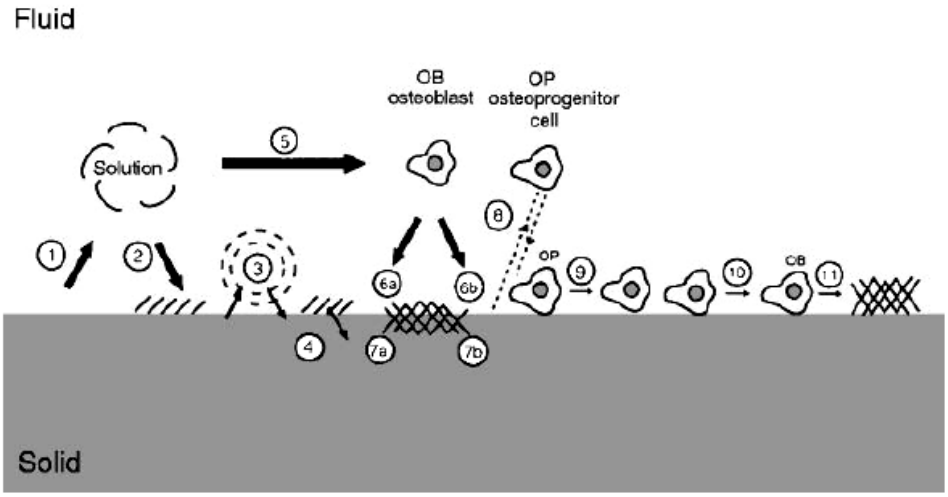

Figure 2. Events at the interface between bioactive ceramics and the surrounding biological environment (Ducheyne and Qui, 1999)

Several physical features, including surface topography, surface energy, the level of porosity, pore size and graft three-dimensional structure of bone substitutes, influence the interaction of the cells with the biomaterials (Figure 3) (Helm, 1951). The signals from the surface topography/charge of the bone substitute are transferred to the cell through changes in the interaction of integrin proteins, the mediators of cell binding to its extracellular matrix, with both intra and extracellular proteins resulting in changes in bone cell phenotypic expression, protein synthesis processes and osteoblastic activity. Further, the morphology of bone substitutes in the form of grooved and porous surfaces influences the cell migration, attachment, orientation and alignment and ultimately differentiation through provision of

compression and tension on the mechanoreceptors of the cells and also vascular invasion (Boyan et al., 2006). The proliferation and differentiation of marrow stromal cells (MSCs) have been shown to be influenced by the pore size as Mygnid et al (2007) demonstrated that pores of 200μm size show faster osteogenic differentiation of MSCs and pores of 500μm size accommodate higher numbers of cells and an increased MSC proliferation rate.

Bone substitutes' surface chemistry, in terms of charge density and net polarity of the charge, determines the hydrophobic or hydrophilic nature of the biomaterial in addition to surface tension or energy of adhesion. This in turn changes the local intermolecular interactions in terms of protein adsorption or the attraction of ions into the biomaterial surface for formation of the ideal host-biomaterial interface (Boyan et al., 2006). Further changes in the surface chemistry of bone substitutes influence the local pH levels, which in turn affects the cellular activities and the rate of bone formation (Hing et al., 2005).

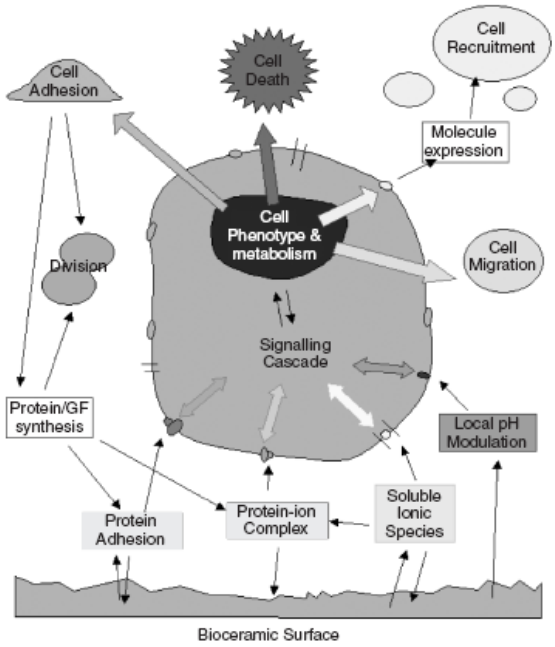

Figure 3 . Bone-bone substitute material communication pathways (Hing et al., 2005)

Dissolution of the bone substitute into its chemical constituents, concomitant with the process of osteogenesis and subsequent remodelling, promotes the ingrowth of

bone tissue and complete replacement of the substitute material with new bone. Random dissolution, phagocytosis or cell mediated resorption are the processes involved in bone substitutes' replacement. Cell mediated resorption of bone substitutes without random dissolution contributes to the elimination of uncontrolled physical degradation of the graft material and optimal material durability and ultimately, superior bone formation (Langstaff, 2001). The mechanism of bone substitute dissolution and resorption will be discussed in detail in the following sections.

Bone substitute materials are required to exhibit similar mechanical strength and load bearing to natural bone. Trabecular and cortical bone are known to show resistance to elastic deformation (Elastic moduli, E, are 10.4 GPa and 18.6 GPa respectively as shown in Table 1). It should be noted that natural bone is anisotropic and exhibits different mechanical properties in different directions based on the orientation of collagen fibres and hydroxyapatite crystals (Brunet-Imbault et al., 2005). Metallic bone substitutes exhibit greater mechanical properties compared to bone however such mechanical strength is not necessary in all instances of bone repair. Mechanical properties of non metallic bone substitutes are influenced by the biomaterial composition, the Ca/P ratio and the ions present, in addition to geometrical variations such as porosity, grain size and crystalline structure (Raynoud et al., 2001) (Table 2). Changes in biomaterial porosity result in changes in the mechanical strength of the material as a result of the reduced resistance of micro and macro crack propagation (Ambard and Mueninghoff, 2006). Graft materials which exhibit lower mechanical strength in comparison with the host bone may cause failure of the constructs and bone repair. As a result, these constructs are only used at places where they are not subject to any significant mechanical loading (Lieberman and Friedlaender, 2005).

Table 2. The mechanical properties of bone and metallic and calcium phosphate implant materials (Kokubo et al., 2003;, Mahmoud et l., 2005, Levy et al., 2007))

Material	Compressive Strength (MPa)	Tensile Strength (MPa)	Young's Modulus (GPa)
Bone			
Cortical Bone	100-230	135-160	17-20
Cancellous Bone	0.15-27	0.2-4	13
Metals			
316 I. Stainless	400	1000	200
Co-Cr alloy	--	900	220
Titanium **6A14V**	--	950	123
Bioglass (45S5)	500	40-60	78
Calcium Phosphates			
Porous	1-10	0.36	14
Dense	30-130	10-28	--

1.2.3.1 Natural bone substitutes

1.2.3.1.1 Coralline/Calcium Carbonate

The carbonate structure of marine species, including mollusc shells, sponges and corals, has been the natural source of many bone and cartilage graft biomaterials. Marine species used as biocompatible biomaterials exhibit porous 3-D structures similar to the structure of natural bone. Natural sea coral, a calcium carbonate ($CaCO_3$), has been the source of many orthopaedics and maxillofacial biomaterials for more than a decade (Ehlrich et al., 2006). Coralline is known to be a resorbable biocompatible material contributing to promotion of bone formation through formation of an aragonite or calcite structure (Richard et al., 1998).

Coral calcium carbonate is known to undergo a surface transformation of the aragonite calcium carbonate to a CaP-rich layer. This CaP-rich layer induces precipitation of a biological apatite, promoting nucleation and consequent bone

formation due to dissolution of synthetic CaP crystals (Richard et al., 1998). The potential of coralline species in controlled adsorption and release of growth factors through modification of their particle sizes or the adsorption conditions, has contributed to their selection as valuable bone graft materials. Coralline bone grafts have proven to be osteoconductive due the mechanism of bone ingrowth into and throughout their porosity when in direct contact with viable bone (Shors, 1999).

Conversion of coralline apatite to hydroxyapatite was achieved hydrothermally (270 °C; 103 MPa;) by Roy and Linnehan in 1974 where the aragonite on the surface of the coralline (calcium carbonate) was completely replaced by a layer rich in calcium and phosphate (Heness and Ben-Nissan, 2004), leaving an underlying scaffold of $CaCO_3$. *In vivo* studies on the mechanism of bone formation by coralline hydroxyapatites have shown the mechanism of rapid degradation of the calcium carbonate composition, concomitant with bone formation on the calcium phosphate component, as the bioactive behaviour of this bone substitute material (Ning et al., 2008).

1.2.3.1.2 Demineralised Bone Matrix

Demineralised bone matrix (DBM) is a processed form of allograft bone with the mineral content removed. Dimeneralised Bone Matrix (DBM) was first used in 1889 in the process of bone graft demineralisation for the purposes of obtaining aseptic tissue (Groeneveld et al., 1998). This was followed by the work of Urist (1965) who identified bone formation when rodent acid treated demineralised bone was implanted into muscle tissue (Kim, Vaccaro, Fessler, 2005). DBM is composed of the organic phase of bone (2%), collagen (93%), growth factors, BMPs and other non-collagenous proteins (5%) (Kenneth et al., 2005). The work of Urist (1965) led to the discovery of BMPs, the non-collagenous glycoproteins in the bone matrix. The presence of BMPs within DBM is known to contribute to the osteogenic property of this material (Laurence et al, 1984). BMPs involved in osteogenesis bond to specific receptors on the surface of mesenchymal stem cells, which transduce the signals for activation of genes that trigger the differentiation of mesenchymal cells to bone through endochondral and also intramembranous ossification (Dvorak et al., 2004).

Different BMP contents have been identified in different DBM preparations: however, BMP-2, BMP-4 and BMP7 (or Osteogenic Protein-1) are amongst the most osteoinductive bone morphogenic proteins (Pietrzak et al., 2006) as they trigger differentiation of osteoprogenitor cells to mature osteoblasts (Einhorn and Lee, 2001). The potential of BMP-2 and BMP-7 in bone generation has led to their therapeutic use in the form of recombinant proteins as replacements for autografts in spinal fusions and tibial non-unions (Lane et al., 2001). Recombinant BMPs have been successfully used in anterior fusions and when compared to autografts, are known to exhibit superior spinal fusion rates (Boden, 2006).

DBM is osteoinductive, osteoconductive and one of the least immunogenic allografts (Guizzardi et al., 1992) as the foreign antigens present in the allograft are removed during the processing period. The collagen component of DBM is known to provide the osteoconductive potential of DBM (Kenneth et al., 2005). The osteoinductive mechanism of bone formation by DBM involves the differentiation of mesenchymal stem cells into osteoblasts, followed by bone matrix synthesis and subsequent tissue calcification (Wang and Glimcher, 1999). The *in vivo* study of DMB by Urist demonstrated the ectopic osteoinductive role of DMB when implanted subcutaneously in muscle of mice animal models (Kenneth et al., 2005). The process of osteoinduction by DBM is known to involve the process of chondrogenesis, where mesenchymal stem cells are differentiated into chondroblasts (Kenneth et al., 2005). This osteoinductive process involves attraction of multinucleated giant cells to the material, followed by the migration of fibroblast-like mesenchymal stem cells to the site. Cartilage formation is known to commence within a week from implantation. The cartilaginous tissue then undergoes mineralization, is resorbed and finally replaced by new bone (Reddi and Huggins, 19972; Groeneveld et al., 1999).

DBM was first used in maxillofacial surgery in 1975 and has since been widely used in both orthopaedics and reconstructive maxillofacial surgery since. Due to the special properties of DBMs, such as low cost, low immunogenicity and ease of availability, DBM bone substitute materials have been widely used in orthopaedics to augment fusion of the spine, repair of graft non-union, osteolytic lesions around total joint biomaterials and also replacement of benign bone cysts (Peterson et al., 2004). DBM is produced from different human and non-human sources. Studies on the use

of xenograft- tissues harvested from one species to use in a different species- DBM have not shown any inflammatory reaction and immunogenic response. This is due to the fact that during the production process of DBM most antigens and proteins triggering an immunogenic response are removed and the BMPs responsible for osteoinduction by this bone substitute are species independent (Urrotia et al., 2008). Studies on the use of xenograft DBM in humans have reported contradicting results, where some discourage the use of it and others count it as a useful alternative. However, DBM derived from autograft seems to show a better clinical outcome when compared to xenograft sources (Lofgren et al., 2000). Commercially available DBM is produced from human bone banks and is available in many forms, including powder, crushed granules, putty, and chips and also in gel-packed syringe. The DBM product of processed cortical bone is in a powder form which is hard to handle. In order to ease the handling and delivery of this material, DBM is mixed with other biocompatible substances known as carriers, such as glycerol (Grafton DBM), gelatine, poloxamer (Accell Connexus DBM) hyaluronic acid and calcium sulphate. The most popular form of DBM is DBM putty or paste (Kenneth et al., 2005). The bone forming potential of DBM is known to be dependent on the demineralisation process, sterilization, carrier choice and the amount and variety of BMPs available within the material (Peterson et al., 2004). Carrier osteoinductivity, resorbablity and biocompatibility are essential factors in the composition of the ideal DBM based bone substitute.

1.2.3.2 Synthetic calcium phosphate bone substitutes

The potential of calcium phosphate based biomaterials in promotion of bone formation have been extensively studied by various scientists. Due to the prominent amounts of calcium phosphates within bone tissue and pathological solid tissues (Dorozhkin, 2007), the use of calcium phosphates in medicine was proposed in the 1890s. Studies of Albee in 1920s on tricalcium phosphate as a bone growth stimulus for enhancing the osteogenic activity of bone in delayed union or pseudarthrosis resulted in formation by this material. Further studies on the affect of the use of calcium phosphates in medicine led to the increase in the popularity of calcium

phosphates as bioactive materials in 1970s and 1980s (Jarcho, 1981, de Groot, 1984). Over recent years calcium phosphate bone substitutes have been widely used in reconstruction of bone tissue predominantly in coating of prosthetic implant devices for promotion of implant-bone bonding and osteointegration (Schnettler et al., 2004).

Calcium phosphate based biomaterials are mixtures of several phases which are synthesised through the reaction of ammonium phosphate with calcium nitrate or calcium hydroxide suspension with phosphoric acid in the form of powder. Different synthesis methods including solid-state, wet chemical (i.e. sol-gel), hydrothermal reactions, micro-emulsion synthesis and mechano-chemical synthesis are used for preparation of calcium phosphates. Each synthesis method produces calcium phosphates of different stoichiometry, density, morphology and crystallinity (Burkes et al., 2006). The produced powder is either transformed into slurry that is cast in a mould by mixing with a binder containing liquid or is dry pressed. This is followed by sintering at high temperatures to densify the powder and to remove the porosity between the particles. Porous biomaterials are produced by using polymer beads that maintain pore space during material processing (Enderle et al., 2005), impregnation of polyurethane foam with calcium phosphate slurry or by incorporation of progens such as oxygen peroxide, naphthalene or sugar molecules (Wnek and Bowlin, 2008) and generation of CO_2 bubbles for production of pores (Miao et al., 2003).

Table 3. Bone hydroxyapatite and different calcium phosphates and their composition (Wopenka and Pasteries, 2005)

Name	**Chemical formula**	**Ca/P ratio**
Stoichiometric hydroxyapatite	$Ca_5(PO4)_3(OH)_2$	1.67
Hydroxyapatite (HA)	$Ca_5(PO_4)_3(OH)_2$	1.67
Carbonated apatite: Calcium carbonate + ß-TCP	$CaCO_3$+ $Ca_3(PO_4)_2$	1.6–2.0,
a-Tricalcium phosphate ß-Tricalcium phosphate	a-$Ca_3(PO_4)_2$? -$Ca_3(PO_4)_2$	1.50 1.50
Calcium pyrophosphate dihydrate	$Ca_2P_2O_7{\cdot}2H_2O$	1.0
Octacalcium phosphate	$Ca_8H_2(PO_4)_6{\cdot}5H_2O$	1.33
Dibasic calcium phosphate	$Ca(HPO_4)$	1.0
Tetracalcium phosphate	$Ca_4(PO_4)_2O$	

Calcium phosphate biomaterials contribute to bone formation by the induction of biological responses in a manner similar to natural bone remodelling (Heise et al., 1990). Calcium phosphate based bone graft materials promote early bone formation within osseous tissue through osteoconduction (Jarcho, 1981) and formation of strong bonds between the biomaterial and host bone and also by osteoinduction within non-osseous tissues (Osborne and Newesley, 1982; Yuan et al., 1998). Studies on calcium phosphate biomaterials have indicated the *in vivo* induction of osteogenesis in many mammals, including monkey, baboons, dog, rabbit, goat and pig, by these biomaterials (Yamasaki et al., 1990; Ripamonti et al., 1991; Yuan et al., 1997; Yuan et al., 2002; Duan et al., 2003). Accumulation of growth factors and other proteins from the body fluids by calcium phosphates *in vitro* (De Groot et al., 1998) has been shown to induce the differentiation of mesenchymal stem cells into osteoblasts (Norman et al, 1994; Okumura et al., 1997).

The ionic transfer of calcium and phosphorous from the solid material via surface hydration of these elements within the biomaterial to the aqueous liquid and also

from the surrounding fluids to the calcium phosphate substrate *in vitro* and *in vivo* influences the bioactivity of calcium phosphates. This ionic transfer is dependant on the material's composition, the environmental conditions *in vitro* and also the implantation site *in vivo*. Changes in the ratio of calcium to phosphorous modify the phase composition of the biomaterial and this in turn influences the rate of ionic exchanges (Barrere et al, 2006). The release of ions could alter the resorption of the calcium phosphate biomaterial if, for example, high concentrations of the calcium ions are released (Heymann and Passuti, 1999).

Further, calcium phosphate biomaterials' surface roughness, due to its role in recruitment and retention of cells and proteins required for bone formation, works in combination with surface physio-chemistry to induce the appropriate biological response (Christophy et al., 2008). As explained before, the presence of micro and macrostructures within bone substitutes enhances the bioactivity (Klein et al., 1993; Blockhuis et al., 2000; Habibovic et al., 2006). Calcium phosphate biomaterials with micro and macro porous structures have been demonstrated to show ectopic bone formation due to the availability of a greater surface area for ionic exchanges, protein adsorption and cell adhesion, in addition to superior vascular penetration (Zhang et al., 2005). Further, strut porosity has been shown to increase *in vivo* bone formation within calcium phosphate based biomaterials and also promote earlier biomaterial osteointegration (Hing et al., 2005). The question here remains as to whether incorporation of strut porosity within biomaterials enhances the osteoinductive property of the biomaterial. However, increasing the strut porosity does reduce the strength of the bone graft material.

Dissolution, composition, surface energy and topography influence the bioactivity of calcium phosphates (Barrere et al., 2006). The dissolution of calcium and phosphate ions and their eventual accumulation and precipitation around the implant results in the formation of a biological apatite which is composed of calcium phosphates formed in a crystalline structure. The mechanism of osteoinduction by calcium phosphates as indicated by Daculsi et al (1990) involves the influence of the apatite precipitation on the surface of biomaterials. The nucleation of this apatite both on the implant surface and also on the proteins, subsequently modifies the implant surface leading to enhanced protein absorption and change in osteoblast cell

adhesion, proliferation, differentiation, maturation and ultimately production of mineralized bone (Porter et al., 2004; Barrere et al., 2006). The dissolution behaviour of calcium phosphates is known to be affected by the crystalline or amorphous features of the CaP. Amorphous biomaterials show faster dissolution; however if in crystalline form, the reduction of the crystal size or incorporation of the elements present in the bone mineral such as silicate and carbonate change the crystal lattice and enhance the dissolution rate (LeGeros, 1988; Barrere et al., 2000). Further, incorporation of proteins, such as bovine serum albumin, causes a change in the crystalline lattice (Liu et al., 2003). In addition, the presence of micro and macroporous structures within the calcium phosphates, influence the dissolution rate of these biomaterials. Thus, it can be elucidated that changes in the biomaterials' chemical composition, leading to physical changes, contribute to the dissolution behaviour of the biomaterials.

The rate of calcium phosphate biomaterials' dissolution influences the resorption behaviour of that biomaterial (Klein et al., 1983). Biomaterial restorability and osteoclastic resorption is known to be dependent on the biomaterial's nature and the physiochemical properties of the material after implantation, including the concentration of the released calcium ions and also the crystallinity and the structure of the CaP biomaterials (LeGeros, 1988; de Bruijn, 1994; Jones et al., 1995). Resorbablity studies on different calcium phosphates have indicated that octacalcium phosphates are more resorbable than ß-tricalcium phosphate and hydroxyapatite, the two most popular calcium phosphates (Kamakura et al., 2002). Natural bone resorption is mediated by acid production by osteoclast cells, which dissolve the small, finely divided carbonate-rich bone salts, exposing the organic matrix for enzymatic degradation. The process of resorption of calcium phosphate biomaterial is known to involve engulfing small biomaterial particles generated as a result of mechanical stress or dissolution at grain boundaries, by macrophages and macrophage polykaryons or osteoclasts in which an acidic environment or enzymatic attack dissolves the biomaterial particles (Boyde et al., 1999; Heymann, 1999). Physiochemical changes such as disintegration, loss of mechanical strength, changes in porosity and dissolution contribute to biodegradation and bioresorbablity of calcium phosphate biomaterials (LeGeros et al., 1988; Kurashina et al., 2002). The

resorption or degradation products of calcium phosphates are naturally metabolized and no abnormal calcium or phosphate levels can be found in the body fluids or organs (Hollander et al., 1991).

The mechanical properties of bone substitute materials are important factors for their use in hard tissue prosthetics. Porous bone substitute materials exhibit similar strength to cancellous bone, with tensile strengths of 5 MPa and compressive strength of up to 40 MPa (depending on level of porosity). Dense bone grafts show greater mechanical strength, however, the bioactivity of these biomaterials is severely compromised due to their smaller surface area (Shi, 2006) (Table 2).

Calcium phosphate bone substitutes and dimeneralised bone matrix (Urrotia et al., 2008) have been the substitutes for auto and allograft bone used in spinal fusions. Silicon substituted Hydroxyapatite specifically, has been found to promote excellent fusion when used in adult patients (Dickerman et al., 2008) due to the effect of its chemical composition, which will be discussed in the following sections.

1.2.3.2.1 Tri-Calcium Phosphates (TCP)

Tri-Calcium Phosphate ($Ca_3(PO_4)_2$) or calcium orthophosphate found in alpha (a) or beta (ß) forms, is a common calcium phosphate based biomaterial. ? eta Tri-Calcium Phosphate (ß-TCP) is one of the first developed calcium phosphate bone graft substitutes with compressive and tensile strengths similar to natural bone (Moore et al., 2000). Accelerated repair of bone defects by the use of tricalcium phosphates was first reported by Albee and Morrison (1920) (Shakelford, 1999). ß-Tricalcium phosphate bone substitute materials are resorbable biocompatible biomaterials with osteoconductive properties (Saikia et al., 2008). *In vivo* analysis of ß-TCP/bone interface has indicated direct biomaterial/ host bone contact and presence of osteocyte cells with elongated processes as the factors contributing to bone formation by this biomaterial (Fujita et al., 2003). ß-TCP is known to promote osteogenic differentiation of marrow stromal cells *in vitro* (Kawagoe et al., 2004; Kotobuki et al., 2006). The mechanism of osteoconduction by ß-TCP is known to involve direct biomaterials/bone contact, osteoclastic resorption and complete

substitution for bone tissue after induction of bone generation (Kamitakahara et al., 2008).

1.2.3.2.2 Synthetic hydroxyapatite

Bone mineral (Ca_5 (OH) $(PO_4)_3$/HA) is the main inorganic component of bone and teeth tissues with Calcium to Phosphate ratio of 1.67 (Biltz and Pellegrino., 1969). Stoichiometric Hydroxyapatite (HA), $Ca_{10}(PO_4)_6(OH)_2$ is the most widely used bone graft biomaterial due to its similar structure to the mineral component of the natural bone (Figure 4) (Heise et al., 1990; Balas et al., 2002).

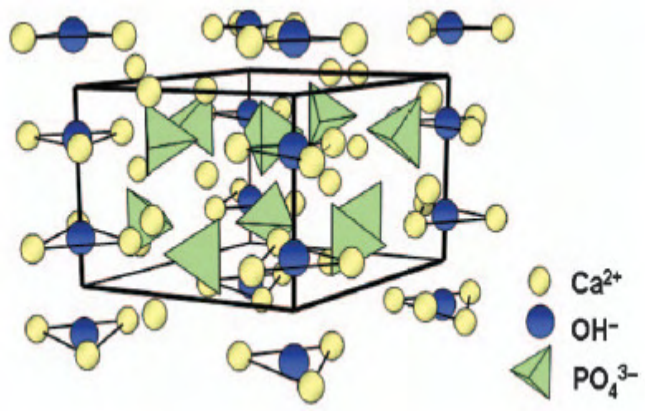

Figure 4. Crystal Structure of HA (Vallet Regi and Acros, 2005)

Despite the understanding of the osteoconduction mechanism by hydroxyapatite, the mechanism of osteoinduction by this biomaterial as a result of chemical composition and/or physical structure is not clearly understood. Studies by Ripamonty et al (1991, 96 and 99) on the induction of osteogenesis on porous HA indicated that bone formation on HA may be through the action of this biomaterial as a medium for adsorption of the circulating BMPs or their storage and controlled release or their expression at the HA-tissue interface. The *in vivo* studies of heterotopic bone formation within baboons indicated mesenchymal condensations at the HA interface and extensive vascular penetration, followed by bone formation within the porous structure, without the presence of any chondrogenic phase (Ripamonti et al., 1993). This indicated the involvement of an intramembranous mechanism of osteoinduction without the involvement of the bone morphogenic

proteins in induction of bone formation by this biomaterial. Bone morphogenic proteins when used often promote bone formation through formation of a cartilage intermediate which is then calcified by endochondral ossification. A study by Okumura et al (1998) in a rat animal model demonstrated that osteoblasts deposit the osteoid matrix, which is not yet calcified, directly on the surface of HA and the osteoid then undergoes maturation into fully mineralized bone. Further, Winter and Simpson (1969) identified the importance of calcification prior to induction of bone formation through an experiment where bone formation was observed within a synthetic polyhydroxyethylemethacrylate sponge implanted in the skin of a pig experimental model, by initial calcification of the polymeric sponge followed by bone formation. This indicated the role of calcification in mechanism of osteoinduction by calcium phosphates (Habibovic et al., 2004).

The analysis of the role of biomaterial structure on the mechanism of osteoinduction has identified that factors such as shape, porosity, pore size and permeability (Ripamonti et al., 1999; Habibovic et al., 2007) of HA biomaterials also contribute to the mechanism of osteoinduction. A study by Van Eeden and Ripamonti et al (1994) indicated that HA samples in block form exhibited heterotopic bone formation in baboons; however, porous HA granules did not indicate any bone formation. Jin et al (2002) demonstrated that the geometry of hydroxyapatite implants in the form of porous particles, porous blocks or honeycomb shaped HA, influences the vascular capillary invasion and consequently the growth, differentiation and phenotypic expression of osteogenic cells. Gray et al (1996) showed that bone formation on inert surfaces is favoured in grooves and crevices with depths similar to that of resorption loci, Howships lacunae left by osteoclasts. Further, the shape and the size of gaps and the discontinuity in osteoblast sheets influence the proliferation rate and the differentiation, function activity of osteoblast cells.

Yuan et al (1999) reported ectopic bone formation due to the effect of the variation in the levels of microporosity by two HA samples with similar chemical and crystallographic structures implanted in the muscle tissue of dog animal models. Such studies indicate that the surface characteristics and geometric parameters are important factors in the osteogenic function of bone substitutes.

Synthetic Hydroxyapatite is widely used as orthopaedic or dental implant coating to promote osteointegration and implant stabilization. Despite these favourable properties of HA, the rate of osteointegration by HA compared to bioactive glasses or glass ceramics is known to be slow.

HA does not degrade significantly and exhibits slow bioresorbability (Pietak et al, 2007; Bjerre et al., 2008). For these reasons, the development of novel HA biomaterials with enhanced efficacy are required (Webster et al., 2001). Biomaterials that exhibit the bone forming properties of HA have been developed by the incorporation of additional phosphorous compounds into the HA structure to form materials such as ß-TCPs which show enhanced solubility and resorbable characteristics, leading to complete substitution for the bone tissue after induction of bone formation (Sato et al., 2005; Kamitakahara et al., 2008). Several scientists have also doped HA with ionic substitutions such as K^+, Mg^{2+}, Na^+, CO_3^{2-} and F^- present in biological HA crystals to enhance the bioactivity of this biomaterial (Webster et al., 2003). Studies on the enhancement of HA bioactivity have shown that incorporation of silicon into the HA structure enhances bone formation through enhanced osteoblast cell activity (Gibson et al., 1999; Patel et al., 2002). A study by Patel et al (2002) on the *in vivo* response of pure HA and carbonate substituted HA demonstrated that the substitution of carbonate groups into HA enhanced the bioactivity of this biomaterial. Carbonate is the major impurity (2-8wt%) of bone mineral. Hydroxyapatite can accommodate carbonate at OH^- and PO^{3-}_4 sites (Zakaria et al., 2005). Studies on carbonate substituted HA have indicated that the presence of carbonate enhances the production of multinucleated cells on the ceramic surface *in vivo* and consequently enhances the bioresorbability of HA. This in turn promotes new bone formation through the mechanism of osteoclasts activity and remodelling processes, which in turn triggers osteoblasts activity and deposition of bone matrix via a coupling process, which was described in section I (Spence et al., 2008).

In 2001 Ergun et al. tested the effect of doping hydroxyapatite with magnesium, zinc, cadmium and yttrium. This study indicated that substitution of trivalent yttrium for calcium ions within HA resulted in the formation of an excess positive charge. Formation of a calcium ion vacancy for each two yttrium ions substituted for one calcium ion and segregation of the yttrium ions to the biomaterial surface was

suggested to contribute to the provision of protein adsorption and consequent cell attachment sites (Urgun et al., 2001). A previous study by Owada et al (1989) on calcium phosphates substituted with other elements for calcium ions, indicated an increase in the amount of surface of hydroxyl groups in relation to the amount of yttrium doped on HA, contributing to the high affinity of this biomaterial for water molecules. This study also indicated a reduction in electrical resistance of yttrium doped. The electric conductivity of this biomaterial, in addition to its water loving nature and the role of these factors in bone formation, contributed to further investigation of this biomaterial as a bone substitute biomaterial (Sato et al., 2006). Further, the *in vitro* study of Webster et al (2001) on osteoblast adhesion to yttrium doped HA showed that yttrium doped hydroxyapatite demonstrates enhanced osteoblast adhesion compared to yttrium free HA through superior calcium absorption and cell adhesion proteins such as vitronectin and collagen. Massa et al (2002) also demonstrated significantly greater osteoblast adhesion on HA doped with trivalent yttrium in comparison with pure HA. A study by Sato et al (2006) indicated superior amounts of calcium deposition by osteoblasts on yttrium doped HA. As cell adhesion to biomaterials contribute directly to their function and differentiation capacity, the results of these studies indicate that, yttrium substitution would contribute to enhancement of osteoblast cells' functions and consequently the amount of bone formation (Webster et al., 2002).

The capability of both calcium phosphate bone substitutes and DBM biomaterials in promotion of bone formation raises the question of "Which of these two groups, calcium phosphate bone substitutes or DBM, promotes superior osteoconduction *in vivo*?"

1.2.4 The effect of silicate ion substitution on bone formation

Rapid bone repair and bone tissue regeneration is an important issue in orthopaedics and maxillofacial surgery. It is desirable for bone formation by bone graft materials to occur in the shortest possible time as the stability and the mechanical properties of the implanted region are greatly affected by the formation of strong bonds between the body cells and the implant (Porter et al., 2004). Bone mineral contains variable deficiencies in Ca, P and OH. A number of cations including magnesium, sodium, silicon and strontium ions that can substitute for the calcium, in addition to a number of anions such as chloride or fluoride that can be substituted for the hydroxyl groups of the HA content of the bone mineral, have been identified (Robinson, 1952; LeGrose, 2002). The substitution of elements in the hydroxyapatite structure contribute to the bioactivity of bone, in particular silicon (8wt%) which is found to be an essential element for skeletal bone and cartilage development (Pietak et al., 2007) have been identified within this tissue. The biological activity of bone mineral and also calcium phosphate biomaterials is known to be enhanced by the presence and incorporation of the substitution elements in the apatite structure. Incorporation of the elemental substitutions influences the solubility, surface chemistry and morphology of the material. Amongst the known substitutions, Silicon (Si) is known as an essential element for a variety of life processes, for example, a metabolite affecting cellular processes and also a regulator of gene expression (Hildebrand et al., 2003). In the 1970s, Carlisle reported silicon as an essential element for normal bone and cartilage growth and development. Carlisle (1970) reported the unique localisation of silicon in active calcification sites of the bone. A further study investigating the effect of silicon deficiency showed the stunted growth of growing chicks and defective bone and connective tissue formation. Further, high concentrations of silicon have been detected in metabolically active osteoblasts (Carlisle, 1976). The role of silicon in bone healing through its effect on vascularisation, bone metabolism and bone matrix mineralisation and organisation has been shown to have a direct connection with the levels of dietary silicon (Schwarz et al., 1977). Hott et al (1993) reported prevention of trabecular bone loss in overiectomized rats by reduction of bone resorption and promotion of bone

formation through a possible effect of silicon on the formation or stabilization of the bone matrix. Calomme and Vanden-Berghe (1996) indicated a positive correlation between silicon concentrations in serum and collagen concentration within cartilage, as well as showing that silicon increases the serum calcium levels. The results suggested the role of silicon in the formation of the extracellular matrix and calcium metabolism. Silicon deficiency has been reported to decrease collagen formation in bone (Seaborn and Nielson, 2002). The results of a recent study by Jugdaohsingh et al (2008) reported the inhibition of growth plate closure and increased longitudinal growth of rats due to silicon deficiency. Soluble silicate ions have been demonstrated to stimulate the expression of type-I collagen and osteoblastic differentiation in osteoblast-like cell cultures (Refitt et al., 2003). Pabruwe et al (2004) demonstrated enhanced *in vivo* osteogenesis of silicon doped alumina. Further, development and structural integrity of connective tissue is known to be dependent on the bioavailability of silicon (Hing et al, 2006). Moreover, this element has been proposed as a factor involved in the formation of the collagen matrix and the mineralisation of bone tissue (Zuo et al., 2008).

With respect to the accumulating data on the role of silicon on the cellular responses and bone formation, substitution of this element has been incorporated into the structure of different biomaterials. Of these biomaterials, Bioglasses with more than 60% silica (SiO_2) content are known to promote bone formation through induction of high local turnover of bone formation and resorption (Valimaki and Aro, 2006). Further compounds such as Pseudowollastonite ($CaSiO_3$) and calcium phosphate based materials with trace levels of Si, such as Silicon substituted HA and Si-TCP, can be named (Pietak et al., 2007). Pseudowollastonite is a highly bioactive silicate mineral ceramic which forms a hydroxyapatite surface layer on an amorphous silica interlayer by releasing calcium and silicate ions into solutions influencing the bioactivity of osteoblasts and bone formation (De Aza et al., 1994 and 2000).

Identification of the factors involved in the stimulation of osteogenesis through the direct effect of cell-implant or through the presence of soluble ions released into the adjacent environment, is essential in understanding the mechanism of bone formation by these biomaterials. Silicate ions are known to stimulate heterogeneous nucleation and precipitation of amorphous calcium phosphate from supersaturated

calcium phosphate solutions (Tanizawa et al., 1995). The improved *in vitro* bioactivity of silicon substituted apatite is known to be affected by the nature of the silicate species, since monomeric silicate ions are known to promote calcium phosphate apatite layers with higher activity in comparison with polymeric silicate species (Ballas et al., 2002). Enhanced metabolic activity and proliferation of human osteoblast-like cells have been reported in culture media supplemented with silicon (Zuo et al., 2008). Ionic products of Bioglass dissolution are known to have a direct effect on gene expression in human osteoblast cells (Xynos et al., 2001). Valerio et al (2003) reported higher collagen production by osteoblasts cultured on bioactive glass containing 60% silica. Phan et al (2003) indicated enhanced proliferation of human osteoblasts on silica containing calcium phosphate particles. Silicon doped-TCP has also been shown to enhance the differentiation of mesenchymal stem cells and osteoblastic activity through formation of a bone-like apatite on the surface of the biomaterial (Camire et al., 2005).

The incorporation of silicate ion in the hydroxyapatite structure substituting phosphorus ions was first reported by Gibson et al (1998) through an aqueous precipitation chemical reaction between calcium hydroxide and orthophosphoric acid solutions. This substitution was then reported to enhance the bioactivity of human osteoblast cells and apatite formation in simulated body fluid *in vitro* (Gibson et al., 1999). Development of silicon substituted HA and its function in enhancement of the rate of bone formation and consequent early bonding of the implant with the host tissue, has contributed to increased use of this osteogenic biomaterial.

In vitro studies on the bioactivity of silicon substituted hydroxyapatite have reported enhanced *in vitro* metabolic activity of human osteosacrcoma cells on SiHA. A study by Botelho et al (2006) indicated increased osteoblastic protein production in human osteoblast cells on SiHA discs compared with pure HA. This study also indicated higher osteoblastic markers expression on 0.8 wt% silicate ion substitution when compared with 1.5wt% silicate substituted HA. A previous study by Porter et al (2003) showed an influence on the dissolution of silicon ions *in vivo* by increasing the level of silicon substitution (0< 0.8wt% <1.5wt%). Another study that investigated different levels of silicon within SiHA showed that 0.8wt% silicon level was the optimal level for the induction of bone formation. This level promoted fast bone

apposition and greater volume of bone ingrowth due to its effects on both bone forming and bone resorbing cells (Hing et al., 2006). Further, *in vivo* studies of the SiHA have indicated enhanced bioactivity of this biomaterial in comparison with pure HA. Patel et al (2002) reported an increase in bone apposition rate at the surface of SiHA implants when compared with pure HA. Further, the presence of organized mineralised collagen fibres within the implant pores at the host bone/SiHA interface was observed by Porter et al (2006).

Despite accumulating evidence indicating the superior SiHA bioactivity compared to normal HA, a detailed understanding of the mechanisms of the increased bioactivity involved has not yet been achieved. So far, studies investigating SiHA bioactivity have proposed a number of different mechanisms. Substitution of silicate ions into the HA structure is known to result in enhanced adsorption of anions to the surface and consequently a reduction of the surface charge of this material to a value more negative than that of HA in solution (Botelho et al., 2002). In addition, silicon substitution within HA is known to enhance the electrostatic, Van Der Waals and surface adhesion of this biomaterial (Vandiver et al., 2003). Protein adhesion, cell morphology and adhesion are affected by a material's surface charge. The negative surface charge of SiHA results in faster SiHA dissolution and the surface precipitation/apatite formation process, when compared to HA as negative charge attracts the positive calcium ions. This, in turn, contributes to SiHA providing a favourable site for the nucleation of an amorphous calcium phosphate apatite layer, providing the ideal conditions for superior bioactivity of this material (Botelho et al., 2002). Further, Porter et al (2003 and 2006) demonstrated the increased rate of HA dissolution by silicate ions' substitution due to smaller SiHA grain size, denser and less ordered grain boundaries' density and triple junctions in SiHA. This increased solubility of SiHA, and consequently the increased concentrations of Si, Ca and P ions at the HA/ceramic interface, is suggested as the contributing factor in the formation of the apatite layer involved in induction of bone apposition. Micro-texture changes including the reduction of the SiHA grain size, have been proposed to enhance osteoblasts attachment by causing conformational changes of cell anchorage proteins on the surface of SiHA and consequently the availability of RGD receptors, which are the cell surface binding domain of several extracellular matrix

proteins involved in cell attachment (Porter et al., 2005; Petty, 1993). Small quantities of silicon and calcium ions have been proposed to stimulate the activity of osteoblastic genes, resulting in increased osteoblast proliferation and differentiation (Hench et al., 2005). Further, Hing et al (2006) demonstrated early bone apposition followed by superior bone ingrowth by porous SiHA (0.8wt%) implants in comparison with HA. Through this study the variation in surface chemistry and structure was proposed as the contributing factor to the activity of the bone forming osteoblast and bone resorbing osteoclast cells. Recent clinical trials have proved silicon substituted calcium phosphate bone substitute to be a preferable alternative to autograft bone for use in spinal fusion impaction grafting (Drew, 2009).

With respect to the accumulating data on the role of silicon in bone formation, the question of the influence of Silicon substitution within calcium phosphates on promotion of bone formation as a sole chemical factor or a combination of chemical and physical factors remains. In general, complex cellular and molecular mechanisms contribute to the process of osteogenesis by calcium phosphate biomaterials. Understanding of the basis of bone regeneration in terms of the expression mode of various growth factor proteins and osteogenic genes contributes to the development of successful bone regeneration mechanisms (Einhorn and Lee, 2001).

1.3 Aim and Hypothesis

The aim of this thesis was to investigate the bone formation by different commercially available calcium phosphate biomaterials *in vivo* in an orthotopic and ectopic site. Further, the role of silicon substitution on the bioactivity of calcium phosphate bone substitutes as osteoinductive biomaterials *in vivo* and also *in vitro* was investigated. In addition, the chemical composition and physical structure on the bioactivity of calcium phosphate biomaterials was analysed.

The hypotheses of this thesis are that:

1. Generally calcium phosphate based bone substitutes demonstrate superior osteoconduction in comparison with DBM based biomaterials.

2. Osteoconduction is influenced by the biomaterial's chemical composition irrespective of structural porosity.
3. Silicon substitution within calcium phosphate bone substitute materials enhances the cellular activities of human marrow stromal cells through regulation of the osteogenic marker genes' expression.

4. Silicon substituted hydroxyapatite biomaterial promotes osteoinduction due to the role of silicon irrespective of the biomaterial's porosity.

5. Incorporation of strut porosity within the biomaterial particles enhances the biomaterial's osteoinductive property.

2 Chapter II. In vivo Osteoconduction by Calcium Phosphate Bone Substitutes: A Comparative Study

2.1 Introduction

Bone grafts are known to be the second most transplanted materials next to blood transfusions (Giannoudis et al., 2005), However, with the invention of a wide range of new bone grafting materials, the choice of the best graft material is an important issue. The ultimate goal of bone graft material is to promote optimal levels of bone formation in the shortest possible time through osteoinductive, osteoconductive or osteogenic mechanisms to replace structural or mechanical functions (Logeart-Aramoglu et al., 2005).

As described in the introductory chapter, a desirable bone substitute material should induce greater bone formation in the shortest possible time with optimal mechanical strength and ultimate resorbablity or remodeling into new bone. In this Chapter, the *in vivo* rate of bone formation by six commercially available calcium phosphate bone substitute materials (ApaPore, Actifuse, BiIonic, CPS, Pro Osteon 500R and Skelite) in comparison with two DBM base bone substitute materials (Grafton Crunch and Accell Connexus DBM putty) was investigated. This was carried out to evaluate the potential of calcium phosphate bone substitutes in promotion of bone formation as a function of their chemical composition in comparison with other bone substitute materials. This study is the largest comparison of bone graft substitute materials carried out to date.

2.2 Calcium phosphate based bone substitute materials

2.2.1 ApaPore: Hydroxyapatite (HA)

ApaPore (HA, $Ca_{10}[PO_4]_6[OH]_2$) is a synthetic phase pure hydroxyapatite biomaterial with a trabecular structure similar to cancellous bone which has been developed by ApaTech Ltd and is used in many clinical applications such as repair of bone defects or spinal fusions (Hing et al., 2005). This biomaterial has a unique, consistent and controlled interconnected micro and macro porous structure (Hing et al., 2003,

Kochhar et al., 2004). ApaPore is designed to absorb blood and bone marrow, contributing to the diffusion of growth factors and osteogenic proteins deep within the structure of the material.

HA was originally thought to be non-resorbable as no chemical dissolution was observed from this material nor was any cell mediated resorption detected (Osborne and Newsley., 1980). However, recent studies have reported that factors such as HA particle surface area influences the resorption and dissolution of this biomaterial (Mangano et al., 2008). As a result, the incorporation of strut porosity has been introduced into the structure of HA in order to enhance the bioactivity of this biomaterial.

2.2.2 Actifuse: Silicon Substituted Hydroxyapatite (SiHA)

Actifuse (Ca_{10} $(PO_4)_{6-x}$ $(SiO_4)_x$ $(OH)_{2-x}$) is a synthetic, 3-D biomaterial with 80% controlled interconnected strut porosity, silicon-substituted (0.8 wt%) hydroxyapatite biomaterial developed by ApaTech Ltd. Gibson et al (1999) first investigated the substitution of silicate ions with phosphate groups within the calcium phosphate structure of hydroxyapatite to test the influence of this element on the bioactivity of HA. Gibson, Best and Bonfield (1998 and 1999) incorporated 0.2, 0.4 and 0.8 wt% silicon into HA through an aqueous precipitation method using Ca $(OH)_2$ and H_3PO_4 followed by sintering of the product at 1200 °C. The Ca/(P+Si) ratio of the prepared samples was kept constant at 1.67, identical to stoichiometric HA and a final substitution of silicon ion into phosphorous sites was obtained (Gibson et al, 1998). This produced single phase silicon substituted HA, which presented identical X-ray diffraction patterns to that of stoichiometric HA with slight structural differences (Gibson et al., 1999).

2.2.3 BiIonic: Yttrium stabilized SiHA

BiIonic or yttrium stabilised silicon substituted HA (Ca_{10-x} Y_x $(PO_4)_{6-x}$ $(SiO_4)_x(OH)_2$, is a newly developed calcium phosphate based biomaterial. Yttrium is an earth metal element which is known to be strongly bound to skeletal tissue and bone surfaces in

the vicinity of vascular channels (MacDonald et al., 1957). A study by MacDonald et al (1957) on the skeletal deposition of yttrium showed the presence of greater amounts of this element in fractured bone when compared with intact bone. Yttrium has been used in yttrium-stabilised Zirconia for orthopaedics and dental purposes (Piconi and Maccauro, 1999) and also to enhance the mechanical properties of ceramics (Gülgün et al., 2002). As previously mentioned, silicon substituted hydroxyapatite (SiHA) is known to exhibit superior bioactivity in comparison with pure hydroxyapatite. However, incorporation of increased concentrations of silicon higher than 5.57 wt% within the HA structure are known to result in structural instability of this biomaterial. Stephen et al 2007, synthesised Y^{3+}/ SiO_4^{4-}co-substituted HA. The co-substitution of Y^{3+} was carried out for Ca^{2+} and SiO_4^{4-} for PO_4^{3-} ions within the HA composition in order to further enhance the stability and also the bioactivity of SiHA (Massa et al., 2001). This in turn would be expected to enhance the bone forming capacity of this biomaterial more than pure HA.

2.2.4 CPS: Calcium Phosphosilicate

Silicocarnotite (CPS)-($Ca_5(PO_4)_2Si0_4$)- is a calcium phosphosilicate originally found in Thomas slag, which is a by-product of steel production (Dickens and Brown, 1970). A study by Kim et al., 2003 showed that silicon substituted hydroxyapatite compounds doped with 3.76 wt% silicate and sintered at 1100°C, undergo decomposition into Calcium Phosphate Silicate (CPS), a-TCP and CaO. The chemical composition of Silicocarnotite is known to posses similarities with that of HA ($Ca_5(PO_4)_3OH$) found in the inorganic phase of human bone tissue (Dickens and Brown, 1970). Within CPS, the PO_4^{3-} anions are substituted by the tetrahedral SiO_4^4 anions which contribute to removal of hydroxyl anions in the HA, compensating for the charge difference. The phosphorous and silicon ions are randomly distributed within the crystalline structure of CPS and isolated SiO_4 and PO_4 tetrahedra are found within the carnonite structure of Silicocarnotite (Ballas et al., 2002).

CPS is produced by mixing of colloidal SiO_2 with stoichiometric solutions of H_3PO_4 and Ca $(NO_3)_2$ at 90°C to from a gel. The gel is then dried at 90°C followed

by 2 hours sintering at 700°C. The dried gel is shaped into pellets and the pellets are then flamed for half an hour at 1600° C followed by heat treatment at 1420° C for 9 hours. The pellets are quenched, re-ground and finally flamed again at 1450° C for 27 hours (Fotheringham, 2006). As Silicocarnotite/CPS exhibits similarities to stoichiometric HA, the bioactive potential of this material has been investigated. The chemical composition of CPS is expected to promote faster dissolution of calcium and phosphate ions and consequently enhanced bone formation by this biomaterial.

2.2.5 Pro Osteon 500R

Pro Osteon 500R is a porous (pores of ~500μm) granular resorbable bone substitute material manufactured by Biomet Inc., composing of a thin HA layer covering a calcium carbonate core. Pro Osteon 500R is produced by hydrothermal transformation of sea coral, which is comprised of calcium carbonate ($CaCO_3$), to HA. Pro Osteon biomaterials either consist of fully reacted HA or a thin layer of HA covering a calcium carbonate core. Calcium carbonates are known to be more soluble than calcium phosphates and the superior solubility of these compounds contributes to their increased rate of resorption. Consequently, a biomaterial which contains a carbonate composition is expected to show an increased resorption rate and also to exhibit earlier replacement of the biomaterial by newly formed bone tissue (Fontaine et al., 2005). Pro Osteon 500R is known to promote osteointegration within 6 months through the generation of woven bone formation followed by remodeling to mature lamellar bone (Walesh et al., 2003).

2.2.6 Skelite

Skelite is a synthetic multiphase silicon stabilised tricalcium phosphate (Si-TCP) based biomaterial with an interconnected open pore structure produced by EBI OsteoStim® used for repair of bone defects. The composition of Skelite consists of 67% Si-TCP and 33% hydroxyapatite (HA)/ß-tricalcium phosphate (ß-TCP). ß-Tricalcium phosphate bone substitute materials are resorbable and biocompatible biomaterials with osteoconductive properties (Saikia et al., 2008). The

biocompatibility of HA and the bioresorbable property of ß-TCP, in addition to the role of silicate ions in the promotion of bone formation, contributed to the development of a biomaterial consisting of both HA and Si-TCP elements commercially known as "Skelite". The HA and TCP within this biomaterial respectively provide stability and solubility and consequently contribute to the resorption rate of Skelite (Combes et al., 2006). The potential of Skelite as a resorbable biomaterial and its contribution to the initiation of the natural bone remodelling process and formation of new bone makes it an ideal bone substitute biomaterial. Skelite is available in granular or block forms with approximate porosity of 70% and an average pore size of 350µm (Leroux et al., 2007). This biomaterial is used for reparation of bone gaps or defects and also spinal fusions.

2.3 DBM based biomaterials

2.3.1 Grafton DBM crunch

Grafton® DBM crunch is a highly water soluble, bioresorbable DBM in a glycerol carrier biomaterial developed by Osteotech. Grafton DBM crunch is composed of demineralised bone fibers mixed with demineralised bone cubes. This biomaterial is used for repairing of segmental defects caused by cancer, tissue damaged by cancer, filling bone voids, augmentation of prosthesis, spinal fusion and also to replace damaged ligaments and tendons (Kim, Vaccaro, Fessler., 2005).

Production of DBM crunch involves the aseptic harvesting of human allograft tissue. The harvested tissue is then sterilised by a low dose electron beam, washed and then sonicated, followed by antibiotic treatment. Demineralisation of the tissue is then carried out by acid treatment to obtain less than 0.5% calcium phosphate; the demineralised tissue is then combined with glycerol, resulting in a product featuring putty like composition. The product obtained is then irradiated (? irradiation) to inactivate HIV-I, Hepatitis- B and C, Cytomegalovirus and poliomyelitis viruses (Peterson et al., 2004).

2.3.2 Accell Connexus DBM Putty

Accell Connexus DBM putty is a poloxamer reverse phase medium carrier form of DBM derived from banked human bone tissue developed by IsoTis Orthobiologics (Peterson et al., 2004). Poloxamers are non-ionic tri-block copolymers composed of central hydrophobic chain flanked by two hydrophilic chains and are used for increasing the water solubility of hydrophobic substances (Karmarkar et al., 2008). DBM putty is an osteoinductive demineralised bone matrix used in orthopaedics for filling gaps and voids within bone tissue that do not require a stable structure. The Connexus DBM putty contains a selection of growth factors, including TGF-beta-1 and a variety of natural human bone morphogenetic proteins including BMP-2, BMP-4 and BMP-7, contributing to the promotion of bone formation by this material (FDA report, 510 (k)). DBM putty is known to thicken at body temperature, adding to the stability within the implanted site.

DBM biomaterials are expected to promote greater osteoconduction compared to calcium phosphate bone substitutes due to the presence of cytokines within their structure. However the rate of bone formation by this group of bone substitutes in comparison with calcium phosphates, which take advantage of the calcium and phosphate ions within their composition for promotion of bone formation, needs to be studied.

2.4 Aims and Hypothesis

The aim of this study is to investigate and compare the rate of osteoconduction by calcium phosphate based bone substitute biomaterials in comparison with DBM based biomaterials.

The hypotheses of this study are that:

1. Calcium phosphate based bone substitute materials promote greater osteoconduction in comparison with DBM based biomaterials at early time points.

2. Osteoconduction is influenced by the biomaterial's chemical composition irrespective of structural porosity.

3. Silicate ion incorporation into the calcium phosphate based biomaterials enhances the bioactivity of these biomaterials.

4. The presence of Yttrium ions within silicon substituted hydroxyapatite further enhances this bioactivity of the biomaterial.

2.5 Materials and Methods

2.5.1 Study design

This study was designed to assess the osteoconduction rate of eight bone substitute materials based on preliminary data collected from a study carried out by Nuss et al., 2006. To achieve significance of $P< 0.05$, the study was designed for comparison of six calcium phosphate based bone substitute biomaterials with two DBM based biomaterials in 5 repeats (n=5) in a femoral condyle site where the overall standard deviation is around 8% (normal distribution with equal variation) with power of 0.8 using the David Shoenfeld's power analysis software. The eight different bone substitute materials investigated are listed below in Table 4.

Table 4. Bone substitute materials. P-G: Porous granules, D-G: Dense granules, P-C: Porous cylinder

Name	Biomaterial	Company	Catalogue
ApaPore (P-G)	HA 80%	ApaTech Ltd.	B011-2005H
Actifuse (P-G)	SiHA 80%	ApaTech Ltd.	B210-2005B
BiIonic (D-G)	Yttrium-SiHA	Dr Ian Gibson	JS115
CPS (D-G)	Silicocarnotite	ApaTech Ltd.	AF5
Pro Osteon 500R (P-G)	Carbonated HA	Biomet Inc.	5RGE10
Skelite ™ (P-C)	Si-TCP	EBI OsteoStim	LNK0420C03
Grafton Crunch	DBM	Musculoskeletal Transparent Foundation	124105
Accell Connexus Putty	DBM	IsoTis Orthobiologics	02-3000-100

2.5.2 Surgery

All procedures in this experiment were performed in accordance with the Animals Act 1986 (Scientific procedure). Seventeen skeletally mature commercially bred sheep aged 4 to 6 years old and weighing between 65 kg to 80 kg were used in this experiment. Prior to surgery, the sheep were premedicated with intramuscular administration of Xylazine 0.1 mg/kg, and anaesthesia induced by intravenous injection of Ketamine 2mg/kg and Midazolam 2.5mg. Approximately ten minutes later anaesthesia was maintained by a Halothane (2%) and Oxygen (25%) mixture. Animals were placed in supine position and the area above the medial aspect of both the right and left femoral condyles were shaved and washed with an iodine scrub in addition to a betadine antiseptic solution. Proximal-distal incisions of ~4 cm were made on the medial aspect of each distal femoral condyle, cutting through the skin, hypodermis layer and along the muscle tissue fibres, exposing the femoral condyle. The periosteum was then scraped from the surface exposing the underlying bone. Two cylindrical defects of 8 ± 0.3 mm in diameter and 15 mm length were created in each condyle using an air powered surgical drill with a 4.5 mm external diameter drill bit. The defects were flushed with sterile saline to remove debris. The selected bone substitute materials (1.2 ml) were then randomly packed into the implantation sites (Figure 5) in a manner that no one animal was implanted with two of the same biomaterial. The incision was then closed using resorbable Vicryl sutures. Animals were allowed full mobilisation as tolerated and at 1, 3 and 6 weeks post surgery, animals were euthanized and the implanted biomaterials retrieved for histomorphometric analysis. After sacrifice the femora were removed, all soft tissue was separated and the femoral condyles collected.

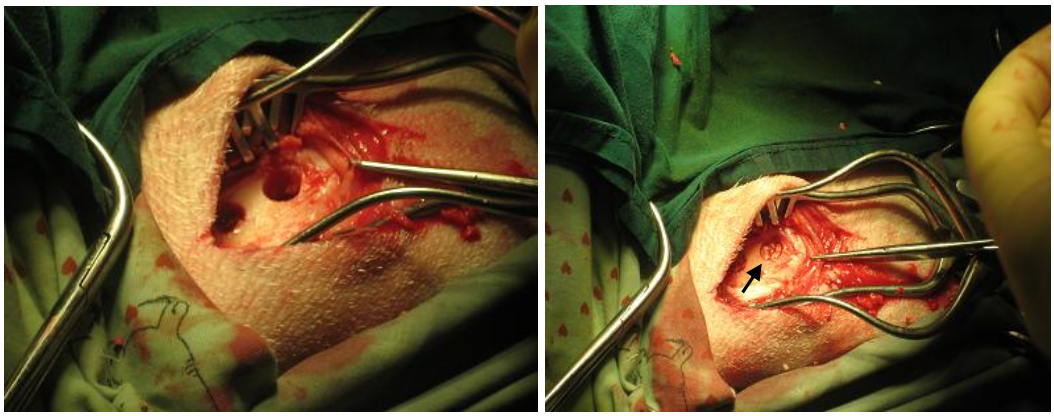

Figure 5. Defects within femoral condyle head filled with test biomaterial

2.5.3 Undecalcified Hard Resin Histology

The fresh femora were fixed by immersion in 10% neutral buffered formalin at room temperature for 7 days. Following this, the samples were prepared for undecalcified hard resin histology. Samples were dehydrated by immersion in industrial methylated spirit (IMS) at increasing dilutions of 30%, 50%, 75%, 85%, 95% and two changes at 100% for three days at each concentration. The samples were then defatted by immersion in chloroform for 3 days to remove lipids and to facilitate the penetration of the embedding medium into the sample. Samples were then cleared of chloroform followed by immersion in 100% IMS for 3 days. A solution of 50:50 LR White™ hard grade resin (London Resin Company Ltd.) and IMS was then prepared and the samples were placed in this solution for 3 days, followed by a final immersion in 100% LR White resin for 6 days during which the samples were kept in a cool, dark and dry area to avoid autopolymerisation of the resin. Following the final processing stage the samples were immersed in fresh hard grade LR White resin in moulding containers. Infiltration of the resin into the samples was aided by application of vacuum pressure for 10 minutes. A catalyst was added to the resin (one drop/10ml) to initiate polymerisation and the samples were placed in a 4 °C refrigerator to allow slow setting and decipation of heat due to the exothermic reaction.

The embedded samples were then sectioned longitudinally through the centre of each defect using an Exakt saw machine (EXAKT, Germany) followed by grinding the prepared sample slide to the desired thickness of ~ 70 μm using the Exakt micro-grinding system (EXAKT, Germany). The prepared thin sections were then polished using the Motopol 2000 machine (Buehler, UK).

In order to carry out histomorphometric analysis, samples were stained with Toluidine Blue for 20 minutes (stains the nuclei and cellular details), followed by 15 minutes of staining with Paragon for the identification of bone within the samples.

2.5.4 Histomorphometry

Comparison of the amount of new bone formation within the different materials was made using histomorphometry techniques. The percentage area occupied with new bone, the percentage new bone in contact with the biomaterial surface and changes in the percentage biomaterial present were quantified using the Axiovision Release 4.6 image analysis system (Zeiss, Germany). Eight images were taken at x5 magnification, four views at the periphery and four views at the centre, of each stained thin section. The images were then overlaid with a grid (10x12 units) and the line-intercept method (Figure 6) was used to quantify percentage area, bone-biomaterial contact and implant area where each line crossed the type of feature being measured.

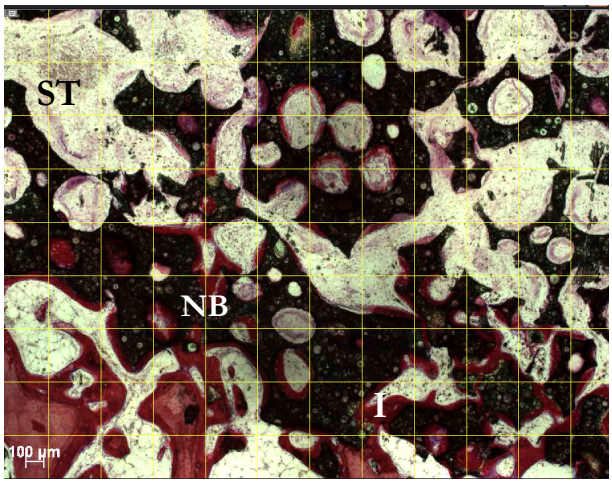

Figure 6. A photo micrograph showing the grid placed over the image and the type of tissue (I: Biomaterial, Red stain/NB: Bone or ST: Soft Tissue) present was measured at each intersection

2.5.5 Back scattered electron microscopy

Back scattered electron microscopy (BSEM) and Energy Dispersive X-Ray analysis (EDAX) were carried out in order to analyse bone formation and the elements present within the bone substitute biomaterials. One thin section sample slide from each biomaterial group was mounted on aluminium stubs and then sputter coated with gold palladium particles using an EMITECH K550 machine. The coated slides were then analysed using a JOEL JSM-5500LV scanning electron microscopy unit and back scattered electron microscopy images of the samples were obtained. Elemental maps of the samples containing new bone were also obtained using Energy Dispersive X-ray microanalysis (EDAX, UK) to investigate the elements present in the newly formed bone and soft tissue next to the implanted biomaterial.

2.5.6 Statistics

Statistical analysis was carried out using SPSS statistics software (SPSS v10.1, SPSS Inc. Chicago, USA). Non parametric data was analysed using Man Whitney U-test and $p < 0.05$ was considered to represent statistical significance.

2.6 Results

2.6.1 Histomorphometry

2.6.1.1 New Bone Area

Histomorphometry results showed bone formation within all biomaterials. The CaP based biomaterials ApaPore (AP), Actifuse (AF), CPS, BiIonic (BI) and Pro Osteon 500R (PO) promoted significantly ($P<0.05$) greater bone formation by 6 weeks with the exception of Skelite (SK) when compared with both DBM putty (CO) and DBM Crunch (CR) (Figure 7).

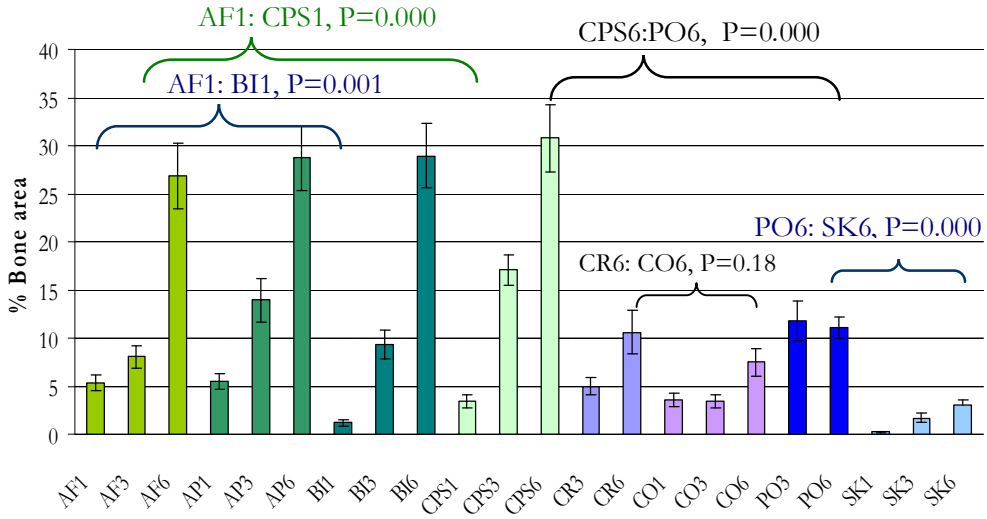

Figure 7. New bone area percentage within Actifuse (AF), ApaPore (AP), BiIonic (BI), CPS, DBM Crunch (CR), DBM putty (CO), Pro Osteon 500R (PO) and Skelite (SK) samples at weeks 1, 3 and 6. (Numbers 1, 3 and 6 next to the letters indicate time point. e.g. AF1: Actifuse at week 1)

Results showed that biomaterials of calcium phosphate composition promoted high levels of bone formation from week 1 to week 6 (Figure 7). At 6 weeks significant levels ($P<0.05$) of new bone were observed within CPS, BiIonic, ApaPore and Actifuse compared to bone formation within these biomaterials at weeks 1 and 3. CPS samples presented the highest level (30.77%) of bone formation at 6 weeks compared to the other groups. Skelite biomaterials exhibited the lowest (3.01%) amount of bone formation at 6 weeks.

BiIonic (28.94), ApaPore (28.70%) and Actifuse (26.83%) samples respectively showed significantly greater bone formation (P=<0.001) compared to Pro Osteon 500R (11.1%) and Skelite (3.01%) samples at week 6. Pro Osteon 500R (PO) biomaterials showed no significant difference (P=0.06) in the amount of newly formed bone from week 3 to 6 (Figure 7).

A significant difference of P< 0.005 was observed between the area of new bone measured within Actifuse (AF1), ApaPore (AP1) and CPS (CPS1) in comparison with BiIonic (BI1) and Skelite (SK1) at week 1 (AP1:BI/SK1, P=0.000; AF1:BI1, P=0.001; AF1: SK1, P=0.000; CPS1:BI1, P=0.009). However, no significant difference was observed between ApaPore and Actifuse samples in comparison with CPS at week 1. CPS (CPS3) and ApaPore (AP3) showed greater bone formation at 3 weeks compared to BiIonic and Actifuse respectively, with a significant difference (P=0.000) between CPS3 and AF3 and BI3. The amount of bone formation within Pro Osteon 500R (PO3 and 6) samples by 6 weeks was not significantly different (PO3:AF3, P=0.82; PO6:BI3, P=0.12; PO6:AP6, P=0.89) from that of Actifuse (AF3), ApaPore and BiIonic (BI3) biomaterials at week 3. The amount of new bone formation at 6 weeks was not significantly different (P> 0.05) when CPS (CPS6), BiIonic (BI6), ApaPore (AP6) and Actifuse (AF6) samples were compared (AF6:AP6, P=0.65; AF6:BI6, P=0.67; CPS6:AF6, P=0.21). Skelite (SK6) samples at 6 weeks showed similar amounts of new bone within CPS (CPS1) samples at week 1.

Both DBM based biomaterials showed the lowest amount of bone formation compared to the calcium phosphate based biomaterials, with the exception of Skelite. DBM Crunch (CR) promoted greater bone formation by week 6 compared to DBM putty (CO), however this difference was not significant (P>0.05) (Figure 7). No significant difference was observed in the amount of bone formation within DBM crunch and DBM putty biomaterials at 3 weeks (Figure 7). The amount of bone area within the DBM putty samples at week 1 did not show any change in comparison with week 3, however significantly more bone was formed by week 6 of the study (CO1: CO6, P=0.01).

2.6.1.2 Bone–Biomaterial Contact

Results showed variable amounts of new bone in contact with the surface of the different biomaterials. Significantly greater bone formation ($P<0.05$) was observed adjacent to the calcium phosphate based biomaterials in comparison to the DBM samples (Figure 8).

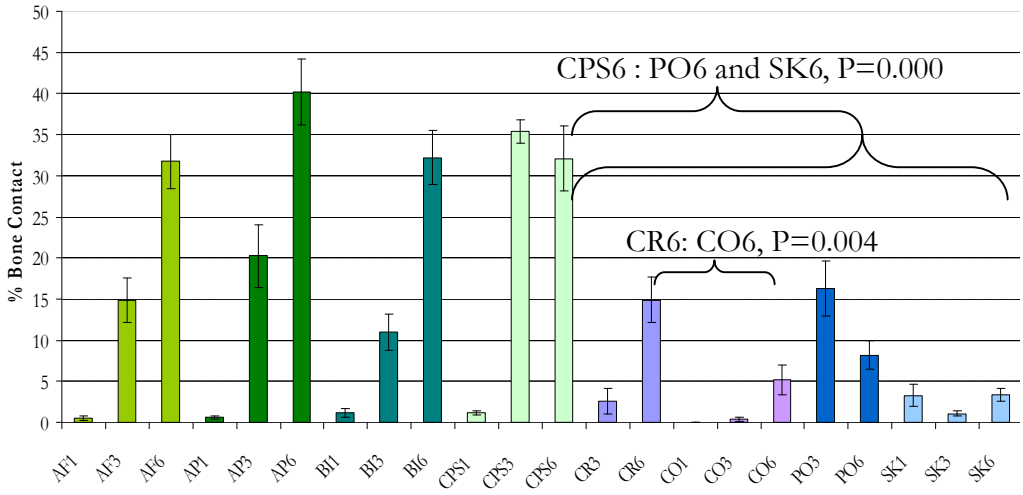

Figure 8. % bone contact for samples at weeks 1, 3 and 6. AF: Actifuse, AP: ApaPore, CO: Connexus, BI: BiIonic, CPS, PO: Pro Osteon 500R, SK: Skelite

ApaPore showed greater bone formation in contact with the surface (40.1%) and Skelite samples indicated the lowest amount of bone contact (3.3%) (Figure 8). Similar to the results obtained for percentage new bone area within the implanted biomaterials, ApaPore (40.1%), CPS (32%), Actifuse (31.7%) and BiIonic (32.2%) demonstrated significantly increased amounts of new bone contact ($P<0.05$) by week 6 compared to Pro Osteon500R and Skelite. Analysis of CPS samples showed a fast and high amount of bone contact by week 3 of the study with a slight decrease in the levels of newly formed bone in contact with the biomaterial surface at week 6 compared to week 3. However, close correlation between the increase in the amount of newly formed bone and the biomaterial surface was observed for ApaPore, Actifuse and BiIonic samples from week 1 to week 6. Levels of bone formed in contact with Pro Osteon 500R samples were observed to be lower at week 6 compared to week 3. Skelite biomaterials showed a decrease in the amount of new

bone in contact with the biomaterial from week 1 to week 3 followed by an increase in bone contact from week 3 to week 6 (Figure 8).

DBM Crunch (CR) samples demonstrated greater bone contact compared with DBM putty (CO) samples at 3 and 6 weeks. Significantly greater new bone contact ($P<0.05$) was observed in both DBM CR and CO samples at 6 weeks compared to samples at week 3 (Figure 8). DMB Crunch showed similar amounts of bone contact at week 6 to ProOsteon 500R at week 3.

2.6.2 Biomaterial Area

Histomorphometry analysis of the percentage implanted material's area within the femoral condyle defects indicated variable changes in the amount of implanted material within the 6 week period of the study (Figure 9).

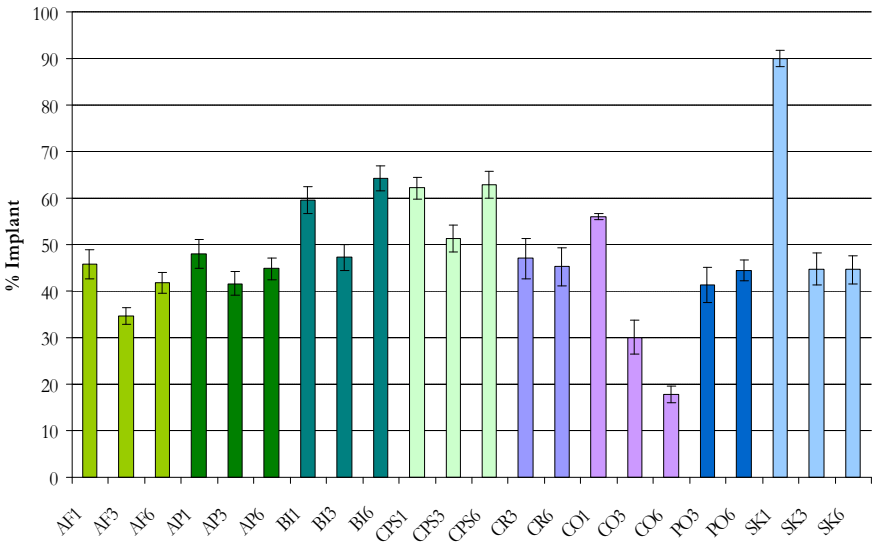

Figure 9. Percentage of biomaterial area within calcium phosphate based and DBM based biomaterials

Results demonstrated resorption of both Skelite and DBM putty samples within 6 weeks. Analysis of Actifuse, ApaPore, BiIonic, CPS and Pro Osteon 500R samples did not show a clear pattern of resorption. These implanted biomaterials were

observed to show a lower biomaterial area at week 3. As the biomaterials area at week 6 were observed to be similar to week 1 based on the histomorphometry results, the lower biomaterial area at week 3 was deduced to be due to the differences in packing of the material into the defects at point of implantation.

Skelite (SK) samples demonstrated a significant reduction (P=<0.001) in percentage of biomaterial area from week 1 to week 6. The area of the implanted material in Skelite samples was observed to reach half the initial implanted amount by week 3, followed by no change in this reduction up to week 6 of the study.

Analysis of the DMB group of biomaterials showed a non-significant reduction from week 3 to week 6 in the area of implanted DBM Crunch (CR) biomaterial. DBM putty (CO) samples, however, demonstrated a significant reduction (P=0.000) in the percentage of biomaterial area from week 1 to weeks 3 and 6.

2.6.3 Dense vs. Porous biomaterials

Analysis of the dense ApaPore (dAP6) and Actifuse (dAF6) samples in comparison with the porous samples (AP6 and AF6) indicated significantly greater bone formation (P=0.000) by week 6 in both porous ApaPore and Actifuse biomaterials. Significantly greater bone formation (AF1: dAF6, P=0.004; AP1; dAP6, P=0.04) was observed in porous samples (AP1 and AF1) at week 1 compared to the dense samples (dAP6 and dAF6) at week 6 (Figure 10).

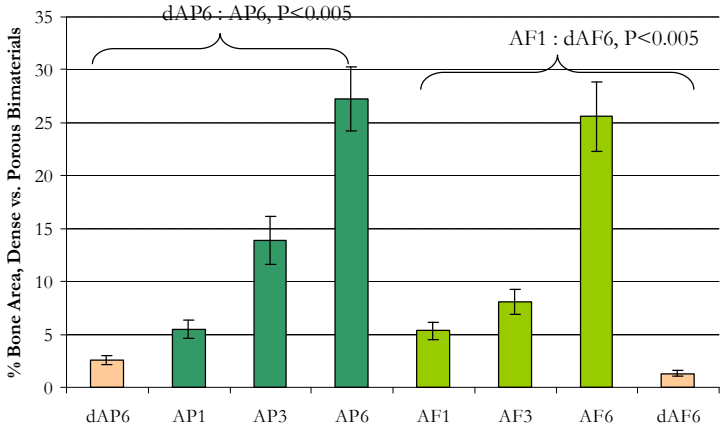

Figure 10. % bone area within porous and dense ApaPore and Actifuse calcium phosphates within 6 weeks

2.6.4 Histological Analysis

2.6.4.1 New Bone Area

Light microscopy analysis showed varying amounts of new bone formation within all groups analysed at weeks 1, 3 and 6. In all groups, woven bone formation was observed to be greater on the periphery of the defects where the biomaterials were in contact with host bone. The amount of bone formation within the centre of the studied biomaterials was observed to be material dependant.

2.6.4.2 Actifuse

Histology and BSEM images of Actifuse showed the presence of woven bone within the scaffold at the periphery and deep within the centre of the implants by week 6. New bone was observed adjacent to the biomaterial surface, within the pores and also in between the biomaterial granules (Figure 11). Bone formation was observed to be initiated by mesenchymal condensation by week 1, followed by bone deposition by osteoblasts and formation of lamellar bone by week 6 of the study. No sign of any inflammatory response was observed.

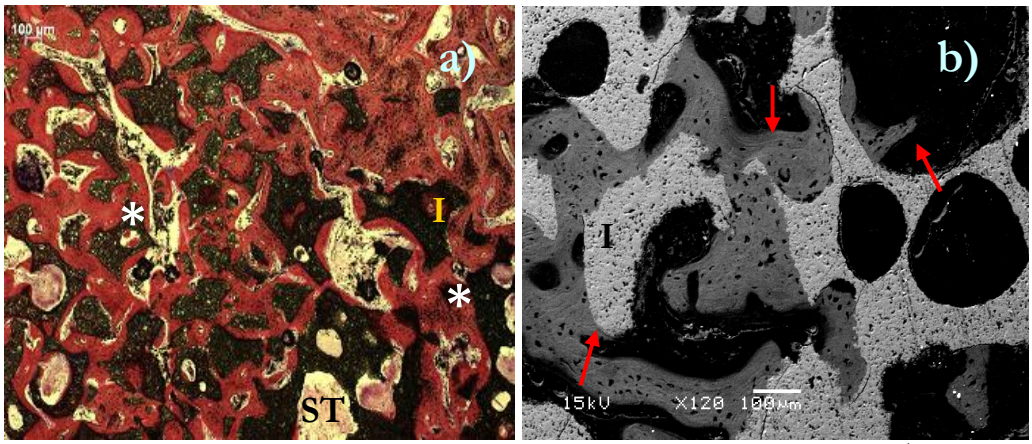

Figure 11. New bone formed within Actifuse at 6 weeks. A) Histology image: "*"/ Red stain indicating new bone. I: Biomaterial, ST: Soft tissue; Bar=100 µm B) BSEM image, Arrows: new bone, I: Actifuse, Bar = 100 µm

High magnification images of the samples showed presence of osteoblasts and centres of ossification and zones of newly deposited bone matrix on the surface of the pore (Figure 12, Figure 13 and Figure 14). Presence of multinucleated giant cells and osteoclasts within the scaffold suggests remodeling of the bone (Figure 16). Lamellar bone was observed by week 6 of the study (Figure 15).

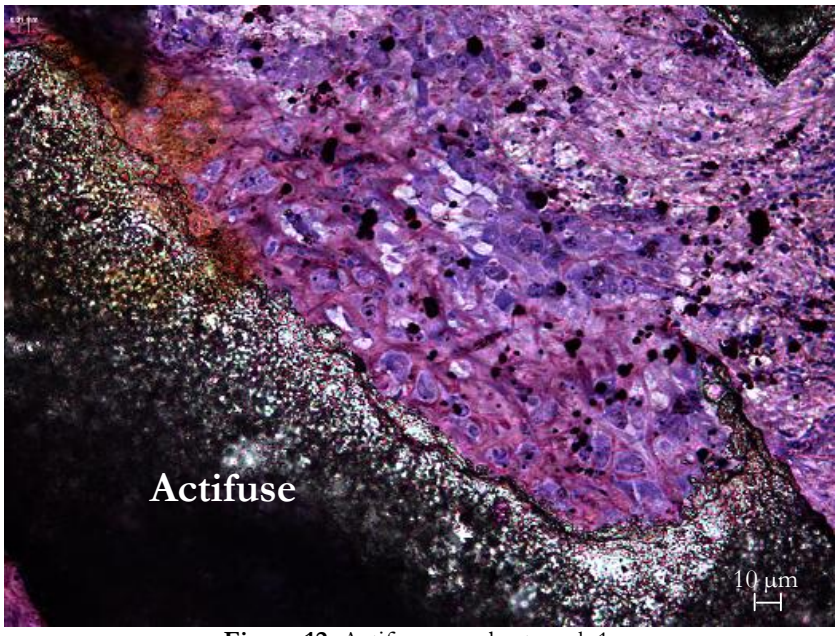

Figure 12. Actifuse sample at week 1.

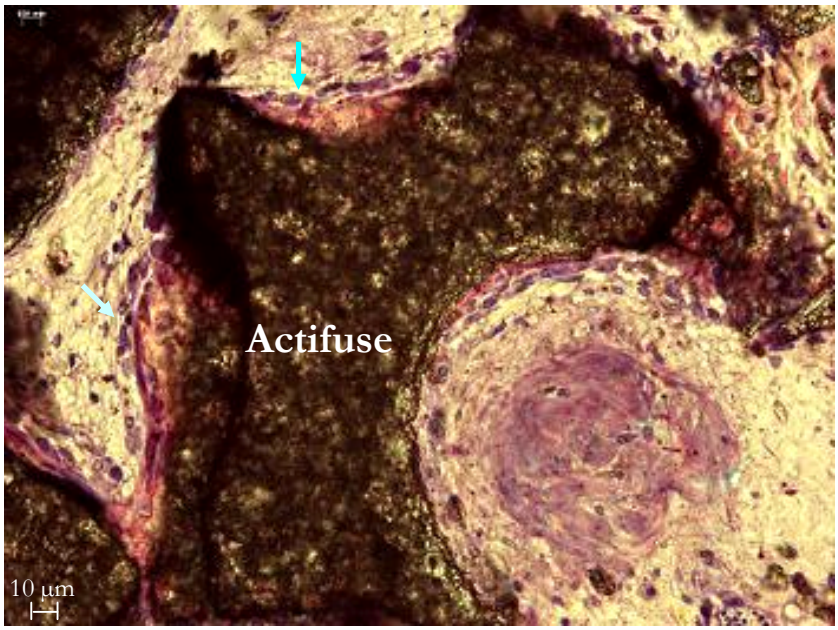

Figure 13. Actifuse at week 3. Red, Bone, Arrows: Osteoblast.

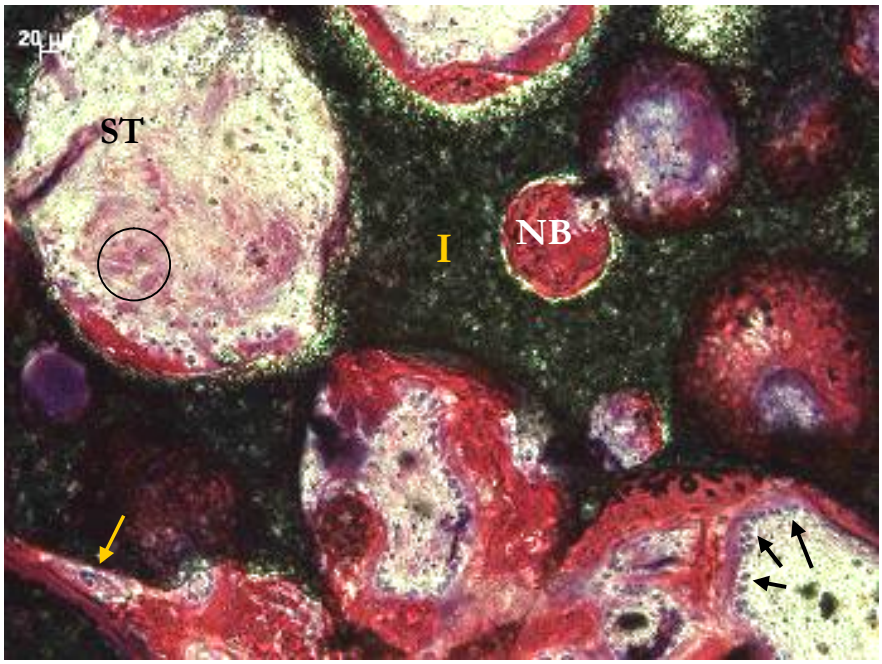

Figure 14. Image of new bone formed within Actifuse at week 6. Arrows: osteoblasts, I: Biomaterial, NB: New bone, ST: Soft tissue. Circle: mesenchymal condensation. Yellow arrow: osteoclasts.

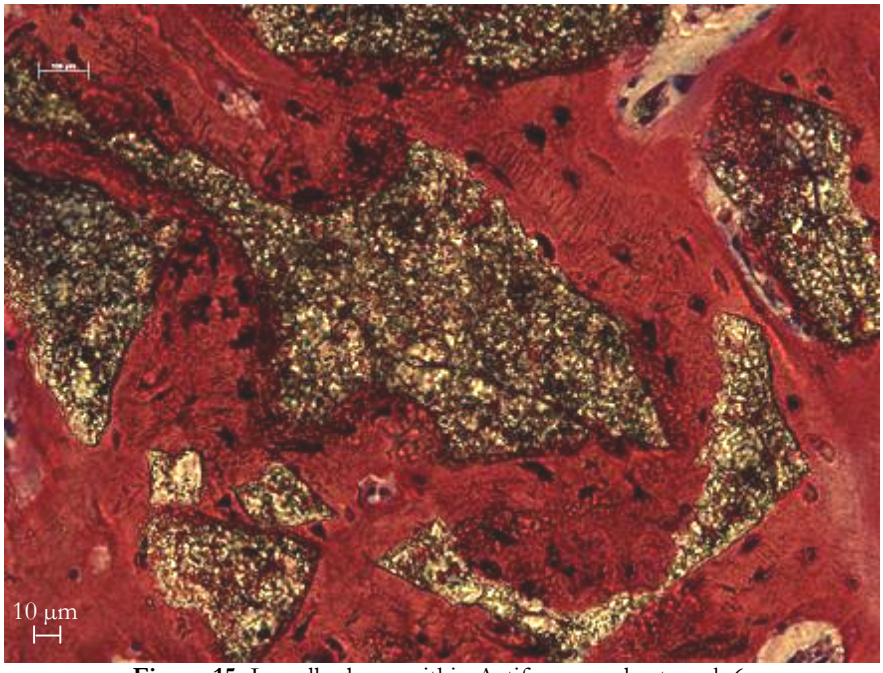

Figure 15. Lamellar bone within Actifuse sample at week 6.

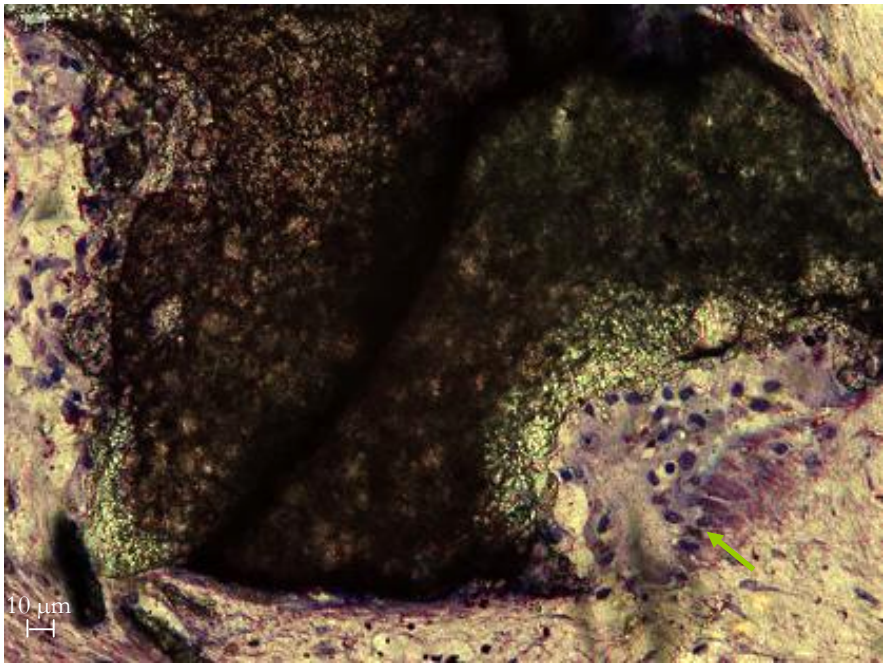

Figure 16. Actifuse at week 3. Arrow: Multinucleated giant cell.

2.6.4.3 ApaPore

Analysis of histological and BSEM (Figure 17 and Figure 18) images of ApaPore samples indicated the presence of bone both in the periphery and also in the centre of the graft. Bone was observed within the biomaterial pores and also in between the ApaPore granules. Zones of mesenchymal condensation were observed on the concave face of the ApaPore pores. Lamellar bone was observed by week 6 of the study (Figure 19).

High magnification images showed the presence of osteoblasts in the vicinity of the newly formed bone adjacent to the biomaterial surface by week 6 (Figure 20). The presence of osteocyte cells and blood vessels (Figure 20) was also observed within the samples (Figure 21). Further osteoclast like foreign body giant cells (FBGC) were identified in the vicinity of ApaPore particles (Figure 20) (Tatrat resistant acid phosphatase (TRAP) would confirm the nature of these cells as osteoaclasts or FBGCs).

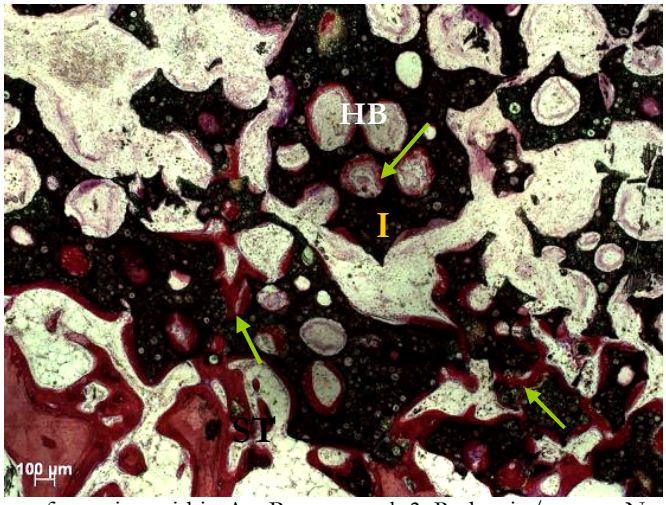

Figure 17. New bone formation within ApaPore at week 3. Red stain/arrows: New bone, I: Implant; ST: Soft tissue. HB: Host bone

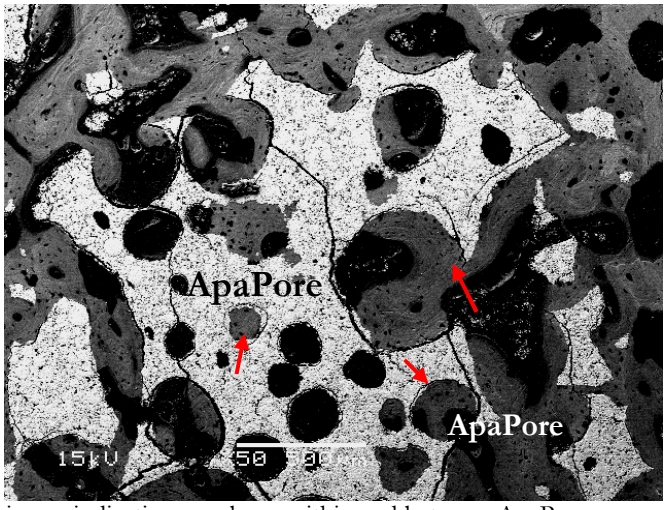

Figure 18. BSEM image indicating new bone within and between ApaPore pores. Arrows: new bone

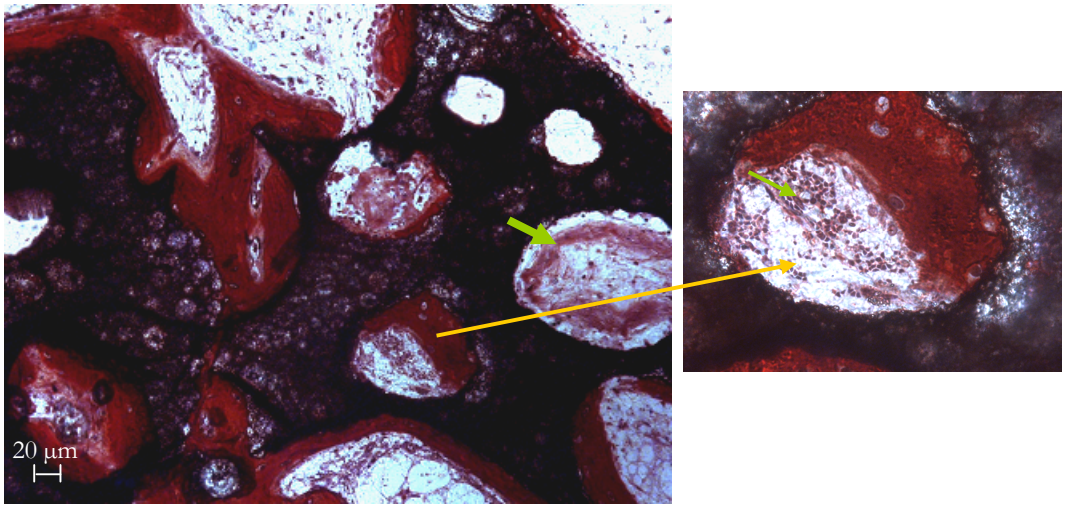

Figure 19. Lamellar bone within ApaPore at 6 weeks. Red stain: Bone; Green Arrow: Mesenchymal condensation.

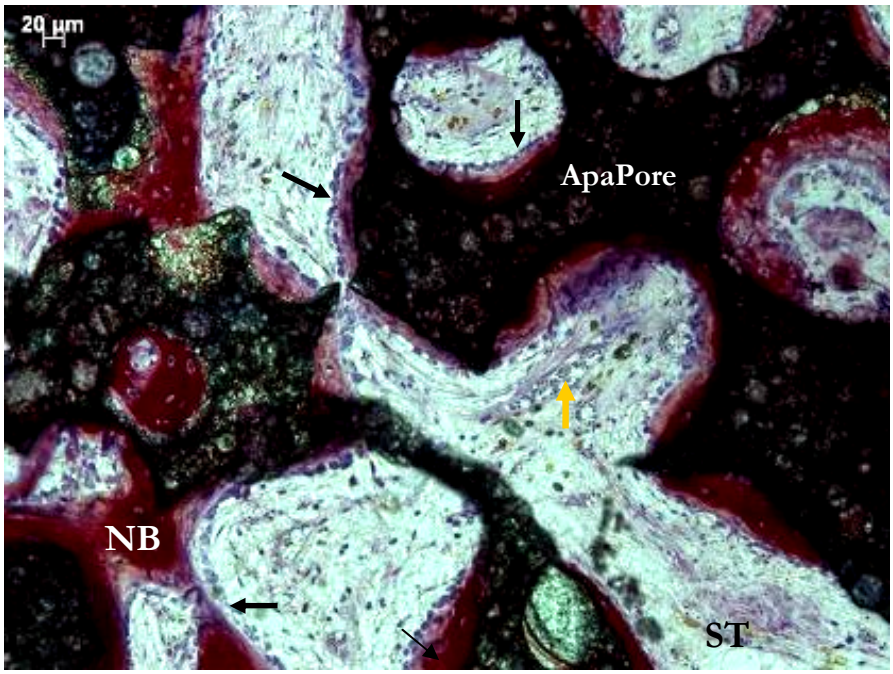

Figure 20. New bone within ApaPore at week 6. Black Arrows: osteoblast. Yellow arrow: Blood vessel, Red stain: NB: New bone, ST: Soft tissue

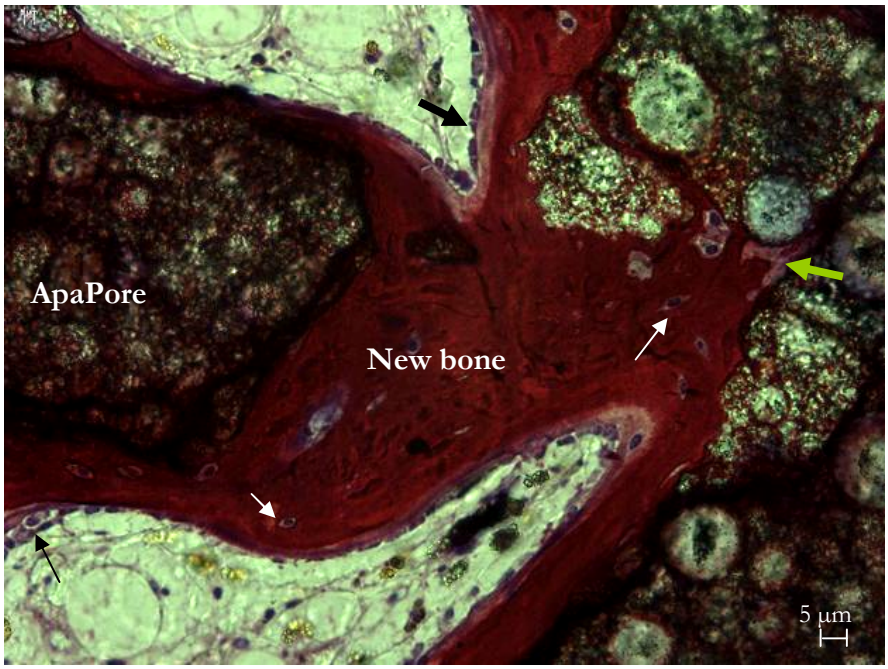

Figure 21. New bone within ApaPore at 6 weeks. Black arrows: osteoblasts, white arrows: osteocytes, Green arrow: osteoclasts and implant resorption zone.

2.6.4.4 BiIonic

Woven bone was observed within BiIonic samples by week 3 of the study (Figure 22, Figure 23). High magnification images indicated the presence of attached osteoblasts on the 1-2 mm dense BiIonic granules surface (Figure 25). Bone formation was observed initially at the periphery of the defects at week 1 and at this time no bone formation was seen within the centre of the defect. By week 6 new bone was observed within the centre of the defects deep within the BiIonic samples (Figure 25).

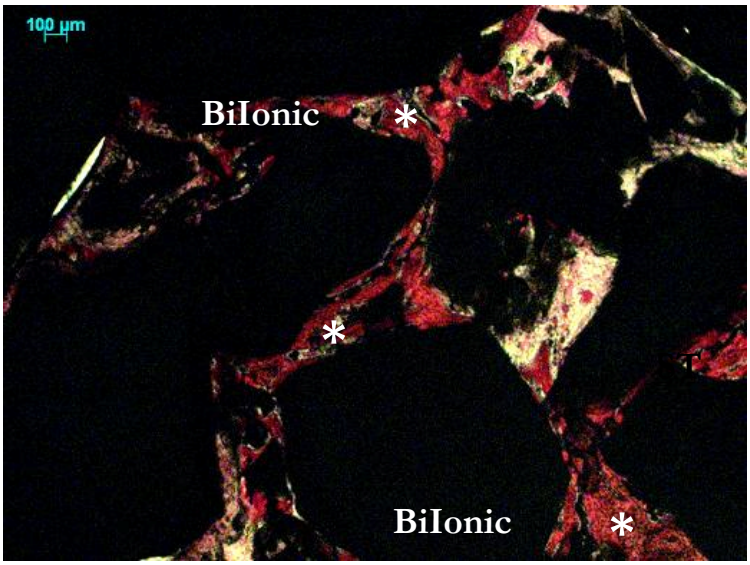

Figure 22. New bone within BiIonic sample at 6 weeks. Red stain/ *: New bone, ST: Soft Tissue

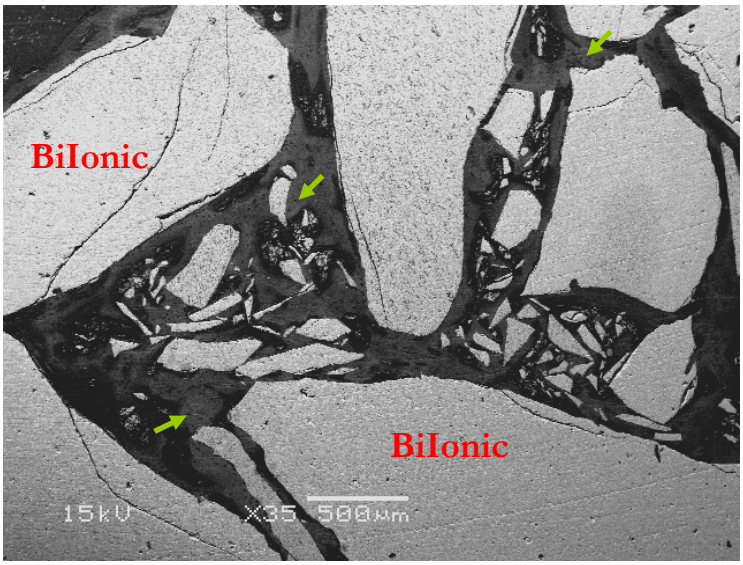

Figure 23. BSEM image indicating new bone within BiIonic. Arrows: New Bone

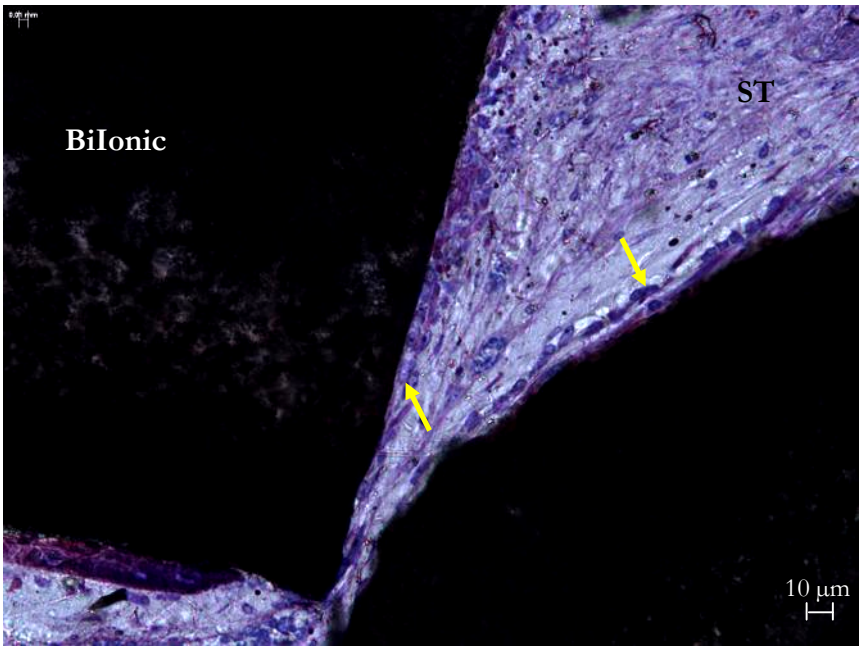

Figure 24. Osteoblast cells surrounding BiIonic particles at 3 weeks. Arrows: Osteoblasts, ST: Soft Tissue.

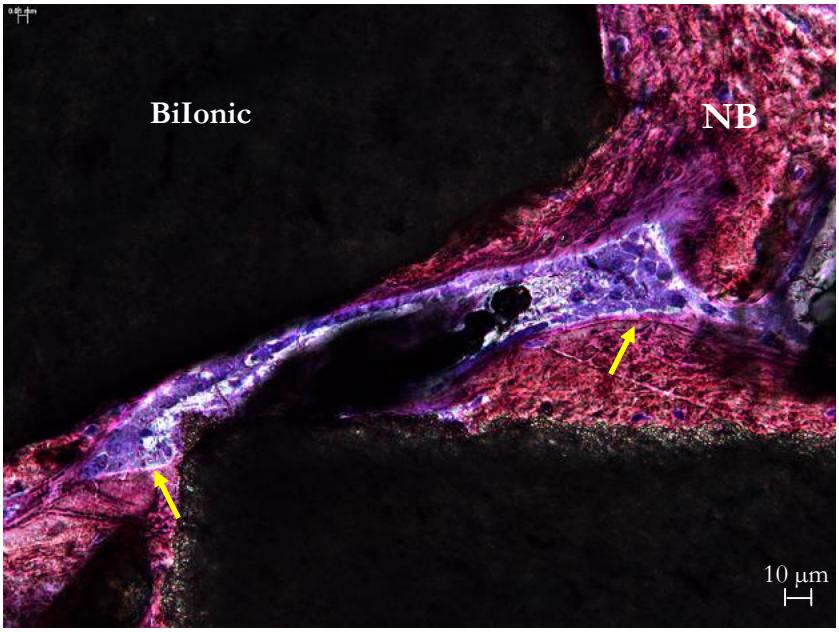

Figure 25. New bone formation within a BiIonic sample at 6 weeks. Arrows: Osteoblasts, NB: New Bone.

2.6.4.5 CPS

Bone formation was observed within all CPS samples at weeks 1, 3 and 6 (Figure 26). BSEM images indicated the presence of new bone in contact with the dense 1-2 mm CPS particles possessing sharp edged structure) and in between the biomaterial particles by week 6. CPS particles were observed to have been resorbed on the edges and the surface deforming into grooved particles (Figure 27, Figure 28). Osteoblasts and blood vessels were observed adjacent to the surface and within the samples (Figure 28, Figure 29).

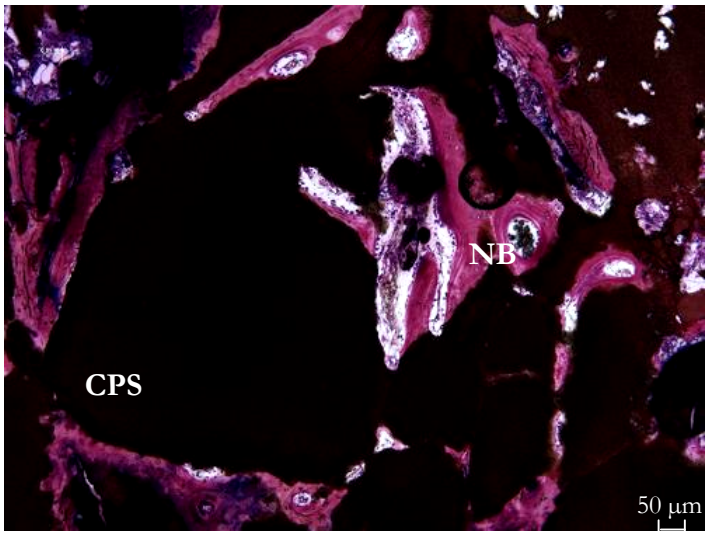

Figure 26. New bone formation within a CPS samples at week 6. Red stain indicating new bone.

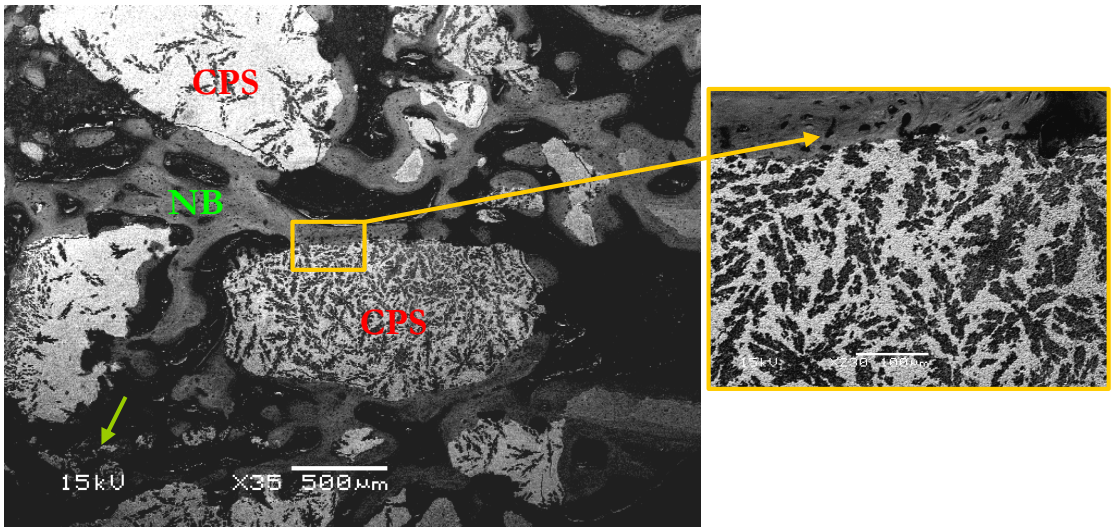

Figure 27. BSEM image indicating new bone within CPS. NB: New bone. Magnified image indicates new bone attachment to CPS. Green arrow indicates material dissolution

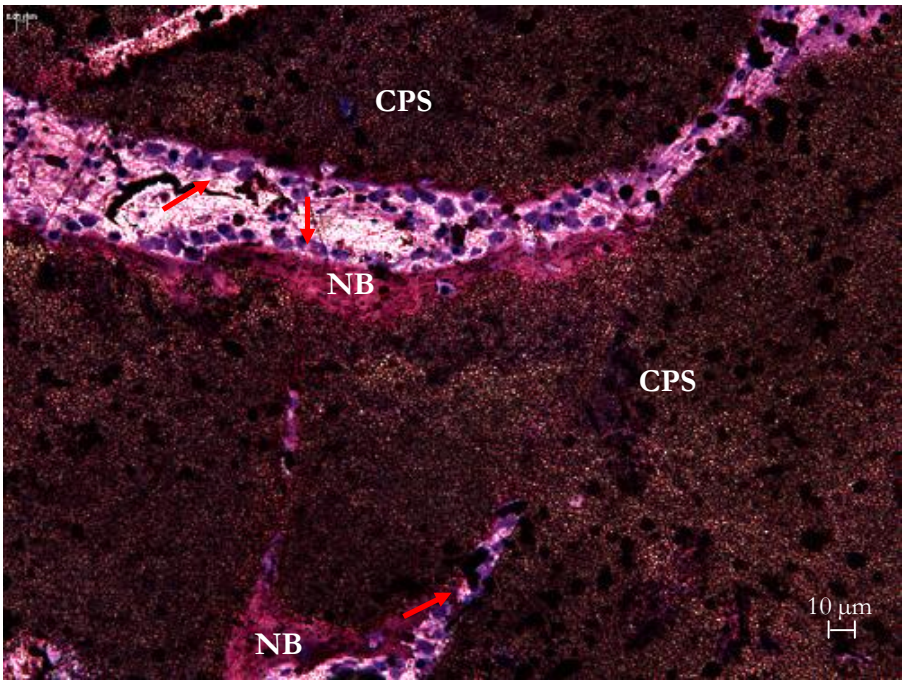

Figure 28. Presence of osteoblasts adjacent to CPS at 6 weeks. NB: New bone.

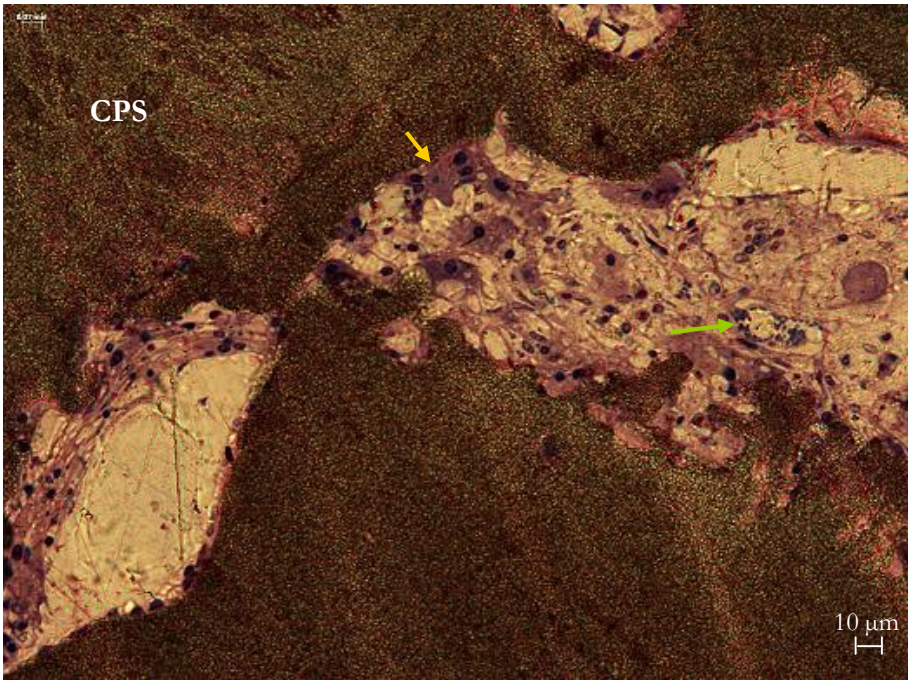

Figure 29. CPS sample at 3 weeks. Yellow arrows: Osteoclasts, Green arrows: blood vessel.

2.6.4.6 Pro Osteon 500R

Woven bone was observed on the surface of Pro Osteon 500R samples by week 6 (Figure 30). Osteoblasts were identified on the surface of the newly formed bone (Figure 31). Analysis of the high magnification images showed bone formation on the surface of the converted HA layer around the calcium carbonate core of the Pro Osteon 500R samples (Figure 31).

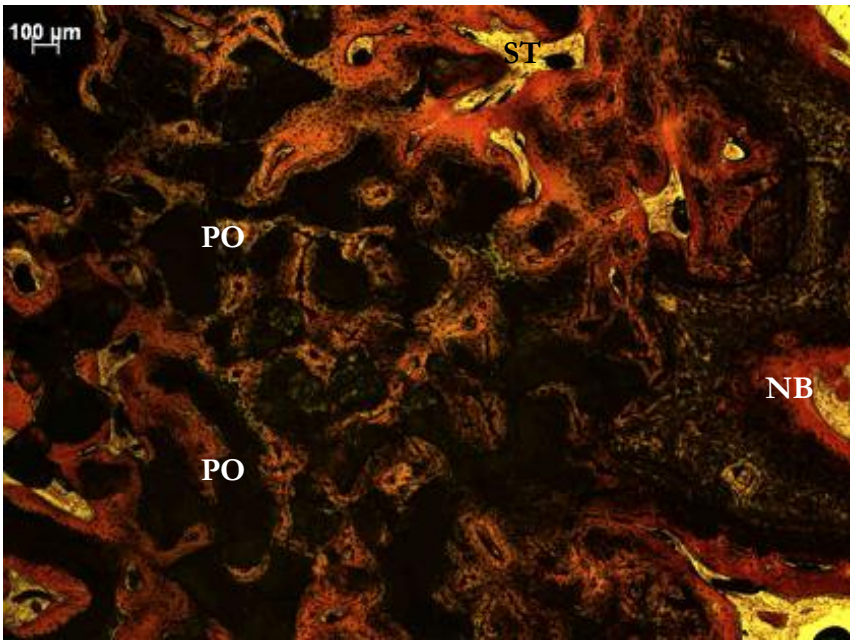

Figure 30. Pro Osteon 500R. Red stain indicating bone. NB: New Bone, ST: Soft Tissue, PO: Pro Osteon 500R

BSEM and histology images of Pro Osteon 500R (PO) samples showed woven bone within the biomaterial particles. New bone was seen to bridge Pro Osteon 500R particles together (Figure 32). Zones of biomaterial resorption were observed starting from the edges of the PO particles deep into the biomaterial particles (Figure 33). Bone formation was formed on the HA layer of the PO particles (Figure 33 and Figure 34). High magnification BSEM and EDAX analysis images showed presence of calcium phosphate precipitation nodules within the samples (Figure 34). Blood vessel formation was also visible within the samples (Figure 31).

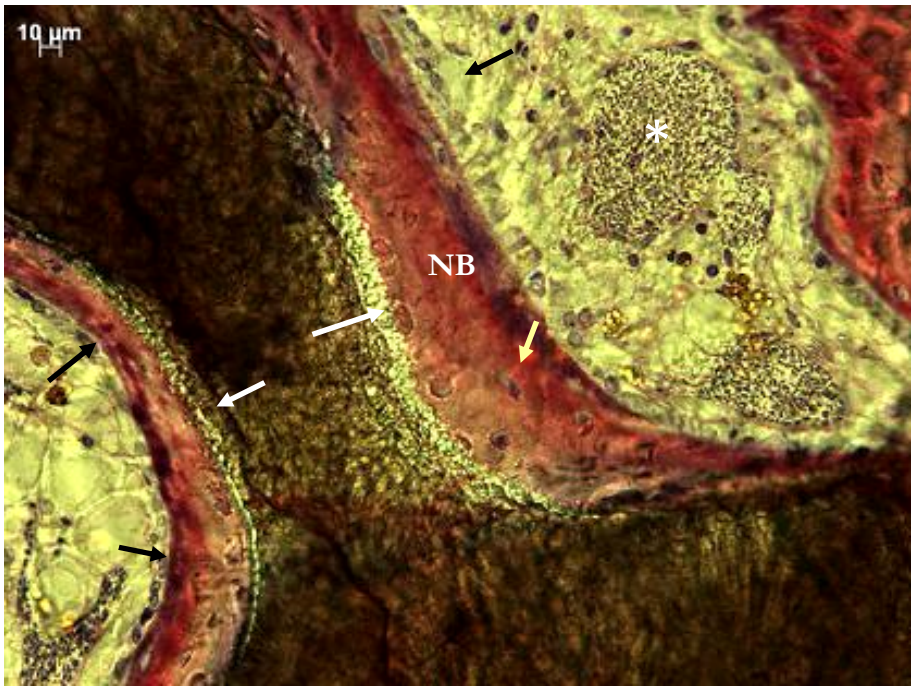

Figure 31. New bone within Pro Osteon 500R. White arrows: HA layer surrounding the PO particle, Star: blood vessels, Black arrows: Osteoblasts, Yellow arrows: Osteocytes and NB: New Bone.

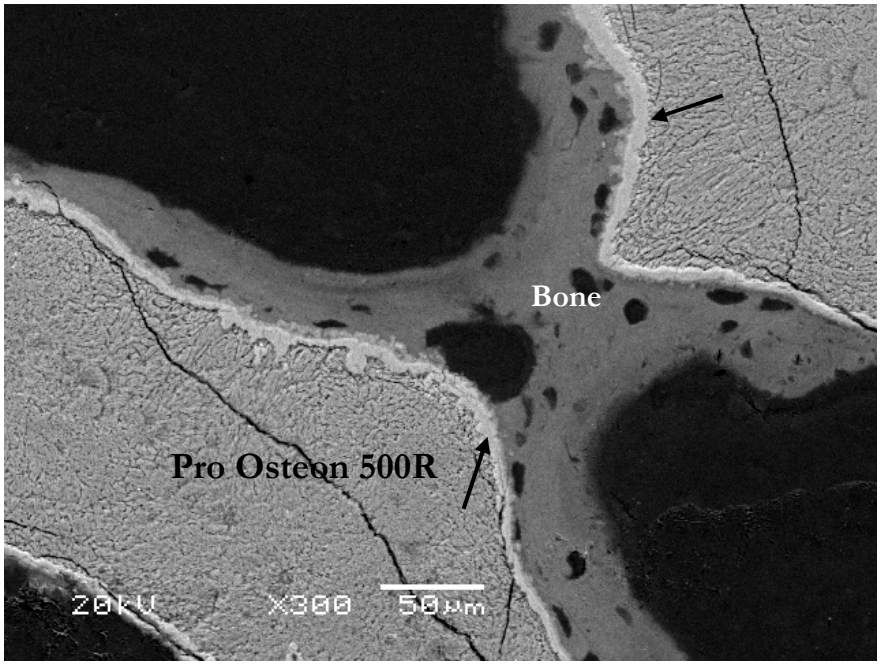

Figure 32. BSEM image indicating bone formation in between Pro Osteon 500R particles. Arrows: HA layer

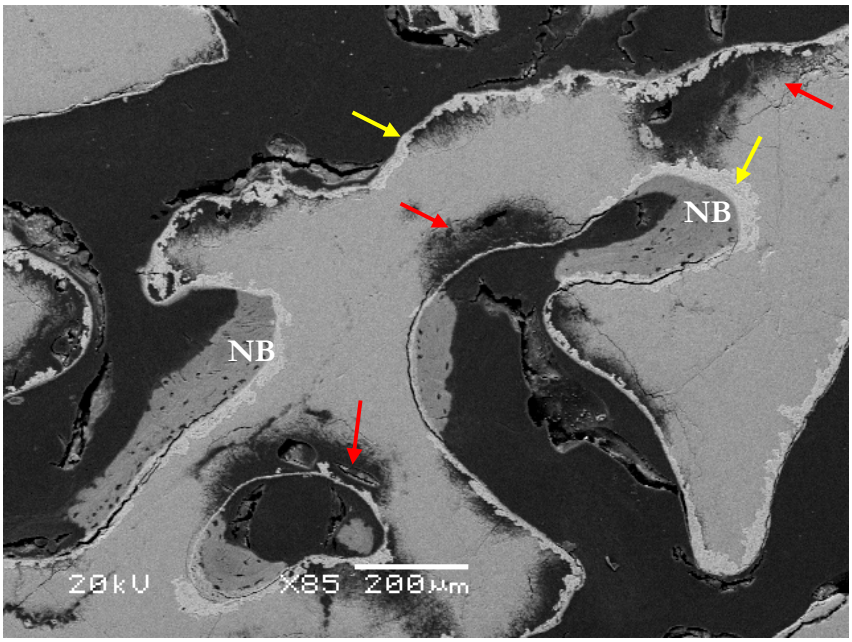

Figure 33. BSEM image indicating bone formation on Pro Osteon 500R and zones of biomaterial resorption. Yellow arrows: HA, Red arrows: resorption zone, NB: New Bone

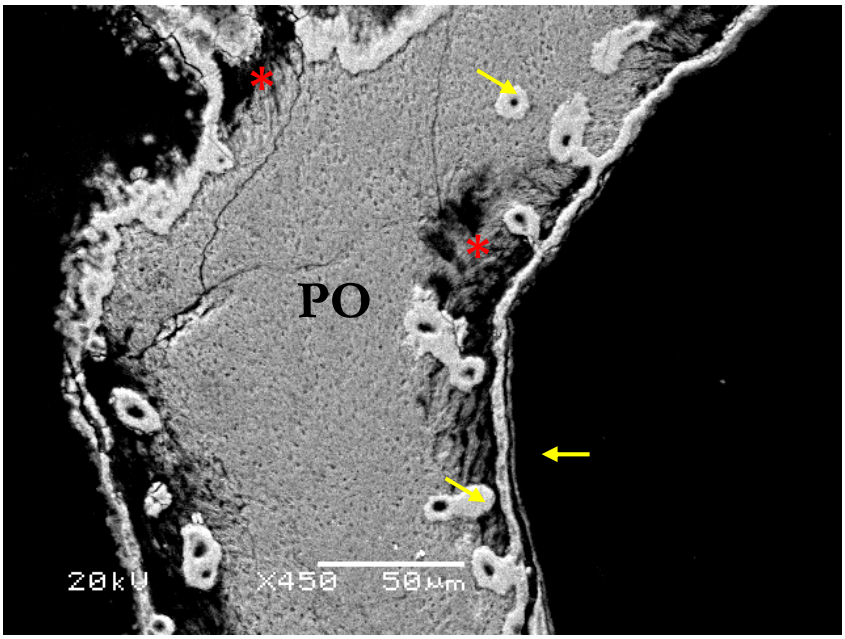

Figure 34. High magnification BSEM image. Zones of Pro Osteon 500R (PO) resorption and presence of CaP nodules. Yellow Arrows: HA, stars *: zones of resorption

EDAX analysis of the layer surrounding the Pro Osteon 500R indicated the calcium carbonate composition of the coral surrounded by the calcium phosphate rich layer of the converted HA. Analysis of elements present within the nodules also demonstrated a calcium phosphate rich composition (Figure 35).

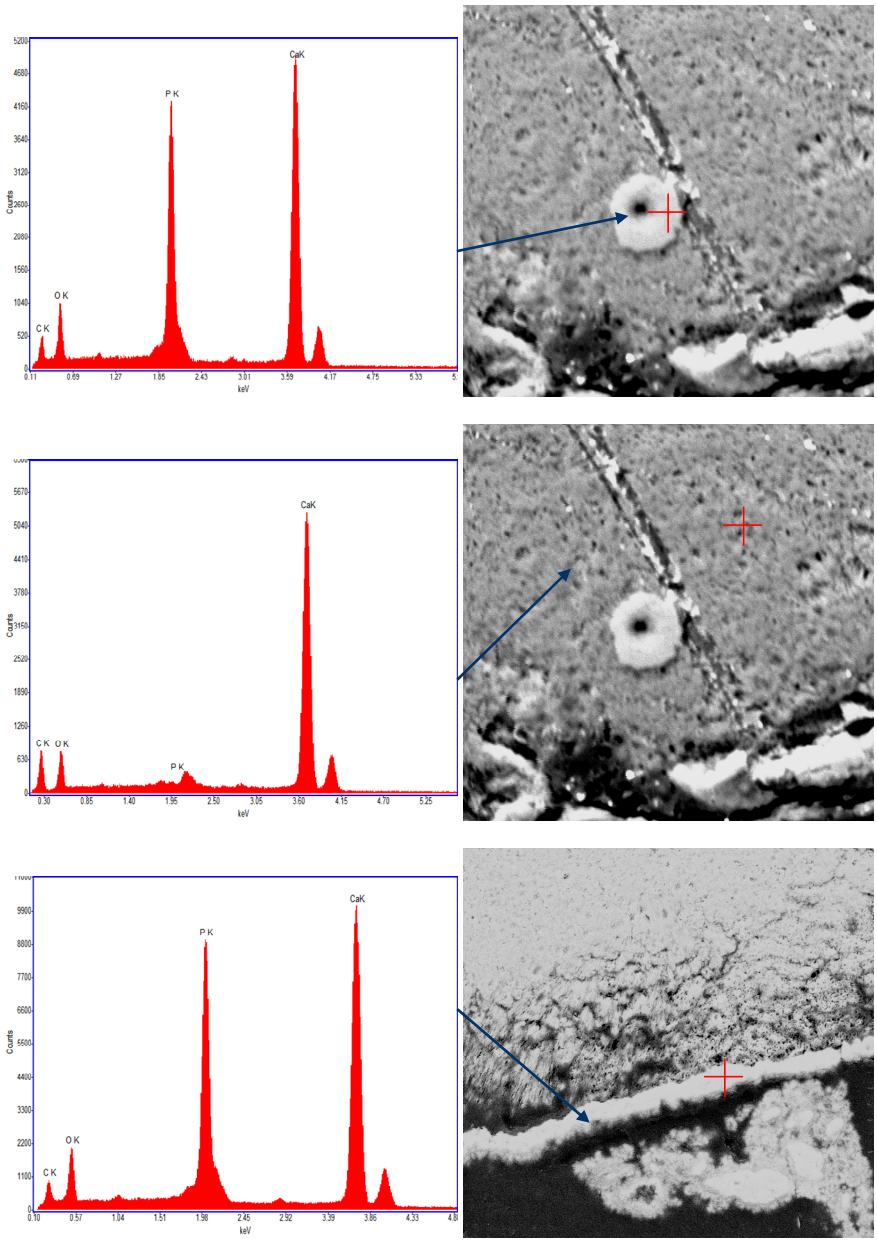

Figure 35. EDAX spectrums of elemental composition of PO samples and the surrounding HA composition

2.6.4.7 Skelite

Skelite samples demonstrated minimal amounts of new bone formation on the surface of the particles within 6 weeks (Figure 36 and Figure 37) and (Figure 38). Analysis showed red stained zones within the samples; however analysis at high magnification did not confirm the red stain as newly formed bone (Figure 38). BSEM images indicated new bone on the surface of the Skelite particles (Figure 37).

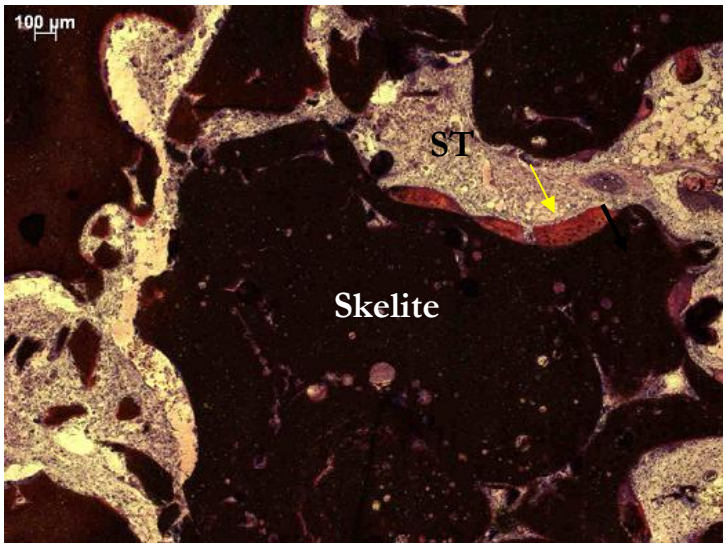

Figure 36. New bone formation on a Skelite at 6 weeks. Red stain/Arrow indicates new bone. ST: Soft tissue

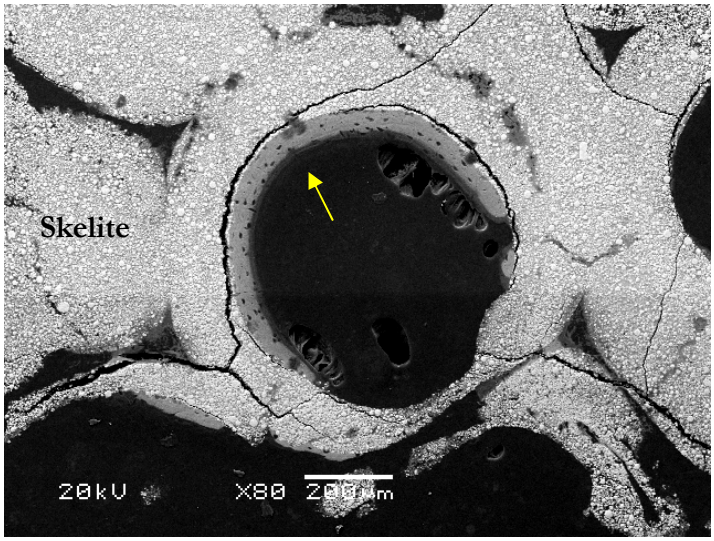

Figure 37. BSEM image indicating new bone within Skelite at 6 weeks

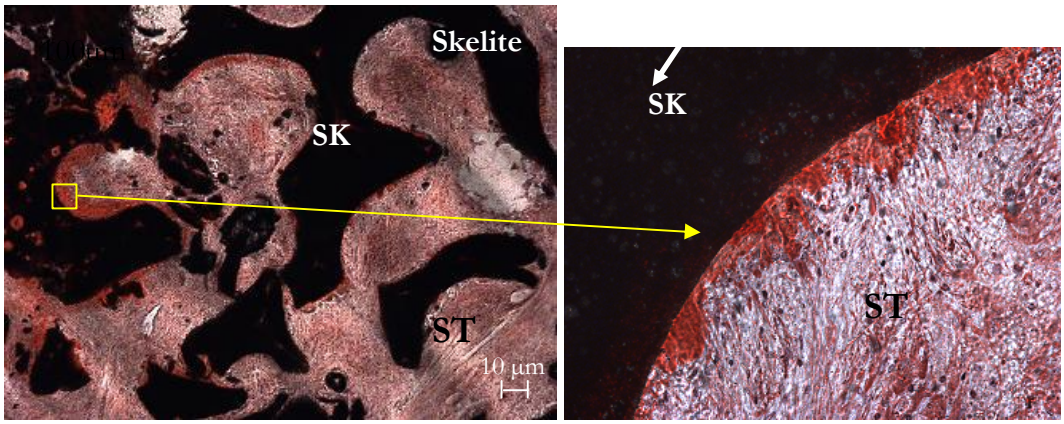

Figure 38. Skelite sample at 3 weeks. SK: Skelite; ST: Soft Tissue.

High magnification analysis of the Skelite samples showed the presence of osteoclasts and multinucleated giant cells indicating presence of active mechanisms of biomaterial resorption (Figure 39, Figure 40 and Figure 41).

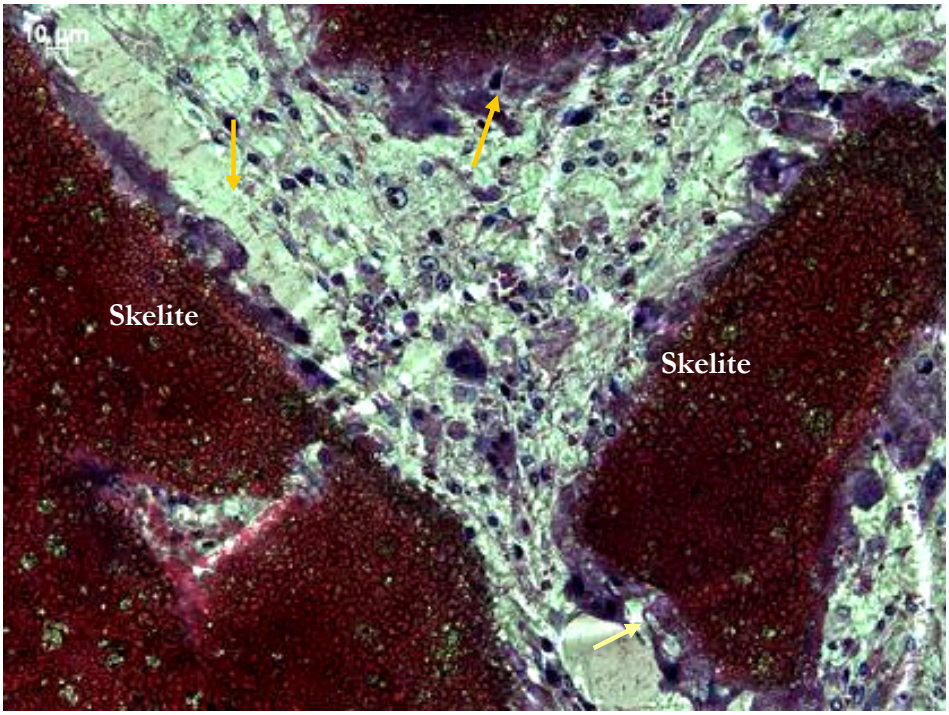

Figure 39. Skelite at 6 weeks. Arrows indicating osteoclasts and nucleated giant cells

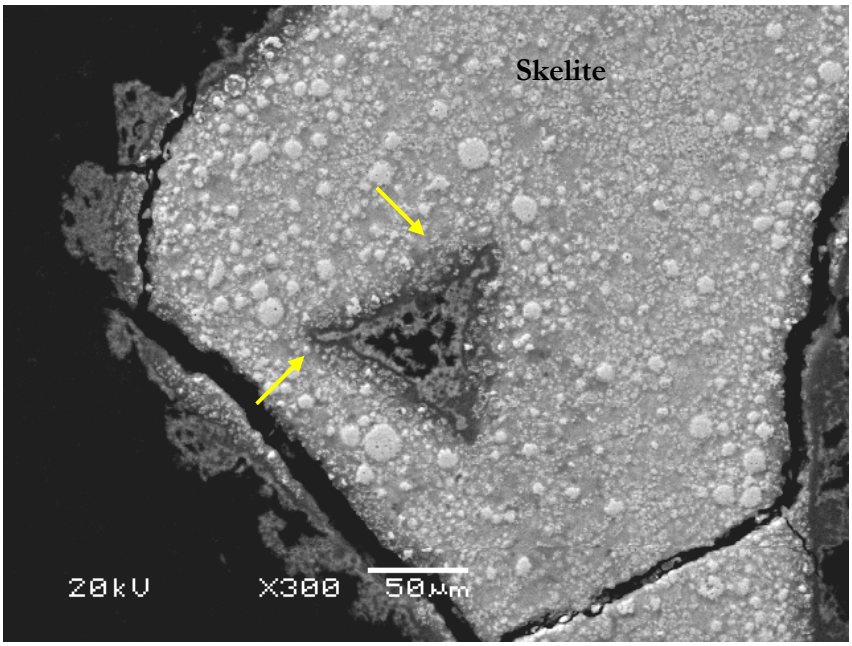

Figure 40. BSEM image. Arrows indicate implant resorption sites within Skelite

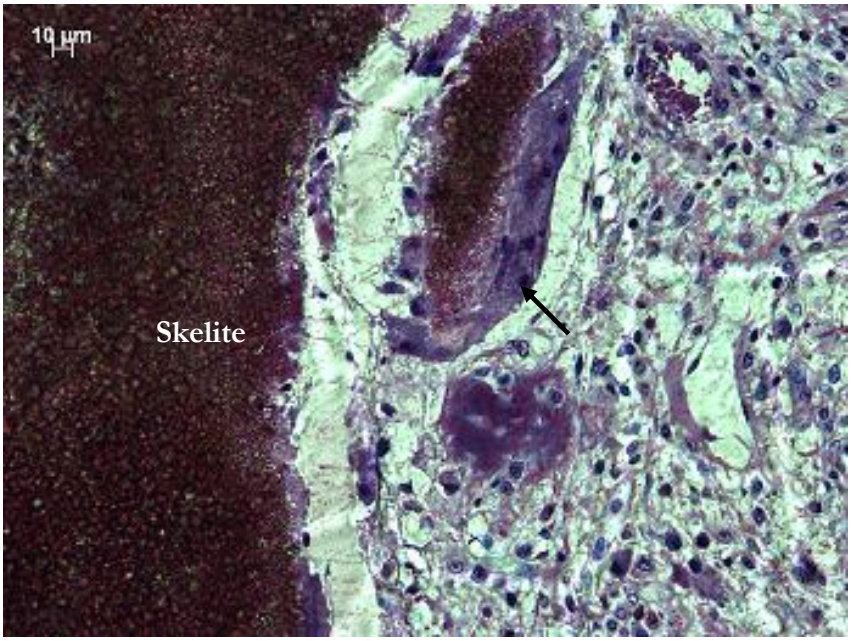

Figure 41. Skelite at 6 weeks. Arrow indicating multinucleated giant cells

2.6.4.8 Grafton DBM Crunch

Minimal bone formation was observed within Grafton crunch samples (Figure 42 and Figure 43). Osteoblasts and osteocytes were also present (Figure 45) on the biomaterial surface indicating new bone formation on the DBM particles (Figure 42 and Figure 45). Remineralisation of DBM particles and presence of multinucleated giant cells was observed adjacent to the Grafton Crunch particles (Figure 44 and Figure 45).

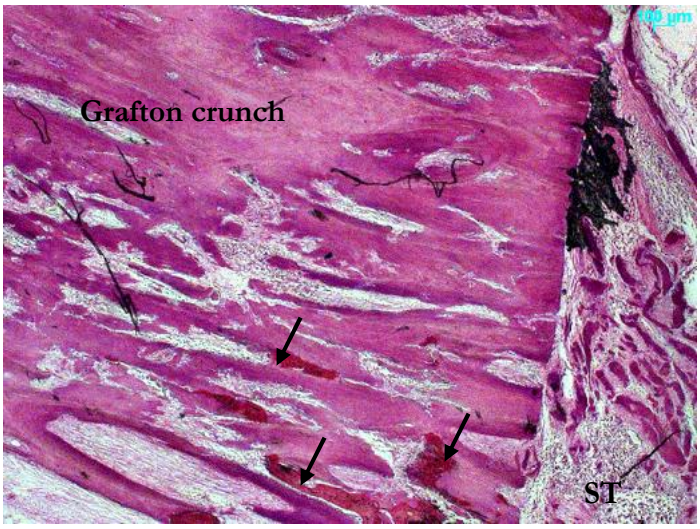

Figure 42. New bone within Grafton crunch at 6 weeks. Arrow indicating remineralised DBM
ST: soft tissue

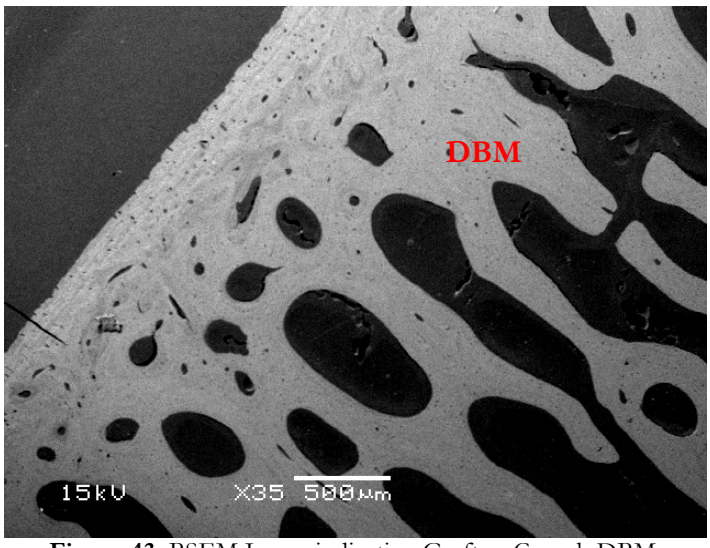

Figure 43. BSEM Image indicating Grafton Crunch DBM.

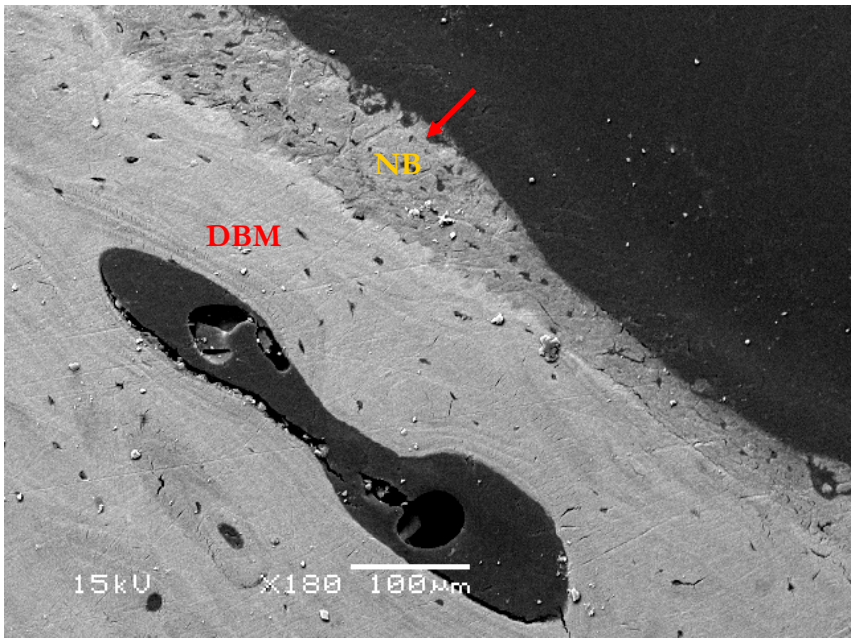

Figure 44. B). Remineralised Grafton Crunch DBM particle. Arrow: bone. NB: New bone

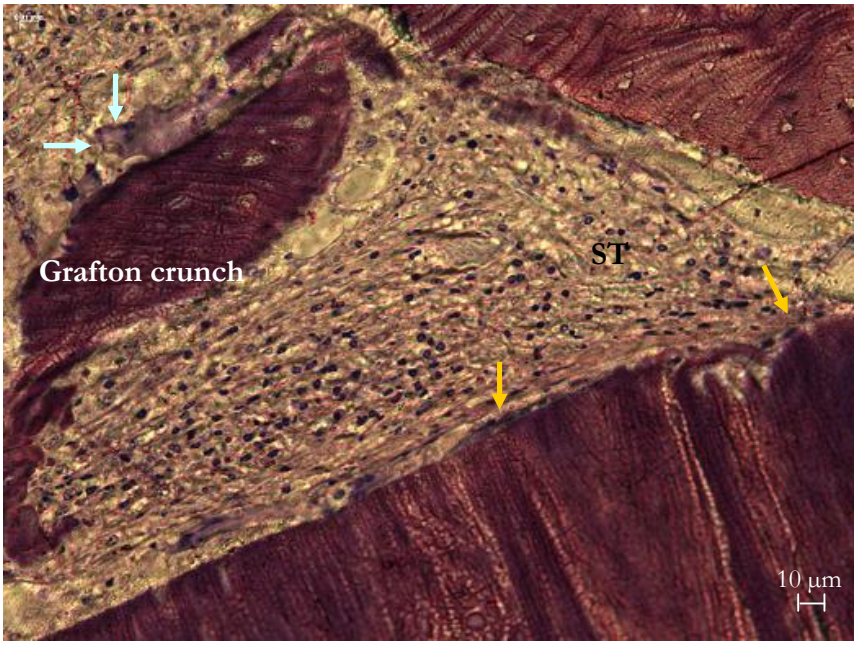

Figure 45. Grafton crunch sample. Blue arrow: multi nucleated giant cell. Yellow arrows: osteoid and osteoblasts.

2.6.4.9 Accell Connexus DBM putty

Histology analysis of the DBM samples showed the presence of minimal amounts of new bone by 6 weeks (Figure 46 and Figure 47). The presence of osteoclasts and multinucleated giant cells was observed in the vicinity of the DBM particles (Figure 48).

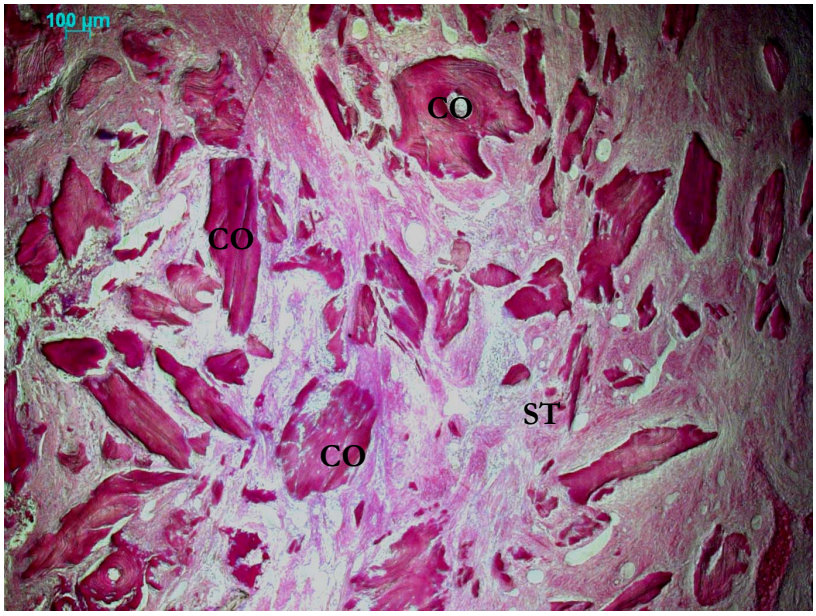

Figure 46. Accell Connexus DBM putty sample at week 6. CO: DBM putty, ST: Soft tissue

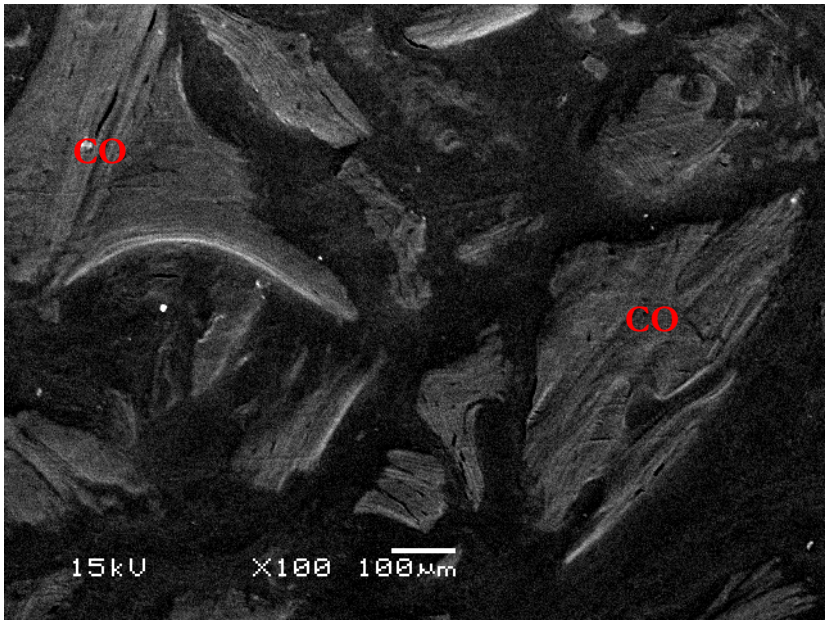

Figure 47. BSEM image of Accell Connexus DBM particles (CO).

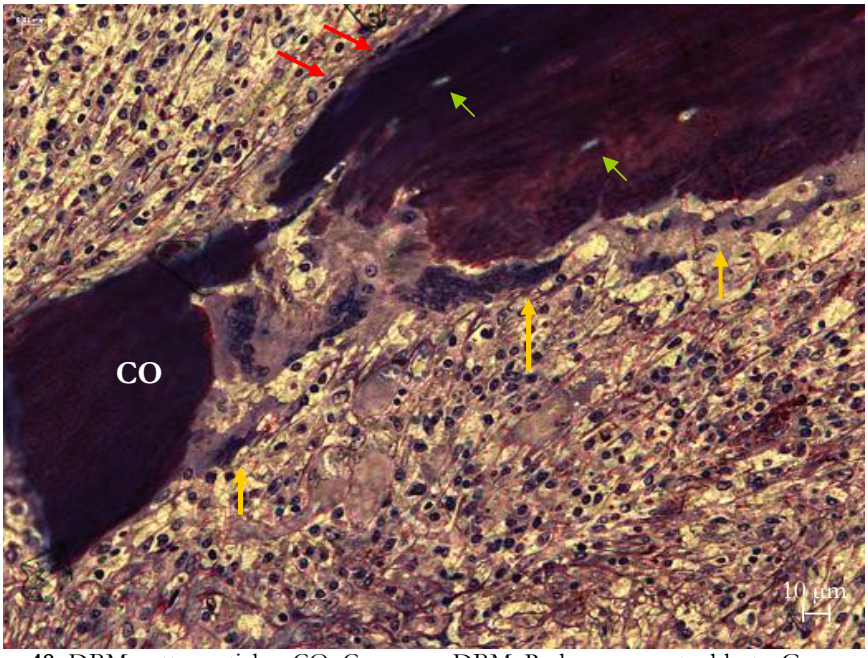

Figure 48. DBM putty particles. CO: Connexus DBM. Red arrows: osteoblasts. Green arrow: Osteocytes, Yellow arrows: osteoclast cells.

2.7 Discussion

The results of this study indicate that all the calcium phosphate bone graft materials ($p=<0.05$) investigated in this study exhibited significantly greater bone formation compared to the DBM based biomaterials. Calcium phosphate based biomaterials have been widely used as osteoconductive materials and the results of this study further confirmed the influence of these biomaterials on bone formation. CPS, BiIonic, Actifuse and ApaPore exhibited the highest amount of bone formation and Pro Osteon 500R and Skelite demonstrated the lowest amount of new bone within 6 weeks. Different mechanisms of bone formation, endochondral ossification in DBM samples and intramembranous ossification in CaP samples, were involved in the process of bone formation within the implanted biomaterials. In this study different mechanisms of bone formation through the effects of chemistry and also microporosity must have contributed to the level of bone formation by the implanted Calcium Phosphates. CPS, ApaPore, Actifuse, Pro Osteon 500R and Skelite particles were of a porous structure and bone formation was observed deep within the pores and in between the biomaterials' particles, whereas BiIonic particles comprised of a dense structure and new bone were observed in contact with the particles surface. It is known that a biomaterial's microstructure influences the rate of bone formation (Karageorgiou and Kaplan, 2005). High porosity and interconnected porous structures are important factors in promotion of biomaterial vascularisation and consequent bone formation through facilitation of cell migration and proteins, growth factors and body fluids' access into the biomaterial structure (Mastrogiocomo et al., 2006). As the results of this study indicated significantly greater bone formation ($P<0.05$) was obtained on CaP biomaterials (Actifuse and ApaPore) with porous structures in comparison with dense particles. However, it should also be noted that the superior bone formation within the porous materials could also have been due to the effect of the extra space in the pores, allowing the growth of more new bone.

Calcium phosphate biomaterials implanted in osseous tissue are known to dissolve and release calcium phosphate ions into their surrounding. The released Ca and P ions result in saturation of the body fluids and formation of a precipitated biological

apatite composed of endogenous proteins on the surface of the material (Daculsi et al., 1990; Villarreal et al., 1998). This is followed by attachment of osteogenic cells to this apatite layer and production of extracellular matrix which undergoes mineralisation by osteoblast cells and formation of woven bone within the biomaterials' pores and along the surface. This process is followed by remodelling of the woven bone by the activity of osteoclast cells (D. Le Nihouannen et al., 2005).
The results of this experiment indicated that some of the materials resorbed quickly, however the release of Ca and P ions alone did not promote enhanced bone formation by these biomaterials in comparison with Actifuse. This indicated that the role of calcium and phosphorous ions is not sufficient for promotion of faster osteoconduction by calcium phosphate biomaterials and the presence of other ions or structural variations also contribute to superior rates of bone formation.

The results of this study indicated 29% bone area and 30% contact of the new bone with ApaPore biomaterial by week 6. The area of new bone within this biomaterial was significantly enhanced from week 3 to week 6. The level of bone contact with ApaPore was observed to increase proportionally from week 1 to week 3 and then week 6. Results of the histomorphometry analysis of this biomaterial indicated no significant change in the area of the ApaPore implants by week 6. However analysis of the histology images exhibited the presence of osteoclast cells within the samples. This indicated resorption of ApaPore particles, although this resorption was not observed to be significant within the period of this study. The results of this study confirm the findings of other studies (Klein et al., 1983; Frayssinet 1993) in terms of the slow resorption rates of this biomaterial. The presence of new bone matrix deposited by osteoblasts and vascular tissue within the macro and micropores of this biomaterial indicated osteoconduction through transfer of cells, body fluids, growth factors and nutrition into this biomaterial.

Analysis of the Actifuse, silicon substituted HA, samples indicated 27% bone area deposited by osteoblasts within the biomaterial's macro and micropores by week 6. Bone formation within this biomaterial was enhanced significantly from week 3 to week 6 ($P<0.05$). New bone formation in contact with Actifuse samples was observed to increase proportionally during the time points of this study with 31%

bone contact by week 6. Presence of osteoblasts on the surface of bone matrix deposited on the surface of the biomaterial and blood vessels within the samples indicated bone formation by Actifuse through the mechanism of chemical composition and structure of this biomaterial. The area of the Actifuse particles within the implanted defects were observed to have reduced by week 6 (45% to 41%), however this reduction was not significant. Silicate ions within SiHA are known to be released from the crystalline lattice of this biomaterial *in vitro* with possible re-precipitation on the surface of the material (Guth et al., 2006). Silicon is known to affect the bioactivity of HA through transformation of the HA surface energy to a more electronegative surface, ideal for apatite formation and also increased solubility of the material by the formation of an apatite similar to the natural bone (Pietak et al., 2007). The surface chemistry of Actifuse is also known to promote greater absorption of growth factors, cell adhesion proteins and osteogenic protein to the surface of this material, enhancing the volume of newly formed bone and formation of mature lamellar bone in a shorter period of time (Hing et al., 2003). The trabecular network formed on Actifuse in known to undergo extensive remodelling, contributing to the formation of an organised and strong bonding between the host bone and the graft material (Porter et al., 2005).

Analysis of the BiIonic samples indicated ~ 29% new bone area within these particles within 6 weeks. Bone formation was observed in between the BiIonic particles. The presence of osteoblast cells depositing bone matrix on the surface of BiIonic particles was detected. Incorporation of Yttrium into the structure of SiHA is known to enhance osteoblast adhesion and consequently osteoconduction by this biomaterial (Massa et al., 2001). Although in studies by Webster et al (2002 and 2004), Sato et al (2006) and Massa et al (2005) Yttrium doped HA is shown to enhance calcium and protein adsorption and consequently adhesion and differentiation of osteoblasts *in vitro,* the results of this study did not indicate that in comparison with HA and SiHA, Yttrium-SiHA promotes any earlier bone formation *in vivo*. Although as the implant area was not significantly changed during the 6 week period of this study and no material disintegration was observed the role of Yttrium on stabilization of SiHA was evident. It should be noted that the implanted BiIonic

particles were in dense form whereas the SiHA and HA particles were porous and the effect of porosity on bone formation should not be neglected. In addition, the mentioned studies were carried out on primary human osteoblast cells and in this study ovine animal models were used and the variation in the effect of biomaterials on different cells should also not be ignored. The level of new bone contact showed a significant increase from week 1 (1.3%) to ~ 32% by week 6 as observed in ApaPore and Actifuse samples. This could be due to the effect of Yttrium promoting protein adsorption and cell attachment to the BiIonic particles (Urgun et al., 2001). The percentage of implanted particles' area did not indicate a significant change from week 1 to week 6.

CPS or the Silicocarnotite samples exhibited ~ 31% bone formation by week 6. As demonstrated in a study by Ballas et al (2002), the substitution of PO_4^{3-} by SiO_4^{4-} within the structure of CPS results in the loss of biomaterial crystallinity, increased surface area and a slight reduction in the pH. This in turn may play a role in the bioactivity of this biomaterial and the formation of the bone-like apatite on the CPS surface and consequently bone formation on the biomaterial particles. The newly formed bone within these samples was observed to show ~ 32% contact with the biomaterial particles. Bone contact with CPS particles was observed to be significantly high ($P<0.05$) by week 6 compared to week 1, However, unlike ApaPore, Actifuse and BiIonic samples, the levels of bone contact with CPS particles was observed to be slightly (~35%), but not significantly, higher at week 3. No significant difference was observed in the area of the implanted CPS particles within the defects on weeks 1 (62.1%) and 6 (62.9%), However as detected for Actifuse, ApaPore and BiIonic samples, the area of CPS particles was reduced on week 3 to ~51%, which was elucidated to be due to human error during packing of the particles at the time of implantation. Further analysis of these samples is required to understand whether the change in implant area on the third week of implantation was due to different packing densities implied by human error during the impaction process or to a biological response. However, as the amount of implanted particles were kept constant for all samples (1.2ml) at the time of implantation, the effect of packing density on this reduction should be minimal.

Further, the results of this study indicated 11% bone area within the defect containing Pro Osteon 500R. There was no difference in the level of bone formation at week 3 compared with week 6. However, the level of bone contact was observed to have reduced from week 3 to week 6, suggesting increased bone formation between the biomaterial particles. The histomorphometry results of this study indicated no significant reduction in the area of the Pro Osteon 500R biomaterials implanted within the femoral condyle defects. However, the histology images obtained for this biomaterial indicated zones of biomaterial resorption as previously shown in studies by Walsh et al., 2003 and Stubb et al., 2004, surrounded by a layer of precipitates identified as calcium phosphate. The study by Doi et al. (1993) indicated that the presence of carbonate in the apatite lattice is known to contribute to the process of resorption in bone tissue. As Pro Osteon 500R is primarily composed of calcium carbonate, the resorption zones observed within this biomaterial may be associated with the removal of calcium carbonate. Presence of osteoclasts surrounding the Pro Osteon 500R confirmed the resorbablity of this biomaterial, as claimed by the manufacturers. A study by Spence at al., 2008 on osteoconductivity of carbonated HA indicated that osteoclast cells influence the bioactivity of the biomaterials through modification of the biomaterial surface in favour of osteoblast cells response to the biomaterial surface and indirect enhancement of osteoconduction through enhanced bio-resorption. The HA converted from calcium carbonate of the coral contributed to the slow biodegradation of the biomaterial due to its low solubility. Further, the HA on the surface of the biomaterial undergoes gradual resorption, whereas fast resorption of the calcium carbonate core of the biomaterial was observed in this study and in the study by Walsh et al., 2003.

Following the 6 week period, the amount of newly formed bone on Skelite samples was observed to be lowest (~3%). The amount of bone formation in contact with the implant particles was not significantly different at weeks 1 and 6 of the study. Histological analysis of Skelite samples indicated the presence of osteoclast and multinucleated giant cells surrounding the biomaterial particles indicating resorption of the particles. Si-TCPs have been shown to reproduce the natural bone remodelling

mechanism by increased binding of osteopontin and osteoclastic proteins to its surface and by recruiting both osteoblasts and osteoclasts to the vicinity (Pietak et al., 2004; Leroux et al., 2007). A study by Mastrogiacomo et al., 2006 investigating the repair of large bone defects by implantation of Skelite, demonstrated that it promoted significant bone formation and integration within the host tissue within two years of implantation. Skelite also exhibited progressive osteoclastic resorption and complete resorption within the two year period of this study. The results of this work do not support the work by Mastrogiacomo et al., 2006 who suggested that resorption or dissolution of this biomaterial was observed with the presence of active new bone deposition. In this study, a cylindrical form of Skelite was used. At the time of implantation and impaction of the biomaterial into the defects, the porous cylinders were fragmented and lost their structural integrity. The histomorphometry results of this study indicated that Skelite particles exhibited a significant reduction ($P<0.05$) in the biomaterial area from week 1 to week 6. The results of this study further confirmed the results of the study by Leroux et al., 2007 indicating the presence of a foreign body reaction for Skelite samples *in vivo* as a result of premature rapid fragmentation of Skelite within the implanted site.

The ideal bone substitute material is expected to promote osteoblastic activity for formation of new bone, in addition to promotion of natural bone remodelling through its resorption by osteoclasts (Langstaff et al., 1999). The resorption rate of a biomaterial is known to depend on the biomaterial's composition, geometry and implantation location (Bohner and Baumgart, 2003). During the 6 week period of this study, Pro Osteon 500R and Skelite demonstrated greater resorption, however the amounts of new bone formed on these biomaterials (Pro Osteon 500R: ~11% and Skelite: ~3%) was significantly lower ($P<0.05$) than the amount of bone formed on ApaPore, Actifuse, BiIonic and CPS samples. As bone formation by these biomaterials is proposed to be the function of a couple processing between resorption and bone deposition, the results of this study suggest that this is not the case with more stable non-resorbable calcium phosphate materials, inducing much larger amounts of bone formation.

DBM biomaterials are known to induce bone formation through osteoinduction and osteoconduction mechanisms (Iian and Ladd, 2003). However, the results of this study showed that the rate of osteoconduction by the tested DBM (Grafton Crunch and Accell Connexus putty) biomaterials was not as high as calcium phosphates by 6 weeks. DBM promotes osteoconduction through apposition of new bone matrix on the DBM particles, followed by mineralisation of this matrix and also remineralisation of the DBM particles, inducing new bone apposition (Hagen et al., 1992). The presence of osteoclast cells within DBM samples indicated resorption of this biomaterial within the implanted site. Studies on resorption of this biomaterial have indicated inconsistent results as some report complete resorption of DBM particles, whereas others have not observed any sign of osteoclastic activity (Groenveld et al., 1998). The histomorphometry and histological results of this study demonstrated a significant reduction ($P<0.05$) in Accell Connexus DBM putty implant area from week 1 to week 6, however DBM Grafton Crunch samples did not resorb significantly during the period of this study. In addition to the low rate of bone formation by DBM biomaterials in comparison with Calcium phosphates, the resorption of the graft and the limited amount of bone for production of these biomaterials are restricting factors in their use (Hagen et al., 1992).

As indicated in various *in vivo* and *in vitro* studies, silicon substitution within the HA structure improves the bioactivity of this biomaterial (Gibson et al., 1999; Patel et al., 2002; Ballas et al., 2002). The histomorphometry results of this study indicated that the incorporation of silicate ion within Actifuse, CPS and BiIonic increased the formation of new bone within theses samples, irrespective of the structural properties of these biomaterials. BiIonic is a dense biomaterial and Actifuse and CPS are porous structures.

2.8 Conclusions

The results of this study indicated that calcium phosphate bone substitute materials promote greater bone formation in comparison with DBM based biomaterials. CPS exhibited the highest amounts of bone formation within the 6 week period of this study. ApaPore, BiIonic, Actifuse, and Pro Osteon 500R respectively demonstrated superior bone formation. Skelite exhibited the lowest amount of bone formation by week 6. Both DBM samples, Grafton Crunch and Accell Connexus putty samples indicated minimal amounts of bone formation by week 6. However Grafton Crunch exhibited greater bone formation in comparison with Accell Connexus putty. ApaPore showed the highest amount of new bone in contact with the biomaterial, followed by Actifuse. Bionic and CPS showed similar amounts of bone contact by week 6, but at lower percentages than bone contact with Actifuse. Percentage of bone contact with Pro Osteon 500R was reduced from week 3 to week 6 of the study. Skelite samples showed the lowest amount of bone contact in comparison with other analysed calcium phosphate based biomaterials. The percentage of bone contact with this biomaterial was similar on week 1 and week 6. The area of implanted ApaPore, Actifuse, BiIonic, CPS and Pro Osteon 500R calcium phosphate based biomaterials particles did not indicate any significant change during the 6 week period of this study. However, Skelite samples exhibited a significant ($P<0.05$) reduction in the area of Skelite particles from week 1 to 6. Grafton Crunch DBM particles did not indicate a significant area reduction, however the area of Accell Connexus putty particles exhibited a significant reduction ($P<0.05$) from week 1 to 6.

Presence of porosity within the biomaterial structure can contribute to increased bone formation. However, it is not essential as, for example, the amount of newly formed bone on dense BiIonic particles was similar to the amount of bone formed on porous ApaPore. This suggests that the chemical composition of a biomaterial has an effect on bone formation irrespective of the structural porosity due to the role of the elements present within its structure.

3 Chapter III. Cellular and Molecular Mechanism of Osteoinductivity by Silicon Substituted Hydroxyapatite

3.1 Introduction

The results of chapter II suggested that the presence of silicate ions (Si) within calcium phosphate based bone substitute materials play a role in the rate of bone formation. Trace amounts of silicon are known to enhance bone formation by increasing osteoblast activity (Keeting et al., 1992). In 1999 Gibson et al demonstrated that the bioactivities of osteoblasts *in vitro* are enhanced on silicon substituted-hydroxyapatite (SiHA). It is known that one common mechanism involved in bone formation by calcium phosphate based biomaterials is the dissolution of calcium and phosphate ions from the biomaterial (Weng et al., 1995) and the deposition of a biological apatite back onto the surface. A study by Xynos et al (2001) also indicated that release of silicate and calcium ions from bioactive glasses lead to an enhanced rate of new bone proliferation due to a process of gene activation and control of the cell cycle. A study that investigated the effect of a physiological concentration of soluble Si on human osteoblast-like cells indicated an increase in osteoblasts' differentiation, proliferation and also collagen production (Reffitt et al., 2003). Botelho et al (2006) demonstrated that 0.8wt% silicon within hydroxyapatite enhanced protein production of human osteoblast cells in addition to enhanced expression of some osteogenic marker genes. Further, human osteoblast-like cells grown on SiHA exhibit enhanced cell adhesion, spreading, extracellular matrix production and mineralisation when compared with HA (Thian et al., 2006). Therefore it is possible that Si HA may induce different gene expression when compared to pure HA.

3.2 Osteoblast Proliferation and Differentiation

Genes encoding transcription factors and osteogenic proteins are known to be involved in the control of the patterning of different skeletal elements, including the

differentiation of the three specific cell types of bone tissue (Karsenty, 1998). This study analysed the proliferation, mineralisation and mRNA expression pattern of angiogenic factor, the VEGF gene, early/late markers of osteogenesis such as Osteopontin, Osteonectin, Osteocalcin, Bone Sialoprotein and transcription factors Cbfa1/RUNX2 and Osterix in hMSCs cultured on this biomaterial in comparison with hMSCs cultured on HA and Therminox discs.

3.2.1 Transcription factors

3.2.1.1 Cbfa1/Runx2

Core binding factor A1 which is a runt (DNA binding transcription factor) related transcription factor from the RUNX family of transcription factors (Cbfa1/Runx2) is involved in transcriptional control of osteoblast differentiation and osteogenesis as its core element (Karsenty and Wagner, 2002). Cbfa1/RUNX2 is expressed in the common ancestor between the stromal cells and osteoblasts known as the osteoprogenitor cells, during the earliest phases of ossification (Otto et al., 1997). Cbfa1 is necessary for differentiation of mesenchymal progenitor cells to osteoblasts, and Cbfa1/RUNX2 is known as an essential factor for the control of bone formation by differentiated osteoblasts (Masato, 2001). Cbfa1 is known to induce expression of osteonectin, osteocalcin and bone sialoprotein osteogenic markers and these genes are known to exhibit Cbfa1 binding sites in their promoters (Ducy et al., 1997; Komori and Kishimoto, 1998). This transcription factor is known to control the expression of other genes encoding osteoblast specific transcription factors such as Osterix (Karsenty and Wagner, 2002). Early stage osteoblast differentiation is known to be positively regulated by Cbfa1 with negative regulation at later stages of osteoblast development (Igarashi et al., 2004).

3.2.1.2 Osterix

Osterix (Osx)/SP7 is an osteoblast specific transcription factor essential for positive regulation of osteoblast differentiation and bone formation (Nakashima et al., 2002; Zhang et al., 2008). Osx deficiency is known to eliminate intramembranous and

endochondral bone formation. Inactivation of the gene encoding for Osx in growing bones is known to delay osteoblast maturation and result in an accumulation of immature osteoblasts and the reduction of osteoblast function in bone formation (Cao et al., 2005; Baek et al., 2008). Osterix is proposed to be involved in the control of osteoblast differentiation by regulating gene expression which is not controlled by Runx2 (Matsubara et al., 2008). Recent studies investigating the function of this transcription factor have demonstrated that Osx induces the expression of osteogenic genes; however, it is not enough for terminal osteogenic differentiation (Yeon-Ju et al., 2006; Kurata et al., 2007).

3.2.2 Osteoblastic marker proteins

As well as gene expression, particularly the expression of transcription factors, protein production by cells is a key function of terminal differentiation and is used to investigate the effect of biomaterials on the differentiation of cells. Osteoblastic differentiation is marked by the production of specific proteins associated with mineralisation and bone formation. The following proteins will be used in this study to investigate the effects of SiHA on osteoblast differentiation.

3.2.2.1 Osteopontin

Osteopontin (OPN), also known as secreted phosphoprotein-1 (SPP1), is an extracellular matrix cell adhesion multifunctional phosphorylated acidic glycoprotein identified by Oldberg et al in 1986. It is expressed in many mineralized and soft tissues including bone, dentin, elastin, muscle, tumours and also in body fluids such as milk, the inner ear and urine (Brown et al., 1992; Gericke et al., 2005). Osteopontin is produced during the early developmental stage by pre-osteoblasts, osteoblasts and also osteoclastic cells and is secreted into osteoid and then integrated within bone (Butler, 1989). This protein is known to be localized in the mineralized phase of bone matrix in endochondral and intramembranous bone (Young et al., 1992). Osteopontin is abundant in the bone matrix and forms strong bonds with hydroxyapatite (Young et al., 1992; Asou et al., 2001). Boskey et al (1994) proposed

that osteopontin stops the growth of hydroxyapatite surfaces at the end of active bone formation. This protein is known to inhibit mineral formation and growth of mineral crystals and proliferation (Hunter et al., 1994; Boskey et al., 2001). Osteopontin is known to be important in the differentiation and recruitment of osteoclast cells (Gericke et al., 2005). It has been suggested that osteopontin contributes to bone resorption by facilitating the attachment of osteoclasts to the extracellular matrix (Fisher et al., 1990; Asou et al., 2001). Remodelling of mature bone depends critically on the presence of osteopontin (Denhardt et al, 2001). An *in vivo* study by Asou et al (2001) demonstrated that the absence of osteopontin impaired angiogenesis, osteoclast accumulation and consequent bone resorption.

3.2.2.2 Osteonectin

Osteonectin/SPARC (secreted protein acidic and rich in cysteine) is a major non-collagenous glycoprotein of the bone matrix with calcium ion binding sites. This protein is involved in tissue remodelling, cellular response to injury and tumour formation (Termine et al., 1981; Turk et al., 2005). Osteonectin is found to be abundant in bone tissue and non-skeletal tissues such as the kidneys' renal tube and the salivary epithelium. Osteonectin is found in osteoblast precursor cells, osteoblasts, newly formed osteocytes and the mineralizing chondroid of the developing bone (Young et al., 1992). This protein is known to be involved in the control of osteoblast and osteoclast cells' proliferation, cell spreading, cell interactions with the extracellular matrix (Tremble et al., 1993; Delany et al., 2000) and also detachment of the cells from the extracellular matrix (Sage et al., 1989), in addition to the modulation of angiogenesis (Turk et al., 2005). Osteonectin is also known to exhibit an affinity with collagen I and hydroxyapatite for the control of mineralization nucleation in bone tissue (Price et al., 1976; Termine et al., 1981; Young et al., 1992).

3.2.2.3 Bone Sialoprotein

Bone sialoprotein (BSP) is a bone extracellular matrix glycoprotein with cell attachment and bio-mineralization functions (Hunter and Goldberg, 1994, Harris et al., 2000). This protein is known to make up 8-12% of the non-collagenous proteins of the bone. Malaval et al (2008) demonstrated that BSP deficiency impairs bone growth and mineralization. Bone sialoprotein is localized in the extrafibrillar mineral of woven bone, dentin, cementum and hypertrophic cartilage (Ganss, 1999). This protein is expressed by mature osteoblast cells localized in active osteogenic cells and sites of *de novo* bone formation and mineral deposition (Harris et al., 2000). This protein exhibits affinity sites for type I collagen and calcium ions and is also known to initiate hydroxyapatite crystal formation in the bone matrix (Young et al., 1992; Ganss, 1999). Hydroxyapatite nucleation, binding and mediation of cell attachment to mineralised tissues, combined with a direct role in mineralisation, are the known functions of bone sialoprotein. Further, this protein is a valuable marker of osteogenic differentiation and specifically terminally differentiated osteoblasts (Ganss et al., 1999; Benson et al., 2000).

3.2.2.4 Osteocalcin

Osteocalcin/ BGP (bone gla/gamma-carboxyglutamate protein) is the most abundant non-collagenous protein expressed specifically in growing bone tissue and is involved in the modulation of bone mineralization and bone turnover (Young et al., 1992). Osteocalcin is expressed late in the process of osteoblast maturation and at the onset of extracellular matrix mineralisation (Bronner and Farach-Carson, 2003). This protein exhibits binding affinity for hydroxyapatite and calcium ions involved in the initiation of tissue mineralization (Hauschka et al., 1975). In addition to its binding properties, osteocalcin is involved in cell signalling and in the recruitment of osteoblasts and osteoclast cells (Hoang et al., 2003). Osteocalcin has been identified as the negative regulator of bone formation through limitation of bone matrix formation and inhibition of calcification and studies have demonstrated that osteocalcin deficient mutant mice exhibited excessive bone matrix deposition by osteoblasts (Wolf, 1996; Ducy et al., 1996 and Luo et al., 1997).

3.2.2.5 Alkaline phosphatase

Alkaline phosphatase is a de-phosphorylation enzyme found in all body tissues, with a tissue specific structure responsible for splitting inorganic phosphates from organic phosphate esters. This enzyme is known to be localised on the surface of osteoblast cells and secreted by these cells into the calcifying matrix, creating an alkaline environment for new bone formation. The presence of this enzyme was first reported in 1923 by Robinson through his study of the biochemical mechanism of bone calcification (Siffert, 1951). Alkaline phosphatase activity is observed at an early stage of osteoblast differentiation with an increase during osteoblast maturation up to the mineralisation phase (Stein et al., 1990). ALP isoenzyme has been proposed to play a role in bone mineralization and deactivation of this gene results in poor mineralisation of cartilage and bone (Hessle et al., 2002).

Bone formation by calcium phosphate biomaterials involves a complex set of cellular and molecular activities, including expression of osteogenic genes and protein synthesis influenced by the chemical composition of the biomaterial. Given the significant role of silicate ion in bone formation and the evident effect of the substitution of this ion into the structure of calcium phosphate biomaterials on the rate of bone formation, study of the influence of this ion on cellular and molecular mechanisms of cell differentiation and proliferation would be an important step in understanding the mechanism of bone formation by silicon substitution.

3.3 Aims and Hypothesis

The aim of this part of this study was to investigate the effect of silicon substituted hydroxyapatite (SiHA) on the osteogenic differentiation of human marrow stromal cells and the osteoinductivity of this biomaterial *in vitro* in comparison with pure hydroxyapatite. The focus of this study was the analysis and comparison of mRNA expression of the VEGF gene, early/late markers of osteogenesis, the osteopontin, osteonectin, osteocalcin, bone sialoprotein genes, in addition to the transcription factors Cbfa1/RUNX2 and Osterix in hMSC grown on SiHA with plain HA.

Hypothesis:

The hypotheses for this part of this study are that:

1. Silicon substituted HA (SiHA) demonstrates *in vitro* osteoinduction through osteoblastic differentiation of hMSCs

2. Compared with HA, SiHA enhances osteogenic differentiation through stimulation of the expression of specific osteogenic marker genes

3. SiHA promotes osteogenesis via enhancement of the bioactivity of hMSCs through its chemical composition irrespective of the influence of osteogenic supplements or surface morphology

3.4 Materials and Methods

In this study human marrow stromal cells were grown on dense SiHA, HA and Therminox cover slip discs for periods of up to 24 days. Cell morphology analysis was carried out using SEM analysis on days 1, 7, 14 and 24. DNA and protein assays on days 3, 12 and 24 were performed to study the bioactivity of these cells on these materials. Further, RNA extraction and RT-PCR analysis was performed to analyse the expression levels of RUNX2, Osterix, Osteopontin, Osteonectin, Osteocalcin, Bone sialoprotein and VEGF genes on days 1, 3, 6, 12 and 24 of the study within hMSCs grown on the discs in normal and osteogenic growth conditions.

3.4.1 Disc production

Hydroxyapatite (Batch no. A00P0B06500) and Silicon-substituted hydroxyapatite (Batch no. B276-2005) powder was provided by ApaTech Ltd. 1 gram of the powder was pressed at 155 Nm^{-2} force using a mechanically operated press machine and metallic dyes specially designed for making dense discs of 11 x 3 mm (Figure 49). The SiHA and HA discs were then sintered in a furnace at 1300°C and 1250°C respectively. The temperature of the sintering furnace was set to increase at a rate of 5°C/min up to the set plateau temperature followed by 2 hours of standstill. The temperature was then reduced down to 26°C at the rate of 10°C/min. the sintered discs were then heat sterilised at 160°C for 1 hour in a dry oven.

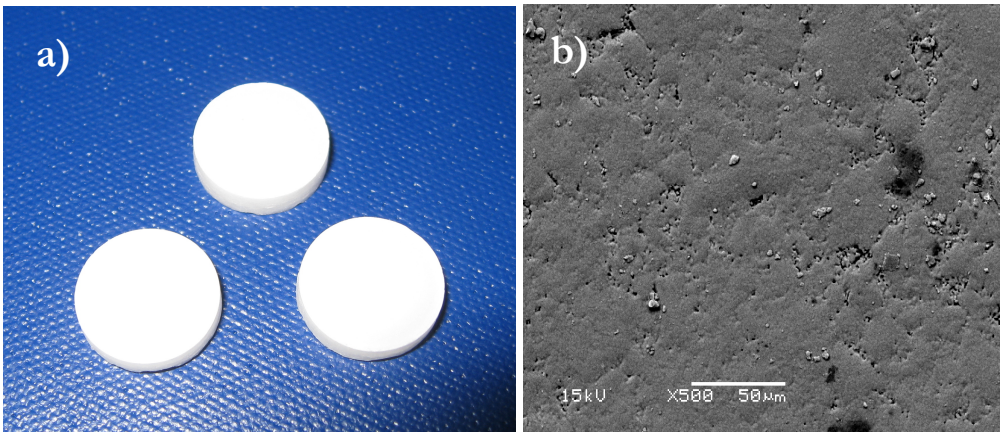

Figure 49. a) Discs of SiHA/HA. b) SEM image of SiHA surface

3.4.2 Human Marrow Stromal Cells (hMSCs) culture

Frozen Human marrow stromal cells of passage 0 suspensions (kindly provided by Dr Michelle Korda, IOMS, UCL) were expanded in culture to obtain the required number of cells. The cryo-preserved cells were initially thawed in a 37°C water bath. The cells were gradually reactivated by the addition of 1:1 increasing concentrations of standard culture medium [Dulbecco's modified eagles medium (DMEM, D6249 Sigma ®), supplemented with 10% fetal calf serum (FCS, First Link, UK) and 100 units/ml penicillin/streptomycin (P/S, 0082, Invitrogen, Paisley, UK)] and centrifugation at 2000 rpm for 5 minutes up to three times. The cell suspension was then centrifuged for 5 minutes at 2000 rpm to obtain the cell pellet. The cell pellet was then separated from the supernatant and re-suspended in 1 ml DMEM using a 19 gauge needle and 1 ml syringe. Following this, the cell suspension was transferred to T25 polystyrene cell culture flasks (Corning® cell culture flask, Sigma Aldrich) containing 4 ml of standard DMEM media, followed by incubation in a humidified incubator with 5% CO_2 supplied at 37°C. Following 7-14 days of incubation and once the cells had covered 70% of the cell culture flask surface, the cells were expanded/passaged to obtain the required number of cells for this study.

In order to expand the number of cells grown in the initial culture flask, the DMEM media was first removed and discarded. The cells were then washed with cold phosphate buffered saline (PBS, P5493, Sigma-Aldrich). The washed cells were then detached from the culture flask by using a 1% Trypsin solution diluted with PBS (0.5% trypsin with EDTA 4Na, Invitrogen. 15400054, UK) solution stock at 37°C for 5 minutes. Following this time and the detachment of the cells, the trypsin solution was neutralised by the addition of a 1:1 concentration of DMEM media. The suspended cells were then centrifuged for 5 min at 2000 rpm and the supernatant was removed. The cell pellet was then re-suspended in 1 ml DMEM media, and a cell viability test was then carried out by using a 1:1 ratio of the suspended cells to 0.4% Trypan Blue solution (T8154, Sigma-Aldrich, UK). The concentration of the cells was then quantified using a Haematocytometer viewed using a phase-contrast light microscope. Trypan Blue stained cells were identified as

dead and the unstained cells were counted as live cells. The cell suspension was then centrifuged for 5 minutes at 2000 rpm and the obtained cell pellet was re-suspended in 1 ml fresh DMEM using a 19 gauge needle and syringe. Cell suspension was then divided into two or three according to the number of counted cells and 4-5,000 cells/cm^2 were seeded in new culture flasks containing DMEM media. Cells were washed and the media was changed every 2-3 days and further passaging (up to passage 3-4) of the cultured cells was carried out upon reaching 70-80% confluency.

3.4.2.1 Characterisation of the Marrow Stromal Cells (MSCs)

The morphology of the human marrow stromal Cells (hMSCs) used in the experiment was monitored under light microscopy at regular intervals during the 24 day course of the study. In order to test the pluripotent characteristic of the MSCs, cells were differentiated along the adipogenic and osteogenic lineages.

3.4.2.1.1 Osteogenic Differentiation

Osteogenic differentiation of the MSCs was carried out in osteogenic supplemented medium. This medium was prepared by the addition of the following osteogenic supplements to DMEM (500 mg/L glucose; 110mg sodium pyruvate/L: L-glutamine; sterile filtered and endotoxin tested, D6249, Sigma®) media.

- 10% Fetal Calf Serum (FCS; First Link, UK)
- 1.0% Penicillin/Streptomycin (P/S, 15070063, Gibes ®; Invitrogen ^{TM})
- x 10^{-7} M Dexamethasone, water soluble (D2915, Sigma®)
- 5.0 x 10^{-4} M Ascorbic Acid
- 0.02 M ß-glycerophosphate, disodium salt, pentahydrate (B69629, Calbiochem)

To make the osteogenic medium, the FCS and P/S were added to the DMEM medium and the differentiation supplements dissolved in 10 ml of DMEM, followed

by sterilisation using a 0.2 μm filter and sterile 10 ml syringe and then added to the prepared DMEM medium. The prepared medium was then added to 50,000 cells seeded in duplicate in 6 well cell culture plates (M8562, Sigma®). A second group of cells were also seeded in culture plates as the experiment control; however for these cells, non-osteogenic supplemented medium/standard DMEM medium was used. The cultured cells were then incubated in 5% CO_2 at 37°C for 24 days. Following this time period, the cells were washed with PBS and fixed using 80% ethanol for 10 minutes before Von Kossa staining for the detection of calcification and mineralisation. Von Kossa staining was carried out by the addition of 2% silver nitrite solution (S2252, Sigma®) to the cells. This was followed by exposure to a bright light for one hour, two washes with distilled water and 5 minutes treatment with 2.5% Sodium Thiosulphate (S7026, Sigma®). The cells were then washed with distilled water and counter stained with 1% Neutral Red (N4638, Sigma®). Stained cell nuclei were then observed under an Olympus BH2 photographic light microscope and the presence of calcium deposition confirmed the osteogenic differentiation of the cells.

3.4.2.1.2 Adipogenic differentiation

Adipogenic differentiation of the MSCs was carried out by culturing 50, 000 cells in adipogenic medium. Preparation of the adipogenic medium was carried out by supplementation of DMEM medium (D6249, Sigma®) with the supplementary factors listed below:

- 20 ml 200 mM L-Glutamin
- 3500 md-glucose
- 10% FCS (First Link, UK)
- 1.0% Penicillin/Streptomycin (P/S, 15070063, Gibes ®; Invitrogen ™)
- 1.0 x 10^{-6} Dexamethasone, water soluble (D2915, Sigma®)
- 200 μM Indomethacin 99% TLC (I7378-5G, Sigma®)
- 500 μM 1-Methyl-3-Isobutylxanthine 99% (IBMX) (I5879, Sigma®)
- 10 μg/ml Insulin from bovine pancreas (I0516-5ML, Sigma®)

The prepared adipogenic medium was added to the cells seeded in 6 well cell culture plates. A control group of cells was also cultured in normal/non-adipogenic supplemented DMEM medium. Samples were incubated at 37°C for a period of 21 days, following which the medium was aspirated from the wells, the cells were washed with PBS and then fixed with 10% formal saline (formaldehyde (11-0705, Sigma) and NaCl solution) for 5 minutes for identification of intracellular lipid within the adipogenic differentiated cells by Oil-Red-O staining. Staining was carried out by rinsing the fixed cells with distilled water, followed by soaking in oil red O stain (O0625, Sigma) for 20 minutes. The cells were then rinsed with distilled water and counterstained with hematoxylin (H3136, Sigma) for 3 minutes. Cells were rinsed with distilled water and then air dried. The red stained lipid molecules and the blue nuclei within the cells were observed under light microscopy.

3.4.3 Cell seeding on discs

To assess the effect of SiHA on the proliferation and differentiation of human marrow stromal cells (hMSCs), three repeats (n=3) of dense SiHA and HA discs were seeded with passage 3 (P3) hMSCs and compared with hMSCs seeded on Therminox discs (Agar scientific, L4350). Osteoblastic differentiation was investigated by observing the morphological changes, osteoblastic marker proteins and osteogenic marker gene expression on SiHA, HA and Therminox coverslips. The prepared sterile SiHA and HA discs were placed in the wells of a 12 well cell culture plate. 50,000 hMSCs suspended in DMEM medium were then dispensed onto the surface of HA, SiHA and Therminox discs and were left for one hour in the incubator to attach. Following this time, 2 ml of standard DMEM culture medium was added to the sample wells and the plates were incubated in 5% CO_2 at 37°C for a period of 24 days, during which timed the samples were tested at days 1, 3, 6, 12 and 24 for their cellular activities. A second group of discs were also seeded with hMSCs in the same manner, however these cells were grown in osteogenic medium in order to evaluate the effect of the osteogenic environment on the cellular activities of the seeded cells.

3.4.4 Osteogenic Differentiation- Morphology

3.4.4.1 Scanning Electron Microscopy

In order to study the morphological changes of cells seeded on SiHA and HA dense discs in comparison with cells seeded on Therminox discs, the discs loaded with cells (n=2) were processed for SEM analysis on days 1, 7, 14 and 24 of the study.

The cell loaded discs were first fixed with the addition of 1.5% glutaraldehyde (R1011, Agar Scientific) in 0.2 M Sodium Cacodylate buffer (BDH Chemicals 30118) for 24 hours at 4°C. Following this time, the glutaraldehyde was removed and the samples were washed with 0.1 M sodium cacodylate buffer for 10 minutes to remove the remaining glutaraldehyde residues. 1% osmium tetroxide in 0.1 M sodium cacodylate was then prepared for staining of the cells and added to the samples for 60 minutes. Following this the samples were washed twice, each time for 5 minutes, with 0.1 M sodium cacodylate buffer. The samples were then dehydrated through increasing concentrations of ethanol (20-100%), twice at each concentration and each for 5 minutes. Following dehydration, hexamethyldisilazane, HMDS, (H4875, Sigma), a transition solvent was added to the samples for the purpose of drying the biological specimens. The samples were then left for 24 hours to air dry following which they were mounted on aluminium discs, sputter coated with a gold-palladium mixture using an Emitech K550 sputter coater (Emitech, UK). Samples were then visualized under a Joel JSM-5500LV Scanning Electron Microscope using the relative Joel User Interface version 4.04 at 15 kV.

3.4.5 Cellular Proliferation

3.4.5.1 Total DNA

To measure the DNA content of the samples, on days 3, 12 and 24 the medium was removed from the culture wells. The cells were washed with PBS solution and then lysed with 1 ml of de-ionized water by repeated freeze-thawing of the cells three times. The lysate was then removed from the wells and used for analysis by using the

Quant-iT™ dsDNA Broad Range Assay kit (Q33, 130, Invitrogen). The assay was performed by transferring 10µl of the lysate into the provided microwell plate in duplicate and adding dsDNA BR reagent and dsDNA BR buffer. This was followed by measuring the fluorescence observed from the samples at 510/590 nm excitation/emission levels. The obtained readings were plotted against a standard curve and the quantity of the DNA content of the cells seeded on SiHA, HA and Therminox cover slip samples was measured.

3.4.5.2 Alamar Blue activity assay

The metabolic activity of the cells seeded on SiHA, HA and Therminox cover slip was measured using the Alamar Blue™ assays on days 1, 3, 6, 12 and 24. To perform this assay the medium was removed from the wells. Alamar blue (10%) was prepared in phenol red free medium and then added to the wells of the test samples and also to an empty well as a control. The samples were incubated for 3 hours following which, 100 µl of the Alamar Blue™ from each sample well was transferred to a micro-well plate and the absorbance levels of the samples were read (Fluoroskan Ascent machine at 510/590 nm). The obtained readings were then compared against standard absorbance values and the results were interpreted.

3.4.6 Osteogenic Protein Expression

The differentiation of the hMSCs on SiHA, HA and Therminox discs was quantified and compared by measuring the level of osteopontin and osteocalcin proteins' secretion by these cells. As the amount of protein produced by cells is relative to the number of cells present, the amount of protein produced by each sample was standardized for a variation in the number of cells grown in each sample over the period of the study. This was done by calculation of the measured protein content of the cells divided by the DNA content of the cells grown on the SiHA, HA and Therminox discs.

3.4.6.1 Total protein assay

The total protein content of the cells seeded on SiHA, HA and Therminox coverslips was measured on days 3, 12 and 24 using Bradford reagent (B6916, Sigma), which has a binding capacity for protein molecules. To run this assay, the culture medium which contained the proteins in solution released from the samples and a set of known concentration BSA (Bovine Serum Albumin) protein standards were transferred to micro-well plates. This was followed by the addition of Bradford reagent and measurement of the absorbance at 595 nm. The obtained readings were then plotted against a standard curve of absorbance versus protein and the concentration of the total protein within the cells was calculated using the obtained measurements.

3.4.6.2 Osteocalcin Assay

To measure osteocalcin protein activity within the cells seeded on SiHA, HA and Therminox discs an osteocalcin assay was performed. To run the assay, the culture medium was removed on days 3, 12 and 24 and levels of osteocalcin protein within the medium was measured using the Metra^{TM} Osteocalcin EIA Kit (8002, Quidel, USA) according to the protocol provided by the manufacturer. The levels of osteocalcin protein within the collected medium were calculated using optical densities measurement of the samples at 405 nm wave length using a Dynatech MR700 plate reader (Dynatech Laboratories, UK).

3.4.6.3 Osteopontin Assay

Levels of osteopontin protein produced by the cells were measured by using the Quantikine ® Human Osteopontin Immunoassay Kit (R&D Systems). To run this assay culture medium from the samples on days 3, 12 and 24 were used as osteopontin is an extracellular protein and the assay was run according to the instructions of the manufacturer. Levels of osteocalcin present within the test samples were calculated by reading the absorbance measurements at 450nm and 540

nm. The obtained readings were then plotted against a standard curve containing a set of known standard concentrations and the osteocalcin content of the test samples was calculated.

3.4.7 Osteogenic Gene Expression

3.4.7.1 Real Time PCR

In order to quantify the expression of osteopontin, osteocalcin, osteonectin, bone sialoprotein, VEGF, RUNX2 and Osterix genes by real time polymerase chain reaction (Q-PCR), mRNA extraction from cells seeded on SiHA, HA and Thermanox cover slips (n=3) was required. mRNA extraction was carried out on days 1, 3, 6, 12 and 24 from 50, 000 cells seeded on SiHA, HA and Thermanox cover slips using QIAGEN RNeasy mini kit (74104, QIAGEN, UK). To carry out the mRNA extraction medium was removed from cell seeded discs within the wells. Cells were washed with PBS and then lysed following the manufacturer's protocol provided by QIAGEN. The amount of RNA extracted was then measures using ND-1000 Nanodrop® spectrophotometer (Labtech Ltd., UK) and the yield of mRNA was calculated in 50 μl volume.

Following mRNA extraction, reverse transcription reaction was carried out to convert the mRNA to complementary DNA (cDNA) for use in later Q-PCR analysis. CDNA was synthesised by using the TaqMan High Capacity cDNA Reverse Transcription Kit (4368813, Applied Biosystems, UK). The mRNA was converted to cDNA by the action of the reverse transcriptase enzyme in combination with dNTPs, Oligo dT, RNAse inhibitor and buffer solutions. The reverse transcription reaction was carried out in a Gene Amp thermal cycler with 10 minutes at 25°C, 2 hours at 37 °C and 5 seconds at 80°C. The synthesized cDNA was then used for amplification in the Q-PCR process.

The generated cDNA was amplified in a real time polymerase chain reaction (QPCR) for quantification of the amount of osteogenic marker genes. QPCR was carried out for specific primers for human Osteopontin, Osteocalcin, Osteonectin, Bone Sialoprotein proteins and VEGF, RUNX2 and Osterix transcription factors.

The QPCR reaction involved the amplification of the cDNA templates by a set of fluorescent oligonucleotide probes, followed by real time quantification of the DNA following each amplification cycle. Quantification of the expression levels of the specified genes was performed at the Genome Centre, Queen Mary University of London by Dr Charles Mein and the calculated quantities were normalised to a housekeeper index for the ATPs and UBC genes.

3.4.8 Statistical analysis

Results obtained in this chapter were compared statistically using the nonparametric tests, Kolmogorov Smirnov Z test and Mann-Whitney U test, which define significant differences between two samples. Any P value less than 0.05 was considered significant.

3.5 Results

3.5.1 Characterisation of MSCs

Light microscopy showed the long spindle like nature of the cultured marrow stromal cells (Figure 50) grown on Therminox. Trypan blue staining showed live and dead cells within the culture flask.

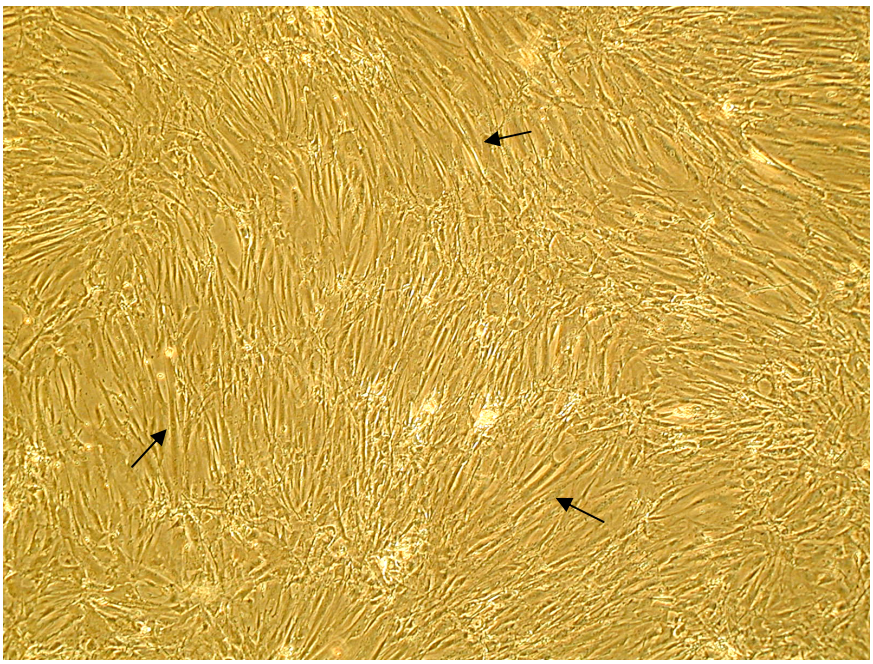

Figure 50. Confluent Passage 3 hMSCs after 14 days. Arrows: Spindle like cells Thermanox cover slips

3.5.1.1 Osteogenic differentiation

Von Kossa staining showed black stained calcium and red stained cells within the cultured cells indicating the presence of calcification and mineralisation of the extracellular matrix of cells grown in osteogenic medium on thermanox cover slips (Figure 51).

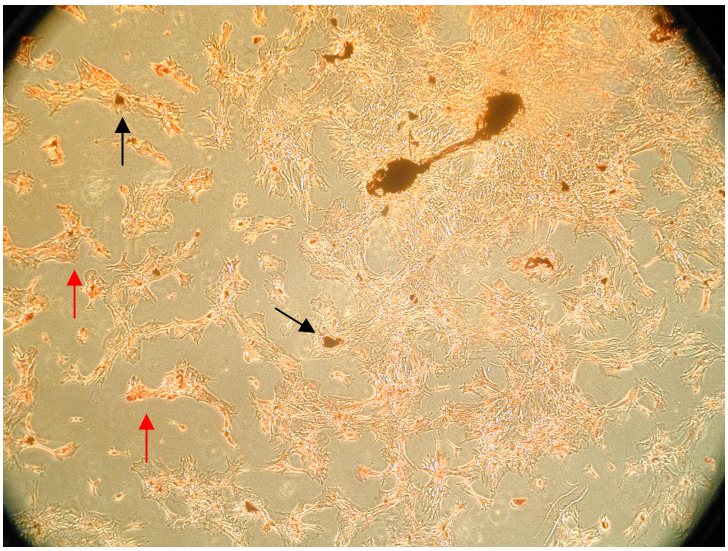

Figure 51. Von Kossa stain indicating mineralisation and calcium deposits within osteogenic differentiated hMSCs on Thermanox discs. Black Arrows: Calcium; Red Arrows: Cells. 2.5 X magnification

3.5.1.2 Adipogenic differentiation

Red stain within the Oil Red O stained cultured cells represented the presence of lipid molecules within the cells confirming the differentiation of the hMSCs into adipocytes (Figure 52).

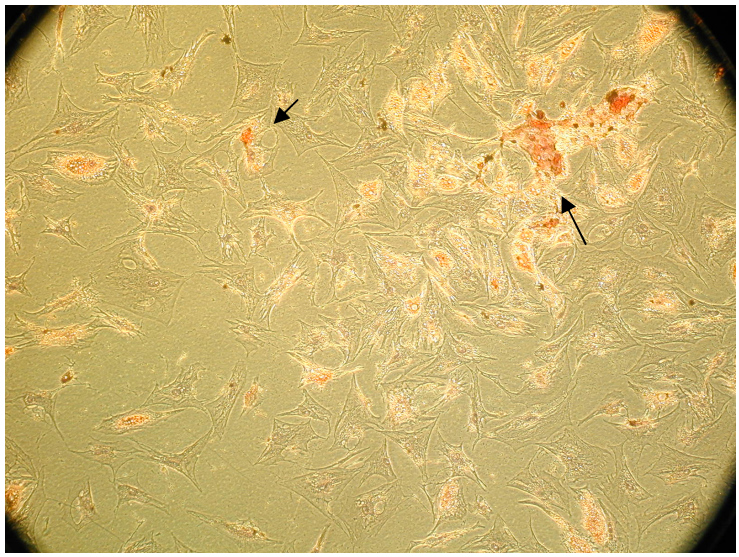

Figure 52. Oil red O stained hMSCs. Arrows: Lipids within the cultured cells on Thermanox discs. 2.5X magnification

3.5.2 Osteoblastic Differentiation- Morphology

3.5.2.1 Scanning Electron Microscopy

Scanning Electron Microscopy (SEM) analysis of the cells on day 1 showed cell attachment at points of contact to all three surfaces. Cells seeded on control samples represented spindle-like morphology (characteristic of fibroblasts). Centrifugal growth of filopodia was observed within the samples (Figure 53). Both HA and SiHA cultures hMSCs indicated a spread out, flat structure at the centre with visible cell processes representing attachment to the surface and also cell-cell contacts. MSCs seeded on SiHA exhibited a more flat morphology covering the surface of the discs; however, cells of spindle-like structure were also observed (Figure 53) as was seen previously under light microscopy (Figure 50).

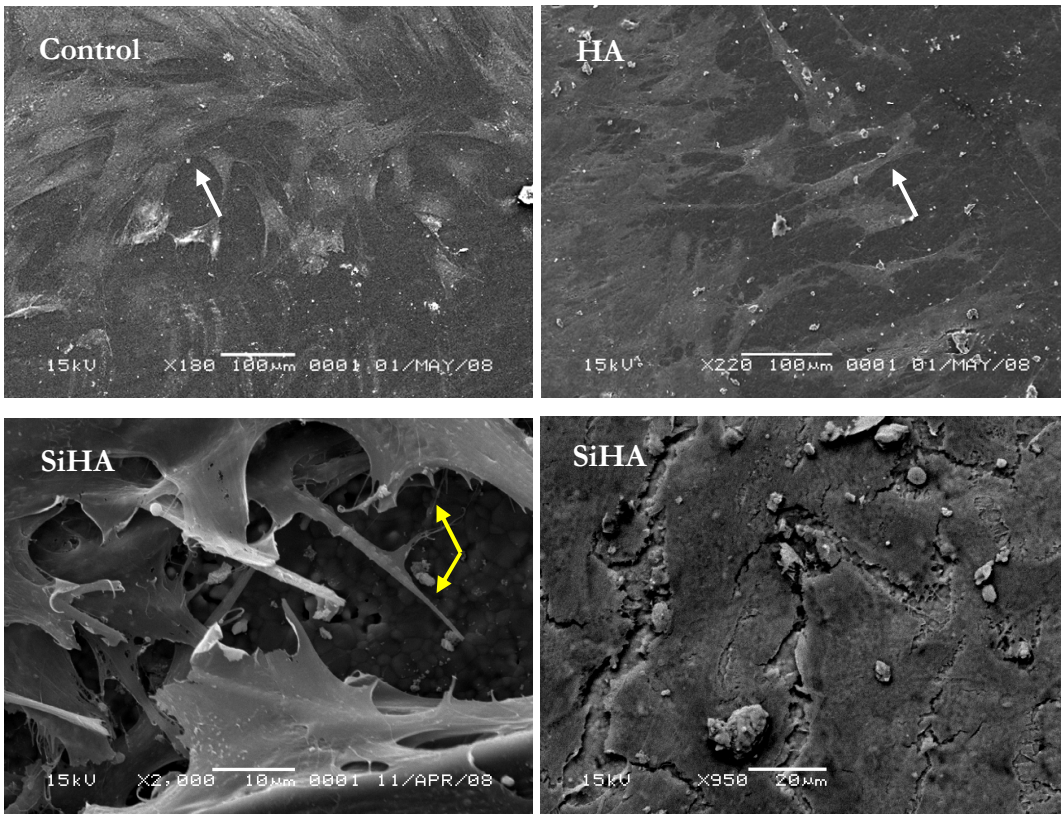

Figure 53. Day 1 hMSC on Control and HA discs. White arrows: adherent hMSCS cells. Yellow arrow: Presence of cell filopodia in contact with SiHA.

MSCs seeded on SiHA discs on day 7 demonstrated a spread out morphology forming a layer over the surfaces of the discs. MSCs seeded on HA discs also demonstrated a spread out cuboidal structure, following the trend reported in other studies (Arcos et al., 2006; Annaz et al., 2004; Thian et al., 2006); however, spindle like cells were also observed on the surface of the biomaterial (Figure 54).

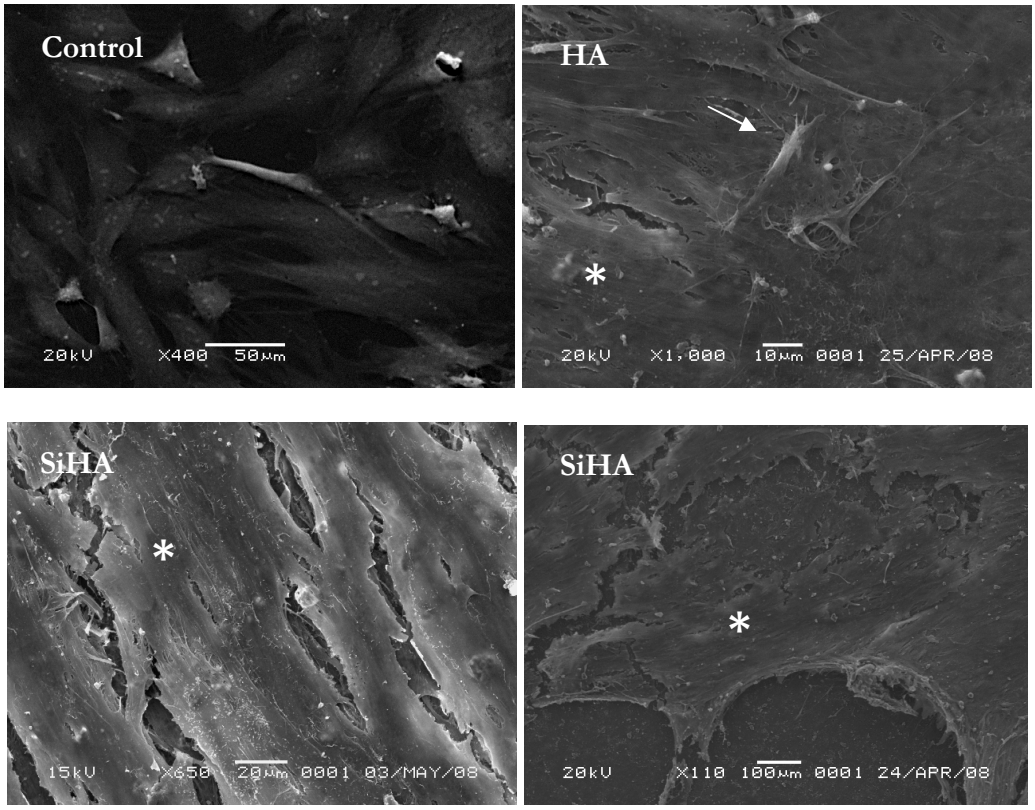

Figure 54 . Day 7 hMSCs on SiHA and HA discs. Arrow: spindle like cell. Stars: Cuboidal cells.

On day 14, hMSCs seeded on Therminox cover slip discs (control) exhibited a well organised cell arrangement formed over the surface of the discs. HA seeded discs exhibited similar morphological structures observed on day 7, however, an increased number of cells with a spread out and flat morphology was observed over the HA surface. SiHA seeded cells exhibited densely packed osteoblastic cuboidal structures coating the surface of the discs (Figure 55).

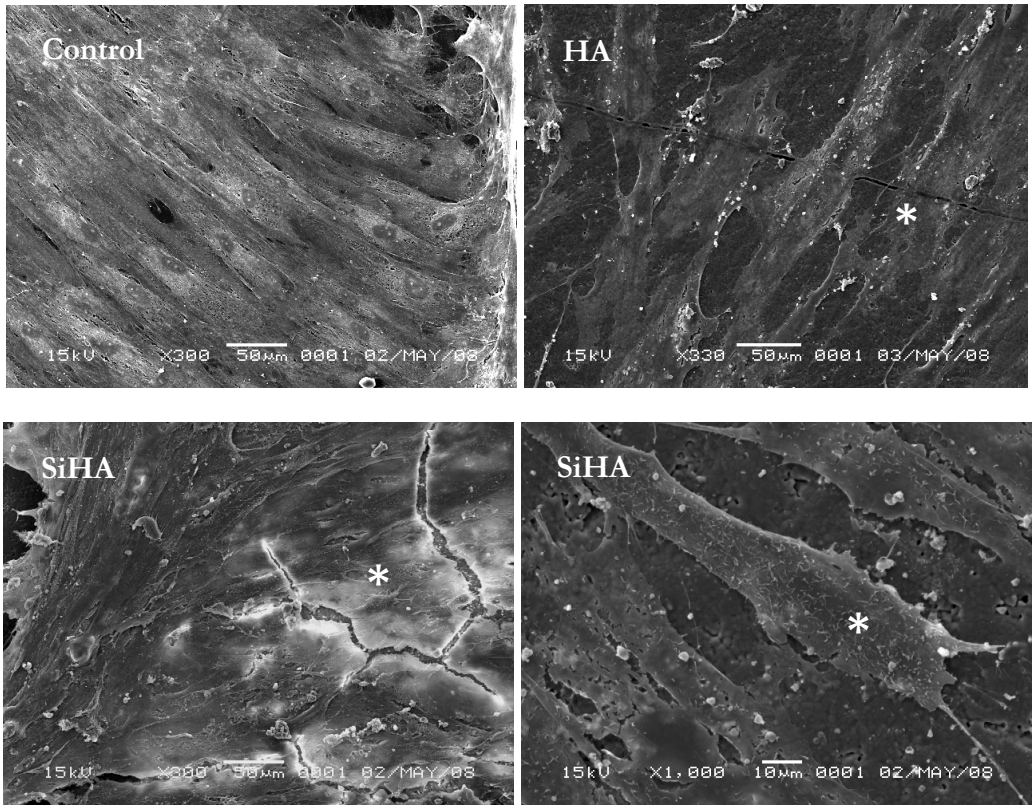

Figure 55. Control, HA and SiHA d14. Stars: cuboidal osteoblasts.

The hMSCs seeded on control discs on day 24 exhibited a spread out structure covering the surface of the Therminox discs; however, spindle like cells making attachment with the disc surface were also observed. Cells seeded on both HA and SiHA discs exhibited flat cuboidal shapes arranged in line forming a layer over the surface of the discs, representing osteoblasts. SiHA discs, however, exhibited the presence of globular calcium phosphate nodules (Kalia et al., 2007, Thian et al., 2006) on the formed cell layer (Figure 56).

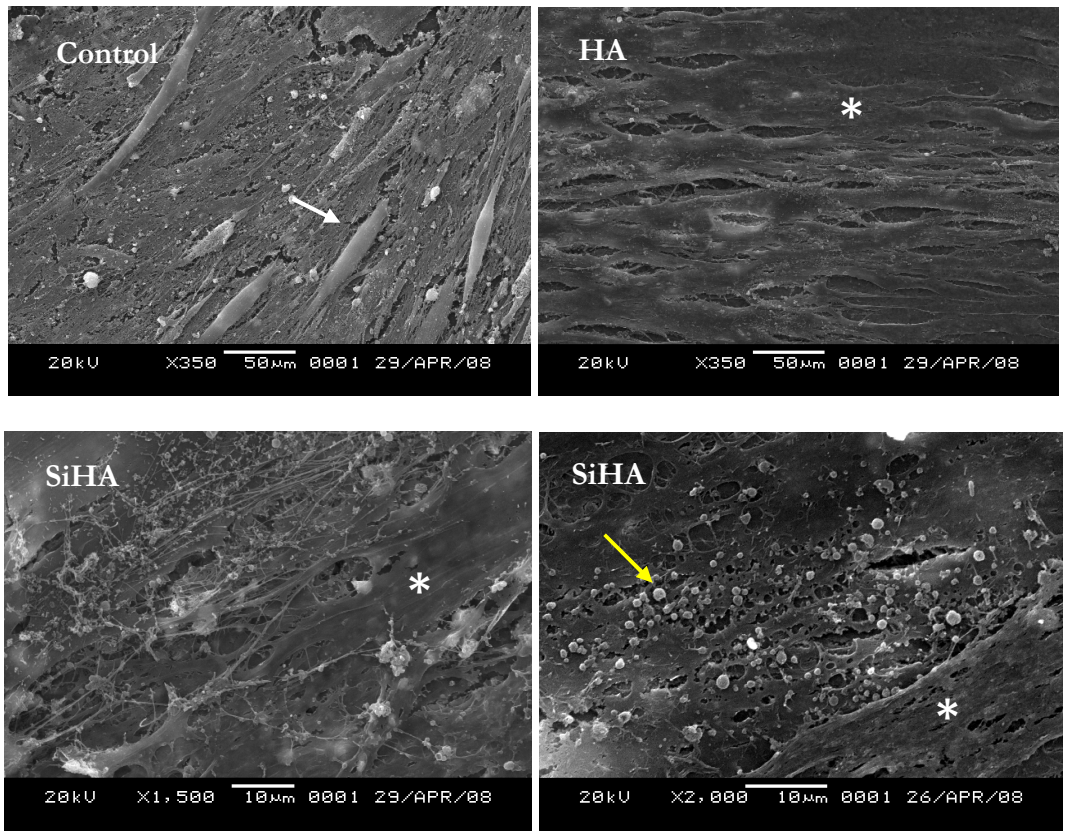

Figure 56. Day 24 hMSCs on Control, HA and SiHA discs. White arrow: Spindle like cells, Star: Osteoblast cells, Yellow arrow: Globular nodules.

3.5.3 Cellular Proliferation

3.5.3.1 Total DNA

Results demonstrated an increase in the amount of DNA from days 3 to 12 in all samples. Cells grown in osteogenic medium ($SiHA^+$ = 1.04±0.13, HA^+ = 1.69±0.39 and $Cntrl^+$= 3.2±1.01) did not indicate any significant difference in levels of DNA content in comparison with cells grown in normal medium ($SiHA^-$ = 1.07±0.34, HA^- = 1.64±0.41 and $Cntrl^-$ = 2.51±0.32) by day 24 of the study. HA (HA^+= 0.83±0.22; HA^- = 0.52±0.09) samples indicated higher DNA content on day 12 in comparison with SiHA ($SiHA^+$= 0±0.01; $SiHA^-$= 0.29±0.24) samples. DNA content of cells seeded on HA (HA^+= 1.69±0.39; HA^- = 1.64±0.41) samples indicated higher levels of DNA in comparison with SiHA ($SiHA^+$ = 1.04±0.13; $SiHA^-$ = 1.07±0.34) seeded cells by day 24. Cells seeded on Therminox cover slip discs ($Cntrl^{-/+}$) exhibited the highest amounts of DNA ($Cntrl^+$ = 3.2±1.01 and $Cntrl^-$ = 2.51±0.32) in comparison with SiHA and HA samples by day 24 of the study (Figure).

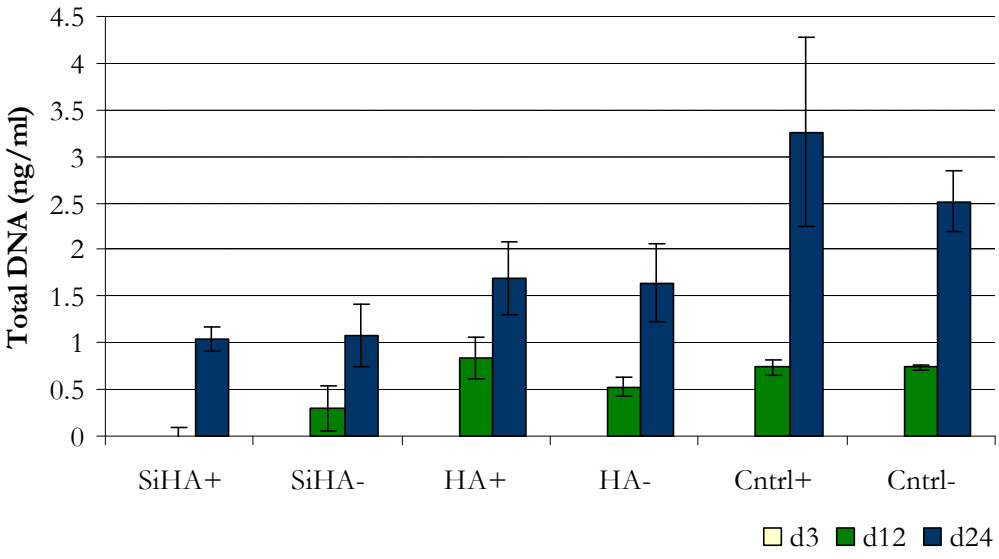

Figure 57. Total DNA content within hMSCs seeded on SiHA, HA and Control discs grown in Normal (-) and Osteogenic (+) medium.

3.5.3.2 Alamar Blue activity assay

Alamar Blue assay results demonstrated that cells seeded on SiHA discs and Therminox discs grown in normal medium ($SiHA^-$= 96.35±12.17 and $Cntrl^-$ =99.44±32.44) exhibited the highest level of cellular activity and cell growth in comparison with other groups by day 24 ($SiHA^+$ =29.98±0.92; HA^+= 55.6±5.30; HA^-= 76.72±7.64; $Cntrl^+$=82.70±16.92. The cellular activity of cells seeded on $SiHA^-$ samples was observed to be higher than other HA and Control groups on days 12 and 6 (Table 5). Cells seeded on HA^- discs indicated higher cellular activity (=38.65±2.6) on day 3 in comparison with the $SiHA^-$ (29.96±14.07), $SiHA^+$ (=7.39±5.55) and cells seeded on HA discs in osteogenic medium (HA^+ = 2.02±0.15). Cellular activity of SiHA ($SiHA^+/^-$) seeded cells were observed to be higher than cells seeded on HA ($HA^+/^-$) discs on day 1 (Figure 58).

Table 5. Mean values (±standard error values) of the cellular activity (RFU/1000s) of hMSCs grown on SiHA, HA and Control discs in osteogenic (+) and normal (-) medium on days1, 3, 6, 12 and 24.

	SiHA+	SiHA-	HA+	HA-	Cntrl+	Cntrl-
d1	22.64±2.74	30.18±4.33	18.16±1.35	17.70±7.64	33.82±5.63	31.46±0.34
d3	7.39±5.55	29.96±14.07	2.02±0.15	38.65±2.6	2.47±0.25	24.45±4.17
d6	20.21±8.30	67.92±6.36	69.03±7.32	38.27±11.71	42.91±40.09	27.09±23.58
d12	25.23±9.92	79.16±3.51	53.19±0.44	45.94±2.93	60.63±17.37	70.44±9.00
d24	29.98±0.92	96.35±12.17	55.60±5.30	76.71±16.91	82.70±16.91	99.44±32.44

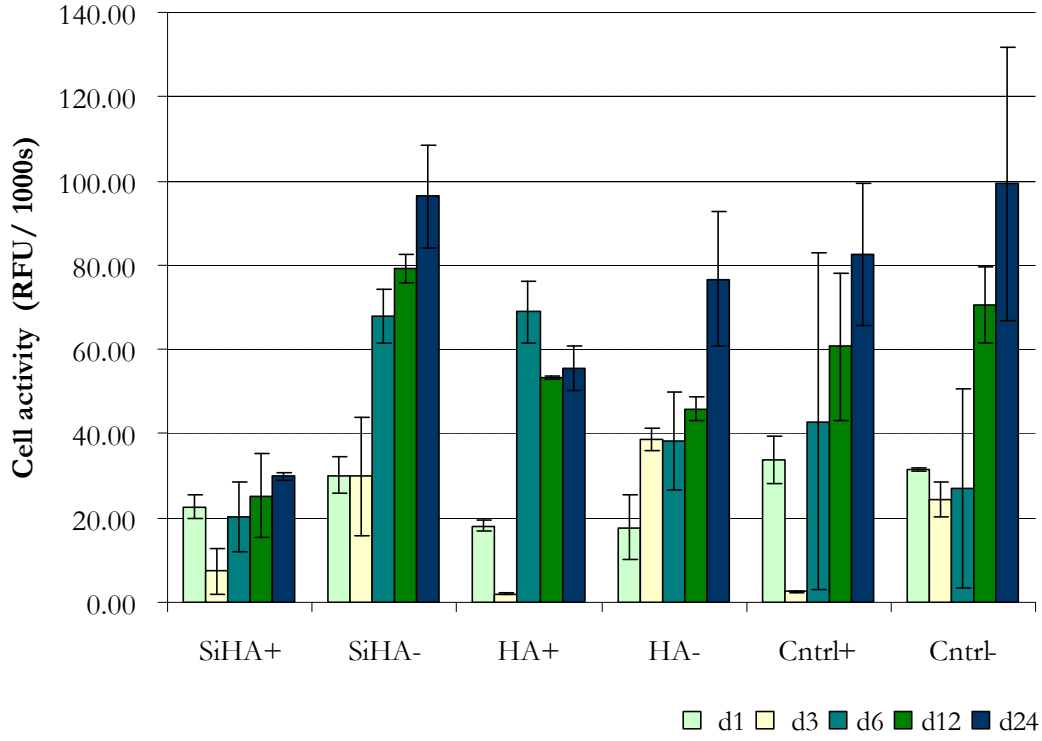

Figure 58. Alamar Blue absorbency of hMSCs seeded on SiHA, HA and Control Therminox disc in Normal (-) and Osteogenic (+) medium within 24 days

3.5.4 Osteoblastic Protein Expression

3.5.4.1 Total protein

Results of the amount of total protein produced by hMSCs seeded on SiHA, HA and Therminox discs indicated higher levels of total protein production by cells seeded on the control ($Cntrl^{+}/^{-}$) samples on days 3 and 24 of the study in comparison with the SiHA and HA seeded cells. Both SiHA ($^{+}/^{-}$) and HA ($^{+}/^{-}$) seeded cells indicated higher levels of protein production on day 12 compared to the control group. No significant difference was observed in the level of protein production in cells grown in normal medium in comparison with osteogenic medium. HA seeded cells ($HA^{+}/^{-}$) indicated slightly higher levels of protein production on day 3 in comparison with SiHA ($^{+}/^{-}$) samples (Figure 59). No significant difference was observed in any of the groups ($P>0.05$).

Normalization of the total protein produced by the cells to the DNA content of the cells indicated that cells seeded on SiHA, HA and control discs grown in both osteogenic and normal medium exhibited highest levels of protein production on day 12. A reduction in the level of total protein/DNA was observed from days 12 to 25, however, cells seeded on SiHA discs in normal medium ($SiHA^{-}$) demonstrated more protein production than other groups (Table 6). None of the groups showed statistically significant results when compared ($P>0.05$).

Table 6. Mean total protein/DNA (ng/ml)/(μg/ml) content of hMSCs seeded on SiHA, HA and Control discs in normal (+) and osteogenic (-) medium on days 3, 12 and 24

Total protein	SiHA+	SiHA-	HA+	HA-	Cntrl+	Cntrl-
d3	0±0	0±0	0±0	0±0	0±0	16591.61±16591.6
d12	10492.80±10492.8	3415.81±1204.5	2485.62±695.0	3507.11±612.3	2313.18±310.0	2270.11±102.1
d24	1590.02±260.7	1920.95±515.48	1174.17±377.4	1211.23±344.5	778.38±244.06	908.23±126.0

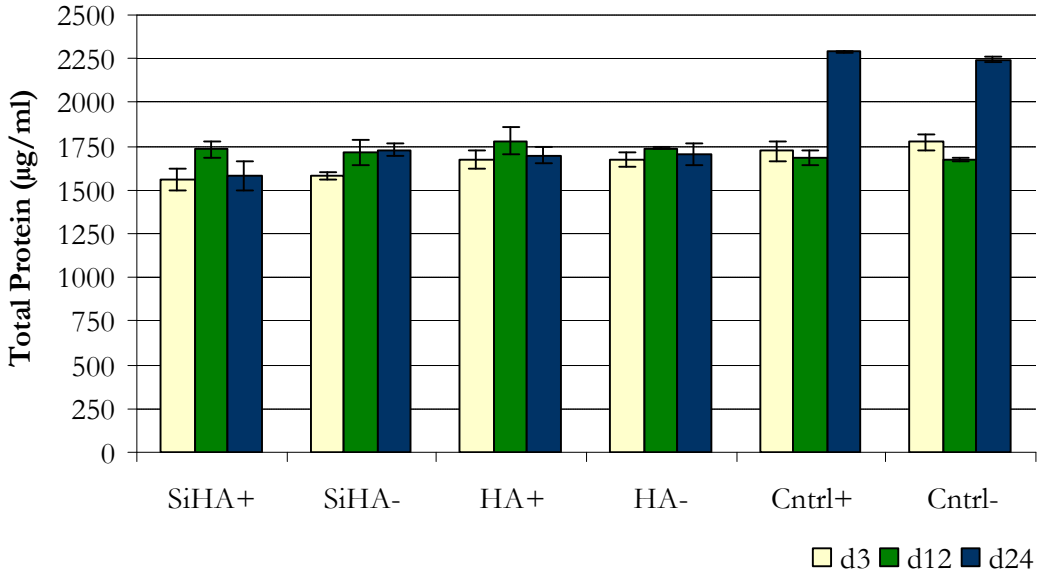

Figure 59. Total protein production within hMSCs seeded on SiHA, HA and Control discs in Osteogenic (+) or Normal medium (-)

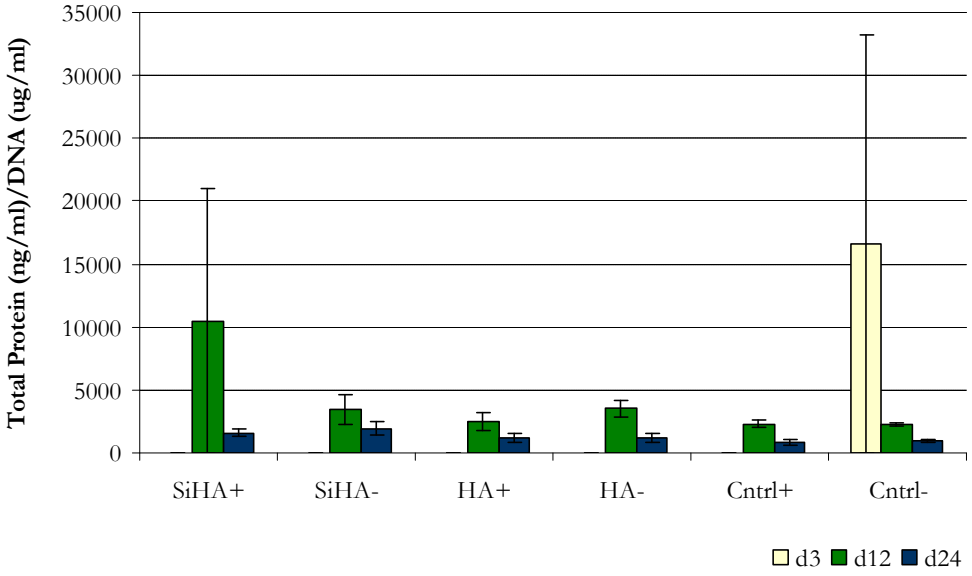

Figure 60. Total protein production normalized to DNA levels

3.5.4.2 Osteocalcin protein production

Normalised results showed higher amounts of osteocalcin protein production by cells grown on SiHA discs by day 24 of the study (Table 7). Levels of osteocalcin protein was highest on day 12 compared with other time points. SiHA seeded cells demonstrated higher amounts of osteocalcin protein compared with HA and control groups on day 12 of the study. SiHA seeded cells showed higher osteocalcin expression on day 24 compared to the control group. Next to SiHA seeded cells, HA samples indicated greater amounts of osteocalcin protein by day 24 compared with the control group. Osteocalcin protein produced by SiHA and HA samples were observed to be higher in cells grown in normal medium ($SiHA^-$ and HA^-) (Figure 61). No statistically significant ($P>0.05$) difference was observed when groups were compared.

Table 7. Mean osteocalcin protein expression values (±standard error values)

Osteocalcin	SiHA+	SiHA-	HA+	HA-	Cntrl+	Cntrl-
d3	0±0	0±0	0±0	0±0	0±0	0±0
d12	0±0	43.48±14.72	14.20±9.40	36.47±5.45	20.78±1.94	19.83±0.82
d24	21±4.96	18.64±6.76	12.87±4.85	12.16±4.91	4.14±1.09	5.94±0.57

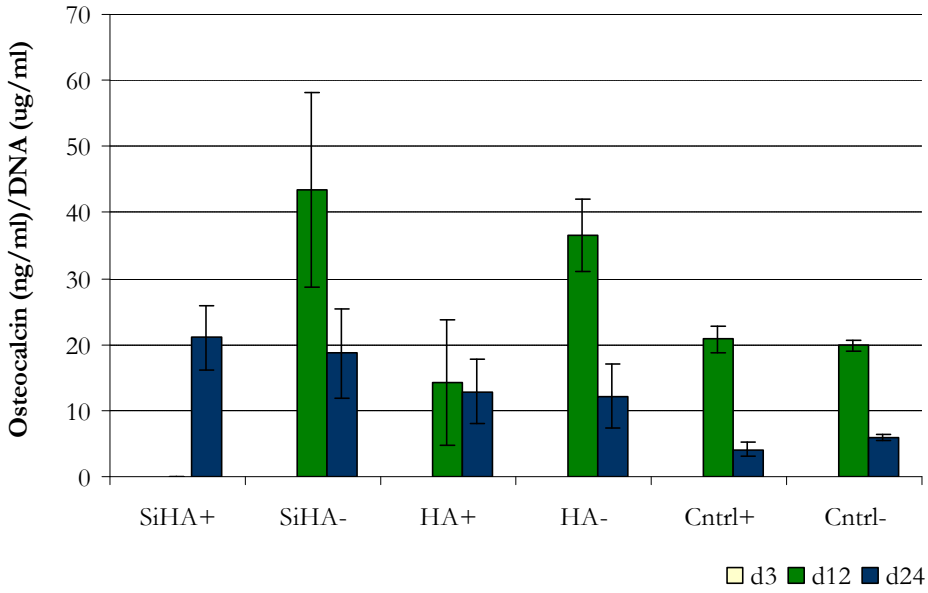

Figure 61. Normalised data for Osteocalcin/DNA production by hMSC seeded on SiHA (SiHA+/-), HA (HA+/-) and control discs (Cntrl+/-) grown in Normal (-) or Osteogenic medium (+)

3.5.4.3 Osteopontin protein production

Protein expression to DNA content data showed significantly ($P<0.05$) greater osteopontin production by the hMSCs seeded on SiHA, HA and control discs on day 12 of the study compared to other time points. The hMSCs seeded on $SiHA^-$ discs demonstrated higher levels of osteopontin production in comparison with HA^- samples on days 12 and 24 (Table 8). Cells seeded on SiHA ($^+/^-$) discs indicated increased osteopontin production by day 24 of the study compared with the HA and control groups, however the levels were not significantly ($P>0.05$) different.

Table 8. Mean osteopontin protein expression values (± standard error values)

Osteopontin	SiHA+	SiHA-	HA+	HA-	Cntrl+	Cntrl-
d3	0±0	0±0	0±0	0±0	0±0	0±0
d12	0.21±0.31	0.16±0.0001	0±0.04	0.32±0.07	0.07±0.01	0.29±0.06
d24	0.64±0.64	0.12±0.01	0.021±0.009	0.085±0.01	0.009±0.001	0.02±0.02

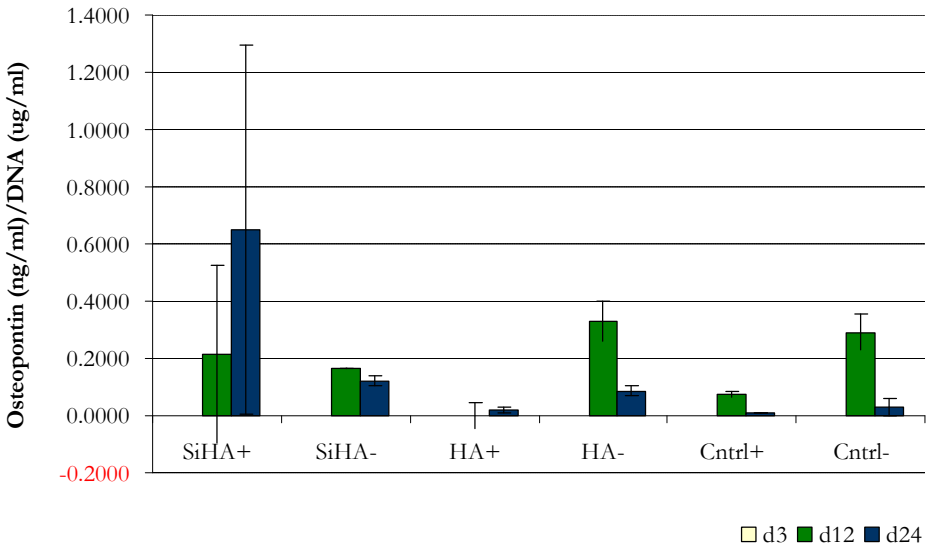

Figure 62. Normalized Osteopontin/DNA production by hMSC seeded on SiHA, HA and Control discs grown in Normal (-) and Osteogenic (+) medium.

.

3.5.5 Osteoblastic gene expression

Analysis of the mRNA expression of osteogenic marker genes and transcription factors of hMSCs grown on SiHA, HA and Therminox discs indicated a set of varying expression levels for the tested genes. The housekeeping genes UBC and ATPs were expressed in all groups. The relative expression of RUNX2 transcription factor indicated significantly higher levels of expression on day 24 of the study in SiHA and HA seeded cells grown in osteogenic medium ($SiHA^+$ and HA^+) compared with other groups. Cells seeded on $SiHA^+$ discs indicated higher RUNX2 expression levels. No significant difference was observed in level of RUNX2 expression on cells seeded on SiHA, HA or control discs on days 1, 3, 6 and 12. At day 1, there was no difference in expression of Osterix transcription factor on all samples. HA and SiHA seeded hMSCs grown in normal medium indicated higher Osterix expression on days 6 and 8, with higher expression of this gene on HA discs (Figure 63).

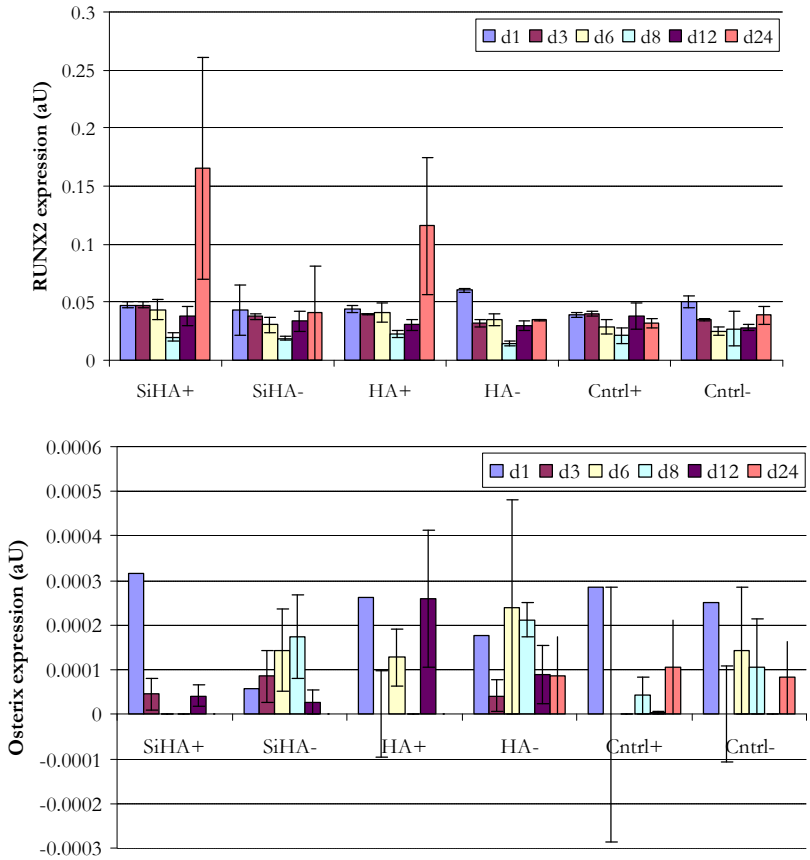

Figure 63. The relative expression of transcription factors RUNX2 and Osterix

The mRNA expression of osteoblast differentiation marker gene, osteopontin, was observed to be higher in SiHA seeded cells grown in osteogenic medium on day 24. HA ($HA^+/^-$) samples indicated higher osteopontin expression on day 24 compared to other groups. No significant difference ($P>0.05$) was observed for osteopontin expression on days 6, 8 and 12 on all samples. SiHA and HA seeded cells in normal medium ($SiHA^-$ and HA^-) expressed higher amounts of osteopontin on day 3 (Figure 64).

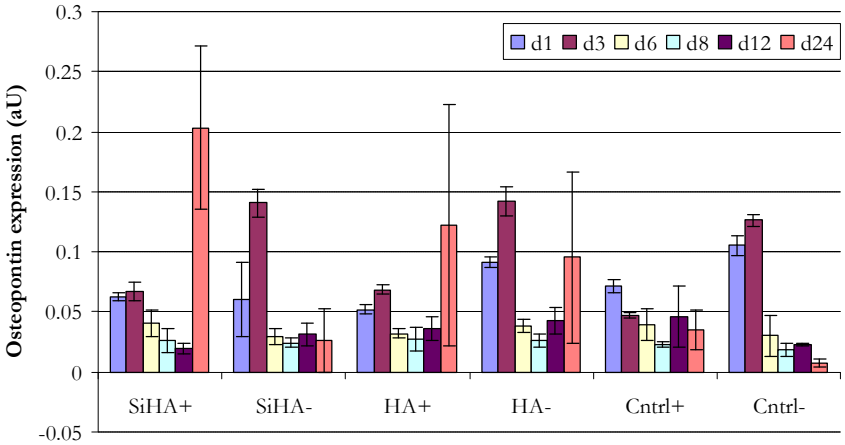

Figure 64. Relative expression levels of osteopontin gene.

The mRNA expression of genes expressed in differentiated osteoblasts forming new bone matrix, the bone sialoprotein and osteonectin genes indicated increase in the levels of bone sialoprotein expression on SiHA ($SiHA^+$ and $SiHA^-$) seeded discs by day 24. Cells seeded on HA discs cultured in osteogenic medium expressed higher levels of bone sialoprotein compared with the control groups (Figure 65) however, these results were not significantly different ($P<0.05$). The mRNA expression of osteonectin gene responsible for mineralisation initiation was observed to be significantly higher on Therminox seeded cells in comparison with cells seeded on SiHA discs on day 24. Expression of this gene was observed to be statistically higher ($P=0.05$) on SiHA discs on days 6 and 8 of the study when compared to other groups (Figure 65). No significant difference ($P>0.05$) in expression of the mineralisation marker, Osteocalcin on any of the samples was observed. However, HA seeded cells cultured in normal medium indicated higher levels of osteocalcin expression on days 1 and 6 compared to other groups (Figure 65).

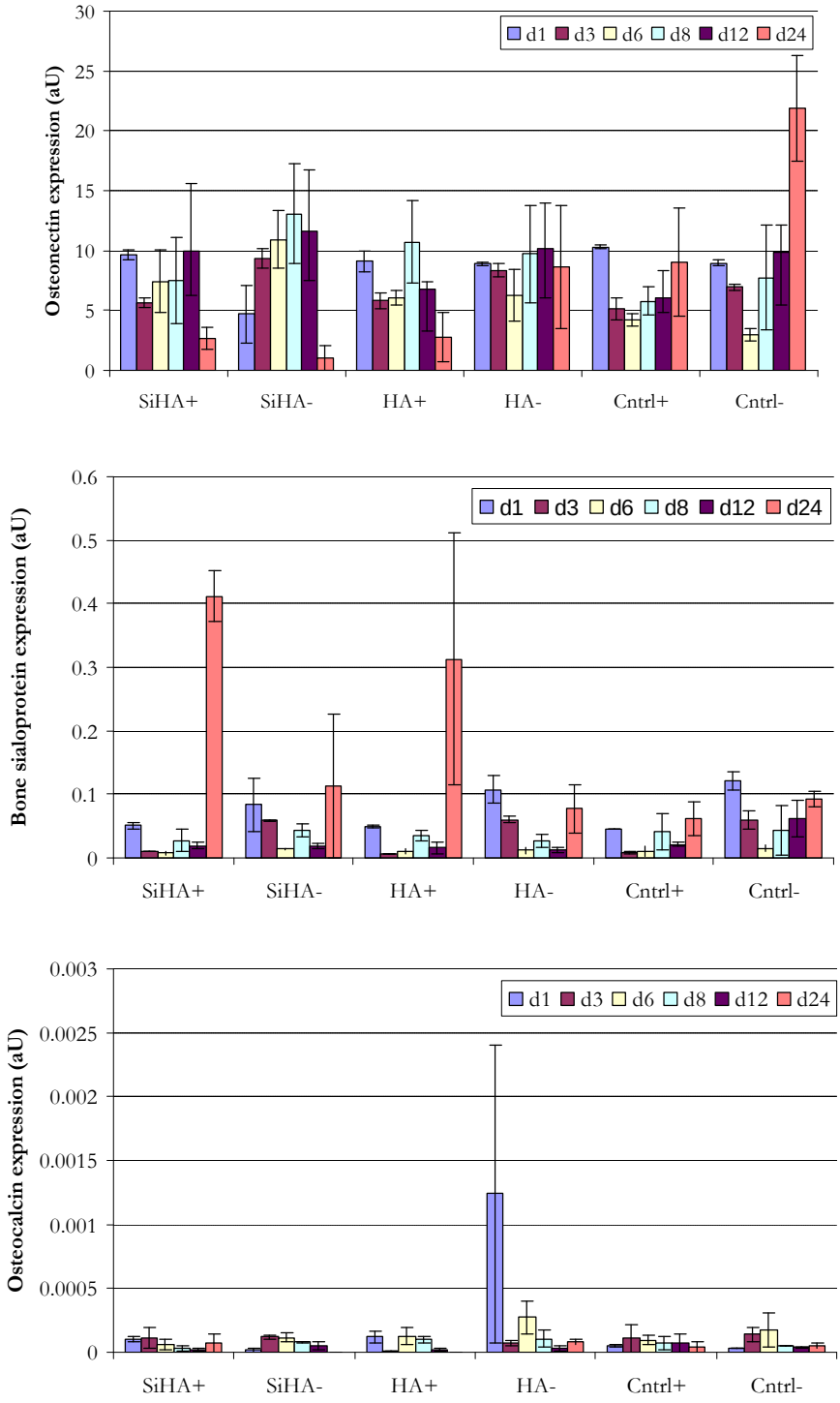

Figure 65. Relative expression of Osteonectin, Bone sialoprotein and Osteocalcin genes.

The mRNA expression of the VEGF gene, the marker for vascularisation mechanism of cells indicated significantly higher levels of expression on SiHA and HA discs grown in normal medium on days 3 and 6 of the study. VEGF expression levels were also observed to be higher on HA and SiHA seeded on day 12 of the study compared with the control group. No significant difference ($P>0.05$) was observed for VEGF expression on SiHA samples compared with HA samples at this time point (Figure 66).

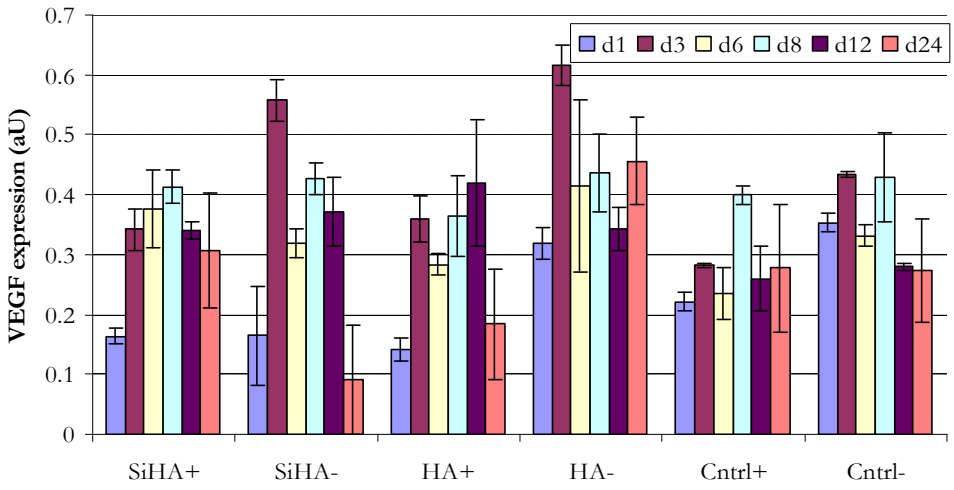

Figure 66. Relative expression of VEGF gene

3.6 Discussion

The aim of this study was to investigate the influence of silicate ion on stimulation of *in vitro* osteoblastic differentiation of hMSCs seeded on dense SiHA discs and the osteoinductivity potential of SiHA bone substitute biomaterial. In this study the morphological changes and the cellular activities involved in osteogenic differentiation of hMSCs by SiHA were analysed. The results of this study indicated that SiHA promoted osteoblastic differentiation of hMSCs *in vitro* in 21 days. The rate of the expression of osteoblastic genes, specifically the vasculogenic gene VEGF, was observed to be different on cells grown on SiHA samples compared to HA. As hydroxyapatite bone substitute materials are calcium phosphate based biomaterials with substantial dissolution properties in vitro, gradual dissolution of HA and release of calcium and phosphate ions and precipitation of the local ions is known as the mechanism of osteogenesis for this biomaterial (Chang et al., 2000; Leewenburgh et al., 2006). Bone marrow cells are reported to undergo osteoblastic differentiation and exhibit upregulated expression levels of Osteopontin, Bone Sialoprotein and ALP messages on HA surfaces (Ozawa and Kasugai, 1996). Wang et al (2003) reported differential expression of osteocalcin, Bone Sialoprotein and osteonectin genes in osteoblasts grown on HA discs. It is known that local release of soluble silicon induces osteogenic differentiation and bone formation by osteoblasts (Reffitt et al., 2003). Silicon substitution within the structure of HA is also known to enhance the bioactivity of human osteoblasts in vitro through combination of the bioactivity of HA with the bioactive properties of silicate ion (Gibson et al., 1999; Brandoff et al., 2006). Further, up regulation of a number of genes expressed by osteoblasts by exposure to ionic products of silica based bioactive glasses have been reported by Gao et al (2001) and Xynos et al (2001). Marrow stromal cells derived from bone marrow stroma because of their regenerative properties and the potential for differentiation into osteoblast, chondrocytes and adipocytes provide the possibility of study of the osteogenic potential of bone graft substitutes. Observational study of the cellular differentiation on SiHA indicated that pluripotent human marrow stromal cells seeded on dense Silicon substituted hydroxyapatite discs

and cultured in normal and osteogenic medium, underwent osteogenic differentiation. Marrow stromal cells are known to undergo differentiation into osteoprogenitor and then maturation into osteoblast cells when cultured under appropriate chemical and physiological conditions (Zue and Chen, 2007). As indicated in a study by Zuo et al (2008), silicon supplementation increases the proliferation and cellular activity of human osteoblast-like cells (Zuo et al 2008). The differentiation of the seeded spindle like hMSCs into flat cuboidal osteoblasts on the surface of SiHA discs, as observed by scanning electron microscopy, was due to the chemical composition of SiHA and the increase in the metabolic activity and cellular proliferation of the seeded hMSCs. The significance of this osteogenic morphology could be further analysed by measurement of the cells' aspect ratios, fluorescent staining of the cells on the test discs or FACS analysis. As dense SiHA discs were used for this study, the influence of porosity on the differentiation of these cells was eliminated in favour of the role of the chemical composition on *in vitro* osteogenic differentiation of the hMS cells. Induction of the osteogenic potential of the seeded hMSC and their differentiation towards the osteogenic phenotype was achieved through culturing in the presence of osteogenic medium. As indicated in a previous study by Castano-Izquierdo et al (2006), secretion of bone-like, possibly extracellular matrix by these cells may have promoted the osteoindution behaviour of these cells seeded on the test materials.

Cell differentiation is controlled by a complex set of cellular and molecular activities and an inverse relationship exists between osteoblast proliferation and differentiation (Malaval et al., 1999). Analysis of the DNA content as a direct measurement of cell number, indicated a higher number on control discs in comparison with HA and SiHA samples. The lowest amount of DNA content was observed on SiHA samples. The proliferation and differentiation of cells are inverse functions, the lower DNA content of hMSCs seeded on SiHA discs concomitant with the flat cuboidal osteoblastic phenotype observed under SEM as early as day 7 indicates earlier differentiation of the SiHA seeded cells in comparison with the HA and control group. It should be noted that in order to evaluate the direct influence of SiHA and HA on the cellular mechanisms of the seeded cells, at the time of the

performance of the required assays (e.g. DNA/ Alamar Blue/ OP and OC assays), the cultured discs were moved to new well plates. This was carried out to avoid detection of signals from cells which had not attached to the disc surface and had fallen to the bottom of the well and consequently were not in direct contact with the test material. For this reason, the higher cell number obtained from the control samples could be due to the difference in the growth of the number of cells attached to the SiHA and HA disc surfaces in comparison with the control Therminox discs.

Alamar Blue absorbency obtained from cells seeded on SiHA, HA and control Therminox discs indicated superior metabolic activity for hMSCs seeded on SiHA discs cultured in normal medium from day 6 to day 24 of the study compared with the HA group. The hMSCs seeded on control discs also indicated similar levels of cellular activity to cells seeded on SiHA discs on day 24 of the study. Analysis of the total protein levels of hMSCs seeded on SiHA, HA and the control discs did not indicate any significant difference between these groups within the period of the study.

The results of this study and the production of osteoblastic marker proteins, in addition to the morphological changes of the hMSCs seeded on SiHA and HA discs, indicated the differentiation of these cells into osteoblasts. Expression of specific transcription factors and proteins are known to contribute to the mechanism of cell differentiation. The initial commitment of mesenchymal stem cells to a particular cell lineage followed by induction of tissue specific patterns of gene expression is required for the process of differentiation (Franceschi, 1999). Osteogenic differentiation involves the expression of transcription factors such as Cbfa1/RUNX2, the osteoblast specific factor, Osterix and osteoblastic proteins including osteopontin, osteonectin, bone sialoprotein and osteocalcin. Neo-vascularisation is known to be an important factor for cell differentiation and the metabolic functions of developing cells (Jarrahay et al., 2005). Vascular Endothelial Growth Factor (VEGF) is known as an important gene involved in angiogenesis and the process of vasculogenesis (Patan, 2000). Vasculogenesis is an essential factor in bone formation by bone substitute materials and the process of bone remodelling and osteoblast differentiation (Sibilla et al., 2006). Formation of an appropriate blood

vessel network is known as one of the factors contributing to the rate of bone formation. Several studies have shown that proliferation, migration and differentiation of osteoblasts is stimulated by VEGF (Furumatsu et al., 2003).

In this study gene expression analysis of RUNX2 transcription factor indicated up regulation of this gene in hMSCs seeded on SiHA and HA discs grown in osteogenic medium by day 24 of the study. However, no significant difference was observed on the level of RUNX2 expression in cells grown in normal medium on SiHA and HA discs in comparison with the control group. Karsenty (1998) has shown that Cbfa1/RUNX2 is a necessary factor for differentiation of mesenchymal progenitor cells to osteoblasts. This transcription factor is known to control the expression of other osteoblast specific transcription factors such as Osterix. (Karsenty and Wagner, 2002). Osterix (Osx) is expressed in osteoblast progenitors downstream of the Cbfa1/RUNX2 gene as Cbfa1 is known to be expressed in Osx deficient mice, while no expression of this gens in observed in Cbfa1 deficient mice (Nakashima et al., 2002). This gene is known as a positive regulator of osteoblast differentiation and bone formation (Baek et al., 2008). Osterix over-expression is known to up regulate the expression of osteocalcin and Cbfa1 genes and to increase the formation of mineralised bone nodules in embryonic stem cells (Guangping et al., 2004). Further, this gene is suggested to exert indirect feedback to Cbfa1 and activation of signalling molecules that lead to osteoblastic differentiation (Tai et al., 2004). Analysis of Osterix expression in this study indicated clear activity of this gene on day 1 of the study, with down regulation in expression levels of this gene on SiHA in comparison with HA and control samples. Down regulation of RUNX2 expression on days 6 and 8 of the study was observed to be concurrent with up regulation of Osterix expression at these time points in cells seeded on all three surfaces. As no clear pattern of expression was observed for expression of this gene on hMSCs seeded on SiHA discs in comparison with HA and control groups, further analysis of the expression of this gene using larger population of cells is required.

Osteopontin is known to be expressed during the early stages of osteoblast proliferation and differentiation and the later mineralisation of the extracellular matrix (Aubin et al., 1995; Denhardt et al., 2001). This protein is known to exhibit an

affinity for binding with HA and regulation of crystal formation and growth for marrow cells differentiation to osteoblasts (Kasugai et al., 1992). The results of this study did not indicate any significant change implied by SiHA on expression of the osteopontin gene; however, this gene was observed to be expressed significantly higher ($P<0.05$) on HA discs compared with hMSCs seeded on control discs by day 24 of this study. However, the results of the osteopontin assay indicated production of higher amounts of osteopontin protein by hMSCs seeded on SiHA discs when compared with the cells seeded on control Therminox discs.

Bone sialoprotein (BSP) is a marker of bone metabolism associated with the osteoid matrix and is expressed in osteoblasts (Sodek et al., 1992; Stork et al, 2000). Analysis of the expression of this gene within hMSCs indicated increased levels of BSP expression by day 24 of the study. This suggested a role of SiHA on osteoinduction of the cells through an effect on mineralisation of the bone matrix. Supplementation of the medium with osteogenic factors was observed to enhance the expression of BSP in both SiHA and HA (SiHA+/HA+) samples.

Osteonectin is a bone-specific protein localized in mineralised bone matrix known for its binding affinity to hydroxyapatite and collagen which nucleate mineral phase deposition (Termine et al, 1981, Bolander et al., 1987). Increased expression of the osteonectin gene on days 6 and 8 of this study indicated an early promotion of the mineralisation by SiHA.

Osteocalcin is a marker of differentiated osteoblasts as it is expressed and secreted by these cells (Garcia-Carasco et al., 1988). The expression of this gene is known to be regulated by the RUNX-2 transcription factor and associated with growth arrest (Stein et al., 1990) and formation of a mineralising matrix (Ducy *et al.*, 1997; Aronow et al., 1990). The results of this study did not indicate any significant influence of SiHA on expression of the osteocalcin gene by hMSCs; however, the results of the osteocalcin protein assay indicated higher levels of osteocalcin secretion by hMSCs seeded on SiHA discs by day 24 of the study compared to the HA and the control group.

Both Osteocalcin and VEGF are critical for bone formation. Expression of the VEGF mRNA was observed to be higher on cells seeded on SiHA and HA discs in

comparison with the control group on days 3 and 6 of the study. This indicates the contribution of SiHA and HA biomaterials to the promotion of early expression of VEGF and consequently the process of vasculogenesis. Increased vascularisation is known to enhance mineralised tissue generation (Murphy et al., 2004). Hing *et al.* (2006) reported increased vascular ingrowth into micro and macroporous SiHA. The increased expression of VEGF in the hMSCs cells may therefore be a contributing factor in the increased vascular ingrowth within SiHA reported by Hing et al.

It is known that factors such as apoptosis and osteoblast heterogeneity which are regulated by maturational age, environmental and micro-environmental conditions at both transcriptional and post-transcriptional levels, contribute to implications for osteoblasts function *in vitro* (Malaval et al., 2006). Therefore it should be noted that the results obtained in this study need further analysis in terms of the use of a larger number of hMSCs samples.

The differences between the levels of DNA and mRNA expression and the relative protein expression for the tested genes at the given time points might have been due to incomplete translation of mRNA to protein at the time of the quantification process or the degradation of the mRNA/DNA, but the presence of the secreted protein due to the long life of the protein compared to the respective mRNA or DNA (Knab et al., 2004).

Further increasing the "n" number in terms of the SiHA and HA disc repeats to higher than 3 and also the use of hMSCs from a number of patients rather than just one, would also contribute to obtaining statistically significant results for the studied genes and protein expression data.

3.7 Conclusions

The ideal bone substitute material should allow for cell migration, attachment, proliferation, differentiation and deposition of mineralised osteoid matrix (Jarrahy et al., 2005). The results of this study indicate that overall Silicon substituted hydroxyapatite promotes the attachment, proliferation and differentiation of hMSCs to osteoblasts *in vitro,* irrespective of the presence of osteogenic supplements. The mechanism of osteoinduction by this biomaterial involves the influence of the chemical composition of SiHA on expression of osteogenic marker genes and secretion of the osteogenic proteins. Early osteogenic differentiation of hMSCs as a result of the earlier ending of cell proliferation and initiation of early bone matrix mineralisation through expression of the osteonectin gene can be the suggested factor involved in osteoinduction by this biomaterial. The current study investigated the in vitro mechanism of osteoinduction by silicon substituted hydroxyapatite. For further evaluation of this biomaterial as an osteoinductive biomaterial, an *in vivo* study of bone formation by SiHA needs to be carried out. It should be noted that bone formation *in vivo* involves a combination of immensely complex and different mechanisms from the in vitro test environment as different biological factors, including circulating body fluids, biological compounds such as proteins and growth factors, influence the mechanism of bone formation by bone substitute materials (Leewenburgh et al., 2006).

4 Chapter IV. Osteoinduction by Silicon substituted HA

4.1 Introduction

The bioactivity of bone graft materials can be enhanced to promote early/greater bone formation by the incorporation of elements present in natural bone into their chemical composition and structure. Gibson et al demonstrated that the incorporation of silicate ions into the structure of stoichiometric hydroxyapatite (HA) increases the bioactivity of this biomaterial. This substitution was shown to enhance the activity of osteoblast cells *in vitro* (Gibson et al., 1999). Further, the presence of silicate ions within the HA structure was demonstrated to accelerate osteoconduction and enhance the rate and amount of bone apposition (Patel et al., 2002). A study by Porter *et al* (2004) demonstrated earlier bone formation by SiHA implants through enhanced bone remodelling processes compared to pure HA. Silicate ion substitution is also known to enhance osteointegration of HA and the formation of a stronger contact between bone and this biomaterial (Vallet-Regi and Arcos, 2005). The level of silicate ion substitution significantly affects the amount of bone formation through osteoconduction. In a study by Hing et al (2006) 0.8wt% substitution was identified as the optimal level for promotion of bone formation.

Osteoconductive and osteoinductive calcium phosphate biomaterials, in combination with supplementary growth factors, bone morphogenic proteins (BMPs) and cell seeding onto the implant surface, are commonly used experimentally to enhance bone tissue regeneration and to make the implant more osteoconductive; however, an ideal bone graft substitute would promote bone formation without the use of supplementary factors. Osteoinduction by cytokines, such as BMPs, promotes bone formation through endochondral ossification (Mizutani and Urist, 1982; Kuboki et al., 2001) whilst osteoinduction by CaP biomaterials usually occurs by direct intramembranous ossification (Le Nihouannen et al., 2005). It has been shown that non calcium phosphate materials, such as natural sponges and titanium, can induce bone formation in non osseous sites (Urist et al., 1965). The process of osteoconduction by Si-HA through direct attachment, proliferation and differentiation of bone forming cells, enhanced bone remodelling, increased

dissolution and enhanced bone apposition rate has been studied by various researchers (Hing et al., 2006, Porter et al., 2006, Patel et al., 2002). Ectopic osteogenesis and osteoinduction by SiHA through stimulation of the differentiation of non osteogenic cells down osteoblastic lineage has not yet been investigated.

This chapter investigates the osteoinductive properties of Si-HA in comparison with pure HA and the effect of this biomaterial's chemical composition and structure on bone formation in non-osseous tissue through implantation in the paraspinalis muscle of sheep. The large size of the animal body allows for the insertion of larger implants and also more implants can be compared in one animal.

New bone formation by bone graft substitutes requires successful initial attraction of cells to the surface of the biomaterial; besides chemical composition as mentioned above, this cellular response is also affected by the surface structure of the biomaterial (Boyan et al., 1996). The presence of interconnected macro (>10μm) and micropores (<5 μm) and the physiochemical properties of the biomaterial determine which and how molecules and cells can absorb, attach and move into the biomaterial's structure (Bronzino, 2006; Boyan et al., 1996; Ripamonti et al., 1999; Christophy et al., 2008). Daculsi et al (1989) demonstrated that the bioactivity of HA and the rate and level of bone formation is enhanced through the incorporation of microporosity. Based on this information, this chapter also investigates the effect of strut porosity on the level of bone formation within SiHA and HA implants.

4.2 Aims and Hypothesis

The aim of this study is to investigate the osteoinductive potential of Silicon substituted hydroxyapatite and the effect of chemistry and strut porosity on bone formation.

The hypotheses for this experiment are that:

1. The presence of silicate ion within hydroxyapatite induces superior bone formation compared to pure HA through osteoinduction when implanted in an ectopic site.

2. Microporosity of ~30% within the biomaterial struts results in greater new bone area compared to 10% or 20% strut porosity.

3. Granular and block implants induce different amounts of bone formation.

4.3 Materials and methods

4.3.1 Study design

To assess the osteoinductive properties of SiHA in comparison with HA, preliminary data was obtained from a study carried out by Patel et al (2002). To achieve significance of $P< 0.05$, the study was designed for comparison of two types of calcium phosphate bone substitute biomaterials in (n=4) an ectopic site where the overall standard deviation is around 8% (normal distribution with equal variation), with power of 0.8 using the Shoenfeld's power analysis software. Using this data eight skeletally mature commercially bred female sheep aged between 4-6 years old and weighing of 65-80kg were used in this experiment to study the osseoinductivity of 0.8wt% SiHA compared to HA. Further, the effect of strut porosity and implant morphology on osseoinduction of Silicon substituted hydroxyapatite (SiHA) and pure stoichiometric hydroxyapatite (HA) biomaterials was investigated. Fifty, HA [ApaPore, ApaTech Ltd. B021-2005] and SiHA [Actifuse, ApaTech Ltd. B008-2005G, B040-2005 and B096-2005A] granules (2-6 mm) and blocks (15x15mm) were randomly and intramuscularly implanted in the paraspinalis muscle of eight sheep for 12 weeks (Figure 68).

To assess the effect of microporosity on bone formation, four SiHA granules and block samples with 10% (SiHA10), 20% (SiHA20) and 30% (SiHA30) strut porosity and HA granules and blocks of 20% (HA20) and 30% (HA20) strut porosity were used. Both HA and SiHA biomaterials manufactured by ApaTech Ltd. contained 80% total porosity (

Table 9).

Table 9. SiHA and HA implants porosity levels

Composition	SiHA10	SiHA20	SiHA30	HA20	HA30
Strut Microporosity	10%	20%	30%	20%	30%
Total Porosity	80%	80%	80%	80%	80%

4.3.2 XRD and XRF Chemical Analysis

X-ray diffraction analysis patterns of HA and SiHA samples did not indicate the presence of any $Ca_3(PO_4)_2$ (TCP) or CaO secondary phases (Figure 67). The Ca/P ratio of HA and Ca/(P+Si) ratio of SiHA found by XRF spectrometry analysis were detected to be 1.67, equivalent to the value of phase pure HA. Further XRF elemental analysis confirmed the levels of silicate ion within SiHA as 0.8wt%.

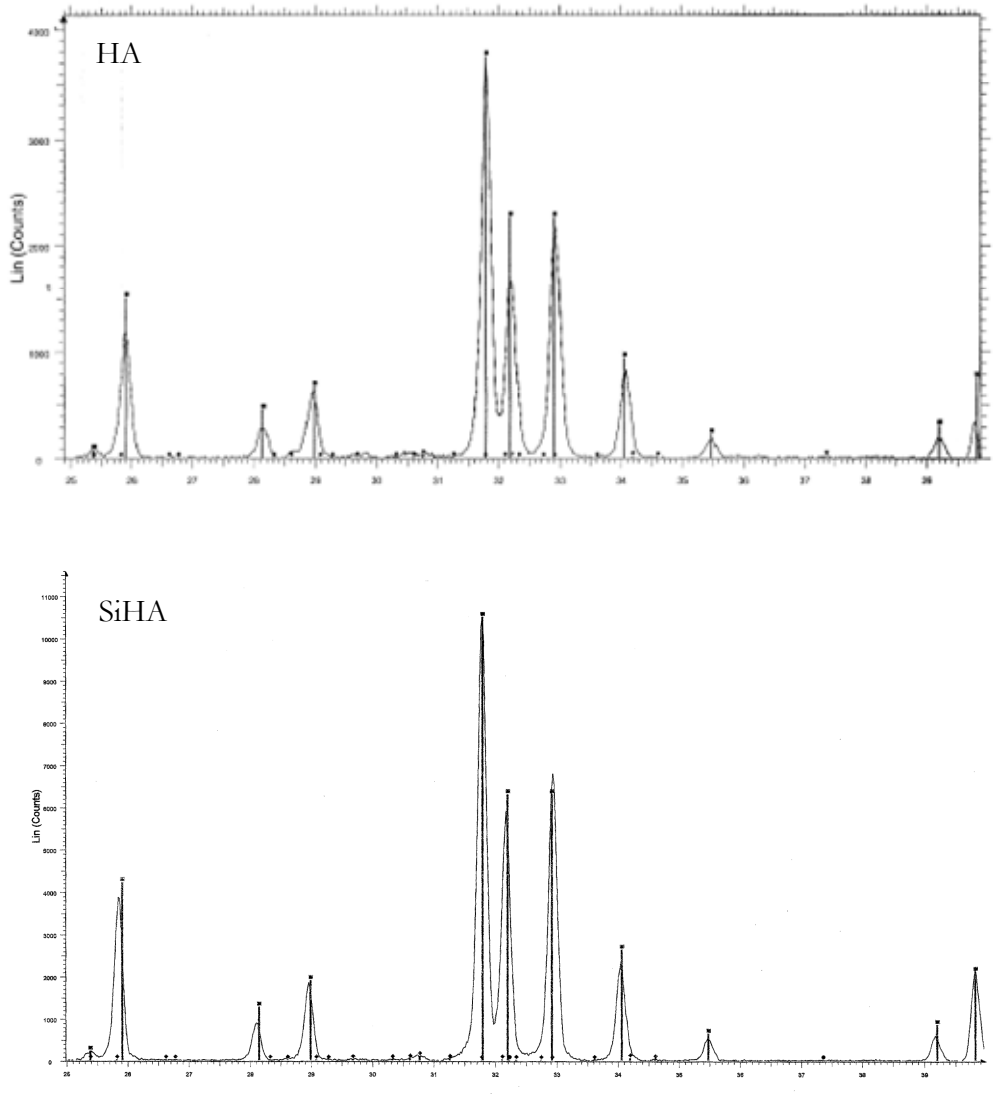

Figure 67. XRD patterns for HA and SiHA samples.

4.3.3 Surgery

All procedures in this experiment were performed in accordance with the Animals Act 1986 (Scientific Procedures) at the Royal Veterinary College, South Mimms. All members of the surgical group held the required Home Office licenses. Sheep used in the operations were starved 12 hours prior to surgery. Each animal was premedicated by intramuscular administration of Xylazine [Rompun 2%] (0.05 ml/kg) 10 minutes before the induction of anaesthesia. The animal was then anaesthetised by intravenous administration of Ketamin [Ketaset] (0.2 ml/kg) and Midazolam [Hypnovel] 2.5 mg. Anaesthesia was then maintained by administration of Halothane (2%) and Oxygen mixture.

The sheep were placed in dorsal recumbency and the fleece on the centre of the animals back above the paraspinous muscle was shaved to expose the skin. The exposed skin was then washed with a solution of Pevidine surgical scrub and water. Surgical scrub was then made into lather to further clean the skin; this process was repeated three times. Sterilization of the surgical site was carried out by washing the site from the centre to the outer areas by using a sterile swab and Pevidine antiseptic solution. The surgical site was further disinfected by wiping the area with Hydrex [Chlorohexadine Gluconate] solution.

The paraspinal muscles along the right and left of the spine adjacent to the lumbar vertebrae were identified and four longitudinal incisions of a few centimetres were then created through the skin, superficial and deep fascia to expose the paraspinal muscles. Blunt longitudinal dissections were then made along the muscle fibre to create a gap within the muscle tissue. The blunt incisions were in line with the fibres of the muscle tissue and not perpendicular to the direction of the fibres. Cylindrical plastic containers of 30mm x 15mm in diameter were lined with stainless steel mesh in order to constrain the HA and SiHA granules in place. Granules of HA/SiHA sterilised with hydrogen peroxide vapour were tipped into the tubes and impacted together by hand using tapping force. Autologous jugular venous blood obtained from the sheep was added to the granules and left to coagulate. The construct was then removed from the container and inserted into the muscle gap. Sterilized HA/SiHA blocks of 15mm x 15mm were then inserted into the muscle gap (Figure

68). The incisions were closed by bringing the layers together using absorbable Vicryl sutures. The animals were recovered from anaesthesia and an intramuscular daily dose of Ceforex (Cefalexin) antibiotic was administered for 5 days post operation.

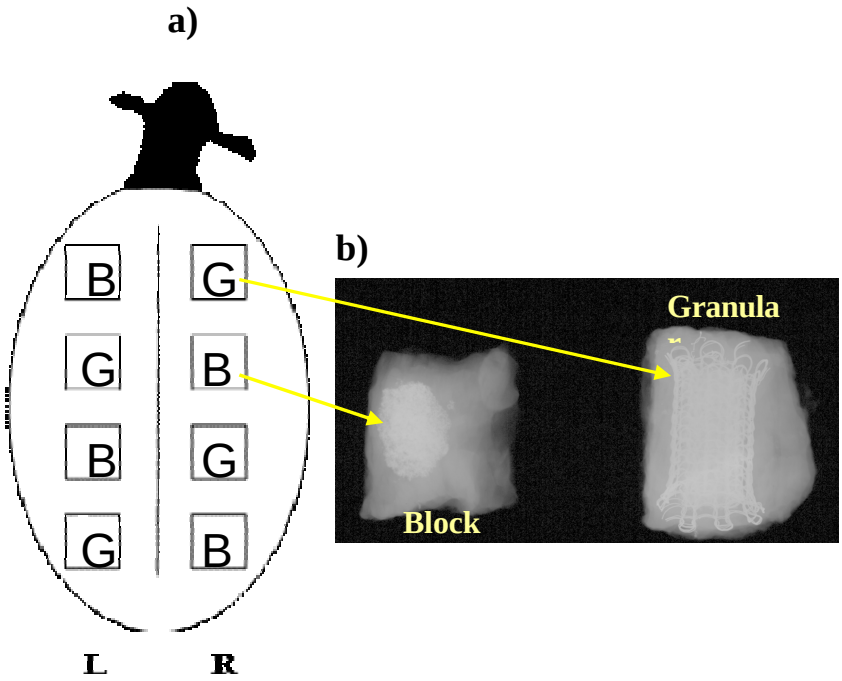

Figure 68. a) Image illustrating the location of the implants. b) Radiograph of granular and block implants.

4.3.4 Undecalcified Hard Resin Histology

Following retrieval of the implants and the surrounding tissue at week 12, the samples were fixed by immersion in 10% neutral buffered formalin at room temperature for 7 days. Histology processing of the samples was carried out as described in chapter II. Dehydration and defatting of the samples were carried out by using increasing concentrations of ethanol and chloroform respectively, followed by infiltration and embedding in 100% LR white resin (London Resin Co Ltd).

Thin sections (100 μm thick) were then made by sectioning the resin embedded samples longitudinally through the centre of the biomaterial using an Exakt saw (Exakt, Germany). The obtained sections, were then ground to the desired thickness by using an Exakt micro-grinding system and then polished to eliminate the scratches on the surface of the sections using the Motopol 2000 machine. The prepared thin

sections were stained for histomorphometric analysis by staining the section with 10% Toluidine Blue for 20 minutes to stain the fibrous tissue, followed by 15 minutes of staining with Paragon, which was prepared by mixing of toludin blue and basic fuchsin in ethanol, to stain the new bone.

4.3.5 Histomorphometry Analysis

The area occupied by the new bone formed within the implanted biomaterial and the new bone contact with the biomaterial was quantified using the Axiovision 4.5 image analysis system. Eight images of each thin section slide were obtained at 5x magnification and the quantification was carried out as percentage of new bone area, new bone contact, percentage of biomaterial and percentage of soft tissue by the use of a grid system as described in chapter II.

4.3.6 BSEM and EDAX Analysis

Back scattered electron microscopy (BSEM) and Energy Dispersive X-Ray analysis (EDAX) were carried in order to analyse bone formation and the elements present within the HA and SiHA samples. One thin section sample slide from each of the porous SiHA and HA groups were mounted on aluminium stubs and then sputter coated with gold palladium particles using an EMITECH K550 machine (Emitech, UK). The coated slides were then analysed using a JOEL JSM-5500LV scanning electron microscopy unit (Joel Techniques, UK) and back scattered electron microscopy images of the samples were obtained. Elemental maps of the samples containing new bone were also obtained using Energy Dispersive X-ray microanalysis (EDAX, UK) to investigate the elements present in the newly formed bone and soft tissue next to the implanted biomaterial.

4.3.7 Statistical analysis

Statistical analysis of the data collected from this experiment was carried out using the statistical software SPSS v10.1. Mann-Witney U statistical test was used to analyse non parametric data and $P < 0.05$ was considered to be significant.

4.4 Results

4.4.1 Histomorphometry

4.4.1.1 Chemistry

4.4.1.1.1 Bone Area

The results of histomorphometric analysis of the Silicon substituted hydroxyapatite (SiHA) samples in comparison with pure HA samples (n=4) indicated significantly (P=0.014) greater bone area within SiHA samples compared to HA samples at 12 weeks (Figure 69).

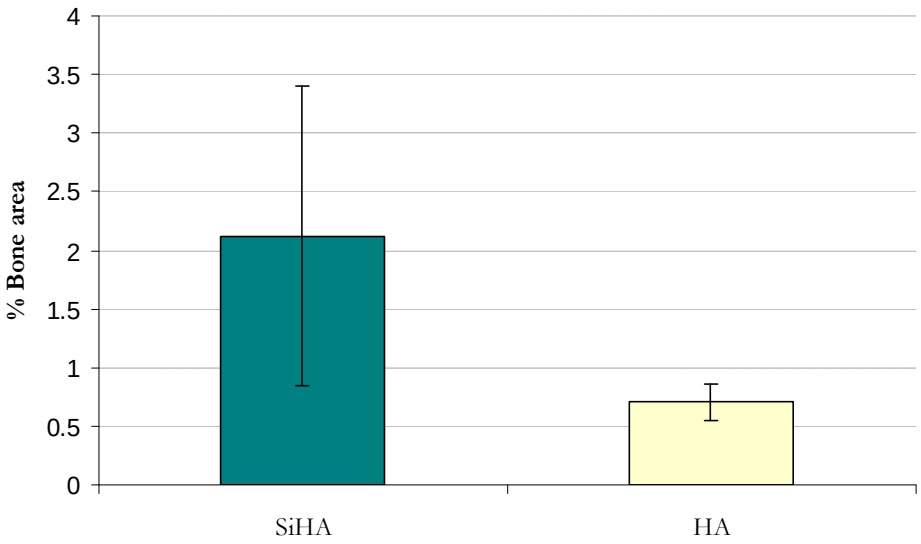

Figure 69. Bone area within SiHA implants compared to HA implants.

4.4.1.1.2 Bone contact

Analysis of new bone contact with the implanted SiHA and HA biomaterials indicated significantly (P=0.005) greater bone contact with SiHA samples compared to HA samples (n=4) (Figure 70).

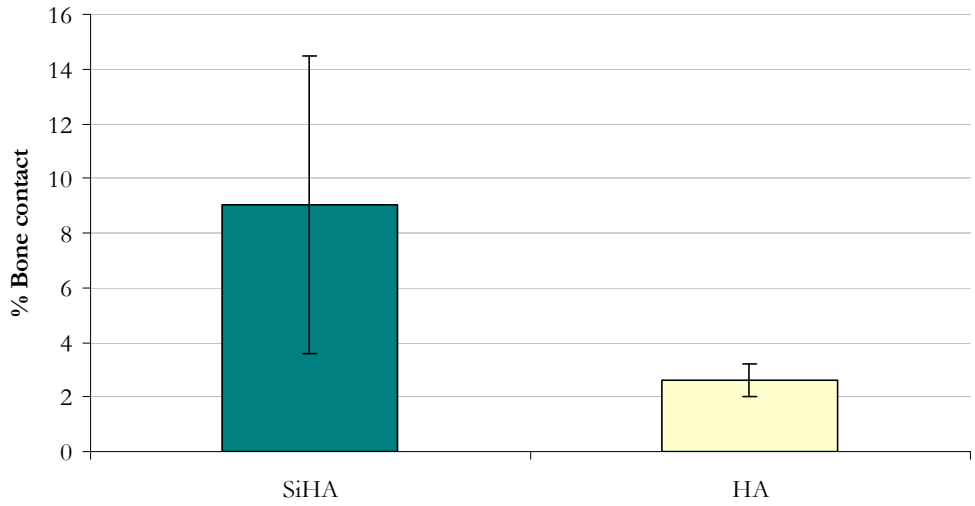

Figure 70. Graph showing % bone contact within SiHA and HA samples.

4.4.1.2 Strut porosity

4.4.1.2.1 Bone Area

Significantly greater (P=0.007) bone formation was observed in SiHA30% samples compared with SiHA20%. More than 4% of the area of SiHA30% samples was filled with new bone (Figure 71).

HA30% samples indicated greater bone formation compared to HA20% samples, however this difference was not significant (P=0.591). Significantly greater (P<0.05) bone formation was promoted by SiHA30% compared to HA30% samples. No bone formation was observed within SiHA10% samples (Figure 71).

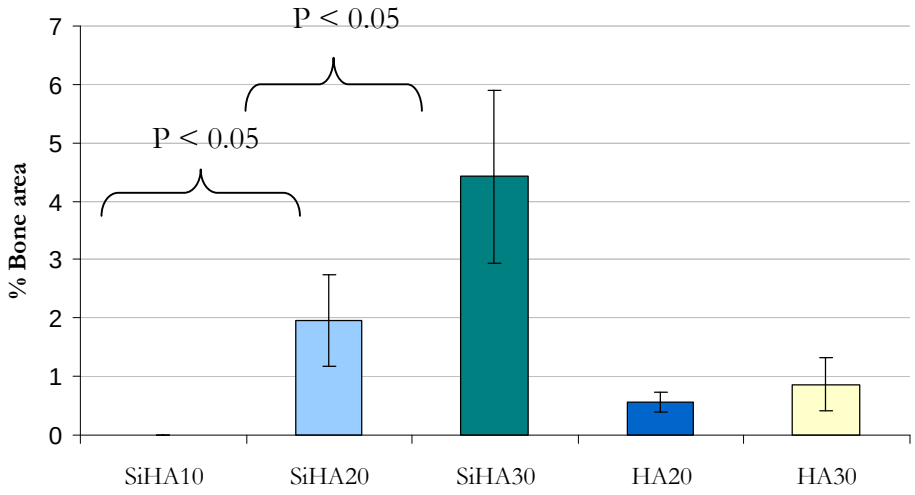

Figure 71. Bone area within SiHA and HA samples with different levels of strut porosity.

4.4.1.2.2 Bone Contact

The results of bone contact between the implant and new bone indicated greater bone contact in samples with the highest (30%) microporosity. Comparison of SiHA30% with SiHA20% and SiHA10% implants showed significantly greater bone contact in SiHA30% samples. HA30% implants also indicate greater bone formation compared to HA20%, however the difference in levels of bone contact between these samples was not significant (Figure 72).

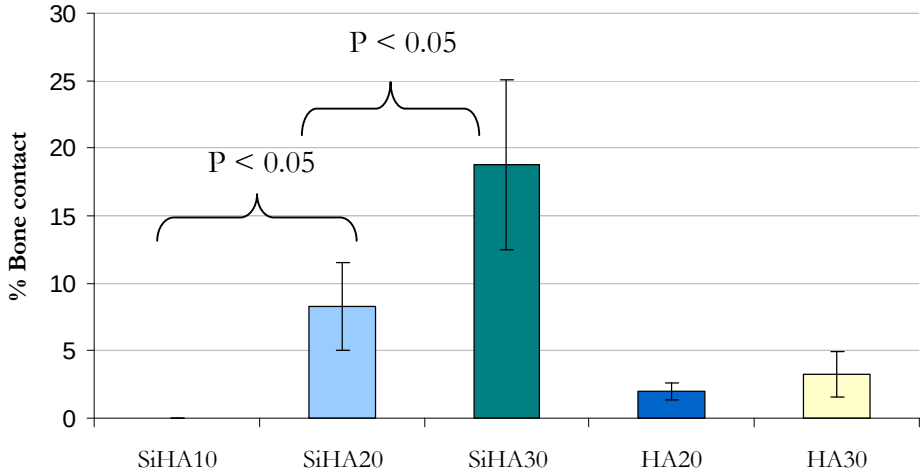

Figure 72. Bone contact measurements for SiHA and HA implants with different strut porosity.

4.4.1.3 Granules vs. Blocks

4.4.1.3.1 Bone Area

Comparison of bone formation within SiHA and HA samples in granular and block forms did not indicate any differences in the amount of bone formation. SiHA20% samples showed greater bone formation in block form compared to granular samples, whereas SiHA30% samples showed greater bone formation within the granular samples compared to the block samples (Figure 73). Greater bone formation was observed within the granular implants of HA20% samples compared to the block implants. Block implants of HA30% implants showed greater bone formation compared to the granules of this material (Figure 73).

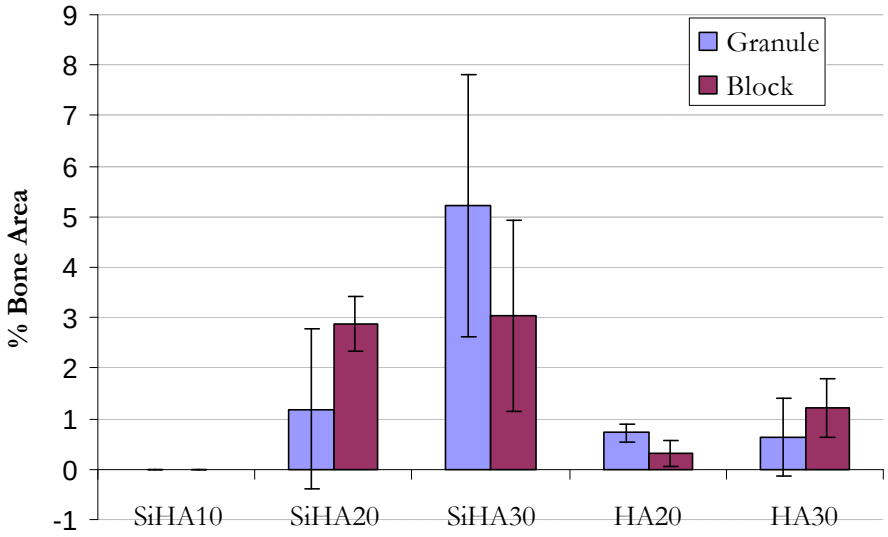

Figure 73. Bone area within granular and blocks of SiHA and HA implants.

4.4.1.3.2 Bone Contact

Comparison of bone contact in granular implants compared to block implants did not indicate any specific differences. Both HA20% and HA30% samples show greater bone contact in block implants. SiHA 30 samples show greater bone attachment for granular implants, whereas SiHA20% samples show greater bone attachment to block implants (Figure 74).

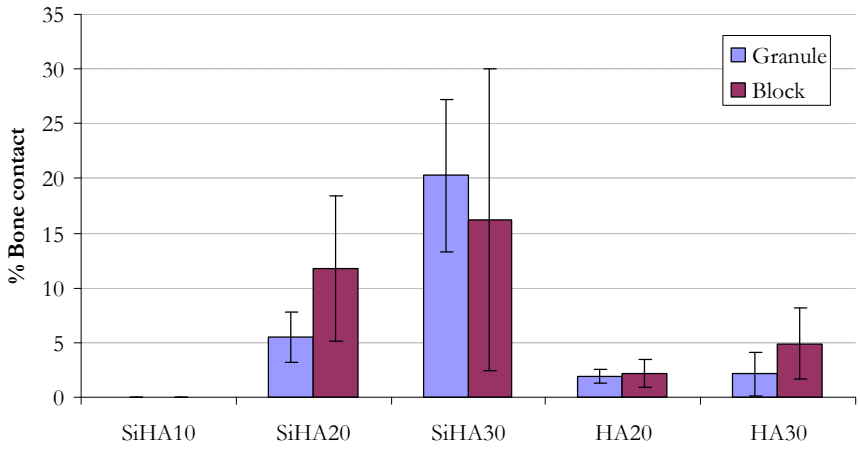

Figure 74. Bone contact in granular and blocks of SiHA and HA samples.

4.4.2 Histology (Light microscopy and SEM analysis)

4.4.2.1 Chemistry

Histological analysis of SiHA and HA samples demonstrated bone formation in both SiHA and HA samples. Light microscopy images indicated extensive osteoinduction through intramembranous ossification within SiHA samples (Figure 75) as no sign of cartilage formation was observed. Bone formation in all samples indicated close association with the implant particles. No sign of inflammatory response was observed within the samples. Presence of osteoblast cells and osteocytes in the vicinity of the implant surfaces indicated active sites of new bone formation (Figure 78).

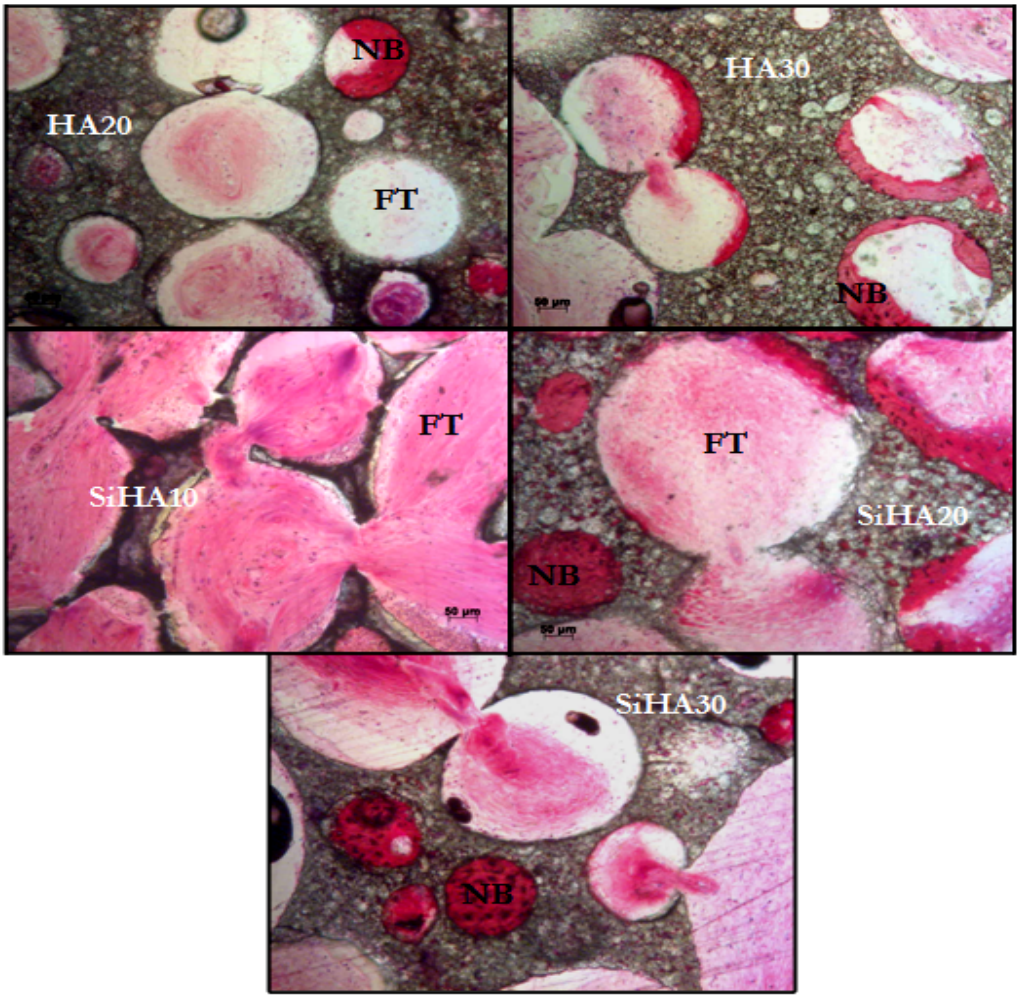

Figure 75. Images illustrating bone formation on HA 20 and 30% and SiHA 10, 20 and 30% samples. FT: Fibrous Tissue. NB: New Bone. No bone formation was observed in SiHA10 samples.

Detailed analysis of light microscopy images indicated the presence of blood cells and fibrous tissue at the implant interface within all groups (Figure 76). Fibrous tissue infiltration within the pores and between the pores of the SiHA and HA samples was observed (Figure 77 and Figure 81). The presence of osteoblasts responsible for bone remodelling was also observed (Figure 77).

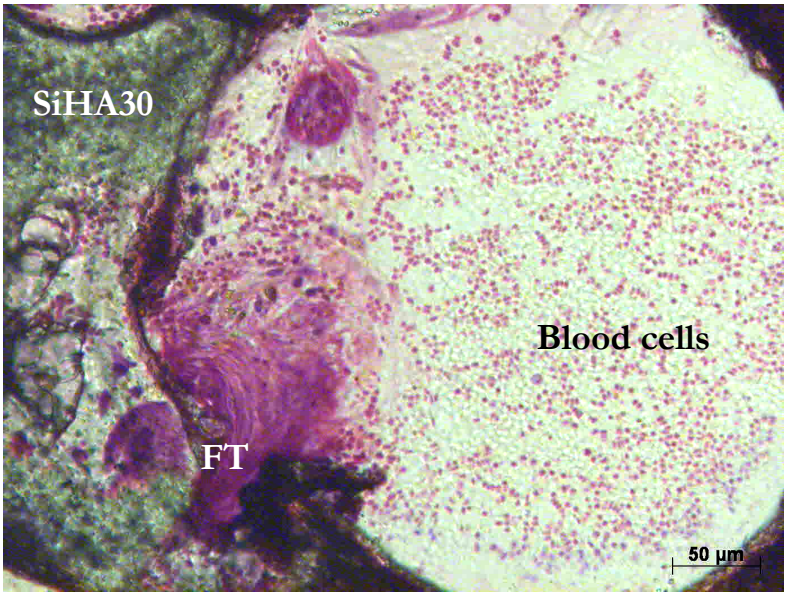

Figure 76. Blood cells at the implant interface within a pore.

Figure 77. Soft tissue infiltration within implant pores. FT: Fibrous tissue, BC: Blood cells.

Zones of osteoid formation by osteoblast cells on the surface of the implant pores were detected as illustrated in Figure 78 (a). New bone deposited by osteoblast cells was observed to be localized circumferentially on the surface of the pores (Figure 78(b)). The centre of the pores represented a zone of undifferentiated mesenchymal tissue (Figure 79). High magnification images of the thin sections indicated zones of osteoid formation within the centre of the biomaterials pores (Figure 79).

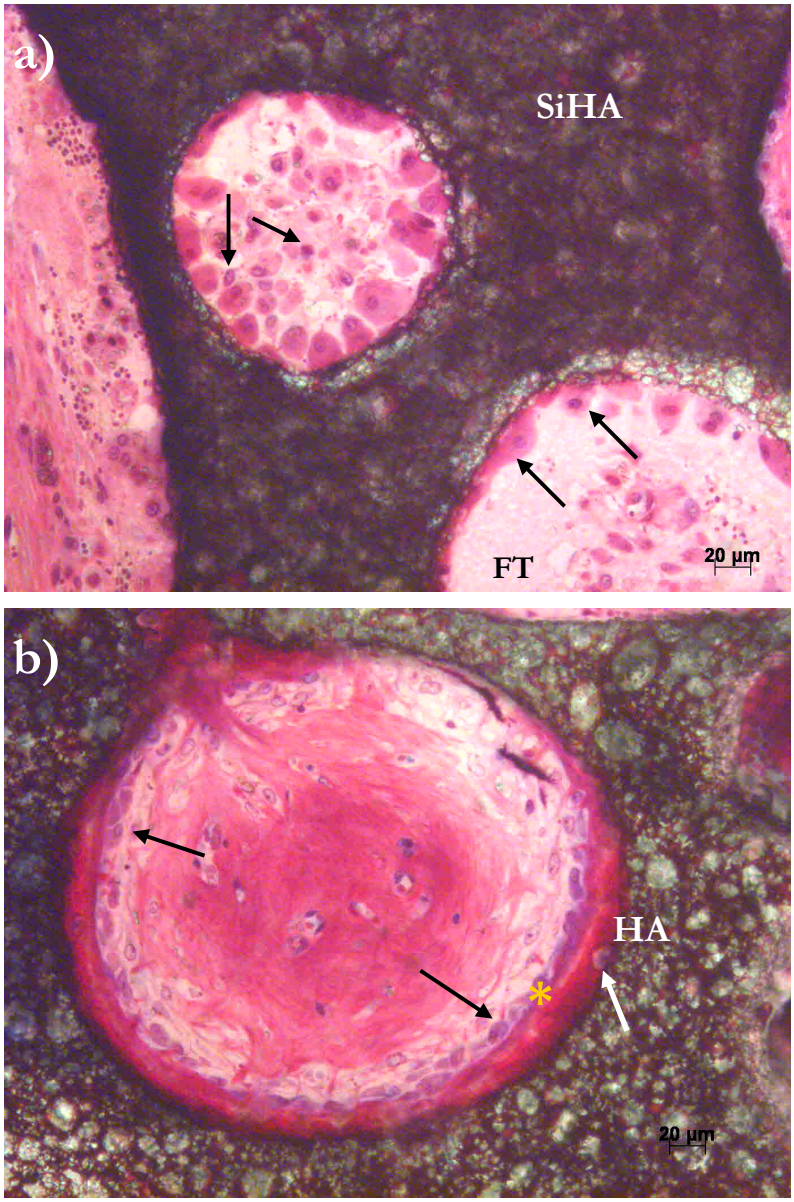

Figure 78. New bone formation within SiHA and HA. Black arrows indicate osteoblasts, white arrow indicates osteocyte. Star indicates bone matrix. FT: Fibrous Tissue.

Figure 79. High magnification image of osteoid formation within SiHA and HA implants.

4.4.2.2 Strut Porosity

Comparison of bone formation within HA and SiHA samples with different strut porosity levels indicated greater bone formation in samples with higher porosity (Figure 80 and Figure 81). SiHA samples indicated greater bone formation compared with HA samples with the same level of strut porosity (Figure 80 and Figure 81).

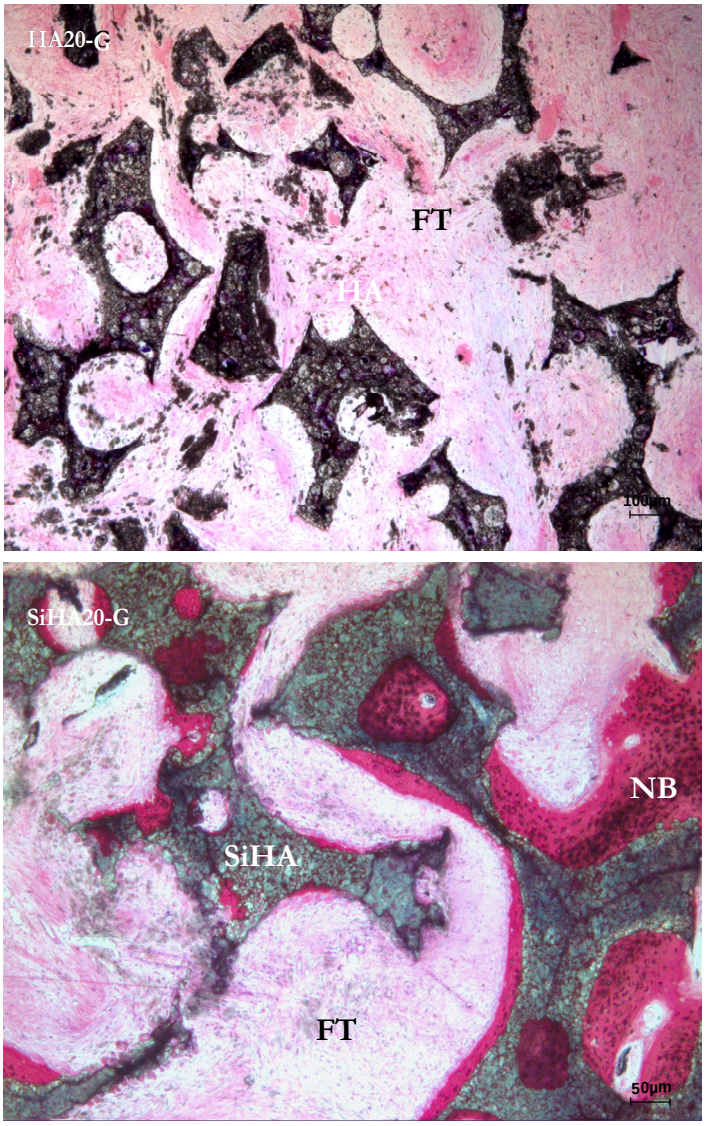

Figure 80. Histology images illustrating new bone within HA20 and SiHA20 implants. NB: New bone, FT: Fibrous tissue.

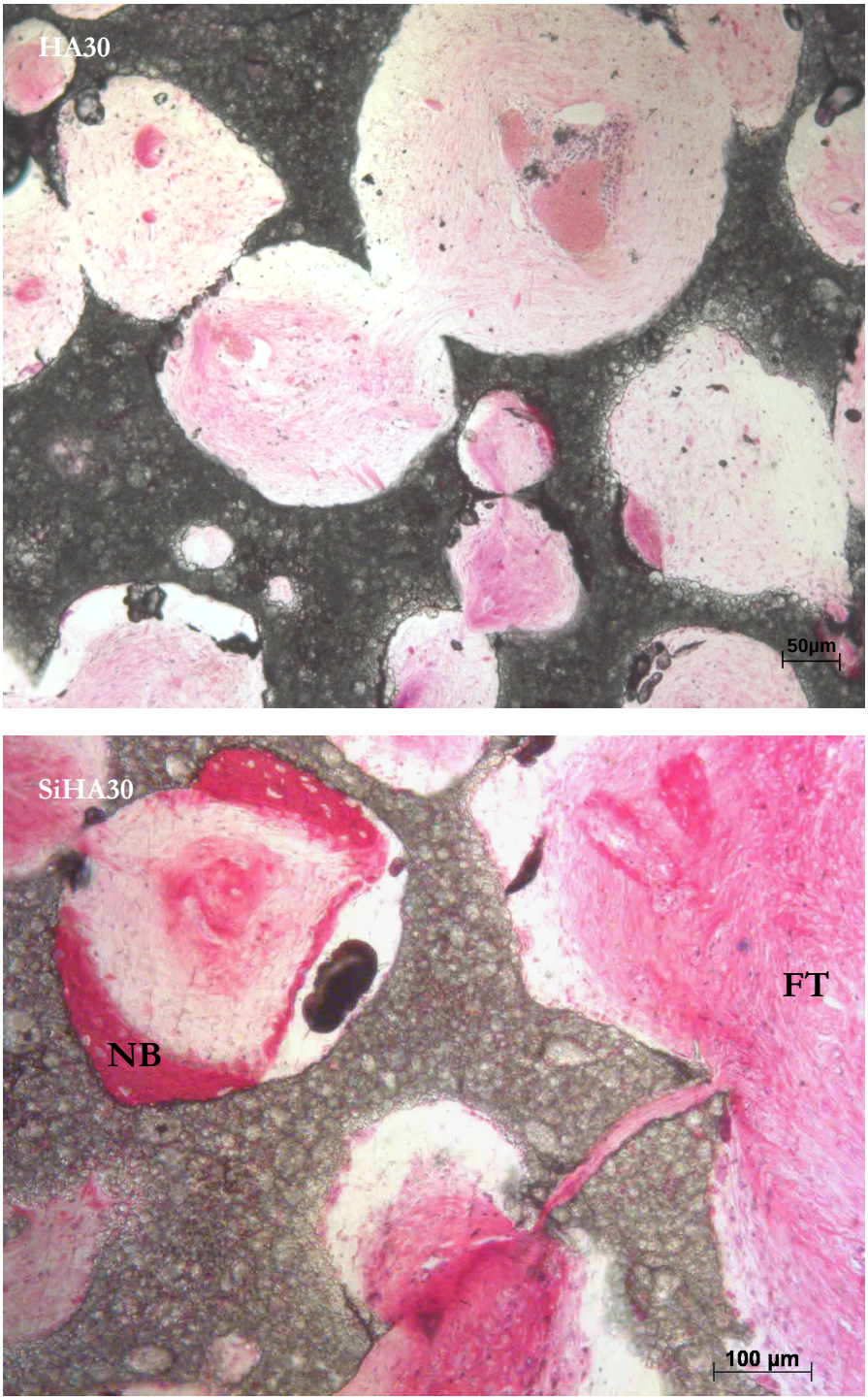

Figure 81. Light microscopy images of newly formed bone within HA30 and SiHA30 samples. NB: New Bone; FT: Fibrous tissue.

Analysis of the back scattered electron microscopy (BSEM) images indicated that all implants presented highly cellular, disorganised woven bone. SiHA30% samples indicated greater bone formation compared to other samples (Figure 82).

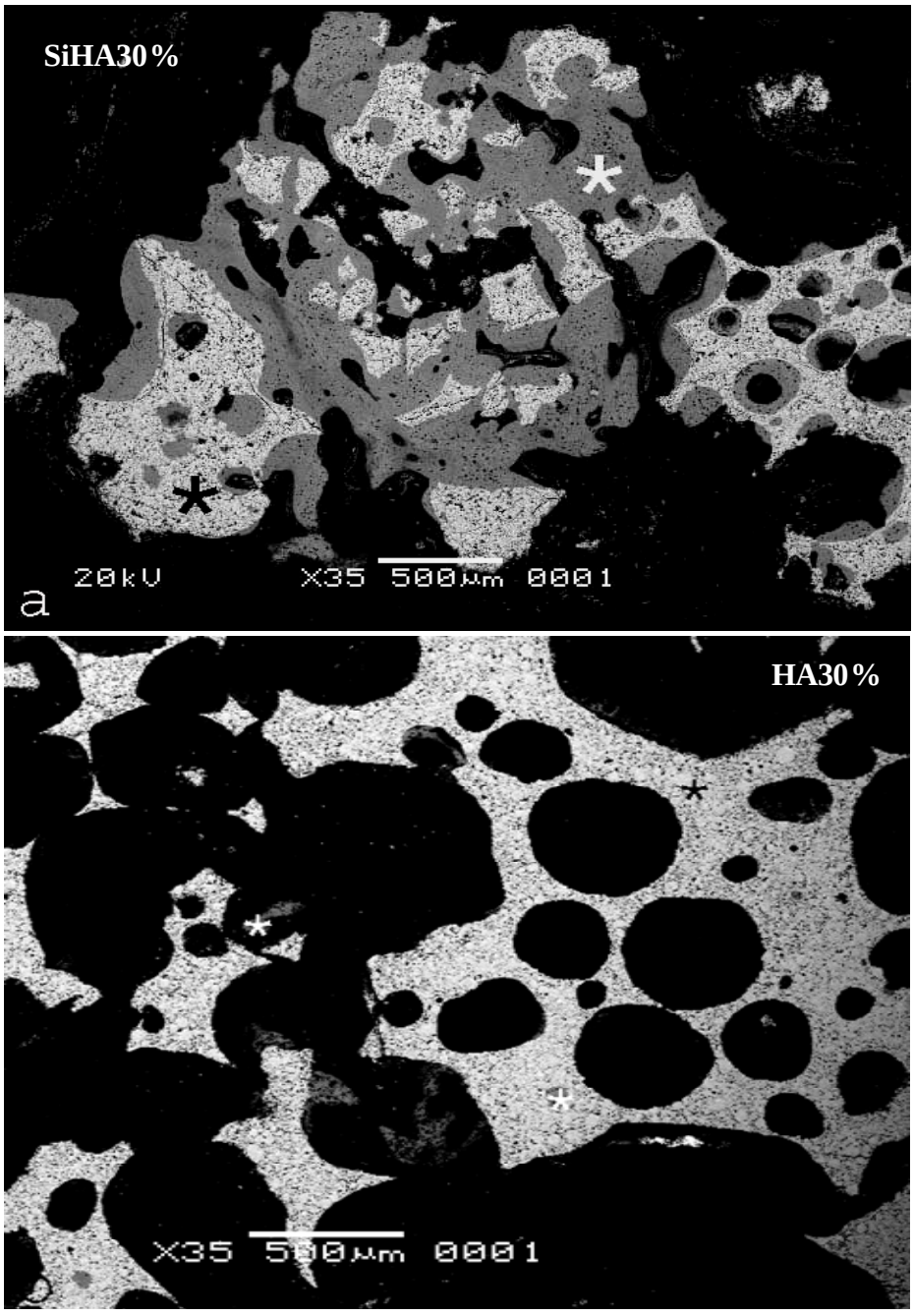

Figure 82. BSEM images illustrating new bone within SiHA30 and HA30% samples. White star indicates woven bone. Black star indicates biomaterial.

Bone formation was observed within macro and micropores of both HA and SiHA samples. High magnification images of thin sections of the implant samples indicated preferential bone formation on the concave surface of the implant pores, within the macropores of the implant and also deep within the micropores. Stained samples and SEM images indicated visible bone formation within pores of less than 20 μm. Zones of newly deposited bone were observed on all samples (Figure 83).

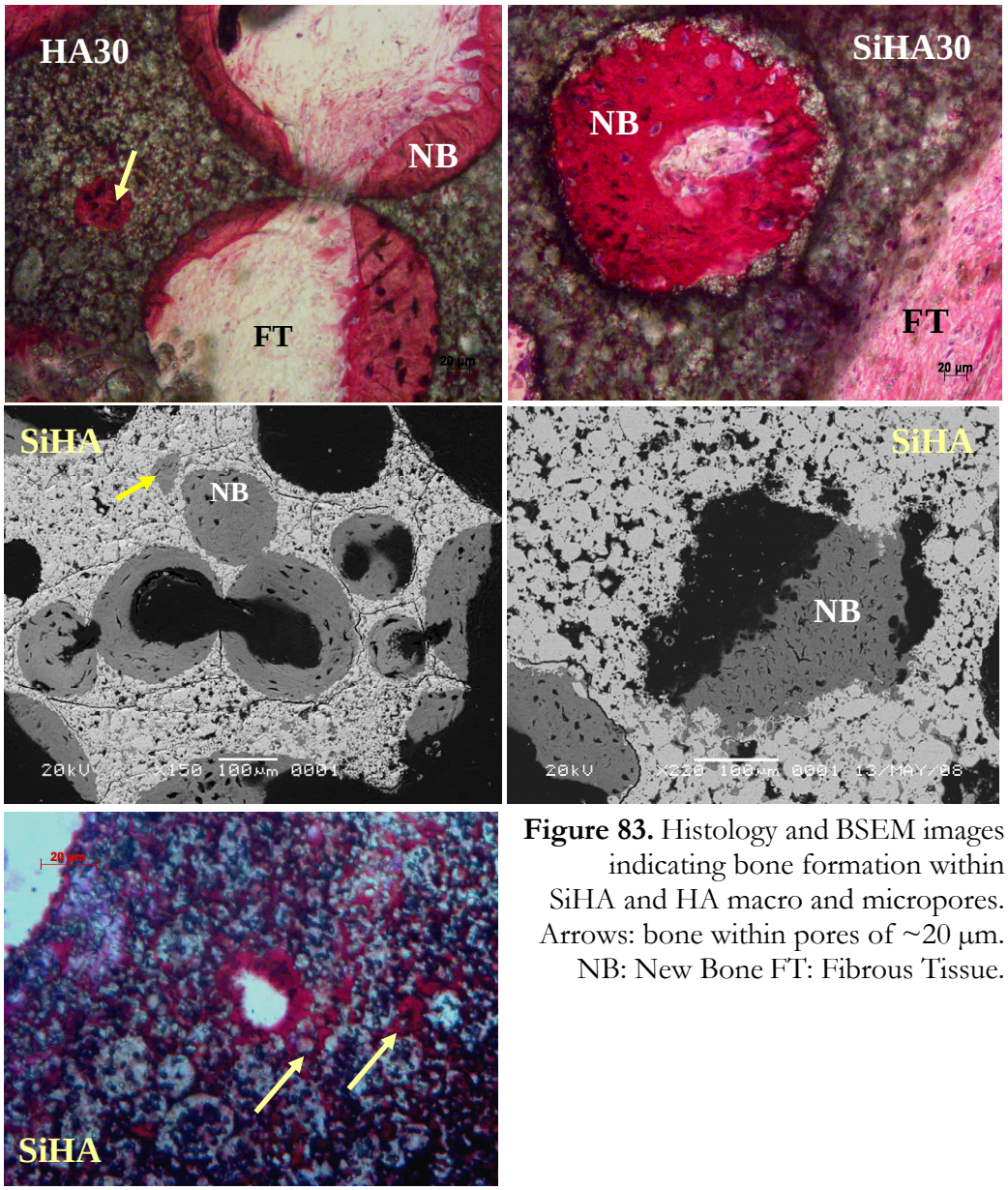

Figure 83. Histology and BSEM images indicating bone formation within SiHA and HA macro and micropores. Arrows: bone within pores of ~20 μm. NB: New Bone FT: Fibrous Tissue.

4.4.2.3 Granules vs. Blocks

Analysis of stained thin section samples of granular and block SiHA and HA samples did not indicate any clear effect due to these morphologic differences on bone formation (Figure 84).

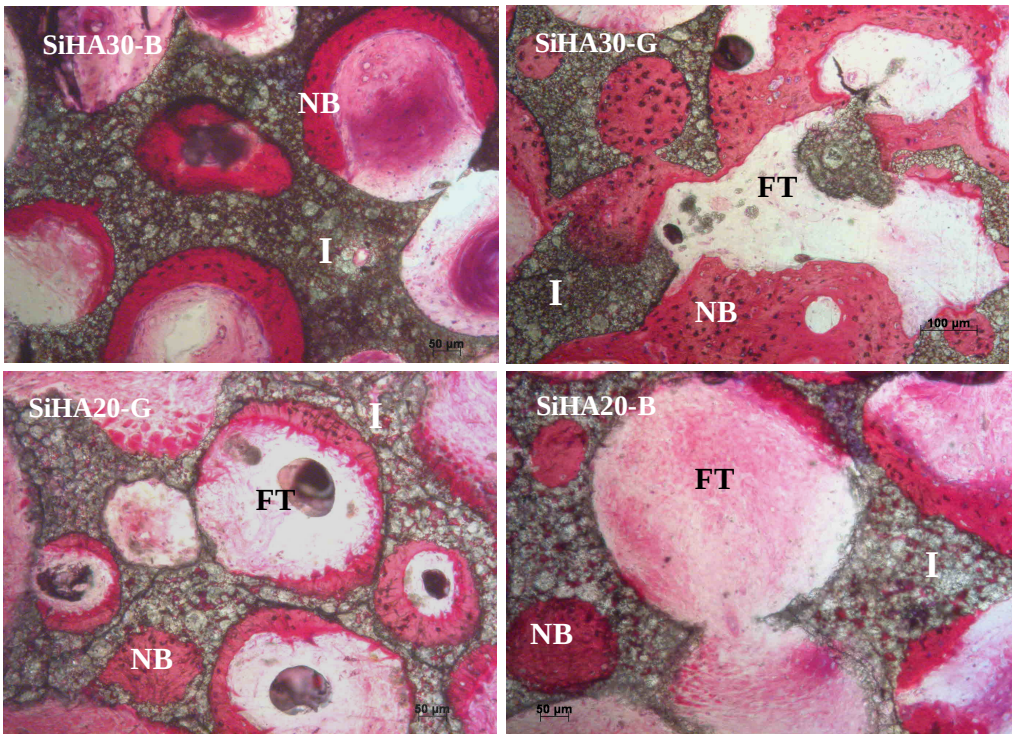

Figure 84. Histology images of block (SiHA30-B) and granular (SiHA30-G) implants illustrating new bone formed within the implant NB: new bone, FT: fibrous tissue.

4.4.2.4 New bone characterisation

EDAX analysis of SiHA samples indicated the presence of Calcium, Phosphorous, Silicon, Oxygen and Carbon elements within the samples. The elemental maps obtained from a section of SiHA sample containing a pore filled with new bone indicated the presence of silicon within the newly formed bone. Silicon was also present in the soft tissue adjacent to the biomaterial, however in lesser levels than within the new bone. Strong signals of carbon were detected within the soft tissue. Peaks of calcium (Ca) and Phosphorous (P) confirmed the new bone composition within both macro and micropores of the samples, as illustrated in Figure 85.

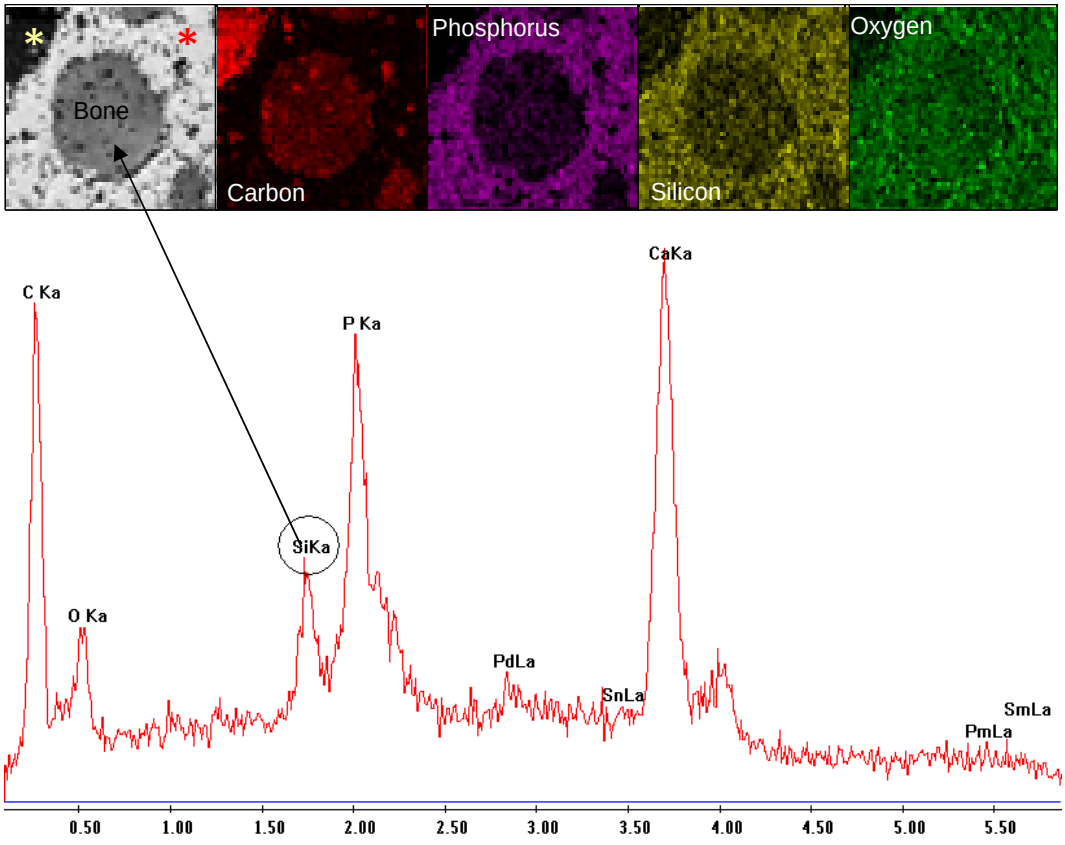

Figure 85. EDAX map of SiHA. Yellow star: Soft tissue, Red star: Implant.

4.5 Discussion

4.5.1 The effect of Silicate ion substitution on osteoinduction

This study demonstrated the chemical influence of Silicon substituted HA on the promotion of bone formation within non-osseous tissue. The paraspinalis muscle was chosen for this study to eliminate the osteoconductive influence of host bone on bone formation. The ovine animal model was selected for this study as the bone metabolism of sheep is more similar to that of humans and sheep represent more similarities in terms of weight, bone, joint structure and bone regeneration (Patel et al., 2005, Nus et al., 2006). In addition, studies carried out on osteoinduction mechanisms have shown that osteoinduction is induced variably depending on the nature of the species. Also, it is known that bone formation is not induced in rat or mice animal models and rabbits present minimal bone formation. Therefore the best models identified so far are known to be those of the large mammals group, sheep (Gossain, et al., 2002) dogs (Yuan et al., 2000) and non-human primates, such as baboons, as demonstrated in many studies by Ripamonti et al (Habibovic et al, 2006). The study by de Bruijn in 1998 also demonstrated bone formation by HA in goat animal models.

The results of this study indicated that at 12 weeks new bone formation was visible within the implanted SiHA and HA granules, and blocks with SiHA samples presented superior bone formation. This study illustrated the role of biomaterial chemistry in promotion of bone formation, irrespective of structural porosity, as comparison of the samples with different porosities indicated that SiHA30% and 20% implants showed the greatest bone formation and attachment compared to HA30% and 20% samples. The *in vivo* interactions between the implant and surrounding tissue engages highly complex mechanisms including many cellular and tissue specific factors, material properties, structural characteristics and numerous other undefined factors (Barrera et al., 2006). Promotion of bone formation on a biomaterial is dependent on the cellular mechanisms that are triggered during the point of implantation and the provoked inflammatory responses leading to tissue repair. Tissue damage triggers immediate cellular responses initially through the

formation of a blood clot which ignites a series of cellular mechanisms (Lanza et al., 1997). In this study, immersion of the SiHA and HA samples into autologous blood was suggested to result in exposure of the biomaterial to host specific substances. Upon insertion of the SiHA and HA granules and blocks coated with blood into the muscle bed, the surface of the biomaterials were covered with a layer of plasma proteins from the host blood, followed by adhesion and activation of platelets. Platelet activation triggers the release of growth factors and cytokines essential for wound healing. This mechanism triggers the attraction of undifferentiated cells towards the surface of the biomaterial and the formation of a blood clot facilitates the movement of the cells through a biological matrix of fibrin and proteins (Gemmel and Park, 2000). This in turn enhances the bonding and the cell-implant interactions, resulting in consequent cell differentiation and implant bioactivity.

As histological analysis showed the presence of blood within the samples, it was concluded that following implantation in the animal body, the ideal living bioreactor, the pores and spaces within the samples were filled with circulating blood. The presence of proteins and growth factors in blood and body fluids, in addition to the recruitment of mesenchymal stem cells present within the muscle tissue into the implant area, were elucidated to have contributed to the initiation of the process of osteoblast differentiation and bone generation (Kilpadi et al., 2001).

Surface roughness and chemistry of the biomaterials influence the initial blood to implant interactions through platelet adhesion and activation, protein adsorption and also cell attachment to the surface of biomaterials (Schwarts and Boyan, 1994; Park and Davis, 2001). Cells' focal attachments with the biomaterial surface determine the shape of cells; this in turn is transduced to the nucleus via the cell cytoskeleton resulting in expression of specific phenotypes. The biomaterial's surface chemistry influences the function of osteoblast cells, which in turn affects the rate of bone formation on the biomaterial (Boyan et al., 1996). Substitution of Silicate ions within HA is known to lower the surface charge of HA and also increase the pH levels in solution to a more alkaline pH (Rashid et al., 2008). It is known that positive and negative surface charges influence osteoblast adhesion to the biomaterial (Teller et al., 2006). Further substitution of 0.8wt% silicate ion is known to increase the

hydrophilicity of HA and contribute to superior protein exchanges. The surface composition is known to influence the protein conformation and consequently adsorption to the surface (Rashid et al., 2008). Protein adhesion to the biomaterial surface is mediated through the activity of the present negative and positive charged groups and their affinity for specific ions available on the biomaterials surface. Cell attachment, on the other hand, is dependant on cell-protein interactions through the RGD sequences. Thus, the negative surface charge of SiHA is suggested to affect the binding efficiency of proteins to the biomaterial surface and consequently influence the cell attachment and bioactivity of this biomaterial. Zuo et al (2008) have shown that Silicon substitution into hydroxyapatite influences the adhesion of human osteoblast-like cells *in vitro*. The influence of the net negative surface charge of SiHA in line with the role of material surface charge on cell adhesion suggests a role for superior osteoinduction in SiHA samples compared to HA samples (Balas et al., 2002).

Enhanced bone formation by SiHA samples compared to HA samples is suggested to be due to the effect of the dissolution of silicate ions into the surrounding area provoking enhanced reactivity of the material and promotion of an osteoinductive biological response (Porter et al., 2004). A study by Guth et al (2006) showed low levels of silicon release from SiHA samples *in vitro*. In my study EDAX analysis of the samples indicated the presence of silicon within the newly formed bone. The observed silicon peaks suggest the incorporation of silicate ions into the new bone from the biomaterial. Silicon substituted HA is known to show localized grain boundary dissolution (Botelho et al., 2002; Porter et al., 2003). *In vitro* studies have shown that soluble silicate ions stimulate the expression of collagen-I in osteoblast-like cell cultures (Zuo et al., 2008). Reprecipitation of the released silicate ions after the initial dissolution from SiHA (Guth et al., 2006) promotes the formation of apatite layers similar to the mineral component of the bone. This apatite layer on the surface of the biomaterial triggers a series of physiological reactions within the surrounding cells and acts as the ideal site for cell attachment, differentiation, growth and maturation (Weng et al., 1997; Porter et al., 2003) and consequently may account for the peripheral organisation of bone formation within the samples. The release of

silicate ions could have resulted in bonding of oxygen to these ions, forming a silicate network that contributes to the organisation of protein elements in a fashion that provides the ideal surface for protein absorption and cell attachment via integrins for connective tissue generation (Thian et al., 2006). This in turn may have stimulated the cells within the surrounding tissue, in this study the muscle tissue, to initiate osteogenesis. Immunohistochemical analysis and protein localisation at the SiHA-bone interface would provide a better understanding of the proteins involved in the mechanism of osteoinduction by this biomaterial.

Further, it can be assumed that the presence of silicate ions within SiHA samples or the surrounding tissue (as was indicated by EDAX analysis) may have influenced the expression of genes involved in osteogenesis, promoting the differentiation of the cells present in the muscle bed into osteoprogenitor and/or osteoblastic cells. *In vivo g*ene expression analysis of the genes involved in osteogenesis through the use of gene expression arrays may contribute to a better understanding of the effect of silicate ion substitution on the mechanism of osteoinduction.

As demonstrated in a study by Nihouannen et al (2005), BMPs are present at the bone HA interface. This suggests a role for HA as the substratum for the adsorption and storage of endogenous circulating BMPs. The local accumulation of BMPs may stimulate the differentiation of stem cells present within the surrounding tissue into osteoblasts.

It should be noted that the levels of bone area and contact within both SiHA (2.12% ± 1.2 and 9.04% ± 5.4 respectively) and HA (0.7% ± 0.1 and 2.6% ± 0.6 respectively) samples within the 12 week period of this study were relatively low. A previous study by Patel et al (2002) reported 37.5% ± 5.9 of bone ingrowth within SiHA granules implanted in femoral condyle defects of rabbit animal models within 23 days. Although species dependant mode of bone formation and differences in the implantation sites should not be ignored, it can be suggested that in this study, however low, the levels of bone formation within the non osseous tissue by 12 weeks demonstrate the osteoinductive potential of SiHA.

4.5.2 The effect of strut porosity and physical structure

Quantitative assessment of bone formation within the strut porosity of the samples indicated significantly greater bone formation within HA and SiHA samples with higher microporosity. Osseous response and bone formation by the implants was clearly affected by the levels of microporosity within the implant structure. The presence of macro and micropores within biomaterials is known to facilitate the penetration of fluids and cells into the core of the biomaterial (Bronzino, 2006). Kuboaki et al (1998) demonstrated the role of porosity in an ectopic rat model of bone formation. Habibovic et al (2005) reported that changes in microporosity contribute to levels of ectopic bone formation. The results of this experiment confirmed that SiHA and HA implants with highest strut porosity (30%) presented greater bone formation (4.41±1.4 and 0.86±0.4 respectively) through osteoinduction compared to the same materials with the lower strut porosity levels (SiHA20%: 1.9±0.7 and SiHA10%: 0). SiHA30% samples demonstrated superior bone formation deep within the biomaterial pores which confirmed the results previously indicated in a study by Gauthier et al (1998) on bone formation within microporous structures. The porous SiHA and HA samples did not show the presence of any chondrogenic phase within the pores and followed the same trend previously described in a study by Ripamonti et al (1996) on ectopic bone formation in porous HA in baboons through intramembranous ossification. Karageorgio and Kaplan (2005) showed that small pores within a biomaterial induce endochondral ossification due to the lower amounts of oxygen tension within the pores, whereas large well vascularised pores induce intramembranous ossification through a superior supply of oxygen and nutrients. Increased concentrations of oxygen through blood supply within the interconnected pores of the SiHA and HA may have contributed to the intramembranous bone formed within these samples.

The enhanced osteoinduction within the samples with higher porosity could be due to the influence of the strut porosity on osteoblasts' guidance, attachment and movement, increased dissolution rate of ions into the surrounding tissue, enhanced ionic exchange rate and vascularisation (Hing et al., 2005;). Deligianni et al (2001) demonstrated increased cell adhesion to HA samples with increased surface

roughness *in vitro*. As stated by Park and Davis (2001), microstructures within a surface influence the initial blood to implant interactions through enhancement of platelet adhesion and activation and also fibrinogen adsorption. This in turn influences the rate of cell attachment and consequent new bone formation.

Detailed analysis of bone formation within SiHA samples in comparison with HA samples indicated that bone formation initiated from the centre of the pores within HA samples, whereas this bone formation seemed to predominately initiate at the concave surface of the pores within SiHA samples. Increased levels of microporosity might have resulted in greater surface area availability for faster dissolution and precipitation of the material and consequent enhanced bio-reactivity of the material. This bone-like apatite layer may have induced the stems cells to undergo osteogenic differentiation or the osteoprogenitor cells to initiate bone mineralisation (Ducheyne and Qui, 1999). The chemical composition of SiHA and the mentioned characteristics of this biomaterial, in addition to the role of porosity and surface area, might have been the contributing factors to attraction and attachment of osteogenic cells and bone formation on the concave of the SiHA pores. Also, the porous structure of the implant might have contributed to formation of a vascular network and increased angiogenesis within both HA and SiHA implants. Vascularisation and vascular derived factors are known to contribute to the coordination of the bone cells' activities (Barou et al., 2002). The enhanced bone formation in the highly porous implants could also have been due to the increased rates of fluid and blood circulation within the implant area and superior provision of proteins important for cell migration and adhesion, such as integrins, growth factors and nutritional factors essential in bone formation (Hing, 2005).

Despite the increase in bone contact and bone area by high porosity implants, it should be noted that increasing the porosity of the biomaterials results in brittleness and reduces the mechanical strength (Gauthier et al., 1998) of the biomaterial, thus engineering a porous bone graft biomaterial with the appropriate mechanical strength and ultimate osteogenic properties is desirable. Nevertheless it should be mentioned that high porosity within the biomaterial structure and its contribution to increased

bone ingrowth could contribute to the mechanical strength of the biomaterial via the presence and the amount of the newly formed bone.

Further, the results of this study showed bone formation within both granules and blocks of SiHA and HA samples. However no specific difference in the role of these structural differences on bone formation in either form was observed. A study by Ripamonti et al (1996) showed bone formation within heterotopic implanted blocks of HA in baboons and no bone formation in HA granules. I my study bone formation was observed within both granular particles and blocks of SiHA and HA samples. In comparison with the other groups, superior bone formation was observed within both SiHA blocks and granules with 30% strut porosity.

In consideration of the above, the effect of host specific responses to the implants and osteoinduction should not be ignored as the concentration of circulating growth factors, proteins and cells have been suggested to influence the rate of bone formation. In addition, increasing the time point of the study from 12 weeks to a longer period of sample incubation within the host animals may also contribute to the identification of the time point by which SiHA biomaterials promote the highest level of bone formation. This in turn would contribute to a better understanding of bone formation in the longer term within Silicon substituted hydroxyapatite biomaterial.

4.6 Conclusions

This study demonstrated that SiHA bone substitute materials induce osteoinduction without the supplementation of BMPs, growth factors or mesenchymal or osteoprogenitor cells as there are disadvantages to the use of supplementary factors, such as their high cost of production and their efficacy in bone formation (Lane, 2001; Maniscalco et al., 2002). Greater bone formation is obtained by SiHA implants compared to HA implants in an ectopic site at 12 weeks. Further incorporation of interconnected micro and macropores within the structure of the HA and SiHA biomaterials contributed to increased bone ingrowth within the implanted biomaterials. Comparison of SiHA and HA samples with 10% : 20% : 30% strut porosity within the implants indicated that greater bone formation was obtained within samples containing the highest level of strut porosity, SiHA30% and HA30%. Further SiHA implants with the highest strut porosity (30%) demonstrated greater bone formation when compared to all other HA and SiHA samples. These results suggest that there is an independent effect of chemistry by the incorporation of Silicate ions into the HA structure on osteoinduction by this biomaterial. However, inclusion of interconnected macro and micro structures within the biomaterial structure results in enhanced ectopic bone formation.

In conclusion, the hypothesis of this study proposing that Silicon substituted HA promotes osteoinduction was proved. Strut porosity was found to enhance the rate of bone formation within biomaterials; however, the effect of granularity nor the effect of block structures of the implanted biomaterials were found to imply any significant contribution to bone formation.

5 Chapter V. Discussion and Conclusions

5.1 Discussion

In this thesis the osteoconductive and the osteoinductive behaviour of calcium phosphate bone substitute materials were investigated at both cellular and molecular levels. In the first experimental chapter, the osteoconductive behaviour of eight commercially available bone substitute materials was compared. A study by Hing et al. (2007) compared the performance of dense calcium sulphate, ultra-porous ß-tricalcium phosphate, and porous silicated calcium phosphate in a rabbit model. However, my study has covered a larger range of bone grafts which were implanted in an ovine model. This experimental model was selected since sheep exhibit closer physical, mechanical and biological similarities to human and the results obtained from this study can be used as guidelines for future use in human clinical applications. In this study the amount of bone formation at 6 weeks, on ApaPore, Actifuse, BiIonic, CPS, ProOsteon 500 R and Skelite calcium phosphate based biomaterials was compared with osteoconduction on two DBM based biomaterials; Grafton Crunch and Accell Connexus putty. The results of this study indicated that calcium phosphate bone graft materials exhibited significantly greater bone ($P<0.05$) formation compared to DBM based biomaterials. However, even with calcium phosphate based bone substitute materials there was a very wide osteoconductive response. CPS, BiIonic, Actifuse and ApaPore biomaterials exhibited the highest amount of bone formation respectively and Pro Osteon 500R and Skelite demonstrated the lowest amount of new bone within the period of the study. In this study, both osseoinductive and osseoconductive mechanisms of bone formation were proposed to have contributed to the rate of bone formation by the implanted Calcium Phosphates; however, as all the samples were implanted in contact with host bone, distinguishing these two mechanisms of bone formation was not possible, as host bone provides both sources of osteoconductive factors and cells and proteins promoting osteoinduction.

Analysis of the mechanism of bone formation within the implanted samples in this experiment and the level of bone formation within the silicon containing biomaterials

(CPS, Actifuse and BiIonic) indicated the potential role of silicon substitution within calcium phosphates on bone formation. As indicated in various *in vivo* and *in vitro* studies, silicon substitution within the HA structure improves the bioactivity of this biomaterial (Gibson et al., 1999; Patel et al., 2002; Ballas et al., 2002). The incorporation of silicate ion within Actifuse, CPS and BiIonic contributed to the formation of new bone within theses samples, irrespective of the effect of strut porosity. It should be noted that levels of new bone formation within Actifuse was not significantly different from that of HA by week 6 of implantation within the femoral defects. However, results of the osteoinduction study indicated formation of significantly higher amount of new bone within SiHA samples by 12 weeks. This suggests that, although presence of silicon may not contribute to greater bone formation compared to pure HA at early stages of implantation, silicon does enhance bone formation at longer time points.

A recent paper by Bohner (2009) has mentioned the lack of experimental evidence supporting the notion that resorbablity of SiHA, which has been assumed by various researchers, is the contributing factor to the release of Si ions and consequent differentiation of osteoblasts. With respect to this, the results of my study provide quantitative evidence that silicate containing calcium phosphates such as Actifuse, CPS or BiIonic which show significant amounts of new bone, do not show any significant material resorption within 6 weeks, with the exception of Skelite (a Si-TCP based material) which exhibited significant material resorption. As a result, it could be concluded that bone formation by Silicated materials is induced by factors other than the role of biomaterial resorption such as the effect of Si ions on expression of osteogenic genes and osteogenic proteins production.

In order to investigate the influence of silicate on stimulation of *in vitro* osteoblastic differentiation of marrow stromal cells, hMSCs were seeded on dense SiHA discs and the osteoinductive potential of SiHA bone substitute biomaterial was monitored. Various studies by Gibson et al. (1999), Guth et al. (2006) and Zou et al. (2009) demonstrated enhanced metabolic activity and cell proliferation through the effect of silicate ions on adhesion, proliferation and differentiation of cells. However most of these studies have used human osteoblast like cells or primary osteoblasts, whereas

this study has employed the use of pluripotent human marrow stromal cells. A study by Xynos et al. (2000) demonstrated the gene expression profile of human osteoblasts on Bioglass 45S5. However, in his study it was not clear whether bone formation was the result of direct cell-biomaterial contact or the effect of the released ions. However, a study by Guth et al. (2006) did demonstrate the release of silicate ions from SiHA into solution. In this study, the osteogenic differentiation of the hMSCs could be speculated to have been due to both cell-biomaterial contact and ionic dissolution of SiHA. The presence of silicon ions within new bone (*in vivo*) and osteoblastic cell differentiation on the surface of the tested discs (*in vitro*) were indicative of the involvement of such mechanisms. Production of osteoblastic marker proteins, in addition to the morphological changes of the hMSCs seeded on SiHA and HA discs, indicated the differentiation of these cells into osteoblasts. Gene expression analysis indicated up regulation of RUNX2, Bone Sialoprotein and VEGF genes in hMSCs seeded on SiHA and HA discs by day 24 of the study. Expression of the VEGF mRNA was observed to be higher on cells seeded on SiHA and HA discs in comparison with the control group on days 3 and 6 of the study. This indicated the contribution of SiHA and HA biomaterials to the promotion of early expression of VEGF and consequently the possible early initiation of vasculogenesis.

In future, work on *in vivo* mRNA gene expression analysis could be carried out to analyse the effect of calcium phosphate bone substitute materials on the expression levels of osteogenic marker genes and the vasculogenic gene, VEGF, involved in the mechanism of osteoconduction. For this purpose, the same femoral condyle model could be employed for RNA extraction and mRNA expression quantification at different time points in implanted calcium phosphate biomaterials.

Further, immunohistochemical analysis of the osteogenic proteins and their cellular localization on *in vivo* implanted calcium phosphate bone substitutes would be the direction for more detailed analysis of the influence of these biomaterials on cellular mechanisms of osteoblastic differentiation and mineralization. It should be noted that immunohistochemical staining is performed on decalcified low temperature resin embedded samples; as the decalcification process may take a long time, resulting in possible protein degeneration and also removal of the CaP component of the

implanted biomaterial samples, in order to obtain accurate results improved techniques of immunohistochemistry need to be developed.

Following the analysis of the role of silicate ion substitution on the osteoblastic differentiation of hMSCs and induction of osteoinduction *in vitro,* the osteoinductive property of SiHA *in vivo* and the effect of silicate ion substitution within HA was analysed as the next step into the study of this biomaterial. Woven bone apposition into the periphery and in the centre of SiHA and HA granules and blocks implanted in paraspinalis muscle of sheep was observed. SiHA promoted osseoinduction in an ectopic site with significantly higher ($P < 0.05$) levels of bone formation in comparison with HA. The osteoinductivity of HA and SiHA was enhanced by the incorporation of strut porosity; however, as shown in chapter four, SiHA promotes superior amounts of bone formation irrespective of its physical structure. It should be mentioned that the 80% porous structure of SiHA can only support bone formation within non-load bearing tissues, therefore, this material is not a suitable candidate for use in load bearing environments. However in spinal fusion procedures where osseoinduction and new bone formation is more important, strut porosity and chemical composition of SiHA contribute to the promotion of rapid bone formation. The study of the effect of strut porosity on osteoinduction confirmed the results previously indicated in a study by Gauthier et al (1998) on bone formation within microporous structures and indicated that increased strut porosity enhances the rate of new bone formation. This can be speculated to be due to communication of osteoblasts with one another through diffusion of chemicals, blood vessels' ingrowth and connective tissue cells with osteogenic potential penetrating across the biomaterial micropores, as indicated in previous studies by Winter in 1970, which showed intramembranous ossification within the pores of an ectopically implanted synthetic sponge.

Future work could utilize cDNA microarrays in order to determine gene expression of cells growing on silicon substituted hydroxyapatite. As long as plain hydroxyapatite is used as control, this would be beneficial because key genes associated with enhanced osteoinduction and osteoconduction on SiHA could be identified. Immunohistochemical analysis could be carried out to obtain a better

understanding of the influence of silicate ions on the expression and localization of osteogenic genes.

5.2 Conclusions

In conclusion, the hypothesis that generally calcium phosphate bone substitute materials promote greater bone formation in comparison with DBM based biomaterials within 6 weeks was proved. The poor performance of DBM in comparison to calcium phosphates is considered to be due to the absence of the calcium phosphate component which plays an essential role in promotion of bone formation. Calcium phosphate based biomaterials are widely used in various orthopaedics and maxillofacial applications, specifically for spinal fusions. The fast rate of bone formation by these biomaterials in comparison to DBMs makes them the ideal group of bone substitute materials where bone regeneration in a short period of time with the appropriate resorption and mechanical properties is required. The presence of strut porosity within the biomaterial structure was shown to enhance new bone formation; however, chemical composition of a biomaterial was observed to contribute to the rate of bone formation irrespective of the structural porosity. Silicon substituted hydroxyapatite was also shown to promote the attachment, proliferation and differentiation of hMSCs to osteoblasts, irrespective of the presence of osteogenic supplements or porosity. The chemical composition of SiHA was shown to contribute to the mechanism of osteoinduction through influencing the expression of osteogenic marker genes and secretion of the osteogenic proteins. Early osteogenic differentiation of hMSCs as a result of the earlier initiation of bone matrix mineralisation through expression of the osteonectin gene, was suggested as on of the factors involved in osteoinduction by this biomaterial. Further, SiHA was proved to induce osteoinduction without the supplementation of BMPs, growth factors or mesenchymal or osteoprogenitor cells. In addition, incorporation of 30% strut porosity within the structure of the HA and SiHA biomaterials contributed to increased bone ingrowth within the implanted biomaterials *in vivo*. These results clarified the independent effect of chemistry on osteoinduction.

In general it was concluded that not only the chemistry of a biomaterial is important for promotion of bone formation, the implant morphology also plays a significant role.

6 Bibliography

- Edith M. Carlisle. (1972). Silicon: an essential element for the chick. Nutrition Classics. Science 178: 619-21, 1972. Rev 40, 210-213.
- B. Trawling, S. Maxwell, ed. (2005). Medicines from the deep sea. The Importance of Protecting the High Seas from Bottom (Natural Resources Defence Council issue paper).
- Ai-Aql, Z., Alagl, A., Graves, D., Gerstenfeld, L., and Einhorn, T. (2008). Molecular mechanisms controlling bone formation during fracture healing and distraction osteogenesis. J Dent Res 87, 107-118.
- Albee, F. (1920). Studies in bone growth: triple calcium phosphate as a stimulus to osteogenesis. Ann Surg 71, 32-39.
- Albrektsson, T., and Johansson, C. (2001). Osteoinduction, osteoconduction and osseointegration. Eur Spine J 10 Suppl 2, S96-101.
- Amaral, M., Lopes, M., Silva, R., and Santos, J. (2002). Densification route and mechanical properties of Si_3N_4-bioglass biocomposites. Biomaterials 23, 857-862.
- Ambard, A., and Mueninghoff, L. (2006). Calcium phosphate cement: review of mechanical and biological properties. J Prosthodont 15, 321-328.
- Annaz, B., Hing, K., Kayser, M., Buckland, T., and Di Silvio, L. (2004a). An ultrastructural study of cellular response to variation in porosity in phase-pure hydroxyapatite. J Microsc 216, 97-109.
- Annaz, B., Hing, K., Kayser, M., Buckland, T., and Di Silvio, L. (2004b). Porosity variation in hydroxyapatite and osteoblast morphology: a scanning electron microscopy study. J Microsc 215, 100-110.
- Anselme, K. (2000). Osteoblast adhesion on biomaterials. Biomaterials 21, 667-681.
- Anselme, K., Bigerelle, M., Noel, B., Dufresne, E., Judas, D., Iost, A., and Hardouin, P. (2000). Qualitative and quantitative study of human osteoblast adhesion on materials with various surface roughnesses. J Biomed Mater Res 49, 155-166.
- Arcos, D., Greenspan, D., and Vallet-Regi, M. (2003). A new quantitative method to evaluate the in vitro bioactivity of melt and sol-gel-derived silicate glasses. J Biomed Mater Res A 65, 344-351.
- Arcos, D., Sánchez-Salcedo, S., Izquierdo-Barba, I., Ruiz, L., González-Calbet, J., and Vallet-Regí, M. (2006). Crystallochemistry, textural properties, and in vitro biocompatibility of different silicon-doped calcium phosphates. J Biomed Mater Res A 78, 762-771.
- Aronow, M., Gerstenfeld, L., Owen, T., Tassinari, M., Stein, G., and Lian, J. (1990). Factors that promote progressive development of the osteoblast phenotype in cultured fetal rat calvaria cells. J Cell Physiol 143, 213-221.

- Asou, Y., Rittling, S., Yoshitake, H., Tsuji, K., Shinomiya, K., Nifuji, A., Denhardt, D., and Noda, M. (2001). Osteopontin facilitates angiogenesis, accumulation of osteoclasts, and resorption in ectopic bone. Endocrinology 142, 1325-1332.
- Ayers, R., Burkes, D., Gottoli, G., Yi, H., Zhim, F., Yahia, L., and Moore, J. (2007). Combustion synthesis of porous biomaterials. J Biomed Mater Res A 81, 634-643.
- Bagambisa, F., Joos, U., and Schilli, W. (1993). Mechanisms and structure of the bond between bone and hydroxyapatite ceramics. J Biomed Mater Res 27, 1047-1055.
- Balas, F., Pérez-Pariente, J., and Vallet-Regí, M. (2003). In vitro bioactivity of silicon-substituted hydroxyapatites. J Biomed Mater Res A 66, 364-375.
- Barou, O., Mekraldi, S., Vico, L., Boivin, G., Alexandre, C., and Lafage-Proust, M. (2002). Relationships between trabecular bone remodeling and bone vascularization: a quantitative study. Bone 30, 604-612.
- Barrere, F., van Blitterswijk, C., and de Groot, K. (2006). Bone regeneration: molecular and cellular interactions with calcium phosphate ceramics. Int J Nanomedicine 1, 317-332.
- Barrere, F., van der Valk, C., Dalmeijer, R., Meijer, G., van Blitterswijk, C., de Groot, K., and Layrolle, P. (2003). Osteogenecity of octacalcium phosphate coatings applied on porous metal implants. J Biomed Mater Res A 66, 779-788.
- Bauer, T. (2007a). An overview of the histology of skeletal substitute materials. Arch Pathol Lab Med 131, 217-224.
- Bauer, T. (2007b). Bone graft substitutes. Skeletal Radiol 36, 1105-1107.
- Bauer, T., and Muschler, G. (2000). Bone graft materials. An overview of the basic science. Clin Orthop Relat Res, 10-27.
- Bauer, T., and Smith, S. (2002). Bioactive materials in orthopaedic surgery: overview and regulatory considerations. Clin Orthop Relat Res, 11-22.
- Baxter, L., Frauchiger, V., Textor, M., ap Gwynn, I., and Richards, R. (2002). Fibroblast and osteoblast adhesion and morphology on calcium phosphate surfaces. Eur Cell Mater 4, 1-17.
- Bell, G. (1952). Bone as a skeletal structure. Br J Nutr 6, 405-409.
- Benson, M., Bargeon, J., Xiao, G., Thomas, P., Kim, A., Cui, Y., and Franceschi, R. (2000). Identification of a homeodomain binding element in the bone sialoprotein gene promoter that is required for its osteoblast-selective expression. J Biol Chem 275, 13907-13917.
- Beresford, J. (1989). Osteogenic stem cells and the stromal system of bone and marrow. Clin Orthop Relat Res, 270-280.
- Bernard, G. (1978). Ultrastructural localization of alkaline phosphatase in initial intramembranous osteogenesis. Clin Orthop Relat Res, 218-225.
- Biltz, R., and Pellegrino, E. (1969). The chemical anatomy of bone. I. A comparative study of bone composition in sixteen vertebrates. J Bone Joint Surg Am 51, 456-466.

- Bjerre, L., Bünger, C., Kassem, M., and Mygind, T. (2008). Flow perfusion culture of human mesenchymal stem cells on silicate-substituted tricalcium phosphate scaffolds. Biomaterials 29, 2616-2627.
- Blair, H., Kahn, A., Crouch, E., Jeffrey, J., and Teitelbaum, S. (1986). Isolated osteoclasts resorb the organic and inorganic components of bone. J Cell Biol 102, 1164-1172.
- Block, J., and Poser, J. (1995). Does xenogeneic demineralized bone matrix have clinical utility as a bone graft substitute? Med Hypotheses 45, 27-32.
- Bloemers, F., Blokhuis, T., Patka, P., Bakker, F., Wippermann, B., and Haarman, H. (2003). Autologous bone versus calcium-phosphate ceramics in treatment of experimental bone defects. J Biomed Mater Res B Appl Biomater 66, 526-531.
- Blokhuis, T., Termaat, M., den Boer, F., Patka, P., Bakker, F., and Haarman, H. (2000). Properties of calcium phosphate ceramics in relation to their in vivo behavior. J Trauma 48, 179-186.
- Bobis, S., Jarocha, D., and Majka, M. (2006). Mesenchymal stem cells: characteristics and clinical applications. Folia Histochem Cytobiol 44, 215-230.
- Boden, S.D. (2006). The use of bone morphogenic proteins in spinal fusion. J Bone Joint Surg Br 88-B: 454-a
- Bohner, M. (2009). Silicon-substituted calcium phosphates - A critical view. Biomaterials 30, 6403-6406.
- Bohner, M., and Baumgart, F. (2004). Theoretical model to determine the effects of geometrical factors on the resorption of calcium phosphate bone substitutes. Biomaterials 25, 3569-3582.
- Bolander, M., and Balian, G. (1986). The use of demineralized bone matrix in the repair of segmental defects. Augmentation with extracted matrix proteins and a comparison with autologous grafts. J Bone Joint Surg Am 68, 1264-1274.
- Bolander, M., Young, M., Fisher, L., Yamada, Y., and Termine, J. (1988). Osteonectin cDNA sequence reveals potential binding regions for calcium and hydroxyapatite and shows homologies with both a basement membrane protein (SPARC) and a serine proteinase inhibitor (ovomucoid). Proc Natl Acad Sci U S A 85, 2919-2923.
- Bonewald, L. (2006). Mechanosensation and Transduction in Osteocytes. Bonekey Osteovision 3, 7-15.
- Bonfield, W. (2006). Designing porous scaffolds for tissue engineering. Philos Transact A Math Phys Eng Sci 364, 227-232.
- Boskey, A., Spevak, L., Paschalis, E., Doty, S., and McKee, M. (2002). Osteopontin deficiency increases mineral content and mineral crystallinity in mouse bone. Calcif Tissue Int 71, 145-154.

- Bostrom, M., and Seigerman, D. (2005). The clinical use of allografts, demineralized bone matrices, synthetic bone graft substitutes and osteoinductive growth factors: a survey study. HSS J 1, 9-18.
- Botelho, C., Brooks, R., Best, S., Lopes, M., Santos, J., Rushton, N., and Bonfield, W. (2006a). Human osteoblast response to silicon-substituted hydroxyapatite. J Biomed Mater Res A 79, 723-730.
- Botelho, C., Brooks, R., Spence, G., McFarlane, I., Lopes, M., Best, S., Santos, J., Rushton, N., and Bonfield, W. (2006b). Differentiation of mononuclear precursors into osteoclasts on the surface of Si-substituted hydroxyapatite. J Biomed Mater Res A 78, 709-720.
- Botelho, C., Lopes, M., Gibson, I., Best, S., and Santos, J. (2002). Structural analysis of Si-substituted hydroxyapatite: zeta potential and X-ray photoelectron spectroscopy. J Mater Sci Mater Med 13, 1123-1127.
- Bourgeois, B., Laboux, O., Obadia, L., Gauthier, O., Betti, E., Aguado, E., Daculsi, G., and Bouler, J. (2003). Calcium-deficient apatite: a first in vivo study concerning bone ingrowth. J Biomed Mater Res A 65, 402-408.
- Boyan, B., Hummert, T., Dean, D., and Schwartz, Z. (1996). Role of material surfaces in regulating bone and cartilage cell response. Biomaterials 17, 137-146.
- Boyde, A. (1999). Osteoconduction in large macroporous hydroxyapatite ceramic implants: evidence for a complementary integration and disintegration mechanism, A. Corsi, ed. (Bone), pp. 579-589.
- Boyle, W., Simonet, W., and Lacey, D. (2003). Osteoclast differentiation and activation. Nature 423, 337-342.
- Brandoff, J., Silber, J., and Vaccaro, A. (2008). Contemporary alternatives to synthetic bone grafts for spine surgery. Am J Orthop 37, 410-414.
- Bronner, F. R.V. Worrell (1999). Orhtopaedics, principles of basic and clinical science,, 1st ed. (Taylor & Francis Ltd). 39-60.
- Brown, K., and Cruess, R. (1982). Bone and cartilage transplantation in orthopaedic surgery. A review. J Bone Joint Surg Am 64, 270-279.
- Butler, W. (1989). The nature and significance of osteopontin. Connect. Tissue Res 23, No. 2-3, 123-136
- Calomme, M., and Vanden Berghe, D. (1997). Supplementation of calves with stabilized orthosilicic acid. Effect on the Si, Ca, Mg, and P concentrations in serum and the collagen concentration in skin and cartilage. Biol Trace Elem Res 56, 153-165.
- Campbell, J., and Kaplan, F. (1992). The role of morphogens in endochondral ossification. Calcif Tissue Int 50, 283-289.

- Cao, Y., Zhou, Z., de Crombrugghe, B., Nakashima, K., Guan, H., Duan, X., Jia, S., and Kleinerman, E. (2005). Osterix, a transcription factor for osteoblast differentiation, mediates antitumor activity in murine osteosarcoma. Cancer Res 65, 1124-1128.
- Caplan, A. Review: mesenchymal stem cells: cell-based reconstructive therapy in orthopedics. Tissue Eng 11, 1198-1211.
- Caporali, E., Rahal, S., Morceli, J., Taga, R., Granjeiro, J., Cestari, T., Mamprim, M., and Correa, M. [Assessment of bovine biomaterials containing bone morphogenetic proteins bound to absorbable hydroxyapatite in rabbit segmental bone defects]. Acta Cir Bras 21, 366-373.
- Carlisle, E. (1970). Silicon: a possible factor in bone calcification. Science 167, 279-280.
- Carlisle, E. (1976). In vivo requirement for silicon in articular cartilage and connective tissue formation in the chick. J Nutr 106, 478-484.
- Carlisle, E. (1980a). A silicon requirement for normal skull formation in chicks. J Nutr 110, 352-359.
- Carlisle, E. (1980b). Biochemical and morphological changes associated with long bone abnormalities in silicon deficiency. J Nutr 110, 1046-1056.
- Carlisle, E. (1981). Silicon: a requirement in bone formation independent of vitamin D1. Calcif Tissue Int 33, 27-34.
- Carlisle, E. (1988). Silicon as a trace nutrient. Sci Total Environ 73, 95-106.
- Chang, Y., Stanford, C., and Keller, J. (2000). Calcium and phosphate supplementation promotes bone cell mineralization: implications for hydroxyapatite (HA)-enhanced bone formation. J Biomed Mater Res 52, 270-278.
- Christophy, C. (2008). Encouraging Nature with Ceramics: The roles of surface roughness and physio-chemistry on cell response to substituted apatites, N. Rashid1, ed. Advances in Science and Technology, pp. 22-30.
- Chung, U., Kawaguchi, H., Takato, T., and Nakamura, K. (2004). Distinct osteogenic mechanisms of bones of distinct origins. J Orthop Sci 9, 410-414.
- Combes, C., Bareille, R., and Rey, C. (2006). Calcium carbonate-calcium phosphate mixed cement compositions for bone reconstruction. J Biomed Mater Res A 79, 318-328.
- Combes, C., and Rey, C. (2002). Adsorption of proteins and calcium phosphate materials bioactivity. Biomaterials 23, 2817-2823.
- Cornuelle, A.G.C., Gronefeld, Diane H. (1997). Radiographic Anatomy & Positioning. McGrow-Hill Medical. 1st ed. pp.83-84
- Dahners, L.E. (1984). Long bone defects treated with demineralized bone, R.R. Jacobs, ed. South Med J. 1985 Aug;78(8):933-4.

- Damien, E., Hing, K., Saeed, S., and Revell, P. (2003). A preliminary study on the enhancement of the osteointegration of a novel synthetic hydroxyapatite scaffold in vivo. J Biomed Mater Res A 66, 241-246.
- De Aza, P., and Luklinska, Z. (2003). Effect of glass-ceramic microstructure on its in vitro bioactivity. J Mater Sci Mater Med 14, 891-898.
- De Aza, P., Luklinska, Z., Martinez, A., Anseau, M., Guitian, F., and De Aza, S. (2000). Morphological and structural study of pseudowollastonite implants in bone. J Microsc 197, 60-67.
- de Boer, H. (1988). The history of bone grafts. Clin Orthop Relat Res, 292-298.
- de Boer, J., Siddappa, R., Gaspar, C., van Apeldoorn, A., Fodde, R., and van Blitterswijk, C. (2004). Wnt signaling inhibits osteogenic differentiation of human mesenchymal stem cells. Bone 34, 818-826.
- de Groot, K. (1985). Clinical usefulness of calcium phosphate ceramics. Zahnarztl Mitt 75, 1938-1940.
- De Groot, K. (1988). Effect of porosity and physicochemical properties on the stability, resorption, and strength of calcium phosphate ceramics. Ann N Y Acad Sci 523, 227-233.
- de Groot, K., Wolke, J., and Jansen, J. (1998). Calcium phosphate coatings for medical implants. Proc Inst Mech Eng H 212, 137-147.
- Delany, A., Amling, M., Priemel, M., Howe, C., Baron, R., and Canalis, E. (2000a). Osteopenia and decreased bone formation in osteonectin-deficient mice. J Clin Invest 105, 1325.
- Delany, A., Amling, M., Priemel, M., Howe, C., Baron, R., and Canalis, E. (2000b). Osteopenia and decreased bone formation in osteonectin-deficient mice. J Clin Invest 105, 915-923.
- Deligianni, D., Katsala, N., Koutsoukos, P., and Missirlis, Y. (2001). Effect of surface roughness of hydroxyapatite on human bone marrow cell adhesion, proliferation, differentiation and detachment strength. Biomaterials 22, 87-96.
- Delloye, C., Cnockaert, N., and Cornu, O. (2003). Bone substitutes in 2003: Overview. Acta Orthop Belg 69, 1-8.
- Delloye, C., Cornu, O., Druez, V., and Barbier, O. (2007). Bone allografts: What they can offer and what they cannot. J Bone Joint Surg Br 89, 574-579.
- Denhardt, David T., Noda, M. O'Regan,, A. W., Pavlin, W., and Berman J. s. (2001). Osteopontin as a means to cope with environmental insults: regulation of inflammation, tissue remodeling, and cell survival. J Clin Invest. 2001 May 1; 107(9): 1055–1061.
- Denissen, H., de Groot, K., Makkes, P., van den Hooff, A., and Klopper, P. (1980). Tissue response to dense apatite implants in rats. J Biomed Mater Res 14, 713-721.

- Dickens, B. (1971). The Crystal Structure of $Cas(P0_4)_2Si0_4$ (Silieo-Carnotite), W.E. Brown, ed. (TMPM Tsehermaks Min. Petr. Mitt.), pp. 1-27.
- Dickerman, R., Reynolds, A., and Morgan, B. Calcium phosphate silicate for spinal fusion: a good alternative to bone morphogenetic protein-2! Spine J 8, 1046-1047.
- Doi, Y., Shibutani, T., Moriwaki, Y., Kajimoto, T., and Iwayama, Y. (1998). Sintered carbonate apatites as bioresorbable bone substitutes. J Biomed Mater Res 39, 603-610.
- Dorozhkin, S.V. (2007). Bioceramics based on calcium orthophosphates. Biomaterials. 2010 Mar;31(7):1465-85. Epub 2009 Dec 7.
- dos Santos, E., Farina, M., Soares, G., and Anselme, K. (2008). Surface energy of hydroxyapatite and beta-tricalcium phosphate ceramics driving serum protein adsorption and osteoblast adhesion. J Mater Sci Mater Med 19, 2307-2316.
- dos Santos, E., Farina, M., Soares, G., and Anselme, K. (2009). Chemical and topographical influence of hydroxyapatite and beta-tricalcium phosphate surfaces on human osteoblastic cell behavior. J Biomed Mater Res A 89, 510-520.
- Duan, Y., Wu, Y., Wang, C., Chen, J., and Zhang, X. (2003). A study of bone-like apatite formation on calcium phosphate ceramics in different kinds of animals in vivo. Sheng Wu Yi Xue Gong Cheng Xue Za Zhi 20, 22-25.
- Ducheyne, P. (1985). Bioglass coatings and bioglass composites as implant materials. J Biomed Mater Res 19, 273-291.
- Ducheyne, P., and Qiu, Q. (1999). Bioactive ceramics: the effect of surface reactivity on bone formation and bone cell function. Biomaterials 20, 2287-2303.
- Ducheyne, P., Radin, S., and King, L. (1993). The effect of calcium phosphate ceramic composition and structure on in vitro behavior. I. Dissolution. J Biomed Mater Res 27, 25-34.
- Effah Kaufmann, E., Ducheyne, P., and Shapiro, I. (2000). Evaluation of osteoblast response to porous bioactive glass (45S5) substrates by RT-PCR analysis. Tissue Eng 6, 19-28.
- Ehrlich, H. (2006). Biomaterial structure in deep-sea bamboo coral (Anthozoa: Gorgonacea: Isididae): perspectives for the development of bone implants and templates for tissue engineering, P. Etnoyer, ed. Materialwissenschaft und Werkstofftechnik 37 (6): 552 – 557
- Einhorn, T., Lane, J., Burstein, A., Kopman, C., and Vigorita, V. (1984). The healing of segmental bone defects induced by demineralized bone matrix. A radiographic and biomechanical study. J Bone Joint Surg Am 66, 274-279.
- Einhorn, T., and Lee, C. Bone regeneration: new findings and potential clinical applications. J Am Acad Orthop Surg 9, 157-165.
- El-Ghannam, A. (2004). Advanced bioceramic composite for bone tissue engineering: design principles and structure-bioactivity relationship. J Biomed Mater Res A 69, 490-501.

- El-Ghannam, A. (2005). Bone reconstruction: from bioceramics to tissue engineering. Expert Rev Med Devices 2, 87-101.
- El-Ghannam, A., Ducheyne, P., and Shapiro, I. (1997). Porous bioactive glass and hydroxyapatite ceramic affect bone cell function in vitro along different time lines. J Biomed Mater Res 36, 167-180.
- Elliot, M., and Edwards, H.J. (1991). Effect of dietary silicon on growth and skeletal development in chickens. J Nutr 121, 201-207.
- Ergun, C., Webster, T., Bizios, R., and Doremus, R. (2002). Hydroxylapatite with substituted magnesium, zinc, cadmium, and yttrium. I. Structure and microstructure. J Biomed Mater Res 59, 305-311.
- Fang, B., Wan, Y., Tang, T., Gao, C., and Dai, K. (2009). Proliferation and osteoblastic differentiation of human bone marrow stromal cells on hydroxyapatite/bacterial cellulose nanocomposite scaffolds. Tissue Eng Part A 15, 1091-1098.
- Fang, T., Salim, A., Xia, W., Nacamuli, R., Guccione, S., Song, H., Carano, R., Filvaroff, E., Bednarski, M., Giaccia, A., et al. (2005). Angiogenesis is required for successful bone induction during distraction osteogenesis. J Bone Miner Res 20, 1114-1124.
- Fellah, B., Gauthier, O., Weiss, P., Chappard, D., and Layrolle, P. (2008). Osteogenicity of biphasic calcium phosphate ceramics and bone autograft in a goat model. Biomaterials 29, 1177-1188.
- Ferguson, C., Alpern, E., Miclau, T., and Helms, J. (1999). Does adult fracture repair recapitulate embryonic skeletal formation? Mech Dev 87, 57-66.
- Fisher, L., McBride, O., Termine, J., and Young, M. (1990). Human bone sialoprotein. Deduced protein sequence and chromosomal localization. J Biol Chem 265, 2347-2351.
- Franceschi, R. (1999). The developmental control of osteoblast-specific gene expression: role of specific transcription factors and the extracellular matrix environment. Crit Rev Oral Biol Med 10, 40-57.
- Franceschi, R., Ge, C., Xiao, G., Roca, H., and Jiang, D. (2007). Transcriptional regulation of osteoblasts. Ann N Y Acad Sci 1116, 196-207.
- Franceschi, R., and Xiao, G. (2003). Regulation of the osteoblast-specific transcription factor, Runx2: responsiveness to multiple signal transduction pathways. J Cell Biochem 88, 446-454.
- Franz-Odendaal, T., Hall, B., and Witten, P. (2006). Buried alive: how osteoblasts become osteocytes. Dev Dyn 235, 176-190.
- Friedlaender, G. (1987). Bone grafts. The basic science rationale for clinical applications. J Bone Joint Surg Am 69, 786-790.
- Fujishiro, T., Bauer, T., Kobayashi, N., Kobayashi, H., Sunwoo, M., Seim, H.r., and Turner, A. (2007). Histological evaluation of an impacted bone graft substitute composed of a

combination of mineralized and demineralized allograft in a sheep vertebral bone defect. J Biomed Mater Res A 82, 538-544.

- Furumatsu, T., Shen, Z., Kawai, A., Nishida, K., Manabe, H., Oohashi, T., Inoue, H., and Ninomiya, Y. (2003). Vascular endothelial growth factor principally acts as the main angiogenic factor in the early stage of human osteoblastogenesis. J Biochem 133, 633-639.
- Gallie, W.E. (1914). The history of a bone graft. J Bone Joint Surg Am. 1914;s2-12:201-212.
- Ganss, B., Kim, R., and Sodek, J. (1999). Bone sialoprotein. Crit Rev Oral Biol Med 10, 79-98.
- Gauthier, O., Bouler, J., Aguado, E., Pilet, P., and Daculsi, G. Macroporous biphasic calcium phosphate ceramics: influence of macropore diameter and macroporosity percentage on bone ingrowth. Biomaterials 19, 133-139.
- Gauthier, O., Goyenvalle, E., Bouler, J., Guicheux, J., Pilet, P., Weiss, P., and Daculsi, G. (2001). Macroporous biphasic calcium phosphate ceramics versus injectable bone substitute: a comparative study 3 and 8 weeks after implantation in rabbit bone. J Mater Sci Mater Med 12, 385-390.
- Georgiade, N., Hanker, J., Levin, S., and Ruff, G. (1993). The use of particulate hydroxyapatite and plaster of Paris in aesthetic and reconstructive surgery. Aesthetic Plast Surg 17, 85-92.
- Gericke, A., Qin, C., Spevak, L., Fujimoto, Y., Butler, W., SÃ¸rensen, E., and Boskey, A. (2005). Importance of phosphorylation for osteopontin regulation of biomineralization. Calcif Tissue Int 77, 45-54.
- Gerstenfeld, L., Cullinane, D., Barnes, G., Graves, D., and Einhorn, T. (2003). Fracture healing as a post-natal developmental process: molecular, spatial, and temporal aspects of its regulation. J Cell Biochem 88, 873-884.
- Giannoudis, P., Dinopoulos, H., and Tsiridis, E. (2005). Bone substitutes: an update. Injury 36 Suppl 3, S20-27.
- Gibson, I. (1999). Enhanced in vitro cell activity and surface apatite layer formation on novel silicon-substituted hydroxyapatites, K. Hing, ed. Bioceramics Vol. 12 (1999) 191-194
- Gibson, I., Best, S., and Bonfield, W. (1999). Chemical characterization of silicon-substituted hydroxyapatite. J Biomed Mater Res 44, 422-428.
- Gibson, I., Ke, S., Best, S., and Bonfield, W. (2001). Effect of powder characteristics on the sinterability of hydroxyapatite powders. J Mater Sci Mater Med 12, 163-171.
- Gibson, I., Rehman, I., Best, S., and Bonfield, W. (2000). Characterization of the transformation from calcium-deficient apatite to beta-tricalcium phosphate. J Mater Sci Mater Med 11, 533-539.
- Gibson, I.R. (2002). Enhanced in vivo response to silicate-substituted hydroxyapatite, K.A. Hing, ed. Key Engineering Materials. Vol 218-220, 203-206

- Gordjestani, M., Dermaut, L., De Ridder, L., Thierens, H., De Waele, P., De Leersnijder Willy, W., and Bosman, F. (2005). Osteopontin and bone metabolism: a histology and scintigraphy study in rats. Int J Oral Maxillofac Surg 34, 794-799.
- Gray, C., Boyde, A., and Jones, S. (1996). Topographically induced bone formation in vitro: implications for bone implants and bone grafts. Bone 18, 115-123.
- Green, A., Jansen, J., van der Waerden, J., and von Recum, A. (1994). Fibroblast response to microtextured silicone surfaces: texture orientation into or out of the surface. J Biomed Mater Res 28, 647-653.
- Green, J. (1994). The physicochemical structure of bone: cellular and noncellular elements. Miner Electrolyte Metab 20, 7-15.
- Greenwald, A., Boden, S., Goldberg, V., Khan, Y., Laurencin, C., and Rosier, R. (2001). Bone-graft substitutes: facts, fictions, and applications. J Bone Joint Surg Am 83-A Suppl 2 Pt 2, 98-103.
- Groeneveld, E., van den Bergh, J., Holzmann, P., ten Bruggenkate, C., Tuinzing, D., and Burger, E. (1999). Mineralization processes in demineralized bone matrix grafts in human maxillary sinus floor elevations. J Biomed Mater Res 48, 393-402.
- Groot, K.D. (1984). Calcium phosphate ceramics: their current status. Contemporary biomaterials, pp. 477-479.
- Guillemin, G., Patat, J., Fournie, J., and Chetail, M. (1987). The use of coral as a bone graft substitute. J Biomed Mater Res 21, 557-567.
- Gulgun, M.A. (2002). Cation Segregation in an Oxide Ceramic with Low Solubility: Yttrium Doped a-Alumina, R.Voytovych, ed. Interface science, pp. 99-110.
- Guoliang, G. (2008). The role of osteocytes in bone metabolism, H.K., Väänänen ed. Bone 3,1. S29
- Habibovic, P., and de Groot, K. (2007). Osteoinductive biomaterials--properties and relevance in bone repair. J Tissue Eng Regen Med 1, 25-32.
- Habibovic, P., Gbureck, U., Doillon, C., Bassett, D., van Blitterswijk, C., and Barralet, J. (2008a). Osteoconduction and osteoinduction of low-temperature 3D printed bioceramic implants. Biomaterials 29, 944-953.
- Habibovic, P., Kruyt, M., Juhl, M., Clyens, S., Martinetti, R., Dolcini, L., Theilgaard, N., and van Blitterswijk, C. (2008b). Comparative in vivo study of six hydroxyapatite-based bone graft substitutes. J Orthop Res 26, 1363-1370.
- Habibovic, P., Sees, T., van den Doel, M., van Blitterswijk, C., and de Groot, K. (2006a). Osteoinduction by biomaterials--physicochemical and structural influences. J Biomed Mater Res A 77, 747-762.

- Habibovic, P., Yuan, H., van den Doel, M., Sees, T., van Blitterswijk, C., and de Groot, K. (2006b). Relevance of osteoinductive biomaterials in critical-sized orthotopic defect. J Orthop Res 24, 867-876.
- Habibovic, P., Yuan, H., van der Valk, C., Meijer, G., van Blitterswijk, C., and de Groot, K. (2005). 3D microenvironment as essential element for osteoinduction by biomaterials. Biomaterials 26, 3565-3575.
- Haddock, S., Debes, J., Nauman, E., Fong, K., Arramon, Y., and Keaveny, T. (1999). Structure-function relationships for coralline hydroxyapatite bone substitute. J Biomed Mater Res 47, 71-78.
- Hadjidakis, D.J. (2006). Bone remodeling, i.I. Roulakis, ed. Ann N Y Acad Sci. 2006 Dec;1092:385-96.
- Hagen, J., Semmelink, J., Klein, C., Prahl-Andersen, B., and Burger, E. (1992). Bone induction by demineralized bone particles: long-term observations of the implant-connective tissue interface. J Biomed Mater Res 26, 897-913.
- Harris, N., Rattray, K., Tye, C., Underhill, T., Somerman, M., D'Errico, J., Chambers, A., Hunter, G., and Goldberg, H. (2000). Functional analysis of bone sialoprotein: identification of the hydroxyapatite-nucleating and cell-binding domains by recombinant peptide expression and site-directed mutagenesis. Bone 27, 795-802.
- Hauschka, P., Lian, J., and Gallop, P. (1975). Direct identification of the calcium-binding amino acid, gamma-carboxyglutamate, in mineralized tissue. Proc Natl Acad Sci USA 72, 3925-3929.
- Haylock, D., and Nilsson, S. (2006). Osteopontin: a bridge between bone and blood. Br J Haematol 134, 467-474.
- Heise, U., Osborn, J., and Duwe, F. (1990). Hydroxyapatite ceramic as a bone substitute. Int Orthop 14, 329-338.
- Hench, L. (1989). Bioceramics and the origin of life. J Biomed Mater Res 23, 685-703.
- Hench, L., and Polak, J. (2002). Third-generation biomedical materials. Science 295, 1014-1017.
- Herten, M., Rothamel, D., Schwarz, F., Friesen, K., Koegler, G., and Becker, J. (2009). Surface- and nonsurface-dependent in vitro effects of bone substitutes on cell viability. Clin Oral Investig 13, 149-155.
- Hessle, L., Johnson, K., Anderson, H., Narisawa, S., Sali, A., Goding, J., Terkeltaub, R., and Millan, J. (2002). Tissue-nonspecific alkaline phosphatase and plasma cell membrane glycoprotein-1 are central antagonistic regulators of bone mineralization. Proc Natl Acad Sci USA 99, 9445-9449.
- Heymann, D. (1999). Bone substitutes: new concepts, N. Passuti, ed. European Journal of Orthopaedic Surgery & Traumatology, 9, pp. 179-184.

- Heymann, D., Delecrin, J., Deschamps, C., Gouin, F., Padrines, M., and Passuti, N. (2001a). In vitro assessment of combining osteogenic cells with macroporous calcium-phosphate ceramics. Rev Chir Orthop Reparatrice Appar Mot 87, 8-17.
- Heymann, D., Guicheux, J., and Rousselle, A. (2001b). Ultrastructural evidence in vitro of osteoclast-induced degradation of calcium phosphate ceramic by simultaneous resorption and phagocytosis mechanisms. Histol Histopathol 16, 37-44.
- Hildebrand, M., Higgins, D., Busser, K., and Volcani, B. (1993). Silicon-responsive cDNA clones isolated from the marine diatom Cylindrotheca fusiformis. Gene 132, 213-218.
- Hill, P. (1998). Bone remodelling. Br J Orthod 25, 101-107.
- Hing, K. (2004). Bone repair in the twenty-first century: biology, chemistry or engineering? Philos Transact A Math Phys Eng Sci 362, 2821-2850.
- Hing, K., Annaz, B., Saeed, S., Revell, P., and Buckland, T. (2005). Microporosity enhances bioactivity of synthetic bone graft substitutes. J Mater Sci Mater Med 16, 467-475.
- Hing, K., Best, S., Tanner, K., Bonfield, W., and Revell, P. (2004). Mediation of bone ingrowth in porous hydroxyapatite bone graft substitutes. J Biomed Mater Res A 68, 187-200.
- Hing, K., Revell, P., Smith, N., and Buckland, T. (2006). Effect of silicon level on rate, quality and progression of bone healing within silicate-substituted porous hydroxyapatite scaffolds. Biomaterials 27, 5014-5026.
- Hing, K., Wilson, L., and Buckland, T. (2007) Comparative performance of three ceramic bone graft substitutes. Spine J 7, 475-490.
- Hing, K.A. (2004). Microporosity affects bioactivity of macroporous hydroxyapatite bone graft substitutes. Key Engineering Materials, pp. 273-276.
- Hing, K.A. (2004). Silicate substitution alters the progression of bone apposition within porous hydroxyapetite bone graft substitutes, S. Seed, ed. Orthopaedics Research Society.
- Hing, K.A. (2005). Bioceramic Bone Graft Substitutes: Influence of Porosity and Chemistry Int. J. Appl. Ceram. Technol, pp. 184-199.
- Hogan, L. (2005). The formation of osseointegration. American Orthopaedics Society.
- Holy, C., Shoichet, M., and Davies, J. (2000). Engineering three-dimensional bone tissue in vitro using biodegradable scaffolds: investigating initial cell-seeding density and culture period. J Biomed Mater Res 51, 376-382.
- Hulbert, S., Young, F., Mathews, R., Klawitter, J., Talbert, C., and Stelling, F. (1970). Potential of ceramic materials as permanently implantable skeletal prostheses. J Biomed Mater Res 4, 433-456.
- Hunter, G., and Goldberg, H. (1994). Modulation of crystal formation by bone phosphoproteins: role of glutamic acid-rich sequences in the nucleation of hydroxyapatite by bone sialoprotein. Biochem J 302 (Pt 1), 175-179.

- Igarashi, M., Kamiya, N., Hasegawa, M., Kasuya, T., Takahashi, T., and Takagi, M. (2004). Inductive effects of dexamethasone on the gene expression of Cbfa1, Osterix and bone atrix proteins during differentiation of cultured primary rat osteoblasts. J Mol Histol 35, 3-10.
- Ikeda, K. (2008a). Assessment of bone quality. Osteocyte function and bone quality. Clin Calcium 18, 321-325.
- Ikeda, K. (2008b). Osteocytes in the pathogenesis of osteoporosis. Geriatr Gerontol Int 8, 213-217.
- Ilan, D.I. (2003). Bone graft substitutes, A.L. Ladd, ed. Operative Techniques in Plastic and Reconstructive Surgery, pp. 151-160.
- J, Aerssen., J, Dequeker., and M, M.J. (1994). Bone tissue composition: biochemical anatomy of bone. Clin Rheumatol. 1994 Dec;13 Suppl 1:54-62.
- Jacobsen, K., Al-Aql, Z., Wan, C., Fitch, J., Stapleton, S., Mason, Z., Cole, R., Gilbert, S., Clemens, T., Morgan, E., et al. (2008). Bone formation during distraction osteogenesis is dependent on both VEGFR1 and VEGFR2 signaling. J Bone Miner Res 23, 596-609.
- Jarcho, M. (1981). Calcium phosphate ceramics as hard tissue prosthetics. Clin Orthop Relat Res, 259-278.
- Jarcho, M. (1986). Biomaterial aspects of calcium phosphates. Properties and applications. Dent Clin North Am 30, 25-47.
- Jin, Q., Takita, H., Kohgo, T., Atsumi, K., Itoh, H., and Kuboki, Y. (2000). Effects of geometry of hydroxyapatite as a cell substratum in BMP-induced ectopic bone formation. J Biomed Mater Res 52, 491-499.
- John, A., Varma, H., and Kumari, T. (2003). Surface reactivity of calcium phosphate based ceramics in a cell culture system. J Biomater Appl 18, 63-78.
- Jones, J., Ehrenfried, L., and Hench, L. (2006a). Optimising bioactive glass scaffolds for bone tissue engineering. Biomaterials 27, 964-973.
- Jones, J., Lee, P., and Hench, L. (2006b). Hierarchical porous materials for tissue engineering. Philos Transact A Math Phys Eng Sci 364, 263-281.
- Jones, J.R. (2009). New trends in bioactive scaffolds: The importance of nanostructure Journal of the European Ceramic Society. 29, 1275-1281.
- Jorgensen, C., Noel, D., Apparailly, F., and Sany, J. (2001). Stem cells for repair of cartilage and bone: the next challenge in osteoarthritis and rheumatoid arthritis. Ann Rheum Dis 60, 305-309.
- Joschek, S., Nies, B., Krotz, R., and Galferich, A. (2000). Chemical and physicochemical characterization of porous hydroxyapatite ceramics made of natural bone. Biomaterials 21, 1645-1658.

- Jukes, J., Both, S., Leusink, A., Sterk, L., van Blitterswijk, C., and de Boer, J. (2008). Endochondral bone tissue engineering using embryonic stem cells. Proc Natl Acad Sci USA 105, 6840-6845.
- Jukes, J.M., Sanne K. Both, Anouk Leusink, Lotus M. Th. Sterk, Clemens A. van Blitterswijk, and Jan de Boer (2008). Endochondral bone tissue engineering using embryonic stem cells.
- Jung, C., Ou, Y., Yeung, F., Frierson, H.J., and Kao, C. (2001). Osteocalcin is incompletely spliced in non-osseous tissues. Gene 271, 143-150.
- Kaback, L., Soung, d.Y., Naik, A., Smith, N., Schwarz, E., O'Keefe, R., and Drissi, H. (2008). Osterix/Sp7 regulates mesenchymal stem cell mediated endochondral ossification. J Cell Physiol 214, 173-182.
- Kale, A., and Di Cesare, P. (1995). Osteoinductive agents. Basic science and clinical applications. Am J Orthop 24, 752-761.
- Kamitakahara, M., Ohtsuki, C., and Miyazaki, T. (2008). Review paper: behavior of ceramic biomaterials derived from tricalcium phosphate in physiological condition. J Biomater Appl 23, 197-212.
- Kanczler, J., and Oreffo, R. (2008). Osteogenesis and angiogenesis: the potential for engineering bone. Eur Cell Mater 15, 100-114.
- Kaplan, F., and Shore, E. (1996). Bone morphogenetic proteins and C-FOS: early signals in endochondral bone formation. Bone 19, 13S-21S.
- Karageorgiou, V., and Kaplan, D. (2005). Porosity of 3D biomaterial scaffolds and osteogenesis. Biomaterials 26, 5474-5491.
- Karsenty, G. (2001). Minireview: transcriptional control of osteoblast differentiation. Endocrinology 142, 2731-2733.
- Karsenty, G., and Wagner, E. (2002). Reaching a genetic and molecular understanding of skeletal development. Dev Cell 2, 389-406.
- KAawagoe, D. (2004). Transparent .Beta.-Tricalcium Phosphate Ceramics Prepared by Spark Plasma Sintering. Journal of the Ceramic Society of Japan, pp. 462-463.
- Kilpadi, K., Chang, P., and Bellis, S. (2001). Hydroxylapatite binds more serum proteins, purified integrins, and osteoblast precursor cells than titanium or steel. J Biomed Mater Res 57, 258-267.
- Kim, H., Kim, U., Vunjak-Novakovic, G., Min, B., and Kaplan, D. (2005). Influence of macroporous protein scaffolds on bone tissue engineering from bone marrow stem cells. Biomaterials 26, 4442-4452.
- Kim, S., Lee, J., Kim, Y., Riu, D., Jung, S., Lee, Y., Chung, S., and Kim, Y. (2003). Synthesis of Si, Mg substituted hydroxyapatites and their sintering behaviors. Biomaterials 24, 1389-1398.

- Klein, C., Abe, Y., Hosono, H., and de Groot, K. (1984a). Different calcium phosphate bioglass ceramics implanted in rabbit cortical bone. An interface study. Biomaterials 5, 362-364.
- Klein, C., Abe, Y., Hosono, H., and de Groot, K. (1987). Comparison of calcium phosphate glass ceramics with apatite ceramics implanted in bone. An interface study--II. Biomaterials 8, 234-236.
- Klein, C., de Blieck-Hogervorst, J., Wolke, J., and de Groot, K. (1990). Studies of the solubility of different calcium phosphate ceramic particles in vitro. Biomaterials 11, 509-512.
- Klein, C., de Groot, K., Chen, W., Li, Y., and Zhang, X. (1994). Osseous substance formation induced in porous calcium phosphate ceramics in soft tissues. Biomaterials 15, 31-34.
- Klein, C., Driessen, A., and de Groot, K. (1984b). Relationship between the degradation behaviour of calcium phosphate ceramics and their physical-chemical characteristics and ultrastructural geometry. Biomaterials 5, 157-160.
- Klein, C., Driessen, A., de Groot, K., and van den Hooff, A. (1983). Biodegradation behavior of various calcium phosphate materials in bone tissue. J Biomed Mater Res 17, 769-784.
- Knaack, D., Goad, M., Aiolova, M., Rey, C., Tofighi, A., Chakravarthy, P., and Lee, D. (1998). Resorbable calcium phosphate bone substitute. J Biomed Mater Res 43, 399-409.
- Knabe, C. (2004). Effect of rapidly resorbable calcium phosphates and a calcium phosphate bone cement on the expression of bonerelated genes and proteins in vitro, G. Berger, ed. Journal of biomedical materials research, pp. 145-154.
- Knabe, C., Berger, G., Gildenhaar, R., Howlett, C., Markovic, B., and Zreiqat, H. (2004). The functional expression of human bone-derived cells grown on rapidly resorbable calcium phosphate ceramics. Biomaterials 25, 335-344.
- Knabe, C., Nicklin, S., Yu, Y., Walsh, W., Radlanski, R., Marks, C., and Hoffmeister, B. (2005a). Growth factor expression following clinical mandibular distraction osteogenesis in humans and its comparison with existing animal studies. J Craniomaxillofac Surg 33, 361-369.
- Knabe, C., Stiller, M., Berger, G., Reif, D., Gildenhaar, R., Howlett, C., and Zreiqat, H. (2005b). The effect of bioactive glass ceramics on the expression of bone-related genes and proteins in vitro. Clin Oral Implants Res 16, 119-127.
- Kokubo, T. (1991). Bioactive glass ceramics: properties and applications. Biomaterials 12, 155-163.
- Kokubo, T., Ito, S., Huang, Z., Hayashi, T., Sakka, S., Kitsugi, T., and Yamamuro, T. (1990a). Ca,P-rich layer formed on high-strength bioactive glass-ceramic A-W. J Biomed Mater Res 24, 331-343.

- Kokubo, T., Kim, H., and Kawashita, M. (2003). Novel bioactive materials with different mechanical properties. Biomaterials 24, 2161-2175.
- Kokubo, T., Kushitani, H., Sakka, S., Kitsugi, T., and Yamamuro, T. (1990b). Solutions able to reproduce in vivo surface-structure changes in bioactive glass-ceramic A-W. J Biomed Mater Res 24, 721-734.
- Komori, T. (1998). Cbfal in bone development, T. Kishimoto, ed. Current opinion in genetics and development, pp. 494-499.
- Kraus, K.H. (2006). Mesenchymal stem cells and bone regeneration, C., Kirker-head ed. Vet Surg. 3: 232-42.
- Kuboki, Y., Jin, Q., and Takita, H. (2001). Geometry of carriers controlling phenotypic expression in BMP-induced osteogenesis and chondrogenesis. J Bone Joint Surg Am 83-A Suppl 1, S105-115.
- Kuboki, Y., Takita, H., Kobayashi, D., Tsuruga, E., Inoue, M., Murata, M., Nagai, N., Dohi, Y., and Ohgushi, H. (1998). BMP-induced osteogenesis on the surface of hydroxyapatite with geometrically feasible and nonfeasible structures: topology of osteogenesis. J Biomed Mater Res 39, 190-199.
- Kurashina, K., Kurita, H., Takeuchi, H., Hirano, M., Klein, C., and de Groot, K. (1995). Osteogenesis in muscle with composite graft of hydroxyapatite and autogenous calvarial periosteum: a preliminary report. Biomaterials 16, 119-123.
- Kurashina, K., Kurita, H., Wu, Q., Ohtsuka, A., and Kobayashi, H. (2002). Ectopic osteogenesis with biphasic ceramics of hydroxyapatite and tricalcium phosphate in rabbits. Biomaterials 23, 407-412.
- Kurioka, K., Umeda, M., Teranobu, O., and Komori, T. (1999). Effect of various properties of hydroxyapatite ceramics on osteoconduction and stability. Kobe J Med Sci 45, 149-163.
- Kohler, P., Ehrnberg, A., and Kreicbergs, A. (1990). Osteogenic enhancement of diaphyseal reconstruction. Comparison of bone grafts in the rabbit. Acta Orthop Scand 61, 42-45.
- Lane, N., Yao, W., Balooch, M., Nalla, R., Balooch, G., Habelitz, S., Kinney, J., and Bonewald, L. (2006). Glucocorticoid-treated mice have localized changes in trabecular bone material properties and osteocyte lacunar size that are not observed in placebo-treated or estrogen-deficient mice. J Bone Miner Res 21, 466-476.
- Langstaff, S., Sayer, M., Smith, T., and Pugh, S. (2001). Resorbable bioceramics based on stabilized calcium phosphates. Part II: evaluation of biological response. Biomaterials 22, 135-150.
- Langstaff, S., Sayer, M., Smith, T., Pugh, S., Hesp, S., and Thompson, W. (1999). Resorbable bioceramics based on stabilized calcium phosphates. Part I: rational design, sample preparation and material characterization. Biomaterials 20, 1727-1741.

- Le Nihouannen, D., Daculsi, G., Saffarzadeh, A., Gauthier, O., Delplace, S., Pilet, P., and Layrolle, P. (2005). Ectopic bone formation by microporous calcium phosphate ceramic particles in sheep muscles. Bone 36, 1086-1093.
- Le Nihouannen, D., Saffarzadeh, A., Aguado, E., Goyenvalle, E., Gauthier, O., Moreau, F., Pilet, P., Spaethe, R., Daculsi, G., and Layrolle, P. (2007). Osteogenic properties of calcium phosphate ceramics and fibrin glue based composites. J Mater Sci Mater Med 18, 225-235.
- Lecanda, F., Avioli, L., and Cheng, S. (1997). Regulation of bone matrix protein expression and induction of differentiation of human osteoblasts and human bone marrow stromal cells by bone morphogenetic protein-2. J Cell Biochem 67, 386-396.
- Lee, Y., Jo, M., Luna, M., Chien, B., Lieberman, J., and Wang, J. (2005). The efficacy of different commercially available demineralized bone matrix substances in an athymic rat model. J Spinal Disord Tech 18, 439-444.
- Leeuwenburgh, S., Wolke, J., Siebers, M., Schoonman, J., and Jansen, J. (2006). In vitro and in vivo reactivity of porous, electrosprayed calcium phosphate coatings. Biomaterials 27, 3368-3378.
- LeGeros, R. (2002). Properties of osteoconductive biomaterials: calcium phosphates. Clin Orthop Relat Res, 81-98.
- LeGeros, R. (2008). Calcium phosphate-based osteoinductive materials. Chem Rev 108, 4742-4753.
- Leroux, T., Perez-Ordonez, B., and von Schroeder, H. (2007). Osteolysis after the use of a silicon-stabilized tricalcium phosphate-based bone substitute in a radius fracture: a case report. J Hand Surg Am 32, 497-500.
- Leupold, J., Barfield, W., An, Y., and Hartsock, L. (2006). A comparison of ProOsteon, DBX, and collagraft in a rabbit model. J Biomed Mater Res B Appl Biomater 79, 292-297.
- Levy S., Van Dalen, M., Agonafer s., Soboyejo, W. O. (2007). Cell sutface interactions and adhesion on bioactive glass 45S5. J Mater Sci: Mater Med. 18, 89-102
- Liao, H., Mutvei, H., Hammarstrom, L., Wurtz, T., and Li, J. (2002). Tissue responses to nacreous implants in rat femur: an in situ hybridization and histochemical study. Biomaterials 23, 2693-2701.
- Liu, X., Morra, M., Carpi, A., and Li, B. (2008). Bioactive calcium silicate ceramics and coatings. Biomed Pharmacother 62, 526-529.
- Lloyd, R., Fisher, D., Schlenker, R., and Miller, S. (1999). Some problems in the skeletal dosimetry of bone-seeking radionuclides. Health Phys 76, 402-412.
- Lopez-Alvarez, M., Solla, E., Gonzalez, P., Serra, J., Leon, B., Marques, A., and Reis, R. (2009). Silicon-hydroxyapatite bioactive coatings (Si-HA) from diatomaceous earth and silica. Study of adhesion and proliferation of osteoblast-like cells. J Mater Sci Mater Med 20, 1131-1136.

- Mabilleau, G., Xia, Z., Hing, K., Buckland, T., and Sabokbar, A. (2007). Osteoclastic responses to phase pure hydroxyapatite (HA) and silicon (SI)-substituted HA. Tissue Engineering 13, 1388-1388.
- MacDonald, N., Lorick, P., and Petriello, L. (1957). Healing bone fractures and simultaneous administration of radioisotopes of sulfur, calcium and yttrium. Am J Physiol 191, 185-188.
- MacDonald, N., Nusbaum, R., Alexander, G., Ezmirlian, F., Spain, P., and Rounds, D. (1952). The skeletal deposition of yttrium. J Biol Chem 195, 837-841.
-
- Malaval, L., Aubin, J., and Vico, L. (2009). Role of the small integrin-binding ligand N-linked glycoprotein (SIBLING), bone sialoprotein (BSP) in bone development and remodeling. Osteoporos Int 20, 1077-1080.
- Malaval, L., Liu, F., Roche, P., and Aubin, J. (1999). Kinetics of osteoprogenitor proliferation and osteoblast differentiation in vitro. J Cell Biochem 74, 616-627.
- Malaval, L., Wade-Gueye, N., Boudiffa, M., Fei, J., Zirngibl, R., Chen, F., Laroche, N., Roux, J., Burt-Pichat, B., Duboeuf, F., et al. (2008). Bone sialoprotein plays a functional role in bone formation and osteoclastogenesis. J Exp Med 205, 1145-1153.
- Mancini, L., Tamma, R., Settanni, M., Camerino, C., Patano, N., Greco, G., Strippoli, M., and Zallone, A. (2007). Osteoblasts cultured on three-dimensional synthetic hydroxyapatite implanted on a chick allantochorial membrane induce ectopic bone marrow differentiation. Ann N Y Acad Sci 1116, 306-315.
- Mangano, C., Piattelli, A., Perrotti, V., and Iezzi, G. (2008). Dense hydroxyapatite inserted into postextraction sockets: a histologic and histomorphometric 20-year case report. J Periodontol 79, 929-933.
- Massa, E.A. (2001). Enhanced Cytocompatibility Properties of Hydroxyapatite Doped with Trivalent Ions, E.B. Slamovich, ed. Materials research society.
- Mastrogiacomo, M., Corsi, A., Francioso, E., Di Comite, M., Monetti, F., Scaglione, S., Favia, A., Crovace, A., Bianco, P., and Cancedda, R. (2006a). Reconstruction of extensive long bone defects in sheep using resorbable bioceramics based on silicon stabilized tricalcium phosphate. Tissue Eng 12, 1261-1273.
- Mastrogiacomo, M., Scaglione, S., Martinetti, R., Dolcini, L., Beltrame, F., Cancedda, R., and Quarto, R. (2006b). Role of scaffold internal structure on in vivo bone formation in macroporous calcium phosphate bioceramics. Biomaterials 27, 3230-3237.
- Matsubara, T., Kida, K., Yamaguchi, A., Hata, K., Ichida, F., Meguro, H., Aburatani, H., Nishimura, R., and Yoneda, T. (2008). BMP2 regulates Osterix through Msx2 and Runx2 during osteoblast differentiation. J Biol Chem 283, 29119-29125.

- Matsushima, A., Kotobuki, N., Tadokoro, M., Kawate, K., Yajima, H., Takakura, Y., and Ohgushi, H. (2009). In vivo osteogenic capability of human mesenchymal cells cultured on hydroxyapatite and on beta-tricalcium phosphate. Artif Organs 33, 474-481.
- Miclau (2005). Common Molecular Mechanisms Regulating Fetal Bone Formation and Adult Fracture Repair.
- Moore, W., Graves, S., and Bain, G. (2001). Synthetic bone graft substitutes. ANZ J Surg 71, 354-361.
- Nakashima, K., Zhou, X., Kunkel, G., Zhang, Z., Deng, J., Behringer, R., and de Crombrugghe, B. (2002). The novel zinc finger-containing transcription factor osterix is required for osteoblast differentiation and bone formation. Cell 108, 17-29.
- Neumann, M. (2006). Composites of calcium phosphate and polymers as bone substitution materials, M. Epple, ed. European journal of trauma, 23, pp. 125-131.
- Nuss, K., Auer, J., Boos, A., and von Rechenberg, B. (2006). An animal model in sheep for biocompatibility testing of biomaterials in cancellous bones. BMC Musculoskelet Disord. 7, 67.
- Ohgushi, H., Miyake, J., and Tateishi, T. (2003). Mesenchymal stem cells and bioceramics: strategies to regenerate the skeleton. Novartis Found Symp 249, 118-127; discussion 127-132, 170-114, 239-141.
- Ohgushi, H., Okumura, M., Tamai, S., Shors, E., and Caplan, A. (1990). Marrow cell induced osteogenesis in porous hydroxyapatite and tricalcium phosphate: a comparative histomorphometric study of ectopic bone formation. J Biomed Mater Res 24, 1563-1570.
- Okada, Y., Kobayashi, M., Fujita, H., Katsura, Y., Matsuoka, H., Takadama, H., Kokubo, T., and Nakamura, T. (1999). Transmission electron microscopic study of interface between bioactive bone cement and bone: comparison of apatite and wollastonite containing glass-ceramic filler with hydroxyapatite and beta-tricalcium phosphate fillers. J Biomed Mater Res 45, 277-284.
- Okumura, M., Ohgushi, H., Dohi, Y., Katuda, T., Tamai, S., Koerten, H., and Tabata, S. (1997). Osteoblastic phenotype expression on the surface of hydroxyapatite ceramics. J Biomed Mater Res 37, 122-129.
- Otto, F., Thornell, A., Crompton, T., Denzel, A., Gilmour, K., Rosewell, I., Stamp, G., Beddington, R., Mundlos, S., Olsen, B., (1997). Cbfa1, a candidate gene for cleidocranial dysplasia syndrome, is essential for osteoblast differentiation and bone development. Cell 89, 765-771.
- Owada, H. (1989). Humidity-Sensitivity of yttrium substituted apatite ceramics, K. Yamashita, ed. Solid State Ionics, 35, 401-404.
- Owen, T., Aronow, M., Barone, L., Bettencourt, B., Stein, G., and Lian, J. (1991). Pleiotropic effects of vitamin D on osteoblast gene expression are related to the proliferative and

differentiated state of the bone cell phenotype: dependency upon basal levels of gene expression, duration of exposure, and bone matrix competency in normal rat osteoblast cultures. Endocrinology 128, 1496-1504.

- Owen, T., Aronow, M., Shalhoub, V., Barone, L., Wilming, L., Tassinari, M., Kennedy, M., Pockwinse, S., Lian, J., and Stein, G. (1990). Progressive development of the rat osteoblast phenotype in vitro: reciprocal relationships in expression of genes associated with osteoblast proliferation and differentiation during formation of the bone extracellular matrix. J Cell Physiol 143, 420-430.
- Ozawa, S., and Kasugai, S. (1996). Evaluation of implant materials (hydroxyapatite, glass-ceramics, titanium) in rat bone marrow stromal cell culture. Biomaterials 17, 23-29.
- Pabbruwe, M., Standard, O., Sorrell, C., and Howlett, C. (2004). Effect of silicon doping on bone formation within alumina porous domains. J Biomed Mater Res A 71, 250-257.
- Papadimitropoulos, A., Mastrogiacomo, M., Peyrin, F., Molinari, E., Komlev, V., Rustichelli, F., and Cancedda, R. (2007). Kinetics of in vivo bone deposition by bone marrow stromal cells within a resorbable porous calcium phosphate scaffold: an X-ray computed microtomography study. Biotechnol Bioeng 98, 271-281.
- Patan, S. (2000). Vasculogenesis and angiogenesis as mechanisms of vascular network formation, growth and remodeling. J Neurooncol 50, 1-15.
- Patel, N. (2001). the in vivo response of phase pure hydroxyapatite and carbonate substituted hydroxyapatite granules of varying size ranges, I.R. Gibson, ed. (Key Engineering Materials), pp. 218-220.
- Patel, N. (2002). A comparative study on the in vivo behaviour of hydroxyapatite and silicon substituted hydroxyapatite granules, I. Gibson, ed. J Mater Sci Mater Med. 12, 1199-206.
- Patel, N., Best, S., Bonfield, W., Gibson, I., Hing, K., Damien, E., and Revell, P. (2002). A comparative study on the in vivo behavior of hydroxyapatite and silicon substituted hydroxyapatite granules. J Mater Sci Mater Med 13, 1199-1206.
- Patel, N., Brooks, R., Clarke, M., Lee, P., Rushton, N., Gibson, I., Best, S., and Bonfield, W. (2005). In vivo assessment of hydroxyapatite and silicate-substituted hydroxyapatite granules using an ovine defect model. J Mater Sci Mater Med 16, 429-440.
- Pederson, L., Ruan, M., Westendorf, J., Khosla, S., and Oursler, M. (2008). Regulation of bone formation by osteoclasts involves Wnt/BMP signaling and the chemokine sphingosine-1-phosphate. Proc Natl Acad Sci U S A 105, 20764-20769.
- Peterson, B., Whang, P., Iglesias, R., Wang, J., and Lieberman, J. (2004). Osteoinductivity of commercially available demineralized bone matrix. Preparations in a spine fusion model. J Bone Joint Surg Am 86-A, 2243-2250.

- Phan, P., Grzanna, M., Chu, J., Polotsky, A., el-Ghannam, A., Van Heerden, D., Hungerford, D., and Frondoza, C. (2003). The effect of silica-containing calcium-phosphate particles on human osteoblasts in vitro. J Biomed Mater Res A 67, 1001-1008.
- Piconi, C., and Maccauro, G. (1999). Zirconia as a ceramic biomaterial. Biomaterials 20, 1-25.
- Pietak, A., Reid, J., and Sayer, M. (2005). Electron spin resonance in silicon substituted apatite and tricalcium phosphate. Biomaterials 26, 3819-3830.
- Pietak, A., Reid, J., Stott, M., and Sayer, M. (2007). Silicon substitution in the calcium phosphate bioceramics. Biomaterials 28, 4023-4032.
- Porter, A. (2006). Nanoscale characterization of the interface between bone and hydroxyapatite implants and the effect of silicon on bone apposition. Micron 37, 681-688.
- Porter, A., Best, S., and Bonfield, W. (2004a). Ultrastructural comparison of hydroxyapatite and silicon-substituted hydroxyapatite for biomedical applications. J Biomed Mater Res A 68, 133-141.
- Porter, A., Botelho, C., Lopes, M., Santos, J., Best, S., and Bonfield, W. (2004b). Ultrastructural comparison of dissolution and apatite precipitation on hydroxyapatite and silicon-substituted hydroxyapatite in vitro and in vivo. J Biomed Mater Res A 69, 670-679.
- Porter, A., Buckland, T., Hing, K., Best, S., and Bonfield, W. (2006). The structure of the bond between bone and porous silicon-substituted hydroxyapatite bioceramic implants. J Biomed Mater Res A 78, 25-33.
- Porter, A., Patel, N., Brooks, R., Best, S., Rushton, N., and Bonfield, W. (2005). Effect of carbonate substitution on the ultrastructural characteristics of hydroxyapatite implants. J Mater Sci Mater Med 16, 899-907.
- Porter, A., Patel, N., Skepper, J., Best, S., and Bonfield, W. (2003). Comparison of in vivo dissolution processes in hydroxyapatite and silicon-substituted hydroxyapatite bioceramics. Biomaterials 24, 4609-4620.
- Porter, A., Patel, N., Skepper, J., Best, S., and Bonfield, W. (2004). Effect of sintered silicate-substituted hydroxyapatite on remodelling processes at the bone-implant interface. Biomaterials 25, 3303-3314.
- Posner, A. (1985a). The mineral of bone. Clin Orthop Relat Res, 200, 87-99.
- Posner, A. (1985b). The structure of bone apatite surfaces. J Biomed Mater Res 19, 241-250.
- Price, P., Otsuka, A., Poser, J., Kristaponis, J., and Raman, N. (1976). Characterization of a gamma-carboxyglutamic acid-containing protein from bone. Proc Natl Acad Sci U S A 73, 1447-1451.
- Pugliarello, M., Vittur, F., de Bernard, B., Bonucci, E., and Ascenzi, A. (1973). Analysis of bone composition at the microscopic level. Calcif Tissue Res 12, 209-216.
- Puleo, D., and Nanci, A. (1999). Understanding and controlling the bone-implant interface. Biomaterials 20, 2311-2321.

- Radin, S., and Ducheyne, P. (1993). The effect of calcium phosphate ceramic composition and structure on in vitro behavior. II. Precipitation. J Biomed Mater Res 27, 35-45.
- Rashid, N. (2004). Effect of silicate substitution on the surface charge of hydroxyapatite, I. Harding, ed. 7th World Biomaterials Congress, Sydney.
- Rashid, N. (2008). Nano-scale manipulation of silicate-substituted apatite chemistry impacts surface charge, hydrophilicity, protein adsorption and cell attachment, I.S. Harding, ed. Int. J. Nano and Biomaterials, 1, 299-319.
- Raynaud, S., Champion, E., Lafon, J., and Bernache-Assollant, D. (2002). Calcium phosphate apatites with variable Ca/P atomic ratio III. Mechanical properties and degradation in solution of hot pressed ceramics. Biomaterials 23, 1081-1089.
- Reddi, A. (1998). Role of morphogenetic proteins in skeletal tissue engineering and regeneration. Nat Biotechnol 16, 247-252.
- Reddi, A. (2000). Morphogenesis and tissue engineering of bone and cartilage: inductive signals, stem cells, and biomimetic biomaterials. Tissue Eng 6, 351-359.
- Redey, S., Nardin, M., Bernache-Assolant, D., Rey, C., Delannoy, P., Sedel, L., and Marie, P. (2000). Behavior of human osteoblastic cells on stoichiometric hydroxyapatite and type A carbonate apatite: role of surface energy. J Biomed Mater Res 50, 353-364.
- Reffitt, D., Ogston, N., Jugdaohsingh, R., Cheung, H., Evans, B., Thompson, R., Powell, J., and Hampson, G. (2003). Orthosilicic acid stimulates collagen type 1 synthesis and osteoblastic differentiation in human osteoblast-like cells in vitro. Bone 32, 127-135.
- Reid, J., Pietak, A., Sayer, M., Dunfield, D., and Smith, T. (2005). Phase formation and evolution in the silicon substituted tricalcium phosphate/apatite system. Biomaterials 26, 2887-2897.
- Rejda, B., Peelen, J., and de Groot, K. (1977). Tri-calcium phosphate as a bone substitute. J Bioeng 1, 93-97.
- Ripamonti, U., Crooks, J., Khoali, L., and Roden, L. (2009). The induction of bone formation by coral-derived calcium carbonate/hydroxyapatite constructs. Biomaterials 30, 1428-1439.
- Ripamonti, U., Heliotis, M., and Ferretti, C. (2007). Bone morphogenetic proteins and the induction of bone formation: from laboratory to patients. Oral Maxillofac Surg Clin North Am 19, 575-589,.
- Ripamonti, U., Ramoshebi, L., Teare, J., Renton, L., and Ferretti, C. (2008). The induction of endochondral bone formation by transforming growth factor-beta(3): experimental studies in the non-human primate Papio ursinus. J Cell Mol Med 12, 1029-1048.
- Rittling, S., Matsumoto, H., McKee, M., Nanci, A., An, X., Novick, K., Kowalski, A., Noda, M., and Denhardt, D. (1998). Mice lacking osteopontin show normal development and bone structure but display altered osteoclast formation in vitro. J Bone Miner Res 13, 1101-1111.

- Roach, H. (1994). Why does bone matrix contain non-collagenous proteins? The possible roles of osteocalcin, osteonectin, osteopontin and bone sialoprotein in bone mineralisation and resorption. Cell Biol Int 18, 617-628.
- Robinson, R. (1952a). An electron-microscopic study of the crystalline inorganic component of bone and its relationship to the organic matrix. J Bone Joint Surg Am 34-A, 389-435; passim.
- Rumpel, E., Wolf, E., Kauschke, E., Bienengraber, V., Bayerlein, T., Gedrange, T., and Proff, P. (2006). The biodegradation of hydroxyapatite bone graft substitutes in vivo. Folia Morphol (Warsz) 65, 43-48.
- Ruppel, M., Miller, L., and Burr, D. (2008). The effect of the microscopic and nanoscale structure on bone fragility. Osteoporos Int 19, 1251-1265.
- Sage, H., Vernon, R., Funk, S., Everitt, E., and Angello, J. (1989). SPARC, a secreted protein associated with cellular proliferation, inhibits cell spreading in vitro and exhibits Ca+2-dependent binding to the extracellular matrix. J Cell Biol 109, 341-356.
- Salasznyk, R., Williams, W., Boskey, A., Batorsky, A., and Plopper, G. (2004). Adhesion to Vitronectin and Collagen I Promotes Osteogenic Differentiation of Human Mesenchymal Stem Cells. J Biomed Biotechnol 2004, 24-34.
- Sato, K., Lewandowski, R., Bui, J., Omary, R., Hunter, R., Kulik, L., Mulcahy, M., Liu, D., Chrisman, H., Resnick, S., et al. Treatment of unresectable primary and metastatic liver cancer with yttrium-90 microspheres (TheraSphere): assessment of hepatic arterial embolization. Cardiovasc Intervent Radiol 29, 522-529.
- Sato, M., Sambito, M., Aslani, A., Kalkhoran, N., Slamovich, E., and Webster, T. (2006). Increased osteoblast functions on undoped and yttrium-doped nanocrystalline hydroxyapatite coatings on titanium. Biomaterials 27, 2358-2369.
- Schnettler (2004). Calcium phosphate-based bone substitutes, J.P. Stahl, ed. European journal of trauma, 30, 219-229.
- Schwartz, Z., and Boyan, B. (1994). Underlying mechanisms at the bone-biomaterial interface. J Cell Biochem 56, 340-347.
- Schwartz, Z., Sela, J., Ramirez, V., Amir, D., and Boyan, B. (1989). Changes in extracellular matrix vesicles during healing of rat tibial bone: a morphometric and biochemical study. Bone 10, 53-60.
- Seaborn, C.O. (1994). Dietary silicon affects acid and alkaline phosphatase and calcium uptake in bone of rats. The Journal of Trace Elements in Experimental Medicine. 7, 11-18.
- Shapiro, F. (2008). Bone development and its relation to fracture repair. The role of mesenchymal osteoblasts and surface osteoblasts. Eur Cell Mater 15, 53-76.

- Sibilla, P., Sereni, A., Aguiari, G., Banzi, M., Manzati, E., Mischiati, C., Trombelli, L., and del Senno, L. (2006). Effects of a hydroxyapatite-based biomaterial on gene expression in osteoblast-like cells. J Dent Res 85, 354-358.
- Spence, G., Phillips, S., Campion, C., Brooks, R., and Rushton, N. (2008). Bone formation in a carbonate-substituted hydroxyapatite implant is inhibited by zoledronate: the importance of bioresorption to osteoconduction. J Bone Joint Surg Br 90, 1635-1640.
- Stains, J., and Civitelli, R. (2005). Cell-to-cell interactions in bone. Biochem Biophys Res Commun 328, 721-727.
- Stein, G., Lian, J., and Owen, T. (1990). Relationship of cell growth to the regulation of tissue-specific gene expression during osteoblast differentiation. FASEB J 4, 3111-3123.
- Steve Weiner, 1 Wolfie Traub, and H. Daniel Wagner (1999). Lamellar Bone: Structure-Function Relations. J Struct Biol., 126(3):241-55.
- Street, J., Bao, M., deGuzman, L., Bunting, S., Peale, F.J., Ferrara, N., Steinmetz, H., Hoeffel, J., Cleland, J., Daugherty, A., et al. (2002). Vascular endothelial growth factor stimulates bone repair by promoting angiogenesis and bone turnover. Proc Natl Acad Sci U S A 99, 9656-9661.
- Stubbs, D., Deakin, M., Chapman-Sheath, P., Bruce, W., Debes, J., Gillies, R., and Walsh, W. (2004). In vivo evaluation of resorbable bone graft substitutes in a rabbit tibial defect model. Biomaterials 25, 5037-5044.
- Tachibana, Y., Ninomiya, S., Kim, Y., and Sekikawa, M. (2003). Tissue response to porous hydroxyapatite ceramic in the human femoral head. J Orthop Sci 8, 549-553.
- Tai, G., Polak, J., Bishop, A., Christodoulou, I., and Buttery, L. Differentiation of osteoblasts from murine embryonic stem cells by overexpression of the transcriptional factor osterix. Tissue Eng 10, 1456-1466.
- Tamai, N., Myoui, A., Tomita, T., Nakase, T., Tanaka, J., Ochi, T., and Yoshikawa, H. (2002). Novel hydroxyapatite ceramics with an interconnective porous structure exhibit superior osteoconduction in vivo. J Biomed Mater Res 59, 110-117.
- Tanaka, K. (1995). Isolated chick osteocytes stimulate formation and bone-resorbing activity of osteoclast-like cells, Y. Yamaguchi, ed. J Bone Miner Metab, 13, 61-70.
- Termine, J., Kleinman, H., Whitson, S., Conn, K., McGarvey, M., and Martin, G. (1981). Osteonectin, a bone-specific protein linking mineral to collagen. Cell 26, 99-105.
- Thian, E., Ahmad, Z., Huang, J., Edirisinghe, M., Jayasinghe, S., Ireland, D., Brooks, R., Rushton, N., Bonfield, W., and Best, S. (2009). The role of surface wettability and surface charge of electrosprayed nanoapatites on the behaviour of osteoblasts. Acta Biomater. 6, 750-755

- Thian, E., Huang, J., Best, S., Barber, Z., and Bonfield, W. (2005a). A new way of incorporating silicon in hydroxyapatite (Si-HA) as thin films. J Mater Sci Mater Med 16, 411-415.
- Thian, E., Huang, J., Best, S., Barber, Z., and Bonfield, W. (2005b). Magnetron co-sputtered silicon-containing hydroxyapatite thin films--an in vitro study. Biomaterials 26, 2947-2956.
- Thian, E., Huang, J., Best, S., Barber, Z., and Bonfield, W. (2006a). Novel silicon-doped hydroxyapatite (Si-HA) for biomedical coatings: an in vitro study using acellular simulated body fluid. J Biomed Mater Res B Appl Biomater 76, 326-333.
- Thian, E., Huang, J., Best, S., Barber, Z., Brooks, R., Rushton, N., and Bonfield, W. (2006b). The response of osteoblasts to nanocrystalline silicon-substituted hydroxyapatite thin films. Biomaterials 27, 2692-2698.
- Thomas, M., Puleo, D., and Al-Sabbagh, M. (2005). Bioactive glass three decades on. J Long Term Eff Med Implants 15, 585-597.
- Tremble, P., Lane, T., Sage, E., and Werb, Z. (1993). SPARC, a secreted protein associated with morphogenesis and tissue remodeling, induces expression of metalloproteinases in fibroblasts through a novel extracellular matrix-dependent pathway. J Cell Biol 121, 1433-1444.
- Trueta, J. (1963). The role of the vessels in osteogenesis. The journal of bone and joint surgery. 45, 402-418
- Tsuruga, E., Takita, H., Itoh, H., Wakisaka, Y., and Kuboki, Y. (1997). Pore size of porous hydroxyapatite as the cell-substratum controls BMP-induced osteogenesis. J Biochem 121, 317-324.
- Ueta, C., Iwamoto, M., Kanatani, N., Yoshida, C., Liu, Y., Enomoto-Iwamoto, M., Ohmori, T., Enomoto, H., Nakata, K., Takada, K., et al. (2001). Skeletal malformations caused by overexpression of Cbfa1 or its dominant negative form in chondrocytes. J Cell Biol 153, 87-100.
- V. I. Putlyaev, V.I. (2006). A new generation of calcium phosphate biomaterials: The role of phase and chemical compositions, T.V. Safronova, ed. Biomaterials. 63, 30-33
- Valerio, P., Pereira, M., Goes, A., and Leite, M. (2004). The effect of ionic products from bioactive glass dissolution on osteoblast proliferation and collagen production. Biomaterials 25, 2941-2948.
- Vallet-regi, M. (2005). Silicon substituted hydroxyapatites. A method to upgrade calcium phosphate based implants, D. Arcos, ed. Journal of materials chemistry, 15, 1509-1516.
- Vallet-RegÃ, M., and Balas, F. (2008). Silica materials for medical applications. Open Biomed Eng J 2, 1-9.

- van Gaalen, S., Dhert, W., van den Muysenberg, A., Oner, F., van Blitterswijk, C., verbout, A., and de Bruijn, J. (2004). Bone tissue engineering for spine fusion: an experimental study on ectopic and orthotopic implants in rats. Tissue Eng 10, 231-239.
- Vandiver, J., Dean, D., Patel, N., Bonfield, W., and Ortiz, C. (2005). Nanoscale variation in surface charge of synthetic hydroxyapatite detected by chemically and spatially specific high-resolution force spectroscopy. Biomaterials 26, 271-283.
- Vandiver, J., Dean, D., Patel, N., Botelho, C., Best, S., Santos, J., Lopes, M., Bonfield, W., and Ortiz, C. (2006). Silicon addition to hydroxyapatite increases nanoscale electrostatic, van der Waals, and adhesive interactions. J Biomed Mater Res A 78, 352-363.
- Viguet-Carrin, S., Garnero, P., and Delmas, P. (2006). The role of collagen in bone strength. Osteoporos Int 17, 319-336.
- Valimaki, V., and Aro, H. (2006). Molecular basis for action of bioactive glasses as bone graft substitute. Scand J Surg 95, 95-102.
- Vaananen, H., Zhao, H., Mulari, M., and Halleen, J. (2000). The cell biology of osteoclast function. J Cell Sci 113 (Pt 3), 377-381.
- Walsh, W., Chapman-Sheath, P., Cain, S., Debes, J., Bruce, W., Svehla, M., and Gillies, R. (2003). A resorbable porous ceramic composite bone graft substitute in a rabbit metaphyseal defect model. J Orthop Res 21, 655-661.
- Wang, C., Duan, Y., Markovic, B., Barbara, J., Howlett, C., Zhang, X., and Zreiqat, H. (2004a). Phenotypic expression of bone-related genes in osteoblasts grown on calcium phosphate ceramics with different phase compositions. Biomaterials 25, 2507-2514.
- Wang, C., Duan, Y., Markovic, B., Barbara, J., Rolfe Howlett, C., Zhang, X., and Zreiqat, H. (2004b). Proliferation and bone-related gene expression of osteoblasts grown on hydroxyapatite ceramics sintered at different temperature. Biomaterials 25, 2949-2956.
- Wang, J., Alanay, A., Mark, D., Kanim, L., Campbell, P., Dawson, E., and Lieberman, J. (2007a). A comparison of commercially available demineralized bone matrix for spinal fusion. Eur Spine J 16, 1233-1240.
- Wang, J., and Glimcher, M. (1999). Characterization of matrix-induced osteogenesis in rat calvarial bone defects: I. Differences in the cellular response to demineralized bone matrix implanted in calvarial defects and in subcutaneous sites. Calcif Tissue Int 65, 156-165.
- Wang, M. (2003). Developing bioactive composite materials for tissue replacement. Biomaterials 24, 2133-2151.
- Wang, Y., Li, S., Wu, D., Zhang, K., Yu, S., and Cui, S. (2003). Bone formation in vitro and in vivo by human bone marrow-derived mesenchymal stem cells. Zhonghua Kou Qiang Yi Xue Za Zhi 38, 467-469.

- Wang, Y., Wan, C., Deng, L., Liu, X., Cao, X., Gilbert, S., Bouxsein, M., Faugere, M., Guldberg, R., Gerstenfeld, L. (2007). The hypoxia-inducible factor alpha pathway couples angiogenesis to osteogenesis during skeletal development. J Clin Invest 117, 1616-1626.
- Wang, Y., Wan, C., Gilbert, S., and Clemens, T. (2007c). Oxygen sensing and osteogenesis. Ann N Y Acad Sci 1117, 1-11.
- Webster, T., Ergun, C., Doremus, R., and Bizios, R. (2002). Hydroxylapatite with substituted magnesium, zinc, cadmium, and yttrium. II. Mechanisms of osteoblast adhesion. J Biomed Mater Res 59, 312-317.
- Webster, T., Massa-Schlueter, E., Smith, J., and Slamovich, E. (2004). Osteoblast response to hydroxyapatite doped with divalent and trivalent cations. Biomaterials 25, 2111-2121.
- Weiner, S. (1998). The material of bone: structure-mechanical function relations, H. Wagner, ed. Annurev Mat Sci. 28: 271-298
- Weng, J., Liu, Q., Wolke, J., Zhang, X., and de Groot, K. (1997). Formation and characteristics of the apatite layer on plasma-sprayed hydroxyapatite coatings in simulated body fluid. Biomaterials 18, 1027-1035.
- Winter, G. (1970). Heterotopic bone formation in a synthetic sponge. Proc R Soc Med 63, 1111-1115.
- Wopenka, B. (2005). A mineralogical perspective on the apatite in bone, J.D. Pasteris, ed. Materials Science and Engineering, 25, 131-143.
- Xiao, G., Jiang, D., Ge, C., Zhao, Z., Lai, Y., Boules, H., Phimphilai, M., Yang, X., Karsenty, G., and Franceschi, R. (2005). Cooperative interactions between activating transcription factor 4 and Runx2/Cbfa1 stimulate osteoblast-specific osteocalcin gene expression. J Biol Chem 280, 30689-30696.
- Xiao, Z., Thomas, R., Hinson, T., and Quarles, L. (1998). Genomic structure and isoform expression of the mouse, rat and human Cbfa1/Osf2 transcription factor. Gene 214, 187-197.
- Xin, R., Leng, Y., Chen, J., and Zhang, Q. (2005). A comparative study of calcium phosphate formation on bioceramics in vitro and in vivo. Biomaterials 26, 6477-6486.
- Xing, L., Schwarz, E., and Boyce, B. (2005). Osteoclast precursors, RANKL/RANK, and immunology. Immunol Rev 208, 19-29.
- Xu, H., Smith, D., and Simon, C. (2004). Strong and bioactive composites containing nano-silica-fused whiskers for bone repair. Biomaterials 25, 4615-4626.
- Xu, J., and Khor, K. (2007). Chemical analysis of silica doped hydroxyapatite biomaterials consolidated by a spark plasma sintering method. J Inorg Biochem 101, 187-195.
- Xu, S., Lin, K., Wang, Z., Chang, J., Wang, L., Lu, J., and Ning, C. (2008). Reconstruction of calvarial defect of rabbits using porous calcium silicate bioactive ceramics. Biomaterials 29, 2588-2596.

- Xue, W., Liu, X., Zheng, X., and Ding, C. (2005). Effect of hydroxyapatite coating crystallinity on dissolution and osseointegration in vivo. J Biomed Mater Res A 74, 553-561.
- Xynos, I., Edgar, A., Buttery, L., Hench, L., and Polak, J. (2001). Gene-expression profiling of human osteoblasts following treatment with the ionic products of Bioglass 45S5 dissolution. J Biomed Mater Res 55, 151-157.
- Yamasaki, H., and Sakai, H. (1992). Osteogenic response to porous hydroxyapatite ceramics under the skin of dogs. Biomaterials 13, 308-312.
- Yang, W., Zhou, D., Yin, G., Chen, H., Xiao, B., and Zhang, Y. (2004). [Study on a new type of apatite/wollastonite porous bioactive glass-ceramic]. Sheng Wu Yi Xue Gong Cheng Xue Za Zhi 21, 913-916.
- Yang, Z., Yuan, H., Zou, P., Tong, W., Qu, S., and Zhang, X. (1997). Osteogenic responses to extraskeletally implanted synthetic porous calcium phosphate ceramics: an early stage histomorphological study in dogs. J Mater Sci Mater Med 8, 697-701.
- Yaszemski, M., Payne, R., Hayes, W., Langer, R., and Mikos, A. (1996). Evolution of bone transplantation: molecular, cellular and tissue strategies to engineer human bone. Biomaterials 17, 175-185.
- Yeh, L., and Lee, J. (1999). Osteogenic protein-1 increases gene expression of vascular endothelial growth factor in primary cultures of fetal rat calvaria cells. Mol Cell Endocrinol 153, 113-124.
- Yokobori, A.J. (1998). Osteogenesis mechanism based on kinetic theory. Biomed Mater Eng 8, 253-257.
- Yoshikawa, H., and Myoui, A. (2005). Bone tissue engineering with porous hydroxyapatite ceramics. J Artif Organs 8, 131-136.
- Yoshikawa, T., and Ohgushi, H. (1999). Autogenous cultured bone graft--bone reconstruction using tissue engineering approach. Ann Chir Gynaecol 88, 186-192.
- Yoshikawa, T., Ohgushi, H., Nakajima, H., Yamada, E., Ichijima, K., Tamai, S., and Ohta, T. (2000). In vivo osteogenic durability of cultured bone in porous ceramics: a novel method for autogenous bone graft substitution. Transplantation 69, 128-134.
- Yoshiko, Y., Candeliere, G., Maeda, N., and Aubin, J. (2007). Osteoblast autonomous Pi regulation via Pit1 plays a role in bone mineralization. Mol Cell Biol 27, 4465-4474.
- Young, J., Rhee, T., Atassi, B., Gates, V., Kulik, L., Mulcahy, M., Larson, A., Ryu, R., Sato, K., Lewandowski, R., et al. (2007). Radiation dose limits and liver toxicities resulting from multiple yttrium-90 radioembolization treatments for hepatocellular carcinoma. J Vasc Interv Radiol 18, 1375-1382.
- Young, M. (2003a). Bone matrix proteins: more than markers. Calcif Tissue Int 72, 2-4.
- Young, M. (2003b). Bone matrix proteins: their function, regulation, and relationship to osteoporosis. Osteoporos Int 14 Suppl 3, S35-42.

- Young, M., Kerr, J., Ibaraki, K., Heegaard, A., and Robey, P. (1992). Structure, expression, and regulation of the major noncollagenous matrix proteins of bone. Clin Orthop Relat Res, 275-294.
- Yuan, H., De Bruijn, J., Li, Y., Feng, J., Yang, Z., De Groot, K., and Zhang, X. (2001a). Bone formation induced by calcium phosphate ceramics in soft tissue of dogs: a comparative study between porous alpha-TCP and beta-TCP. J Mater Sci Mater Med 12, 7-13.
- Yuan, H., de Bruijn, J., Zhang, X., van Blitterswijk, C., and de Groot, K. (2001b). Bone induction by porous glass ceramic made from Bioglass (45S5). J Biomed Mater Res 58, 270-276.
- Yuan, H., Kurashina, K., de Bruijn, J., Li, Y., de Groot, K., and Zhang, X. (1999). A preliminary study on osteoinduction of two kinds of calcium phosphate ceramics. Biomaterials 20, 1799-1806.
- Yuan, H., Li, Y., de Bruijn, J., de Groot, K., and Zhang, X. (2000). Tissue responses of calcium phosphate cement: a study in dogs. Biomaterials 21, 1283-1290.
- Yuan, H., van Blitterswijk, C., de Groot, K., and de Bruijn, J. (2006a). A comparison of bone formation in biphasic calcium phosphate (BCP) and hydroxyapatite (HA) implanted in muscle and bone of dogs at different time periods. J Biomed Mater Res A 78, 139-147.
- Yuan, H., van Blitterswijk, C., de Groot, K., and de Bruijn, J. (2006b). Cross-species comparison of ectopic bone formation in biphasic calcium phosphate (BCP) and hydroxyapatite (HA) scaffolds. Tissue Eng 12, 1607-1615.
- Yuan, H., Van Den Doel, M., Li, S., Van Blitterswijk, C., De Groot, K., and De Bruijn, J. (2002). A comparison of the osteoinductive potential of two calcium phosphate ceramics implanted intramuscularly in goats. J Mater Sci Mater Med 13, 1271-1275.
- Yuan, H., Yang, Z., De Bruij, J., De Groot, K., and Zhang, X. (2001c). Material-dependent bone induction by calcium phosphate ceramics: a 2.5-year study in dog. Biomaterials 22, 2617-2623.
- Yuan, H., Yang, Z., Li, Y., Zhang, X., De Bruijn, J., and De Groot, K. (1998a). Osteoinduction by calcium phosphate biomaterials. J Mater Sci Mater Med 9, 723-726.
- Yuan, H., Zou, P., Yang, Z., Zhang, X., De Bruijn, J., and De Groot, K. (1998b). Bone morphogenetic protein and ceramic-induced osteogenesis. J Mater Sci Mater Med 9, 717-721.
- Zhang, C., Cho, K., Huang, Y., Lyons, J., Zhou, X., Sinha, K., McCrea, P., and de Crombrugghe, B. (2008). Inhibition of Wnt signaling by the osteoblast-specific transcription factor Osterix. Proc Natl Acad Sci U S A 105, 6936-6941.
- Zhang, W., Zhou, D., Yang, W., Yin, G., and Ou, J. (2007). A novel europium doped apatite/wollastonite porous magnetic bioactive glass ceramic. Sheng Wu Yi Xue Gong Cheng Xue Za Zhi 24, 785-789.

- Zhao, L., and Chang, J. (2004). Preparation and characterization of macroporous chitosan/wollastonite composite scaffolds for tissue engineering. J Mater Sci Mater Med 15, 625-629.
- Zhu, X., Fan, H., Xiao, Y., Li, D., Zhang, H., Luxbacher, T., and Zhang, X. (2009). Effect of surface structure on protein adsorption to biphasic calcium-phosphate ceramics in vitro and in vivo. Acta Biomater 5, 1311-1318.
- Zhu, X., Ganss, B., Goldberg, H., and Sodek, J. (2001). Synthesis and processing of bone sialoproteins during de novo bone formation in vitro. Biochem Cell Biol 79, 737-746.
- Zou, S., Huang, J., Best, S., and Bonfield, W. (2005). Crystal imperfection studies of pure and silicon substituted hydroxyapatite using Raman and XRD. J Mater Sci Mater Med 16, 1143-1148.
- Zou, S., Ireland, D., Brooks, R., Rushton, N., and Best, S. (2009). The effects of silicate ions on human osteoblast adhesion, proliferation, and differentiation. J Biomed Mater Res B Appl Biomater 90, 123-130.
- Zreiqat, H., Markovic, B., Walsh, W., and Howlett, C. (1996). A novel technique for quantitative detection of mRNA expression in human bone derived cells cultured on biomaterials. J Biomed Mater Res 33, 217-223.
- Zur Nieden, N., Kempka, G., and Ahr, H. (2003). In vitro differentiation of embryonic stem cells into mineralized osteoblasts. Differentiation 71, 18-27.

7 Conference presentations

- Samizadeh S, Hing, KA, Buckland, T, Coathup M, Blunn, GW. 2010. Are Calcium Phosphates or DBM better bone graft substitutes?. 56th Annual Meeting of the Orthopaedics Research Society.

- Hing K., Coathup M., Samizadeh S., 2009. The relative importance of strut porosity and chemistry on osteoinductivity of bioceramic bone graft substitutes. 33rd International Conference and Exposition on Advanced Ceramics and Composites.

- Samizadeh S, Coathup M, Amogbokpa J, Fang SC, Hing KA, Buckland T, Blunn G W**.** 2008. Osseoinduction by calcium phosphate bone substitutes as a function of chemical composition and structure. World Biomaterials Congress.

- Samizadeh S, Coathup M, Amogbokpa J, Fang SC, Hing KA, Buckland T, Blunn G W**.** 2007. Osseoinduction by calcium phosphate bone substitutes as a function of chemical composition and structure. 56th British Orthopaedics Research Society.

- Samizadeh S, Coathup M, Amogbokpa J, Fang SC, Hing KA, Buckland T, Blunn G W**.** 2007. Osseoinduction by calcium phosphate bone substitutes as a function of chemical composition and structure. 53rd Annual Meeting of the Orthopaedics Research Society.